

Instytut Chemii Bioorganicznej
Polskiej Akademii Nauk



Proteomiczna, metabolomiczna i lipidomiczna analiza krwi
w poszukiwaniu mechanizmów progresji miażdżycy
w przewlekłej chorobie nerek

mgr inż. Joanna Tracz

Praca doktorska wykonana w Zakładzie Proteomiki Biomedycznej

Promotor: dr hab. Magdalena Łuczak, prof. IChB PAN

Poznań 2021

Pragnę złożyć najserdeczniejsze podziękowania mojemu promotorowi

Dr hab. Magdalenie Łuczak, prof. IChB PAN

za przekazaną wiedzę, ogromny wkład w mój rozwój naukowy, nieocenione wsparcie merytoryczne oraz pomoc przy realizacji i redagowaniu niniejszej pracy, a także wyrazić wdzięczność za cenne wskazówki oraz inspirujące dyskusje, które były dla mnie motywacją do poszukiwania rozwiązań napotkanych problemów biologicznych.

Swoje podziękowania kieruję również do

Dr. Łukasza Marcza

za nieocenione wsparcie przy pracy z aparaturą badawczą oraz przekazaną wiedzę, a także życzliwość i wnikliwe uwagi przy redagowaniu niniejszej rozprawy.

Dr Annie Wojakowskiej dziękuję

za twórcze rozmowy, cenne rady oraz ogromne pokłady optymizmu.

Dziękuję Kolegom i Koleżankom

z **Europejskiego Centrum Bioinformatyki i Genomiki**

za stworzenie milej atmosfery pracy.

Szczególne wyrazy wdzięczności składam również mojej **Rodzinie i Przyjaciołom**,
a w szczególności **Marcinowi**, za wiarę we mnie i okazane wsparcie.

Przedłożona rozprawa doktorska została sfinansowana z projektu badawczego
Narodowego Centrum Nauki OPUS 10
„Poszukiwanie molekularnych mechanizmów progresji miażdżycy
w przewlekłej chorobie nerek”
nr 2015/19/B/NZ2/02450

SPIS TREŚCI

Wykaz skrótów	6
Streszczenie.....	7
Abstract	9
1. Wprowadzenie	11
1.1. Przewlekła choroba nerek.....	11
1.2. Patogeneza rozwoju zmian miażdżycowych	13
1.3. Badania multiomiczne prowadzone z wykorzystaniem spektrometrii mas	14
1.3.1. Proteomika	16
1.3.2. Lipidomika	17
1.3.3. Metabolomika	18
2. Cel pracy	19
3. Materiał i metody badawcze.....	20
3.1. Analiza proteomiczna.....	20
3.2. Analiza lipidomiczna.....	21
3.3. Analiza metabolomiczna	21
4. Skrótowe omówienie publikacji, będących wynikiem pracy doktorskiej	22
4.1. Applying Proteomics and Integrative „Omics” Strategies to Decipher the Chronic Kidney Disease-Related Atherosclerosis	22
4.2. Proteomic Profiling of Leukocytes Reveals Dysregulation of Adhesion and Integrin Proteins in Chronic Kidney Disease-Related Atherosclerosis	23
4.3. Mass-Spectrometry-Based Lipidomics Reveals Differential Changes in the Accumulated Lipid Classes in Chronic Kidney Disease.....	24
5. Wnioski	28
6. Bibliografia	29
7. Dorobek naukowy	33
8. Załączniki	36

Wykaz artykułów zawarty w rozprawie doktorskiej:

1. **Tracz J.**, Luczak M.
Applying Proteomics and Integrative „Omics” Strategies to Decipher the Chronic Kidney Disease-Related Atherosclerosis. *International Journal of Molecular Sciences* 2021, 22, 7492 (IF₂₀₂₀=5.923, IF_{5-letni}=6.132, 140 pkt MNiSW)
2. **Tracz J.**, Handschuh L., Lalowski M., Marczak Ł., Kostka-Jeziorny K., Perek B., Wanic-Kossowska M., Podkowińska A., Tykarski A., Formanowicz D., Luczak M.
Proteomic Profiling of Leukocytes Reveals Dysregulation of Adhesion and Integrin Proteins in Chronic Kidney Disease-Related Atherosclerosis. *Journal of Proteome Research* 2021, 20, 6 (IF₂₀₂₀=4.466, IF_{5-letni}=4.352, 100 pkt MNiSW)
3. Marczak L., Idkowiak J., **Tracz J.**, Stobiecki M., Perek B., Kostka-Jeziorny K., Tykarski A., Wanic-Kossowska M., Borowski M., Osuch M., Formanowicz D., Luczak M.
Mass-Spectrometry-Based Lipidomics Reveals Differential Changes in the Accumulated Lipid Classes in Chronic Kidney Disease. *Metabolites* 2021, 11, 275 (IF₂₀₂₀=4.932, IF_{5-letni}=4.98, 70 pkt MNiSW)

Artykuły niewchodzące w skład rozprawy doktorskiej:

1. Malecki P., Mania A., **Tracz J.**, Łuczak M., Mazur-Melewska K., Figlerowicz, M.
Adipocytokines as Risk Factors for Development of Nonalcoholic Fatty Liver Disease in Children. *Journal of Clinical and Experimental Hepatology* 2021 (70 pkt MNiSW)
2. Malecki P., **Tracz J.**, Łuczak M., Figlerowicz M., Mazur-Melewska K., Służewski W., Mania A.
Serum proteome assessment in nonalcoholic fatty liver disease in children: a preliminary study. *Expert Review of Proteomics* 2020, 17 (IF₂₀₁₉=3.614, IF_{5-letni}=3.805, 100 pkt MNiSW)
3. Waliczek M., Bąchor R., Kijewska M., Gąszczyk D., Panek-Laszczyńska K., Konieczny A., Dąbrowska K., Witkiewicz W., Marek-Bukowiec K., **Tracz J.**, Łuczak M., Szewczuk Z., Stefanowicz P.
Isobaric duplex based on a combination of 16O/18O enzymatic exchange and labeling with pyrylium salts. *Analytica Chimica Acta* 2019, 1048 (IF₂₀₁₈=5.256, IF_{5-letni}=6.228, 100 pkt MNiSW)
4. Zdarta A., **Tracz J.**, Luczak M., Guzik U., Kaczorek E.
Hydrocarbon-induced changes in proteins and fatty acids profiles of *Raoultella ornithinolytica* M03. *Journal of Proteomics* 2017, 164 (IF₂₀₁₆=3.914, IF_{5-letni}=4.02, 100 pkt MNiSW)

WYKAZ SKRÓTÓW

CKD	– przewlekła choroba nerek (<i>ang. <u>chronic kidney disease</u></i>)
CKD-A	– miażdżyca związana z przewlekłą chorobą nerek (<i>ang. <u>CKD-related atherosclerosis</u></i>)
CVD	– choroba sercowo-naczyniowa (<i>ang. <u>cardiovascular disease</u></i>)
ELISA	– test immunoenzymosorbcyjny (<i>ang. <u>enzyme-linked immunosorbent assay</u></i>)
ESI	– jonizacja poprzez elektrorozpraszanie (<i>ang. <u>electrospray ionization</u></i>)
GC-MS	– chromatografia gazowa sprzężona ze spektrometrią mas (<i>ang. <u>gas chromatography/mass spectrometry</u></i>)
GFR	– współczynnik filtracji kłębuszkowej (<i>ang. <u>glomerular filtration rate</u></i>)
HDL	– lipoproteina o wysokiej gęstości (<i>ang. <u>high-density lipoprotein</u></i>)
HV	– zdrowy ochotnik (<i>ang. <u>healthy volunteer</u></i>)
LC-MS/MS	– chromatografia cieczowa sprzężona z tandemową spektrometrią mas (<i>ang. <u>liquid chromatography coupled with tandem mass spectrometry</u></i>)
LDL	– lipoproteina o niskiej gęstości (<i>ang. <u>low-density lipoprotein</u></i>)
MS	– spektrometria mas (<i>ang. <u>mass spectrometry</u></i>)
MS/MS	– tandemowa spektrometria mas (<i>ang. <u>tandem mass spectrometry</u></i>)
PCA	– analiza głównych składowych (<i>ang. <u>principal component analysis</u></i>)
SRM/MRM	– metoda monitorowania wybranych/wielu reakcji następczych (<i>ang. <u>single/multiple reaction monitoring</u></i>)
WB	– western blot

STRESZCZENIE

Przewlekła choroba nerek (*ang. chronic kidney disease, CKD*) charakteryzuje się długotrwałą, progresywną oraz nieodwracalną utratą funkcji nerek, która w ostatnim stadium wymaga leczenia nerkozastępczego. Zaburzenie powoduje gromadzenie w organizmie produktów ubocznych metabolizmu, co naraża pacjentów na rozwój wielu schorzeń towarzyszących. Jednym z nich jest bardzo szybko postępująca miażdżyca związana z CKD (*ang. chronic kidney disease-related atherosclerosis, CKD-A*) oraz jej konsekwencje w postaci choroby sercowo-naczyniowej (*ang. cardiovascular disease, CVD*) i jej powikłań, które są główną przyczyną śmierci wśród pacjentów z CKD. W kilku badaniach wykazano, że charakter zmian miażdżycowych, pojawiających się w dysfunkcyjnych naczyniach krwionośnych w CKD różni się od tych występujących w klasycznej CVD, sugerując zaangażowanie innych mechanizmów molekularnych w rozwój CKD-A. Jednak patomechanizm akceleracji CVD w CKD nie został do tej pory w pełni wyjaśniony.

Nadrzędnym celem badań prowadzonych w ramach rozprawy doktorskiej była próba pogłębienia wiedzy na temat procesów i szlaków zaangażowanych w rozwój CKD-A. Rozprawa doktorska ma formę spójnego tematycznie zbioru artykułów, składającego się z pracy przeglądowej oraz dwóch prac eksperymentalnych. W pracy przeglądowej omówiono wszechstronne zastosowanie różnych podejść „omicznych”, ze szczególnym uwzględnieniem proteomiki do badania CKD i potencjał wykorzystania biologii systemów oraz badań integracyjnych do analizy patomechanizmu, leżącego u podstaw progresji CKD-A. Następnie przeprowadzono kompleksową analizę proteomu frakcji leukocytów oraz metabolomiczną i lipidomiczną analizę osocza, z wykorzystaniem metod opartych na spektrometrii mas (MS). Materiał badawczy uzyskano od dwóch grup pacjentów z różnym stopniem zaawansowania CKD i tym samym z różną progresją miażdżycy oraz dwóch grup z klasyczną CVD, również różniących się pod względem zaawansowania miażdżycy, lecz bez objawów dysfunkcji nerek. Jako referencję wykorzystano materiał zebrany od zdrowych ochotników. Uzyskane wyniki zostały częściowo zweryfikowane na poziomie białek i mRNA z wykorzystaniem takich technik jak ELISA, western blot, ddPCR oraz celowanej analizy MS wykonanej w trybie MRM. Przeprowadzone analizy statystyczne i bioinformatyczne pozwoliły wskazać procesy oraz szlaki molekularne zaangażowane w rozwój i progresję CKD-A.

Zidentyfikowane zmiany akumulacji białek ujawniły zaburzenia mechanizmów zapalnych w CKD-A związane z procesem transmigracji komórek przez śródbłonek naczyń. Wykazano, że w CKD może dochodzić do nasilenia mobilizacji i adhezji leukocytów na powierzchni śródbłonka, lecz procesy odpowiedzialne za reorganizację cytoszkieletu i polaryzację komórki, niezbędne do ukończenia procesu migracji, są najprawdopodobniej zahamowane. W tej sytuacji może dochodzić do agregacji komórek na powierzchni śródbłonka, lokalnego stanu zapalnego i dysfunkcji śródbłonka, promujących procesy aterogenne. W konsekwencji obserwujemy nasilenie programowanej śmierci komórek silnie skorelowane ze zmianami na poziomie molekuł adhezyjnych.

W pracy, po raz pierwszy scharakteryzowano również unikalny profil lipidomiczny pacjentów z miażdżycą niezwiązaną i związaną z CKD, wskazując na obniżony poziom akumulacji sfingomielin, cholesterolu i jego estrów, fosfatydylocholin, ceramidów i fosfatydyloetanoloamin w CKD w porównaniu do CVD. Wykazano również podwyższony poziom akumulacji triacylogliceroli

w CKD, jednak szczegółowa analiza związków będących substratami dla tych lipidów, jak również LDL i HDL, pokazała, że w tym przypadku dużo większą rolę mogą odgrywać zaburzenia w procesie syntezy bądź degradacji tych cząsteczek, a nie ich ogólnego poziomu, co może mieć wpływ na ich aterogenne i anty-aterogenne właściwości. Przeprowadzone analizy korelacyjne sugerują, że unikalny profil lipidowy może być związany z nasileniem stanu zapalnego, towarzyszącego dysfunkcji nerek.

Podsumowując, zidentyfikowano wiele zmian na poziomie białek, lipidów i niskocząsteczkowych metabolitów, które wskazują między innymi na zaburzenia mechanizmów zapalnych, w szczególności systemicznego stanu zapalnego, migracji, apoptozy i procesu koagulacji, a co za tym idzie homeostazy śródbłonka i leukocytów w CKD-A. Bezpośrednie porównanie akumulacji molekuł u pacjentów z klasyczną CVD oraz CKD przybliżyło nas do zrozumienia mechanizmu molekularnego przyspieszonego rozwoju CKD-A. Zaprezentowane wyniki wspierają postulowaną teorię „odwróconej epidemiologii” w CKD, a przyszłe badania powinny skupić się między innymi na mechanistycznych badaniach procesu diapedezy poszczególnych subpopulacji leukocytów w CKD.

ABSTRACT

Chronic kidney disease (CKD) is characterized by prolonged, progressive and irreversible loss of kidney function, which requires a renal replacement therapy in the last stage. The disorder causes the accumulation of intermediate products of metabolism in the body, which exposes patients to the development of many accompanying diseases. One of them is the rapidly progressive CKD-related atherosclerosis (CKD-A) and its consequences in the form of cardiovascular disease (CVD) as well as its complications, which are the major cause of mortality among CKD patients. Several studies have shown that nature of atherosclerotic lesions appearing in dysfunctional blood vessels in CKD differs from those in classical CVD, suggesting the involvement of other molecular mechanisms in the development of CKD-A. However, the pathomechanism of CVD acceleration in CKD has not been fully elucidated so far.

The main goal of the doctoral dissertation was an attempt to extend the knowledge about the processes and pathways involved in the development of CKD-A. The results presented in this doctoral dissertation were published as the review article and two experimental papers. In review, the versatile utilization of various "omics" approaches, with particular emphasis on proteomics for the study of CKD, was discussed. Moreover, the potential of using systems biology and integrative studies to analyze the pathomechanism underlying CKD-A progression, was emphasized. Then, a comprehensive proteome analysis of the leukocyte fraction as well as the metabolomic and lipidomic analysis of plasma using methods based on mass spectrometry (MS), were performed. The biological material was obtained from two groups of patients with different severity of CKD and thus different progression of atherosclerosis, and two groups with classical CVD, also different in the context of atherosclerosis progression, but without any symptoms of renal dysfunction. As a reference, material collected from healthy volunteers, was used. The obtained results were partially verified at the level of proteins and mRNA utilizing the techniques such as ELISA, western blot, ddPCR and MS targeted analysis in the MRM mode. The performed statistical and bioinformatics analyzes allowed to indicate the processes and molecular pathways involved in the development and progression of CKD-A.

The identified changes in protein accumulation revealed disturbances in the inflammatory mechanisms in CKD-A related to the process of cells transmigration through the vascular endothelium. It has been shown that in CKD mobilization and adhesion of leukocytes on the endothelial surface may be increased, but the processes responsible for the reorganization of the cytoskeleton and cell polarization, necessary to complete the migration process are most likely inhibited. In this situation, cell aggregation on the endothelial surface, local inflammation and endothelial dysfunction, promoting atherogenic processes, might be observed. As a consequence the intensification of programmed cell death strongly correlated with changes at the level of adhesive molecules, was observed.

The unique lipidomic profile of plasma in CKD-A and CVD was also demonstrated for the first time. The reduced level of accumulation of sphingomyelins, cholesterol and its esters, phosphatidylcholines, ceramides and phosphatidylethanolamines in CKD compared to CVD, were indicated. An increased level of triacylglycerol accumulation in CKD was also demonstrated, but a detailed analysis of compounds that are substrates for these lipids, and thus LDL and HDL, showed that in this case, disturbances in the synthesis or degradation of these molecules may play a much greater role than their level, which may affect their atherogenic and anti-atherogenic properties. The performed analyzes of correlation suggested that the unique lipid profile may also be associated with the severity of inflammation accompanying renal dysfunction.

In conclusion, a lot of changes at the level of proteins, lipids and low-molecular-weight metabolites, were demonstrated, indicating, among others, disturbance of inflammatory mechanisms, in particular systemic inflammation, migration, apoptosis and the coagulation process, and thus endothelial and leukocyte homeostasis in CKD-A. A direct comparison of the accumulation of molecules in patients with classical CVD and CKD provides better understanding the molecular mechanism of accelerated CKD-A development. The presented results support the postulated "reverse epidemiology" theory in CKD, and future research should focus, among other, on mechanistic studies of the diapedesis process of individual leukocyte subpopulations in CKD.

WPROWADZENIE

1.1. PRZEWLEKŁA CHOROBA NEREK

Przewlekła choroba nerek (*ang. chronic kidney disease, CKD*) jest złożonym oraz wielobjawowym stanem chorobowym, który jest następstwem uszkodzenia nefronów i pogarszania się funkcji nerek.^{1,2} Schorzenie diagnozuje i monitoruje się w oparciu o pomiar poziomu współczynnika filtracji kłębuszkowej (*ang. glomerular filtration rate, GFR* [mL/min/1.73 m²]), określającego ilość przesączonego osocza w jednostce czasu przez kłębuszki nerkowe z wytworzeniem moczu pierwotnego. Ważną rolę w ocenie schorzenia odgrywają również inne wskaźniki zaburzenia nerek, tj. proteinuria wyrażona jako stosunek stężenia albuminy do kreatyniny, nieprawidłowości w osadzie moczu oraz badania obrazowe.³ Na podstawie tych parametrów można ocenić stadium zaawansowania choroby i oszacować ryzyko dalszego jej rozwoju (Tabela 1). Wraz z pogarszającą się kondycją nerek poziom wskaźnika GFR obniża się, pojawiają się coraz liczniejsze nieprawidłowości w osadzie moczu oraz badaniach obrazowych. Ostatecznie u pacjentów z CKD rozwija się schyłkowa niewydolność nerek (CKD5), która wymaga specjalistycznego leczenia nerkozastępczego, w postaci dializy lub transplantacji. Brak prawidłowej funkcji nerek powoduje gromadzenie w organizmie produktów ubocznych metabolizmu i narażenie pacjentów na rozwój wielu schorzeń towarzyszących.⁴ Jednym z takich schorzeń jest szybko postępująca miażdżycza związana z CKD (*ang. chronic kidney disease –related atherosclerosis, CKD-A*), oraz jej konsekwencje w postaci powikłań sercowo-naczyniowych, stanowiących przeważającą przyczynę śmierci wśród pacjentów z CKD.⁵ Badania epidemiologiczne ujawniły, że wszystkie stadia CKD są skorelowane z podwyższonym ryzykiem miażdżycy, które drastycznie wzrasta u pacjentów rozpoczynających dializy, osiągając wartości nawet od 20- do 1000-krotnie wyższe w porównaniu do populacji ogólnej.⁶ Miażdżycza jest bardzo złożonym, wieloczynnikowym procesem zapalno-fibroproliferacyjnym, który charakteryzuje się tworzeniem swoistych zmian w ścianie naczyń, obejmujących nacieki zapalne, gromadzenie lipidów oraz włóknienie.⁷ Nasilenie tych zmian prowadzi do pojawienia się blaszek miażdżycowych oraz nekrotycznego rdzenia, powodując ostatecznie dysfunkcję naczynia.⁷ Występowanie i stopień zaawansowania zmian miażdżycowych ściśle koreluje z obecnością czynników ryzyka choroby sercowo-naczyniowej, które możemy podzielić na tradycyjne oraz nietradycyjne. Do pierwszej grupy zalicza się czynniki takie jak: otyłość, nadciśnienie, dyslipidemia, nikotynizm oraz cukrzyce. Do drugiej grupy należą między innymi podwyższony stres oksydacyjny, stan zapalny, zaburzenie procesów krzepnięcia, gromadzenie toksyn mocznicowych i zaburzenie gospodarki fosforanowo-wapniowej.⁸ Długotrwałe działanie tradycyjnych czynników ryzyka jest uznawane za kluczowe w rozwoju klasycznej choroby sercowo-naczyniowej (*ang. cardiovascular disease, CVD*). Miażdżycza związana z CKD postępuje o wiele szybciej i sugeruje się, że jej rozwój związany jest głównie z występowaniem nietradycyjnych czynników, które współdziałają z czynnikami tradycyjnymi.^{9,10} Dodatkowo, wśród pacjentów z CKD często obserwuje się zjawisko tzw. „odwróconej epidemiologii”, czyli paradoksalną odwrotną zależność między małym stężeniem cholesterolu, a dużym ryzykiem wystąpienia komplikacji sercowo-naczyniowych.^{11,12} Ponadto w CKD-A, wykazano wzmożone procesy zwapnienia naczyń

oraz bardziej nieorganiczny skład blaszek miażdżycowych, w porównaniu do klasycznej CVD, niezwiązanej z dysfunkcją nerek.¹³

Tabela 1. Klasyfikacja CKD na podstawie parametru eGFR (*ang. estimated GFR*) i poziomu albuminurii¹ wraz z oceną ryzyka progresji choroby: kolor zielony – niskie ryzyko (brak CKD przy nieobecności innych markerów zaburzenia funkcji nerek), kolor żółty – umiarkowanie podwyższone ryzyko, kolor pomarańczowy – wysokie ryzyko, kolor czerwony – bardzo wysokie ryzyko. ACR – wskaźnik albumina/kreatynina.

Ocena stadium CKD na podstawie eGFR i albuminurii			Poziom albuminurii ACR		
			A1	A2	A3
Stadia CKD	GFR [mL/min/1.73 m ²]	Funkcja nerek	Przedział albuminurii	Przedział albuminurii	Przedział albuminurii
			<30mg/g <3 mg/mmol	30-300 mg/g 3-30 mg/mmol	>300 mg/g >30 mg/mmol
CKD1	≥90	Nieznacznie zmniejszona			
CKD2	60-89	Lekko obniżona			
CKD3a	45-59	Umiarkowanie obniżona			
CKD3b	30-44	Umiarkowanie – poważnie obniżona			
CKD4	15-29	Znacząco obniżona			
CKD5	<15	Niewydolność nerek			

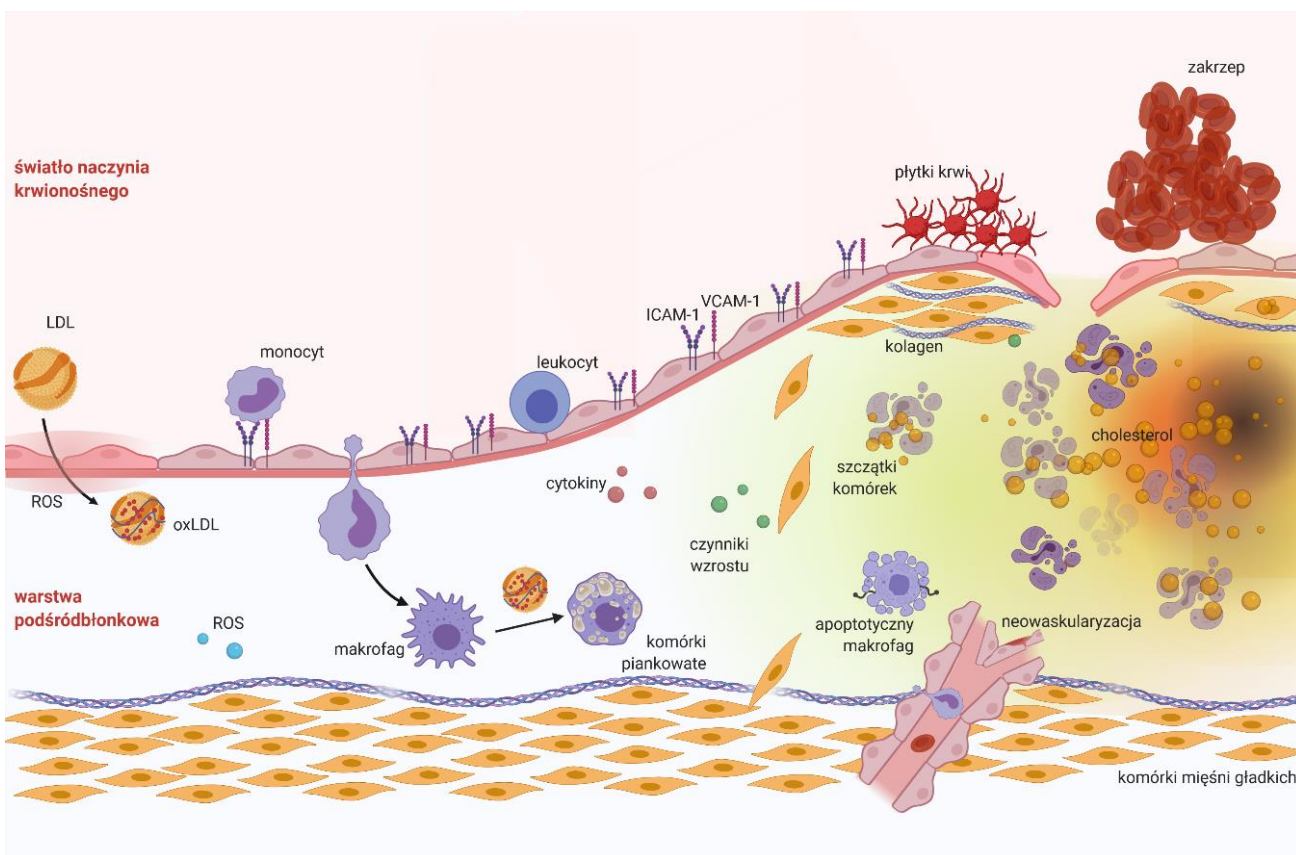
↓ progresja CKD

→ progresja CKD

Pomimo wielu lat badań obraz zmian, inicjujących oraz przyspieszających rozwój miażdżycy w CKD, pozostaje nie w pełni wyjaśniony. Niepowodzenia te mogą wynikać z niezwykle skomplikowanych i wielopłaszczyznowych procesów, toczących się w organizmie pacjenta, które są pogłębione przez dializy, zabieg konieczny w schyłkowym stadium choroby. Najnowsze doniesienia wskazują na bliską funkcjonalną zależność pomiędzy chorobami nerek, a CVD,¹⁴⁻¹⁶ lecz pomimo tych spostrzeżeń wielu badaczy wciąż wyklucza pacjentów z CKD z dużych badań klinicznych nad strategią leczenia miażdżycy oraz innych schorzeń sercowo-naczyniowych.¹⁷ Większość prezentowanych w dostępnym piśmiennictwie naukowym badań, skupia się na wczesnej diagnostyce CKD, a kwestie dotyczące miażdżycy są często pomijane. W tym kontekście pacjenci z CKD zestawiani są najczęściej ze zdrowymi ochotnikami (*ang. healthy volunteer, HV*), nieprzyjmującymi żadnych leków, podczas gdy leczenie chorych jest często bardzo złożone. Wydaje się, że badania porównawcze CKD-A oraz CVD, mają większy potencjał i mogą pozwolić na odróżnienie efektów wynikających z dysfunkcji nerek od tych związanych z rozwojem samej choroby sercowo-naczyniowej. Takie podejście może przybliżyć nas do zrozumienia mechanizmów szybko postępującej miażdżycy u pacjentów z CKD.

1.2. PATOGENEZA ROZWOJU ZMIAN MIAŻDŻYCOWYCH

W klasycznej CVD, nasilenie czynników ryzyka, takich jak otyłość, nadciśnienie, nikotynizm, hipercholesterolemia oraz hiperglikemia, zwykle prowadzi do uszkodzenia funkcji komórek śródbłonka naczyń, co przy podwyższonym poziomie lipidów we krwi sprzyja ich przenikaniu do głębszych warstw ściany naczynia. Przenikające w ten sposób cząsteczki LDL są zatrzymywane i utleniane w przestrzeni podśródbłonkowej na skutek nasilonych reakcji wolnorodnikowych (Rycina 1).¹⁸ Utlenione cząsteczki LDL indukują wzmożoną produkcję cząsteczek adhezyjnych, takich jak E-selektyny, VCAM1 (*ang. vascular adhesion molecule 1*) i ICAM1 (*ang. intercellular adhesion molecule 1*), które są uznawane za markery uszkodzenia komórek śródbłonka. Zwiększona obecność cząsteczek adhezyjnych na powierzchni śródbłonka stymuluje wiązanie monocytów i ich przenikanie na drodze diapedezy do warstwy podśródbłonkowej,¹⁹ gdzie różnicują w makrofagi i pochłaniają utlenione lipidy, przekształcając się w komórki piankowate (Rycina 1).²⁰ W takich warunkach dochodzi do nasilenia aktywacji śródbłonka, przenikania innych komórek układu immunologicznego, nasilenia mechanizmów odpowiedzi immunologicznej oraz produkcji cytokin prozapalnych, co sprzyja zwiększeniu objętości blaszek miażdżycowych (Rycina 1). Wzrost blaszki miażdżycowej prowadzi również do miejscowego niedotlenienia tkanek, co sprzyja procesowi neowaskularyzacji.²¹ Ponadto, wydzielane przez płytki krwi czynniki wzrostu i mitogeny wywołują odpowiedź proliferacyjną komórek mięśni gładkich, stabilizujących powstałą blaszkę miażdżycową. Dodatkowo, adhezja i agregacja płytek krwi na powierzchni śródbłonka sprzyja epizodom zakrzepowym.²² Na skutek toczących się procesów miażdżycorodnych, komórki piankowate mogą ulegać apoptozie, a uwolnione szczątki komórek i złogi lipidowe budują nekrotyczny rdzeń blaszki miażdżycowej. Wszystkie te procesy ostatecznie przyczyniają się do dysfunkcji naczynia (Rycina 1).



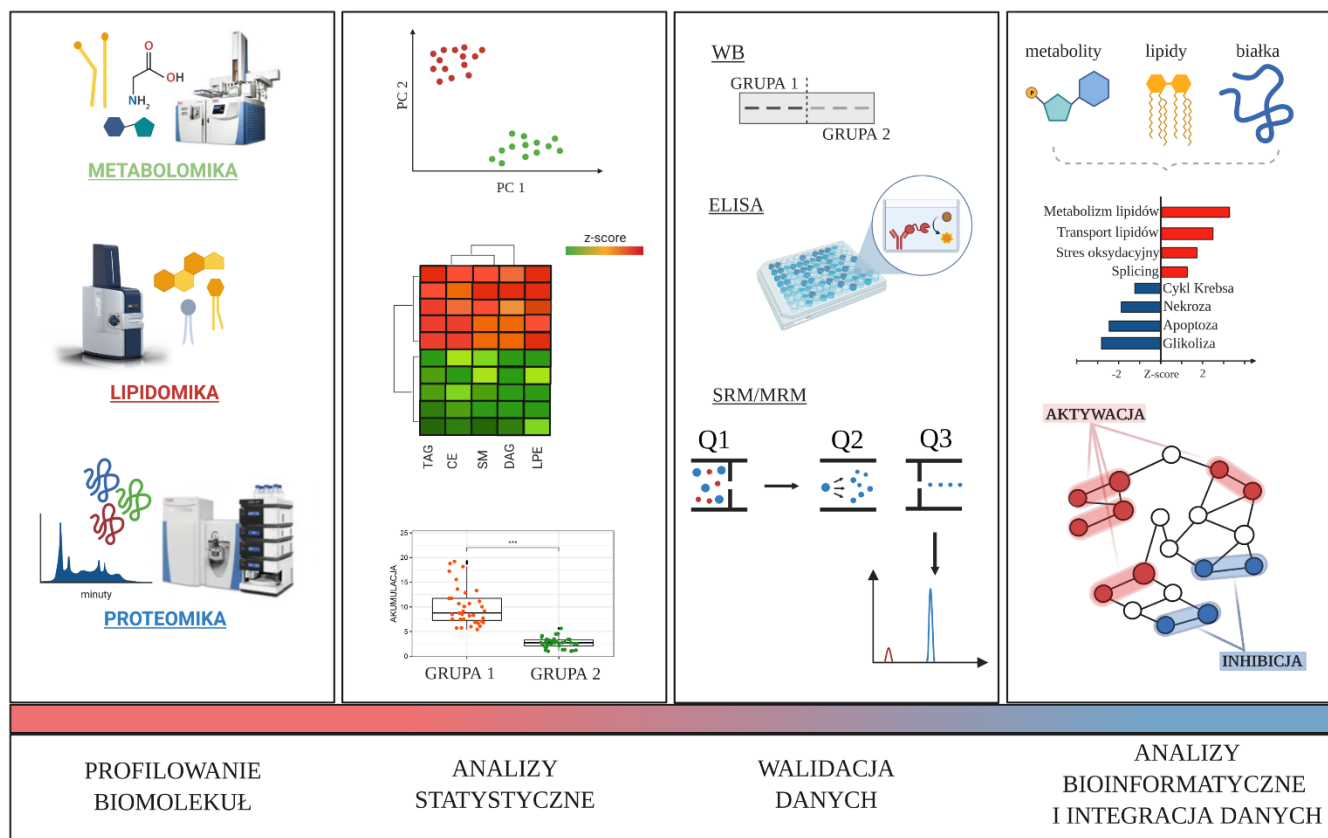
Rycina 1. Schemat prezentujący patogenezę zmian miażdżycowych, wykonany na podstawie¹⁹ z wykorzystaniem narzędzia BioRender.com.

1.3. BADANIA MULTIOMICZNE PROWADZONE Z WYKORZYSTANIEM SPEKTROMETRII MAS

Wysokoprzepustowe techniki „omiczne” są coraz częściej stosowane w analizach biomedycznych, a przedmiotem ich badań są geny, mRNA, białka, lipidy oraz niskocząsteczkowe metabolity pierwotne i wtórne analizowane w ujęciu całościowym.²³ Strategia multiomiczna umożliwia identyfikację oraz ocenę ilościową setek, a nawet tysięcy związków, których poziom akumulacji jest zaburzony podczas rozwoju choroby. Ilość danych uzyskanych w tego rodzaju analizach jest ogromna i wymaga uporządkowania, co jest możliwe z wykorzystaniem narzędzi biostatystyki i bioinformatyki. Jednym z pierwszych etapów usystematyzowania danych jest przeprowadzenie szeregu analiz statystycznych, w tym określenie poziomu istotności statystycznej, wariacji, wielkości efektu oraz znalezienia prawidłowości pomiędzy zmiennymi, np. poprzez analizę głównych składowych (*ang. principal component analysis, PCA*) i grupowanie hierarchiczne. Etap ten prowadzi do określenia zbioru cząsteczek różnicujących badane grupy eksperymentalne, a uzyskany zestaw danych można wykorzystać jako macierzę do przeprowadzenia funkcjonalnych analiz bioinformatycznych. Efektem jest wytypowanie szlaków i procesów zaburzonych podczas rozwoju choroby, w które cząsteczki różnicujące są zaangażowane, jak również określenie kierunkowości zmian oraz interakcji pomiędzy zidentyfikowanymi zaburzeniami. Końcowym etapem takiego podejścia powinna być integracja wielkoskalowych danych, w celu budowania modeli ułatwiających zrozumienie zjawisk zachodzących w badanych procesach. W analizach multiomicznych stosuje się technikę spektrometrii mas (*ang. mass*

spectrometry, **MS**), której upowszechnienie w biochemii i medycynie można dostrzec w ostatnich dekadach przy badaniu białek, lipidów i metabolitów. Analizy bazujące na MS wykorzystuje się do identyfikacji i oceny ilościowej badanych związków, a procedura analityczna obejmuje kilka kluczowych etapów, w tym przygotowanie materiału biologicznego, jakościowe i ilościowe profilowanie biomolekuł z wykorzystaniem techniki MS oraz obróbkę uzyskanych danych.²⁴ Model postępowania przy przygotowywaniu materiału do analizy zależy od rodzaju użytego materiału biologicznego oraz badanych związków i obejmuje m.in. dla analiz proteomicznych: homogenizację tkanek, liżę komórek, separację, oczyszczanie białek i ich trawienie, natomiast dla analiz metabolomicznych ekstrakcję związków oraz ich derywatyzację.^{25,26} Profilowanie biomolekuł oraz obróbka uzyskanych danych jest zależna od wielu zmiennych, dlatego zostanie szerzej opisana w dalszej części pracy.

Do badań „omicznych” zwykle wykorzystuje się tandemowe spektrometry mas (*ang. tandem mass spectrometer*, **MS/MS**), wykorzystujące, tzw. miękkie metody jonizacji, które z reguły wyposażone są w dwa analizatory przedzielone komorą zderzeń.²⁴ Zastosowanie trybu MS/MS zwiększa czułość i selektywność oznaczeń oraz umożliwia bardziej precyzyjną ocenę identyfikowanych związków, w tym m.in. określenie sekwencji aminokwasowej białek.²⁴ Nieocenionym narzędziem w biomedycynie okazało się również sprzężenie spektrometrii mas z chromatografią ciekłą (*ang. liquid chromatography coupled with tandem mass spectrometry*, **LC-MS/MS**) lub gazową (*ang. gas chromatography/mass spectrometry*, **GC-MS**) jako wielowymiarowych metod separacji złożonych mieszanin.²⁷ Jedną z podstawowych zalet technik łączonych jest zmniejszenie zjawiska supresji jonów, a tym samym zwiększenie liczby wykrywanych molekuł w analizie MS, w porównaniu do technik polegających na bezpośrednim wprowadzaniu próbki do źródła jonów. Techniki sprzężone wykorzystywane rutynowo w proteomice, lipidomice i metabolomice, zastosować można w dwóch strategiach analitycznych – niecelowanej oraz celowanej.²⁷ Przedmiotem analiz niecelowanych jest identyfikacja i ilościowa ocena możliwie, jak największej liczby badanych molekuł. Zastosowanie tego podejścia stosuje się w celu wyznaczenia hipotezy badawczej, ponieważ umożliwia poznanie i charakteryzację zmian, zachodzących w odpowiedzi na badany czynnik w ujęciu całościowym, bez koncentrowania się na pojedynczych związkach. Natomiast, analizy celowane, bazujące na technikach MS przeprowadza się w celu identyfikacji i ilościowej analizy wybranych, interesujących nas związków i wykorzystuje najczęściej jako metodę weryfikacji wyników otrzymanych w uprzednio przeprowadzonych badaniach. Do tego celu stosuje się metody monitorowania reakcji następczych typu SRM lub MRM (*ang. single/multiple reaction monitoring*).²⁸ Technika ta polega na monitorowaniu przejść jonu macierzystego w wybrany jon potomny powstały w wyniku fragmentacji i pomiarze intensywności tego sygnału. Schemat prezentujący poszczególne etapy wysokoprzepustowych analiz multiomicznych, bazujących na MS przedstawiono na Rycinie 2.



Rycina 2. Schemat metodyki profilowania biomolekuł za pomocą wysokoprzepustowych analiz bazujących na MS wykonany z wykorzystaniem narzędzia BioRender.com.

1.3.1. PROTEOMIKA

Przyczyny lub następstwa stanów chorobowych mogą mieć odzwierciedlenie w zaburzeniach dynamiki proteomu, obejmujące zmiany w akumulacji, strukturze, modyfikacji i interakcji białek. Monitorowanie tych zmian pozwala na identyfikację zjawisk, które mogą być przyczyną lub następstwem choroby. Szczególnie istotna w tym kontekście jest proteomika porównawcza, która polega na porównaniu uzyskanych profili peptydowo-białkowych prób pochodzących od różnych grup eksperymentalnych, a tym samym wskazaniu unikatowych zmian towarzyszących badanym stanom patologicznym. Najpowszechniejszą z metod stosowanych do tego celu jest niecelowana analiza proteomiczna typu „shotgun”, bazująca na MS.²⁹ W technice tej wszystkie białka obecne w badanych próbach poddaje się trawieniu enzymatycznemu, a uzyskaną mieszaninę peptydów rozdziela się z wykorzystaniem chromatografii ciekowej (*ang. liquid chromatography, LC*), sprzężonej z tandemowym spektrometrem mas (LC-MS/MS), stosując jonizację typu elektrorozpraszanie (*ang. electrospray ionization, ESI*). Wprowadzane do spektrometru jony peptydów są fragmentowane, a uzyskane widma fragmentacyjne są wykorzystywane do ustalenia sekwencji aminokwasowej badanych peptydów, a następnie białek.²⁹ Do oceny ilościowej białek stosuje się pomiar intensywności sygnału, wykorzystując metody ze znakowaniem białek/peptydów znacznikami izotopowymi lub izotopowymi bądź metodę bez znakowania (*ang. label-free*).³⁰ Pomimo dużej efektywności metod ze znakowaniem, ich stosowanie jest czasochłonne i kosztowne, a analiza uzyskanych wyników dość skomplikowana, dlatego dużą popularnością cieszy się metoda bez znakowania. W tej metodzie

konieczna jest analiza dużej liczby próbek, w celu zapewnienia wiarygodności uzyskanych wyników, a względne zmiany akumulacji peptydów/białek określa się poprzez porównanie intensywności sygnałów pomiędzy poszczególnymi analitami uzyskanymi w trybie MS.³⁰ Otrzymane w analizie LC-MS/MS widma masowe oraz chromatogramy przetwarza się w dedykowanych do tego celu programach (np. Proteome Discoverer, MaxQuant^{31,32}), które umożliwiają identyfikację i ocenę względnego poziomu akumulacji białek w próbce. Uzyskane dane należy poddać analizom statystycznym, w celu wytypowania białek różnicujących badane grupy eksperymentalne.³³ Za białko różnicujące powszechnie przyjmuje się białko zidentyfikowane przez co najmniej 2 unikalne peptydy i którego poziom akumulacji jest zmieniony w porównywanych grupach w sposób statystycznie istotny. Niezwykle ważna jest również tzw. krotność zmian (*ang. fold change, FC*) pomiędzy analizowanymi grupami eksperymentalnymi.³⁴ Wytypowaną listę białek różnicujących analizuje się, stosując narzędzia bioinformatyczne, np. PANTHER czy Ingenuity Pathway Analysis (IPA).³⁵ Wynikiem tych analiz jest informacja o funkcjach molekularnych, procesach oraz szlakach biologicznych, w które białka różnicujące są zaangażowane.³⁶ Otrzymane wyniki należy potwierdzić za pomocą alternatywnych technik laboratoryjnych. W tym celu wykorzystuje się metody immunoenzymatyczne, bazujące na specyficznych przeciwciałach (western blot lub ELISA), celowane analizy LC-MS/MS typu SRM lub MRM oraz weryfikację otrzymanych wyników na innych poziomach molekularnych, np. analizując poziomy mRNA badanych białek.

1.3.2. LIPIDOMIKA

Ogromna różnorodność związków lipidowych, występujących w materiale biologicznym powoduje, że scharakteryzowanie całego lipidomu w jednym podejściu jest niebywałym wyzwaniem, nie tylko ze względu na strukturalną różnorodność lipidów, ale również z uwagi na ogromną liczbę związków, występujących w bardzo niskich stężeniach. Lipidy stanowią element strukturalny błon komórkowych oraz pełnią rolę modulatorów aktywności białek i cząsteczek sygnałowych. Ze względu na pełnioną przez te molekuly funkcję, zrozumienie zmian pojawiających się w lipidomie może dopełnić obraz zaburzeń patologicznych w danym schorzeniu, ujawniony w proteomie. Stosując niecelowane analizy lipidów uzyskuje się dane o specyficznej jakościowej i ilościowej sygnaturze składu lipidowego badanego materiału biologicznego. Określenie profilu lipidowego wymaga zastosowania szeregu procedur przygotowania próbek oraz technik analitycznych.³⁷ Pierwszym etapem jest ekstrakcja, która powinna zapewniać odzysk większości lipidów lub grup związków lipidowych, których dotyczy analiza.³⁸⁻⁴¹ W niektórych przypadkach dodatkowo stosuje się frakcjonowanie, używając różnych technik separacji tj. chromatografii cienkwarstwowej, ekstrakcji do fazy stałej lub LC. Jedną z najistotniejszych metod identyfikacji lipidów jest spektrometria mas sprzężona z rozdziałem chromatograficznym, bądź bezpośrednia technika badawcza, w której próbki są wprowadzane do spektrometru z pominięciem separacji chromatograficznej (*ang. direct infusion, DI*), tzw. technika „shotgun lipidomics”.⁴² W tym podejściu analitycznym, identyfikacji dokonuje się w oparciu o dokładność pomiaru wartości stosunku m/z i obserwację charakterystycznych odejść cząsteczek obojętnych lub jonów fragmentacyjnych na widmach MSⁿ. Zaletą tej metody, w odniesieniu do technik łączonych LC-MS i GC-MS jest wysoka przepustowość, krótki czas zbierania danych i powtarzalność. Natomiast słabszą stroną tego podejścia jest zjawisko supresji jonów, które może prowadzić do rejestracji uboższego profilu lipidowego oraz utrudniona analiza związków izomerycznych, powszechnych wśród lipidów. Otrzymane, w wyniku analizy MS, dane są

przetwarzane z wykorzystaniem specjalistycznego oprogramowania (SimLipid, LipidXplorer⁴³ itp.) w celu identyfikacji molekuł oraz określenia względnego poziomu ich akumulacji. Uzyskane wyniki, podobnie jak w analizach proteomicznych, są analizowane statystycznie. Do weryfikacji wybranych wyników można wykorzystać metody celowane lub uzupełnić otrzymane wyniki o podejście metabolomiczne GC-MS, jako technikę pozwalającą na analizę kwasów tłuszczowych, steroli czy glicerolu. Lipidomika jest stosunkowo nową, ale szybko rozwijającą się gałęzią nauki, którą zainteresowanie wzrasta. Niestety, ze względu na niewielką dostępność narzędzi bioinformatycznych oraz wciąż ubogie w informacje bazy danych, możliwości przeprowadzenia funkcjonalnych analiz lipidów są bardzo ograniczone.

1.3.3. METABOLOMIKA

Metabolity są niskocząsteczkowymi związkami (<1500 Da), które biorą udział w przemianach metabolicznych i są zaangażowane we wszystkie funkcje żywego organizmu, regulując prawidłowe funkcjonowanie komórek, w tym m.in. wzrost, oddychanie, procesy translacyjne i transkrypcyjne. Wśród metabolitów można wyróżnić takie związki jak aminokwasy, lipidy, cukry, alkohole i nukleotydy. Ze względu na tak ogromną różnorodność związków chemicznych, wchodzących w skład metabolomu, bardzo trudno jest go oznaczyć przy wykorzystaniu jednej platformy metabolomicznej. Wachlarz metod wykorzystywanych do oceny jakościowej i ilościowej badanego metabolomu jest bardzo szeroki, natomiast jednymi z najczęściej stosowanych metod są podejścia LC-MS oraz GC-MS.⁴⁴ Pierwszym etapem procedury profilowania jest ekstrakcja metabolitów, której schemat postępowania zależy od badanego materiału biologicznego, rodzaju metabolitów, który chcemy badać i wybranego systemu analitycznego. Podejście LC-MS jest dedykowane do oznaczania niepolarnych i średniopolarnych metabolitów o wyższej masie cząsteczkowej, a przygotowanie próbek wymaga etapu deproteinizacji oraz ekstrakcji metabolitów z wykorzystaniem organicznych rozpuszczalników.⁴⁴ Analiza GC-MS wymaga bardziej skomplikowanej procedury przygotowania prób dla związków nielotnych i obejmuje, oprócz deproteinizacji również derywatyzację przeprowadzaną w celu zwiększenia lotności i stabilności termicznej metabolitów, co wpływa na poprawę rozdzielczości chromatograficznej i selektywności oznaczeń.⁴⁵ Taka procedura poszerza spektrum analizowanych cząsteczek, umożliwiając oznaczenie zarówno tłuszczów i estrów o niskiej polarności, a także metabolitów o wysokiej polarności, aminokwasów, kwasów organicznych oraz cukrów. Uzyskane w analizach metabolomicznych złożone zbiory danych poddawane są wstępnemu przetwarzaniu, w tym redukcji szumów oraz dekonwolucji.⁴⁶ Kolejnym etapem procesu analizy danych jest identyfikacja metabolitów poprzez porównanie uzyskanych widm, czasów retencji oraz wzorów fragmentacji z biblioteką, następnie określana jest akumulacja zidentyfikowanych związków oraz przeprowadzane są analizy statystyczne. Do weryfikacji otrzymanych rezultatów można wykorzystać analizy celowane przy użyciu standardów wewnętrznych w porównaniu z krzywymi wzorcowymi. Niestety metabolomiczne bazy danych nie są w pełni kompletne, co utrudnia wnioskowanie. Chociaż prace nad rozszerzeniem baz danych metabolitów oraz ich funkcjonalnością ciągle trwają, napotykaną są problemy z identyfikacją wielu związków. Niemniej jednak, metabolomika jest bardzo ważną dziedziną, która wraz z pozostałymi naukami „-omicznymi” może dostarczyć cennych informacji, pozwalających w możliwie pełny sposób zrozumieć patomechanizmy rozwoju różnych chorób.

CEL PRACY

Celem badań podjętych w ramach niniejszej rozprawy doktorskiej było pogłębienie wiedzy na temat podstaw molekularnych rozwoju miażdżycy w CKD z wykorzystaniem wysokoprzepustowych analiz proteomicznych, metabolomicznych i lipidomicznych wybranych składników krwi. Moje szczególne zainteresowanie skupiało się na określeniu szlaków i sieci sygnałowych, które różnicują inicjację i progresję miażdżycy związanej z CKD w porównaniu do klasycznej CVD, a tym samym wytypowanie zaburzeń zaangażowanych w rozwój CKD-A.

Cele szczegółowe pracy doktorskiej:

Cel 1. Scharakteryzowanie profilu białkowego leukocytów, pochodzących od pacjentów w różnych stadiach CKD, CVD oraz grupy HV.

Cel 2. Scharakteryzowanie lipidomu i metabolomu osocza pacjentów w różnych stadiach CKD, CVD i grupy HV.

Cel 3. Walidacja wyników uzyskanych podczas realizacji celu 1 i 2 na różnych poziomach „omicznych”.

Cel 4. Identyfikacja szlaków i sieci sygnałowych związanych z rozwojem i progresją CKD-A.

Osiągnięcie wyżej wymienionych celów wymagało realizacji następujących zadań:

1. Dokonania przeglądu danych literaturowych dotyczących stanu wiedzy na temat potencjalnych mechanizmów progresji miażdżycy w CKD i wykorzystania w ich badaniu metod „omicznych”.
2. Zebrania próbek od 300 osób i izolacji osocza oraz całkowitej frakcji leukocytów z krwi obwodowej pacjentów w różnych stadiach CKD, CVD, a także grupy HV.
3. Oceny jakościowej uzyskanego materiału komórkowego z wykorzystaniem mikroskopii konfokalnej oraz cytometrii przepływowej, wraz z oceną odsetka komórek podlegających apoptozie.
4. Przeprowadzenia analizy proteomicznej leukocytów z wykorzystaniem metody nano-LC-MS/MS.
5. Przeprowadzenia analizy lipidomicznej osocza z wykorzystaniem wysokoprzepustowej techniki MS.
6. Przeprowadzenia analizy metabolomicznej uzyskanego osocza z użyciem metody GC-MS.
7. Zdefiniowania różnic jakościowych i ilościowych w proteomie frakcji leukocytów oraz w lipidomie i metabolomie osocza pomiędzy pacjentami różniącymi się progresją CKD i CVD.
8. Szczegółowego zweryfikowania otrzymanych rezultatów na poziomie białek, mRNA oraz niskocząsteczkowych metabolitów.
9. Przeprowadzenia funkcjonalnych analiz bioinformatycznych w celu wytypowania szlaków i sieci sygnałowych zaangażowanych w patogenezę miażdżycy u pacjentów z CKD i CVD.

MATERIAŁ I METODY BADAWCZE

Material do badań stanowiła krew obwodowa, pochodząca od 45 zdrowych ochotników oraz 255 pacjentów zakwalifikowanych do 4 grup badawczych w zależności od stopnia zaawansowania choroby sercowo-naczyniowej i miażdżycy oraz dysfunkcji nerek. Kwalifikacja pacjentów do poszczególnych grup badawczych prowadzona była przez wykwalifikowanych klinicystów na podstawie specjalistycznych, biochemicznych i obrazowych badań, historii choroby oraz zgodnie z wytycznymi NICE¹ i KDIGO³. Pacjentów z CKD podzielono na dwie grupy badawcze: CKD1-2, pacjenci w początkowym stadium CKD z wczesną postacią miażdżycy oraz CKD5, hemodializowani pacjenci w schyłkowym stadium CKD z zaawansowanymi symptomami miażdżycy. Pacjentów z klasyczną chorobą sercowo-naczyniową, CVD, również podzielono na dwie grupy: CVD1, pacjenci w początkowym stadium oraz CVD2, pacjenci z zaawansowaną postacią choroby sercowo-naczyniowej i miażdżycy. Obie grupy CVD nie wykazywały żadnych dysfunkcji nerek. Kryterium wykluczania pacjentów obejmowało cukrzycę, chorobę nowotworową oraz aktywną infekcję. Materiał badawczy został zebrany dzięki współpracy z dr n. med. Katarzyną Kostką-Jeziorny z Kliniki Hipertensjologii, Angiologii i Chorób Wewnętrznych i prof. dr hab. n. med. Bartłomiejem Perkiem z Kliniki Kardiochirurgii, Szpitala Klinicznego Przemienienia Pańskiego Uniwersytetu Medycznego w Poznaniu, oraz dr n. med. Aliną Podkowińską ze stacji dializ Dravis sp. z o.o. Z otrzymanej krwi obwodowej wyizolowano osocze oraz całkowitą frakcję leukocytów. Podczas realizacji niniejszej rozprawy doktorskiej jako podstawową technikę analityczną stosowano spektrometrię mas sprzężoną z techniką chromatografii ciekowej, gazowej lub ze zintegrowaną platformą TriVersa NanoMate (Advion BioSciences, Ltd., Ithaca, NY, USA) do przeprowadzenia odpowiednio analizy proteomicznej, metabolomicznej i lipidomicznej.

3.1. ANALIZA PROTEOMICZNA

Analizę proteomiczną zastosowano do badania zmian proteomu całkowitej frakcji leukocytów. Zebrany materiał komórkowy poddano lizie i przeprowadzono enzymatyczne trawienie białek. Otrzymaną mieszaninę peptydów analizowano z wykorzystaniem podejścia bezznacznikowego „*label-free*” i systemu nano-LC-MS/MS złożonego z wysokorozdzielczego spektrometru Q-Exactive z analizatorem typu Orbitrap (Thermo Fisher Scientific, Niemcy) sprzężonego z nanochromatografem ciekowym Dionex 3000 (Thermo Fisher Scientific, Niemcy). Otrzymane widma masowe i chromatogramy analizowano z użyciem oprogramowania MaxQuant i Proteome Discoverer w celu przeprowadzenia identyfikacji i określenia akumulacji białek. Uzyskane dane poddano analizom statystycznym, w tym zastosowano test Chi kwadrat dla zmiennych nominalnych, test Shapiro-Wilk’a do sprawdzenia rozkładu normalnego zmiennych ilościowych oraz test Levene’a do określenia jednorodności wariancji. Wyniki zgodne z rozkładem normalnym i wykazujące jednorodność wariancji analizowano, wykorzystując testy parametryczne: analizę wariancji (ANOVA) wykorzystano do porównania więcej niż dwóch grup, natomiast test t-Studenta dla porównania pomiędzy dwoma grupami. Dane, które nie spełniały założeń rozkładu normalnego analizowano odpowiednio testem Kruskal’a-Wallis’a i Mann’a-Whitney’a. Dodatkowo określono miary wielkości efektu zgodnie

z formułą g Hedgesa. Za białko różnicujące uznano białka zidentyfikowane z wykorzystaniem co najmniej 2 unikalnych peptydów, które różniły się poziomem akumulacji o co najmniej 40% z zachowaniem istotności statystycznej <0.05 , i wykazywały współczynnik wielkości efektu wyższy niż 0.5. Do badań wykorzystano również analizy korelacyjne Pearson'a i Spearman'a. Białka różnicujące poddano bioinformatycznym analizom funkcjonalnym w oprogramowaniu Perseus i Ingenuity Pathway Analysis (IPA) do identyfikacji nadreprezentowanych szlaków sygnałowych, funkcji biologicznych, zaburzeń chorobowych oraz do określenia cząsteczek regulujących procesy, w które zaangażowane są identyfikowane białka różnicujące. Kierunkowość obserwowanych zmian określono wykorzystując algorytm IPA z-score, przewidując inhibicję przy wartościach $<- 2$ oraz aktywację przy wartościach >2 . Weryfikację otrzymanych w analizie proteomicznej wyników przeprowadzono, stosując następujące techniki: ilościowa analiza PCR techniką emulsyjną, *ddPCR*; MRM i techniki immunoenzymatyczne (ELISA i western blot). Ponadto, ocenę morfologii, żywotności oraz odsetka apoptotycznych i nekrotycznych komórek wykonano z użyciem cytometrii przepływowej i mikroskopii konfokalnej, dzięki współpracy z dr Agnieszką Fedoruk–Wyszomirską oraz dr Dorotą Gurdą z Pracowni Analiz Struktur Subkomórkowych IChB PAN kierowanej przez prof. dr hab. Elżbę Wyszko.

3.2. ANALIZA LIPIDOMICZNA

Ekstrakcję lipidów wykonano z użyciem eteru tert-butyloowo-metylowego, MTBE.³⁸ Do zbadania zmian na poziomie lipidomu osocza wykorzystano podejście *shotgun*, stosując spektrometr Q-Exactive Orbitrap (Thermo Fisher Scientific, Niemcy) sprzężony ze zrobotyzowanym źródłem jonów typu nanoESI TriVersa NanoMate (Advion BioSciences Ltd.). Do identyfikacji poszczególnych lipidów wykorzystano oprogramowanie LipidXplorer. Lipidy identyfikowano na podstawie wartości m/z odczytanych z widm masowych uzyskanych podczas analiz MS w trybie jonów dodatnich. Na podstawie intensywności sygnałów określano natomiast ich względny poziom akumulacji. Analizę porównawczą zarówno lipidów jak i ich klas przeprowadzono, stosując szereg analiz statystycznych, m.in. U-Mann-Whitney'a, t-Studenta oraz ANOVA i Kruskal-Wallis'a, a także nadzorowaną oraz nienadzorowaną analizę PCA. Listę różnicujących lipidów i klas lipidów wytypowano, stosując następujące założenia: wartość statystyczna $p < 0.05$ oraz $FC \geq 1.5$. Funkcjonalne analizy bioinformatyczne wykonano, wykorzystując narzędzie LION⁴⁷.

3.3. ANALIZA METABOLOMICZNA

Analizę metabolomu przeprowadzono na osoczu, wykorzystując technikę GC-MS (TRACE 1310 GC, TSQ8000 MS). Próbki przygotowywano poprzez deproteinizację oraz derywatyzację. Przeprowadzono profilowanie metabolomiczne osocza, jednakże w dalszej części skupiono się na analizie komponentów i prekursorów lipidów: kwasów tłuszczowych, cholesterolu i glicerolu. Akumulację poszczególnych analitów oceniano poprzez wykreślenie pola powierzchni pików jonów o wartości m/z oraz czasie retencji, ustalonych na podstawie danych literaturowych. Uzyskane dane normalizowano do całkowitego prądu jonowego, a uzyskane wyniki analizowano statystycznie, stosując m.in. testy U-Mann-Whitney'a, t-Studenta, ANOVA i Kruskal-Wallis'a oraz analizy korelacyjne.

SKRÓTOWE OMÓWIENIE PUBLIKACJI, BĘDĄCYCH WYNIKIEM PRACY DOKTORSKIEJ

4.1. APPLYING PROTEOMICS AND INTEGRATIVE „OMICS” STRATEGIES TO DECIPHER THE CHRONIC KIDNEY DISEASE-RELATED ATHEROSCLEROSIS

Tracz J., Luczak M.

International Journal of Molecular Sciences. 2021, 22, 7492.

<https://doi.org/10.3390/ijms22147492>

W niniejszym artykule przeglądowym podsumowałam dostępną w piśmiennictwie naukowym wiedzę na temat mechanizmów molekularnych zaangażowanych w rozwój CKD-A. Szczególną uwagę zwróciłam na te badania, w których zastosowano wysokoprzepustowe analizy „omiczne”, uzupełnione o funkcjonalne analizy bioinformatyczne, a uzyskane wyniki zweryfikowano alternatywnymi technikami. Praca przeglądowa w pierwszej części przedstawia zwięzły opis schorzenia oraz podstawy teoretyczne wysokoprzepustowych strategii proteomicznych wykorzystywanych w badaniach biomedycznych. Główną część pracy stanowi analiza dotychczasowych doniesień, opisujących patogenne procesy uczestniczące w rozwoju CKD-A i została ona podzielona na 4 podrozdziały. Pierwszy podrozdział opisuje zaburzenia związane z metabolizmem lipidów, drugi przedstawia zmiany związane ze zwapnieniem naczyń, natomiast trzeci prezentuje mechanizmy związane z rozwojem stanu zapalnego i dysfunkcji śródbłonna. Podrozdział czwarty przedstawia możliwości wielowymiarowej strategii multiomicznej jako przyszłościowego podejścia w poszerzaniu wiedzy na temat procesów leżących u podstaw szybko postępującej miażdżycy w CKD. W pracy zasugerowałam, że w kontekście obecnego stanu naszej wiedzy, stosowanie wielowymiarowych analiz „omicznych” skorelowanych z funkcjonalnymi analizami bioinformatycznymi może być bardziej przydatne do badania mechanizmów leżących u podstaw procesów patologicznych niż do poszukiwania diagnostycznych biomarkerów, które wciąż wzbudzają wiele kontrowersji. Podkreśliłam również, że tylko porównanie chorych z CKD i CVD, w jednym badaniu, może dostarczyć cennych informacji na temat progresji miażdżycy w CKD-A.

4.2. PROTEOMIC PROFILING OF LEUKOCYTES REVEALS DYSREGULATION OF ADHESION AND INTEGRIN PROTEINS IN CHRONIC KIDNEY DISEASE-RELATED ATHEROSCLEROSIS

Tracz J., Handschuh L., Lalowski M., Marczak Ł., Kostka-Jeziorny K., Perek B., Wanic-Kossowska M., Podkowińska A., Tykarski A., Formanowicz D., Luczak M.

Journal of Proteome Research. 2021, 20, 6, 3053-3067.

<https://doi.org/10.1021/acs.jproteome.0c00883>

W niniejszej publikacji skupiłam się na porównawczej analizie proteomu całkowitej frakcji leukocytów, wyizolowanej od pacjentów z CKD-A i CVD oraz HV. Kierunek badań został wyznaczony przez wcześniejsze rezultaty otrzymane przez zespół, w którym realizowałam swoją rozprawę doktorską. Przeprowadzone uprzednio w zespole, porównawcze analizy proteomiczne osocza pacjentów z różnym stopniem zaawansowania CKD i CVD, wykazały kilkakrotnie wyższy poziom akumulacji białek ostrej fazy oraz białek związanych z procesami zapalnymi w grupie z zaawansowaną CKD w porównaniu do CVD.^{48,49} Również w pracach innych zespołów, analizujących niezależnie grupy pacjentów z CKD lub CVD, wykazano podwyższony poziom akumulacji białek zapalnych oraz sugerowano, że obie jednostki chorobowe są ściśle związane z systemicznym stanem zapalnym.^{50,51} Jednak badania naszego zespołu sugerowały, że procesy zapalne mogą odgrywać dużo istotniejszą rolę w progresji miażdżycy związanej z CKD. Ponieważ to leukocyty uczestniczą w procesach prozapalnych podczas inicjacji i progresji miażdżycy, założyłam, że porównawcza analiza proteomiczna tej frakcji komórek może dostarczyć cennych i unikatowych informacji na temat mechanizmów przyspieszonego rozwoju CKD-A oraz procesów, które temu towarzyszą.

Przeprowadzona analiza proteomiczna wykazała, że największe różnice w profilach białkowych wykazują dwie grupy pacjentów o podobnych, zaawansowanych symptomach miażdżycy, ale różniących się funkcjonowaniem nerek grupa CKD5 (pacjenci hemodializowani) oraz CVD2 (prawidłowa funkcja nerek). Co więcej, grupy z początkowymi symptomami miażdżycy – CKD1-2 (wczesne objawy dysfunkcji nerek) oraz CVD1 (brak dysfunkcji nerek) wykazały duże podobieństwo w profilu proteomicznym, co jest zgodne z wcześniejszymi doniesieniami zespołu.^{49,52} Zidentyfikowane białka różnicujące poddałam analizom bioinformatycznym, które wskazały, że grupy CKD5 oraz CVD2 różnią się istotnie profilami białek, uczestniczącymi w aktywacji i adhezji leukocytów do śródbłonka (Rycina 1 i 2 w artykule). Obserwowane poziomy akumulacji białek zaangażowanych w te procesy sugerowały ich aktywację w CKD-A w porównaniu z CVD. Jednakże, w przypadku innych procesów, również związanych z diapedezą leukocytów, takich jak wynacznienie leukocytów czy szlak sygnałowy aktywny, przeprowadzona analiza nie ujawniła kierunku obserwowanych zmian, pomimo wysokiej istotności statystycznej obserwowanych zmian w akumulacji poszczególnych białek. Aby przyjrzeć się bliżej temu zjawisku zbadalam poziom wybranych białek, zarówno tych zidentyfikowanych w niecelowanej analizie, jak i wybranych na podstawie przeglądu literatury naukowej, jako uczestniczących we wskazanych szlakach. W tym celu wykorzystałam analizy celowane oparte o technikę ELISA, MRM i WB. Zbadalam również poziom niektórych transkryptów metodą ddPCR. Wykonane analizy walidacyjne częściowo potwierdziły wcześniejsze rezultaty (Rycina 3 w artykule). Po przeanalizowaniu otrzymanych wyników ustaliliśmy, że poziom akumulacji większości białek zaangażowanych we wczesny etap diapedezy, czyli aktywacji i wychwytu leukocytów

oraz ich toczenia się na powierzchni komórek śródbłonka naczyń krwionośnych, jest podwyższony w grupie CKD5 w porównaniu do CVD2 (Rycina 4 w artykule). Odwrotną sytuację zauważyliśmy w przypadku białek zaangażowanych w późną fazę transmigracji leukocytów, związaną z polaryzacją cytoszkieletu aktynowego, dla których poziom akumulacji białek był wyraźnie obniżony (Rycina 4 w artykule). Na tej podstawie zasugerowaliśmy, że w zaawansowanym stadium CKD może dochodzić do zaburzenia procesu transmigracji leukocytów. Z jednej strony możemy mieć do czynienia z ich aktywacją i nagromadzeniem na powierzchni śródbłonka poprzez mechanizm związany z integrzynami, a z drugiej, z obniżeniem ich zdolności do reorganizacji cytoszkieletu niezbędnej do ukończenia procesu transmigracji. W tej sytuacji może dochodzić do zaburzenia funkcji śródbłonka oraz akceleracji procesu tworzenia blaszek miażdżycowych. Co ciekawe, w grupie CKD5 w porównaniu do CVD2, zaobserwowałam również aktywację procesów związanych ze śmiercią komórki. Wyniki te zostały potwierdzone z wykorzystaniem cytometrii przepływowej oraz mikroskopii konfokalnej, które wykazały istotnie zwiększony odsetek komórek, będących w trakcie procesu apoptozy w grupie CKD5 w porównaniu do CVD2. Co więcej, przeprowadzone analizy korelacyjne ujawniły, że wiele białek zaangażowanych w apoptozę wykazuje pozytywną korelację z grupą białek zaangażowanych w adhezję i migrację komórek. Na podstawie tych wyników zasugerowałam powiązanie procesów programowanej śmierci komórki z zaburzeniami transmigracji leukocytów. W kolejnym etapie pracy postanowiłam sprawdzić, które cząsteczki mogą być odpowiedzialne za regulację zaburzonych procesów. Zidentyfikowałam TGFB1 jako najbardziej prawdopodobny regulator odpowiedzialny za kontrolę diapedezy komórek, ale również procesów apoptozy i nekrozy.

Podsumowując, w niniejszym artykule po raz pierwszy scharakteryzowałam proteom leukocytów pacjentów z CKD-A i wykazałam deregulację białek zaangażowanych w różne fazy transmigracji leukocytów. Nowym odkryciem była również identyfikacja białek zaangażowanych w apoptotyczną śmierć komórki, wykazujących podwyższony poziom akumulacji w CKD-A. Te wyniki zostały funkcjonalnie potwierdzone na poziomie komórkowym. Wysunęliśmy hipotezę, że rozregulowanie różnych etapów diapedezy może prowadzić do zmian w integralności komórkowej i powodować śmierć komórki. Wyniki te wskazują na nowe zaburzenia, pojawiające się w progresji CKD-A i sugerują dalszy kierunek badań.

4.3. MASS-SPECTROMETRY-BASED LIPIDOMICS REVEALS DIFFERENTIAL CHANGES IN THE ACCUMULATED LIPID CLASSES IN CHRONIC KIDNEY DISEASE

Marczak L., Idkowiak J., **Tracz J.**, Stobiecki M., Perek B., Kostka-Jeziorny K., Tykarski A., Wanic-Kossowska M., Borowski M., Osuch M., Formanowicz D., Luczak M.

Metabolites 2021, 11, 275.

<https://doi.org/10.3390/metabo11050275>

Podwyższony poziom cholesterolu i związany z tym wzrost stężenia frakcji LDL są kluczowe w rozwoju zmian miażdżycowych i w konsekwencji komplikacji sercowo-naczyniowych.⁵³ Pomimo tego, u pacjentów z CKD często obserwuje się „odwrotną epidemiologię”, czyli niskie stężenie cholesterolu całkowitego i frakcji HDL oraz normalne lub wręcz niskie stężenie frakcji LDL skorelowane z wysokim ryzykiem rozwoju miażdżycy.^{11,54,55} Poprzednie badania zespołu, w którym realizowałam pracę doktorską ujawniły znaczące zmiany w poziomie białek osocza zaangażowanych w metabolizm i transport lipidów, w tym lipidów budujących cząsteczki lipoproteinowe HDL i LDL.⁵⁶

Dlatego w niniejszej pracy postanowiliśmy przyjrzeć się zmianom w akumulacji poszczególnych lipidów osocza w CKD oraz CVD. Według mojej wiedzy, prezentowana w pracy porównawcza analiza lipidomu osocza u pacjentów z klasyczną CVD oraz CKD-A stanowi pierwsze tego typu dostępne opracowanie.

Otrzymane w analizie profile lipidów wyraźnie różniły obie grupy CKD (CKD1-2 i CKD5) od grup CVD2 i HV, sugerując unikalny profil lipidomiczny związany z dysfunkcją nerek. Porównując grupy CKD5 oraz CVD2, czyli grupy o podobnym stopniu zaawansowania miażdżycy, ale różniące się funkcją nerek, zidentyfikowaliśmy wzrost poziomu triacylogliceroli (TAG) w CKD5 oraz obniżenie poziomu cholesterolu i jego estrów (CE), fosfatydylocholin, ceramidów, fosfatydyloetanoloamin i sfingomielin w porównaniu do grupy CVD2 (Rycina 2 w artykule). Dodatkowo, zmiany w poziomie CE były pozytywnie skorelowane z poziomem białka CRP oraz współczynnikiem eGFR, co zasugerowało związek z progresją dysfunkcji nerek i potwierdzało sugerowaną w literaturze „odwroconą epidemiologię”. Unikalny profil wykazaliśmy również dla poszczególnych lipidów osocza w CKD i CVD, a uzyskane wyniki nie tylko wskazywały na różne mechanizmy dyslipidemii w CKD-A i klasycznej CVD, ale również wzmocniły naszą hipotezę, że mechanizm progresji miażdżycy może być odmienny w początkowych i schyłkowych stadiach CKD.

W ramach tej pracy przeprowadziliśmy również profilowanie metabolitów, wykorzystując analizę niecelowaną opartą na GC-MS, obejmującą identyfikację i relatywną ocenę ilościową związków niskocząsteczkowych, takich jak aminokwasy, kwasy tłuszczowe, cukry, czy też alkohole alifatyczne. W wyniku tych badań wygenerowane zostały złożone zbiory danych, zawierające tysiące rejestrowanych sygnałów. Jednak w niniejszej pracy skupiono się jedynie na wybranych sygnałach, pochodzących od powszechnych prekursorów lub komponentów lipidów, pozostałe wyniki pozostają w opracowaniu. W szczególności zależało nam na oznaczeniu poziomu akumulacji kwasów tłuszczowych i glicerolu, komponentach budujących cząsteczki TAG, jak również lipoprotein LDL i HDL. Podwyższenie poziomu akumulacji wszystkich zidentyfikowanych TAG w obu grupach CKD, nie było dla nas zaskoczeniem, ponieważ podobne zmiany ujawniły standardowe badania surowicy przeprowadzone w szpitalnych klinikach. Jednak chcieliśmy się nieco bliżej przyjrzeć tym wynikom. Ponadto, analizy GC-MS wykorzystaliśmy do dodatkowej weryfikacji poziomu cholesterolu w badanych próbkach. Brak dobrze wystandaryzowanych badań walidacyjnych, stanowi bowiem wciąż słabą stronę badań lipidomicznych.

Zidentyfikowałam 7 różnych kwasów tłuszczowych (Rycina 7 w artykule), których poziom był wyraźnie obniżony w grupie z zaawansowaną CKD w porównaniu do CVD, co było zaskakujące biorąc pod uwagę podwyższony poziom TAG w CKD5 wykazany w standardowych analizach laboratoryjnych, jak i lipidomicznych. Z drugiej strony, poziom glicerolu był najwyższy w CKD5 w porównaniu do wszystkich pozostałych grup. Dodatkowo wykazaliśmy, że zmiany te silnie korelują z progresją dysfunkcji nerek i stanem zapalnym. Tak unikatowy obraz dyslipidemii może sugerować, że standardowe testy laboratoryjne profilu lipidowego mogą być niewystarczające do właściwej oceny ryzyka rozwoju CVD w przypadku pacjentów z CKD. Przeprowadzone analizy pozwoliły również na potwierdzenie obniżonej akumulacji cholesterolu w grupie CKD5, i tym samym walidację wyników uzyskanych innymi technikami. Uprzednie badania zespołu sugerowały, że skład białkowy lipoprotein HDL i LDL może wykazywać różnice pomiędzy CVD i CKD.⁵⁶ Wyniki prezentowane w niniejszej pracy wyraźnie sugerują, że podobne zmiany mogą również dotyczyć komponentu lipidowego, a z pewnością umacniają naszą wcześniejszą hipotezę, że mechanizm molekularny akceleracji miażdżycy w CKD-A może być inny w porównaniu do miażdżycy niezwiązanej z dysfunkcją nerek.

W pracy podjęliśmy również próby analizy funkcjonalnej uzyskanych wyników, co nie było łatwe ze względu na wciąż ubogą dostępność do narzędzi bioinformatycznych do analizy wyników lipidomicznych. Wykorzystaliśmy w tym celu oprogramowanie LION, a uzyskane wyniki sugerowały, że główną funkcją lipidów, biorących udział w progresji CKD może być magazynowanie lipidów

i tworzenie kropelek lipidowych, związane z cząsteczkami TAG, DAG, ale także różnych fosfolipidów (Rycina 5 w artykule).

Podsumowując, scharakteryzowaliśmy unikalny profil lipidomiczny u pacjentów z CKD-A i CVD w bezpośrednim porównaniu, co do tej pory nie zostało przedstawione. Wykazaliśmy zróżnicowany poziom akumulacji wielu lipidów oraz kwasów tłuszczowych w obu schorzeniach, sugerując różne mechanizmy dyslipidemii w miażdżycy klasycznej oraz związanej z CKD. Ponadto, zasugerowaliśmy, że na właściwości pro-aterogenne lipidów i lipoprotein mogą wpływać zaburzenia, wynikające z procesów syntezy lipidów, a nie bezpośrednio z poziomu ich akumulacji.

INNE PUBLIKACJE, NIEWCHODZĄCE W SKŁAD ROZPRAWY DOKTORSKIEJ

Oprócz prac, wchodzących w skład rozprawy doktorskiej, jestem współautorem 4 innych prac eksperymentalnych.⁵⁷⁻⁶⁰ Prace te nie stanowiły głównego wątku mojej pracy doktorskiej, ale pozwoliły poszerzyć moją wiedzę w dziedzinie spektrometrii mas i proteomiki oraz rozwinąć, a następnie udoskonalić mój warsztat metodologiczny. Pierwsza z prac⁵⁷ jest rezultatem badań, które prowadziłam w ramach pracy magisterskiej wykonanej we współpracy z zespołem prof. dr hab. inż. Ewy Kaczorek z Zakładu Chemii Organicznej, Politechniki Poznańskiej oraz Instytutu Chemii Bioorganicznej PAN w Poznaniu. Podczas jej realizacji oceniałam wpływ pochodnych benzenu na zmiany we właściwościach powierzchniowych oraz profilu białek membranowych i cytozolowych szczepu bakteryjnego *Raoutella ornithinolytica*. Kolejna z prac, w której jestem współautorem, przedstawia pionierskie podejście znakowania peptydów z wykorzystaniem znaczników izobarycznych opartych na solach pyryliowych.⁵⁹ Opracowana technika ma potencjalne zastosowanie do analizy przesiewowej próbek biologicznych, w miejsce dostępnych na rynku standardowych, ale kosztownych technik typu iTRAQ czy TMT. Pracę realizowano we współpracy z Zespołem Chemii i Stereochemii Peptydów i Białek, Uniwersytetu Wrocławskiego kierowanym przez prof. dr hab. Zbigniewa Szewczuka. Moim wkładem w tę pracę była optymalizacja i przeprowadzenie procedury przygotowania próbek biologicznych do znakowania. Dwie kolejne prace koncentrowały się na poszukiwaniach biomarkerów oraz zaburzeń, towarzyszących rozwojowi niealkoholowej stłuszczeniowej choroby wątroby wśród dzieci i powstały w wyniku współpracy z zespołem prof. dr hab. n. med. Magdaleny Figlerowicz z Kliniki Chorób Zakaźnych i Neurologii Dziecięcej Uniwersytetu Medycznego w Poznaniu.^{58,60} W pracy byłam odpowiedzialna za optymalizację oraz przeprowadzenie porównawczej analizy proteomicznej osocza z wykorzystaniem techniki spektrometrii mas nano-LC-MS/MS, a następnie analizę uzyskanych wyników.

WNIOSKI

Proteomika, metabolomika oraz lipidomika są podejściami badawczymi, pozwalającymi na wskazanie w ujęciu całościowym procesów i szlaków biologicznych, towarzyszących badanym schorzeniom. Te podejścia wprowadzają nowe możliwości lepszego zrozumienia patogenezы chorób poprzez rozszyfrowywanie wzajemnych złożoności i powiązań pomiędzy badanymi molekułami oraz procesami, w które są one zaangażowane, co często prowadzi do formułowania nowych hipotez badawczych. Wdrażanie wysokoprzepustowych analiz opartych o technikę MS do badań biomedycznych dostarcza unikatowych wyników w badaniach podstawowych oraz dąży do zastosowania uzyskanej wiedzy w praktyce klinicznej. Wykorzystane w pracy strategie: proteomiczna, metabolomiczna i lipidomiczna pozwoliły na wyciągnięcie następujących wniosków:

1. Obraz zaburzeń w postaci zmienionej akumulacji białek, metabolitów oraz lipidów w CKD-A potwierdza, że patomechanizm obserwowanych zmian może być podobny w początkowych stadiach CKD-A i CVD. Jednak w zaawansowanym stadium CKD-A mechanizm molekularny progresji choroby sercowo-naczyniowej wydaje się odmienny w porównaniu do klasycznej CVD. Co więcej, tylko część z obserwowanych zmian skorelowana była z progresją dysfunkcji nerek, co może sugerować, że są one raczej specyficznie związane z rozwojem samej choroby sercowo-naczyniowej.
2. Deregulacja białek zaangażowanych w różne etapy procesu diapedezy leukocytów może działać prozapalnie na mikrośrodowisko, a tym samym nasilać dysfunkcję śródbłonna i produkcję czynników prozapalnych m.in. TGFβ1, który promuje zwłóknienie i zwapnienie naczyń w CKD-A. W konsekwencji obserwujemy wzmożenie procesu programowanej śmierci komórki silnie skorelowane ze zmianami na poziomie molekuł adhezyjnych, nasilenie systemicznego stanu zapalnego i progresję zmian miażdżycowych w zaawansowanych stadiach CKD-A.
3. Właściwości pro-aterogenne lipidów i lipoprotein w CKD-A, wynikają raczej z zaburzeń procesów ich syntezy, a w konsekwencji zmiany ich składu lub struktury, a nie bezpośrednio z zaburzeń w stężeniu. Z tego względu standardowe badania biomedyczne profilu lipidowego mogą być niewystarczające w ocenie predyspozycji do akceleracji zmian miażdżycowych u pacjentów z CKD.
4. Zademonstrowany unikalny profil lipidomiczny dla CKD-A nie tylko potwierdza postulowaną w literaturze naukowej teorię „odwróconej epidemiologii” w CKD, ale zwraca również uwagę na ścisły związek ze stanem zapalnym.
5. Uzyskane wyniki pozwalają wyznaczyć kierunki przyszłych badań, które powinny dotyczyć funkcjonalnych i mechanistycznych analiz procesów adhezji i migracji leukocytów oraz dogłębnej analizy „omicznej” poszczególnych subpopulacji leukocytów, w tym monocytów i limfocytów T, które są komórkami szczególnie istotnymi podczas rozwoju miażdżycy. Również analizy poziomu cytokin w CVD i CKD powinny uzupełnić obraz udziału stanu zapalnego w progresji CKD-A.

BIBLIOGRAFIA

1. NICE Clinical Guidelines. Chronic Kidney Disease: Early Identification and Management of Chronic Kidney Disease in Adults in Primary and Secondary Care. *Natl Clin Guidel Centre*. 2014;182:113–120.
2. Webster AC, Nagler E V, Morton RL, Masson P. Chronic Kidney Disease. *Lancet*. 2017;389(10075):1238-1252. doi:10.1016/S0140-6736(16)32064-5
3. Levin A, Stevens PE, Bilous RW, et al. Kidney disease: Improving global outcomes (KDIGO) CKD work group. KDIGO 2012 clinical practice guideline for the evaluation and management of chronic kidney disease. *Kidney Int Suppl*. 2013;3(1):1-150. doi:10.1038/kisup.2012.73
4. Thomas R, Kanso A, Sedor JR. Chronic kidney disease and its complications. *Prim Care*. 2008;35(2):329-344. doi:10.1016/j.pop.2008.01.008
5. Vallianou NG, Mitesh S, Gkogkou A, Geladari E. Chronic Kidney Disease and Cardiovascular Disease: Is there Any Relationship? *Curr Cardiol Rev*. 2019;15(1):55-63. doi:10.2174/1573403X14666180711124825
6. Schiffrin EL, Lipman ML, Mann JFE. Chronic kidney disease: effects on the cardiovascular system. *Circulation*. 2007;116(1):85-97. doi:10.1161/CIRCULATIONAHA.106.678342
7. Frostegård J. Immunity, atherosclerosis and cardiovascular disease. *BMC Med*. 2013;11:117. doi:10.1186/1741-7015-11-117
8. Drüeke TB, Massy ZA. Atherosclerosis in CKD: Differences from the general population. *Nat Rev Nephrol*. 2010;6(12):723-735. doi:10.1038/nrneph.2010.143
9. Weiner DE, Tighiouart H, Elsayed EF, et al. The relationship between nontraditional risk factors and outcomes in individuals with stage 3 to 4 CKD. *Am J Kidney Dis*. 2008;51(2):212-223. doi:10.1053/j.ajkd.2007.10.035
10. Chen J, Mohler ER, Xie D, et al. Traditional and non-traditional risk factors for incident peripheral arterial disease among patients with chronic kidney disease. *Nephrol Dial Transplant*. 2016;31(7):1145-1151. doi:10.1093/ndt/gfv418
11. Kalantar-Zadeh K, Block G, Humphreys MH, Kopple JD. Reverse epidemiology of cardiovascular risk factors in maintenance dialysis patients. *Kidney Int*. 2003;63(3):793-808. doi:10.1046/j.1523-1755.2003.00803.x
12. Tonelli M, Muntner P, Lloyd A, et al. Association between LDL-C and Risk of Myocardial Infarction in CKD. *J Am Soc Nephrol*. 2013;24(6):979-986. doi:10.1681/ASN.2012080870
13. Kato K, Yonetsu T, Jia H, et al. Nonculprit Coronary Plaque Characteristics of Chronic Kidney Disease. *Circ Cardiovasc Imaging*. 2013;6(3):448-456. doi:10.1161/CIRCIMAGING.112.000165
14. Perez-Gomez MV, Bartsch L-A, Castillo-Rodriguez E, et al. Clarifying the concept of chronic kidney disease for non-nephrologists. *Clin Kidney J*. 2019;12(2):258-268. doi:10.1093/CKJ/SFZ007
15. Davoodi G, Mehrabi Pari S, Rezvafard M, et al. Glomerular filtration rate is related to severity of obstructive coronary artery disease in patients undergoing coronary angiography. *Int Urol Nephrol* 2011 444. 2011;44(4):1161-1168. doi:10.1007/S11255-011-0070-3
16. Khalique O, Aronow WS, Ahn C, et al. Relation of Moderate or Severe Reduction in Glomerular

- Filtration Rate to Number of Coronary Arteries Narrowed >50% in Patients Undergoing Coronary Angiography for Suspected Coronary Artery Disease. *Am J Cardiol.* 2007;100(3):415-416. doi:10.1016/J.AMJCARD.2007.03.038
17. Maini R, Wong DB, Addison D, Chiang E, Weisbord SD, Jneid H. Persistent Underrepresentation of Kidney Disease in Randomized, Controlled Trials of Cardiovascular Disease in the Contemporary Era. *J Am Soc Nephrol.* 2018;29(12):2782-2786. doi:10.1681/ASN.2018070674
 18. Wu M-Y, Li C-J, Hou M-F, Chu P-Y. New Insights into the Role of Inflammation in the Pathogenesis of Atherosclerosis. *Int J Mol Sci.* 2017;18(10). doi:10.3390/ijms18102034
 19. Steidl DC, Kaufmann BA. Ultrasound Imaging for Risk Assessment in Atherosclerosis. 2015;16(5):9749-9769. doi:10.3390/IJMS16059749
 20. Singh RB, Mengi SA, Xu Y-J, Arneja AS, Dhalla NS. Pathogenesis of atherosclerosis: A multifactorial process. *Exp Clin Cardiol.* 2002;7(1):40-53.
 21. Falk E, Shah PK, Fuster V. Coronary plaque disruption. *Circulation.* 1995;92(3):657-671. doi:10.1161/01.CIR.92.3.657
 22. Badimon L, Padró T, Vilahur G. Atherosclerosis, platelets and thrombosis in acute ischaemic heart disease. *Eur Hear journal Acute Cardiovasc care.* 2012;1(1):60-74. doi:10.1177/2048872612441582
 23. Sun Y V, Hu Y-J. Integrative Analysis of Multi-omics Data for Discovery and Functional Studies of Complex Human Diseases. *Adv Genet.* 2016;93:147-190. doi:10.1016/bs.adgen.2015.11.004
 24. Danikiewicz W. *Spektrometria Mas*: Wydawnictwo Naukowe PWN. Warszawa 2020.
 25. Muddiman DC, Alexander R, Ivanov, Alexander V, Lazarev (Eds): Sample preparation in biological mass spectrometry. *Anal Bioanal Chem.* 2012;404(5):1331-1332. doi:10.1007/s00216-012-6260-8
 26. Perez- Riverol Y, Moreno P. Scalable Data Analysis in Proteomics and Metabolomics Using BioContainers and Workflows Engines. *Proteomics.* 2020;20(9):1900147. doi:10.1002/pmic.201900147
 27. Drabik A, Kraj A, Silberring J. *Proteomika i Metabolomika* . Wydawnictwo Uniwersytetu Warszawskiego. Warszawa 2019.
 28. Lange V, Picotti P, Dörmann B, Aebersold R. Selected reaction monitoring for quantitative proteomics: a tutorial. *Mol Syst Biol.* 2008;4:222. doi:10.1038/msb.2008.61
 29. Zhang Y, Fonslow BR, Shan B, Baek M-C, Yates JR, III. Protein analysis by shotgun/bottom-up proteomics. *Chem Rev.* 2013;113(4):2343-2394. doi:10.1021/cr3003533
 30. Anand S, Samuel M, Ang C-S, Keerthikumar S, Mathivanan S. Label-Based and Label-Free Strategies for Protein Quantitation. *Methods Mol Biol.* 2017;1549:31-43. doi:10.1007/978-1-4939-6740-7_4
 31. Palomba A, Abbondio M, Fiorito G, Uzzau S, Pagnozzi D, Tanca A. Comparative Evaluation of MaxQuant and Proteome Discoverer MS1-Based Protein Quantification Tools. *J Proteome Res.* 2021;20(7):3497-3507. doi:10.1021/ACS.JPROTEOME.1C00143
 32. Cox J, Mann M. MaxQuant enables high peptide identification rates, individualized p.p.b.-range mass accuracies and proteome-wide protein quantification. *Nat Biotechnol.* 2008;26(12):1367-1372. doi:10.1038/nbt.1511
 33. Lualdi M, Fasano M. Statistical analysis of proteomics data: A review on feature selection. *J Proteomics.* 2019;198:18-26. doi:10.1016/J.JPROT.2018.12.004
 34. Levin Y. The role of statistical power analysis in quantitative proteomics. *Proteomics.* 2011;11(12):2565-2567. doi:10.1002/pmic.201100033

35. Mi H, Muruganujan A, Casagrande JT, Thomas PD. Large-scale gene function analysis with the panther classification system. *Nat Protoc.* 2013;8(8):1551-1566. doi:10.1038/nprot.2013.092
36. Schmidt A, Forne I, Imhof A. Bioinformatic analysis of proteomics data. *BMC Syst Biol.* 2014;8. doi:10.1186/1752-0509-8-S2-S3
37. Holčápek M, Liebisch G, Ekroos K. Lipidomic Analysis. *Anal Chem.* 2018;90(7):4249-4257. doi:10.1021/acs.analchem.7b05395
38. Matyash V, Liebisch G, Kurzchalia T V, Shevchenko A, Schwudke D. Lipid extraction by methyl-tert-butyl ether for high-throughput lipidomics. *J Lipid Res.* 2008;49(5):1137-1146. doi:10.1194/jlr.D700041-JLR200
39. Bligh EG, Dyer WJ. A rapid method of total lipid extraction and purification. *Can J Biochem Physiol.* 1959;37(8):911-917. doi:10.1139/O59-099
40. Folch J, Lees M, Sloane Stanley GH. A simple method for the isolation and purification of total lipides from animal tissues. *J Biol Chem.* 1957;226(1):497-509.
41. Löfgren L, Ståhlman M, Forsberg G-B, Saarinen S, Nilsson R, Hansson GI. The BUMÉ method: a novel automated chloroform-free 96-well total lipid extraction method for blood plasma. *J Lipid Res.* 2012;53(8):1690-1700. doi:10.1194/jlr.D023036
42. Hsu F-F. Mass spectrometry-based shotgun lipidomics - a critical review from the technical point of view. *Anal Bioanal Chem.* 2018;410(25):6387-6409. doi:10.1007/s00216-018-1252-y
43. Herzog R, Schuhmann K, Schwudke D, et al. LipidXplorer: A Software for Consensual Cross-Platform Lipidomics. *PLoS One.* 2012;7(1):e29851. doi:10.1371/journal.pone.0029851
44. Ortmayr K, Causon TJ, Hann S, Koellensperger G. Increasing selectivity and coverage in LC-MS based metabolome analysis. *TrAC Trends Anal Chem.* 2016;82:358-366. doi:10.1016/J.TRAC.2016.06.011
45. Fiehn O. Metabolomics by Gas Chromatography-Mass Spectrometry: Combined Targeted and Untargeted Profiling. *Curr Protoc Mol Biol.* 2016;114:30.4.1-30.4.32. doi:10.1002/0471142727.mb3004s114
46. Di Guida R, Engel J, Allwood JW, et al. Non-targeted UHPLC-MS metabolomic data processing methods: a comparative investigation of normalisation, missing value imputation, transformation and scaling. *Metabolomics.* 2016;12(5):93. doi:10.1007/s11306-016-1030-9
47. Molenaar MR, Jeucken A, Wassenaar TA, van de Lest CHA, Brouwers JF, Helms JB. LION/web: a web-based ontology enrichment tool for lipidomic data analysis. *Gigascience.* 2019;8(6):061. doi:10.1093/gigascience/giz061
48. Luczak M, Formanowicz D, Pawliczak E, Wanic-Kossowska M, Wykretowicz A, Figlerowicz M. Chronic kidney disease-related atherosclerosis - proteomic studies of blood plasma. *Proteome Sci.* 2011;9(1):25. doi:10.1186/1477-5956-9-25
49. Luczak M, Suszynska-Zajczyk J, Marczak L, et al. Label-Free Quantitative Proteomics Reveals Differences in Molecular Mechanism of Atherosclerosis Related and Non-Related to Chronic Kidney Disease. *Int J Mol Sci.* 2016;17(5). doi:10.3390/ijms17050631
50. Glorieux G, Mullen W, Duranton F, et al. New insights in molecular mechanisms involved in chronic kidney disease using high-resolution plasma proteome analysis. *Nephrol Dial Transplant.* 2015;30(11):1842-1852. doi:10.1093/ndt/gfv254
51. Wallentin L, Eriksson N, Olszowka M, et al. Plasma proteins associated with cardiovascular death in patients with chronic coronary heart disease: A retrospective study. *PLOS Med.* 2021;18(1):e1003513. doi:10.1371/journal.pmed.1003513

52. Luczak M, Formanowicz D, Marczak Ł, et al. ITRAQ-based proteomic analysis of plasma reveals abnormalities in lipid metabolism proteins in chronic kidney disease-related atherosclerosis. *Sci Rep.* 2016;6:32511. doi:10.1038/srep32511
53. Hao W, Friedman A. The LDL-HDL Profile Determines the Risk of Atherosclerosis: A Mathematical Model. Yang X-F, ed. *PLoS One.* 2014;9(3):e90497. doi:10.1371/journal.pone.0090497
54. Kaysen GA. New insights into lipid metabolism in chronic kidney disease. *J Ren Nutr.* 2011;21(1):120-123. doi:10.1053/j.jrn.2010.10.017
55. Kalantar-Zadeh K, Kilpatrick RD, McAllister CJ, Greenland S, Kopple JD. Reverse Epidemiology of Hypertension and Cardiovascular Death in the Hemodialysis Population. *Hypertension.* 2005;45(4):811-817. doi:10.1161/01.HYP.0000154895.18269.67
56. Luczak M, Formanowicz D, Marczak Ł, et al. iTRAQ-based proteomic analysis of plasma reveals abnormalities in lipid metabolism proteins in chronic kidney disease-related atherosclerosis. *Sci Rep.* 2016;6(1):32511. doi:10.1038/srep32511
57. Zdarta A, Tracz J, Luczak M, Guzik U, Kaczorek E. Hydrocarbon-induced changes in proteins and fatty acids profiles of *Raoultella ornithinolytica* M03. *J Proteomics.* 2017;164:43-51. doi:10.1016/j.jprot.2017.05.028
58. Malecki P, Mania A, Tracz J, Łuczak M, Mazur-Melewska K, Figlerowicz M. Adipocytokines as Risk Factors for Development of Nonalcoholic Fatty Liver Disease in Children. *J Clin Exp Hepatol.* March 2021. doi:10.1016/J.JCEH.2021.03.002
59. Waliczek M, Bąchor R, Kijewska M, et al. Isobaric duplex based on a combination of 16O/18O enzymatic exchange and labeling with pyrylium salts. *Anal Chim Acta.* 2019;1048:96-104. doi:10.1016/J.ACA.2018.10.012
60. Malecki P, Tracz J, Łuczak M, et al. Serum proteome assessment in nonalcoholic fatty liver disease in children: a preliminary study. 2020;17(7-8):623-632. doi:10.1080/14789450.2020.1810020

DOROBEK NAUKOWY

PUBLIKACJE

1. **Tracz J.**, Luczak M., Applying Proteomics and Integrative „Omics” Strategies to Decipher the Chronic Kidney Disease-Related Atherosclerosis. *International Journal of Molecular Sciences*. 2021, 22, 7492. (IF₂₀₂₀=5.923, IF_{5-letni}=6.132, 140 pkt MNiSW)
2. **Tracz J.**, Handschuh L., Lalowski M., Marczak Ł., Kostka-Jeziorny K., Perek B., Wanic-Kossowska M., Podkowińska A., Tykarski A., Formanowicz D., Luczak M., Proteomic Profiling of Leukocytes Reveals Dysregulation of Adhesion and Integrin Proteins in Chronic Kidney Disease-Related Atherosclerosis. *Journal of Proteome Research*. 2021, 20, 6, 3053-3067. (IF₂₀₂₀=4.466, IF_{5-letni}=4.352, 100 pkt MNiSW)
3. Marczak L., Idkowiak J., **Tracz J.**, Stobiecki M., Perek B., Kostka-Jeziorny K., Tykarski A., Wanic-Kossowska M., Borowski M., Osuch M., Formanowicz D., Luczak M., Mass-Spectrometry-Based Lipidomics Reveals Differential Changes in the Accumulated Lipid Classes in Chronic Kidney Disease. *Metabolites*. 2021, 11, 275. (IF₂₀₂₀=4.932, IF_{5-letni}=4.98, 70 pkt MNiSW)
4. Malecki, P., Mania, A., **Tracz, J.**, Łuczak, M., Mazur-Melewska, K., Figlerowicz, M., Adipocytokines as Risk Factors for Development of Nonalcoholic Fatty Liver Disease in Children. *Journal of Clinical and Experimental Hepatology* 2021 (70 pkt MNiSW)
5. Malecki, P., **Tracz, J.**, Łuczak, M., Figlerowicz, M., Mazur-Melewska, K., Służewski, W., Mania, A., Serum proteome assessment in nonalcoholic fatty liver disease in children: a preliminary study. *Expert Review of Proteomics* 2020, 17. (IF₂₀₁₉=3.614, IF_{5-letni}=3.805, 100 pkt MNiSW)
6. Waliczek, M., Bąchor, R., Kijewska, M., Gąszczyk, D., Panek-Laszczyńska, K., Konieczny, A., Dąbrowska, K., Witkiewicz, W., Marek-Bukowiec, K., **Tracz, J.**, Łuczak M., Szewczuk Z., Stefanowicz P., Isobaric duplex based on a combination of 16O/18O enzymatic exchange and labeling with pyrylium salts. *Analytica Chimica Acta* 2019. (IF₂₀₁₈=5.256, IF_{5-letni}=6.228, 100 pkt MNiSW)
7. Zdarta, A., **Tracz, J.**, Luczak, M., Guzik, U., Kaczorek, E., Hydrocarbon-induced changes in proteins and fatty acids profiles of *Raoultella ornithinolytica* M03. *Journal of Proteomics* 2017, 164, 43–51. (IF₂₀₁₆=3.914, IF_{5-letni}=4.02, 100 pkt MNiSW)

KONFERENCJE

Prezentacje plakatowe

1. M. Luczak, D. Formanowicz, **J. Tracz**, E. Pawliczak, K. Schwermer, M. Wanic-Kossowska, *The Influence of Duration of Peritoneal Dialysis on the Proteomic and Metabolomic Profiles of Plasma and Peritoneal Fluid*, Journal of the American Society of Nephrology 28 (2017): 865. Kidney Week 2017, Nowy Orlean, Stany Zjednoczone, 31.10-5.11.2017

2. **J. Tracz**, K. Kostka-Jeziorny, B. Perek, A. Podkowinska, D. Formanowicz, M. Luczak, *Analysis of the leukocytes proteome in atherosclerosis related and non-related to chronic kidney disease*, Journal of Proteomics and Bioinformatics 10:11 (2017): 77. 9th International Conference and Expo on Proteomic and Molecular Medicine, Paryż, Francja, 13-15.11.2017
3. **J. Tracz**, K. Kostka-Jeziorny, B. Perek, A. Podkowinska, D. Formanowicz, M. Luczak, *LC-MS/MS analysis of the leukocytes proteome and oxidative stress biomarkers in atherosclerosis related and non-related to chronic kidney disease*, Materiały konferencyjne (2018): 51. 6th Conference of Polish Mass Spectrometry Society, Warszawa, Polska, 23-26.04.2018
4. Ł. Marczak, J. Idkowiak, **J. Tracz**, M. Łuczak, B. Perek, K. Kostka-Jeziorny, A. Podkowinska, M. Stobiecki, *Lipidomic analysis of patients suffering from cardiovascular disease related to chronic kidney disease*, Materiały konferencyjne (2018): 67. 6th Conference of Polish Mass Spectrometry Society, Warszawa, Polska, 23-26.04.2018
5. **J. Tracz**, K. Kostka-Jeziorny, B. Perek, A. Podkowinska, D. Formanowicz, M. Luczak, *LC-MS/MS analysis of the monocytes CD14+ proteome in atherosclerosis related and non-related to chronic kidney disease*, Materiały konferencyjne (2018): 126. III Kongres BIO2018, Gdańsk, Polska 18-21.09.2018
6. Ł. Marczak, J. Idkowiak, **J. Tracz**, M. Łuczak, B. Perek, K. Kostka-Jeziorny, A. Podkowinska, M. Stobiecki, *Analysis of serum lipid fraction of patients suffering from cardiovascular disease related to chronic kidney disease*, Materiały konferencyjne (2018): 101. III Kongres BIO2018, Gdańsk, Polska 18-21.09.2018
7. **J. Tracz**, K. Kostka-Jeziorny, B. Perek, A. Podkowinska, D. Formanowicz, M. Luczak, *Analysis of the CD14+ monocytes proteome in atherosclerosis related and non-related to chronic kidney disease*, World Structural and Molecular Biology Conference, Rzym, Włochy 26-28.11.2018

Prezentacje ustne

1. **J. Tracz**, *Badanie mechanizmów molekularnych progresji miażdżycy w przewlekłej chorobie nerek z wykorzystaniem analiz proteomicznych i metabolomicznych krwi*, Seminarium IChB PAN. Poznań, Polska 6.05.2019
2. **J. Tracz**, K. Kostka-Jeziorny, B. Perek, A. Podkowinska, D. Formanowicz, M. Luczak, *Proteomic analysis of monocytes in cardiovascular disease related to chronic kidney disease*, 13th Central and Eastern European Proteomic Conference, Ustroń, Polska 23-25.09.2019
3. **J. Tracz**, K. Kostka-Jeziorny, B. Perek, A. Podkowińska, D. Formanowicz, M. Łuczak, *Analiza proteomiczna monocytów w miażdżycy związanej z przewlekłą chorobą nerek*, II Polskie Spotkanie Użytkowników Orbitrapów, Wrocław, Polska 21.11.2019
4. **J. Tracz**, K. Kostka-Jeziorny, B. Perek, A. Podkowińska, D. Formanowicz, M. Łuczak, *Analiza proteomiczna komórek układu immunologicznego w progresji miażdżycy związanej z przewlekłą chorobą nerek*, BioOrg 2019 III Ogólnopolskie Sympozjum Chemii Bioorganicznej, Organicznej i Biomateriałów, Poznań, Polska 7.12.2019

PROJEKTY BADAWCZE

1. Grant dla Młodych Naukowców ICHB PAN 2018/2019
Optymalizacja metody profilowania białek zawierających grupy karbonylowe w osoczu z wykorzystaniem technik spektrometrii mas.
Kierownik projektu
2. NCN OPUS 2015/19/B/NZ2/02450
Poszukiwanie molekularnych mechanizmów progresji miażdżycy w przewlekłej chorobie nerek.
Doktorant

STYPENDIA NAUKOWE

2020/2021 Stypendium dla najlepszych doktorantów Środowiskowego Studium Doktoranckiego IChB PAN

2019/2020 Stypendium dla najlepszych doktorantów Środowiskowego Studium Doktoranckiego IChB PAN

2017/2018 Stypendium dla najlepszych doktorantów Środowiskowego Studium Doktoranckiego IChB PAN

ZAŁĄCZNIKI

1. OŚWIADCZENIA O WKŁADZIE PRACY KANDYDATA W ARTYKUŁY ZAWARTE W ROZPRAWIE DOKTORSKIEJ.

2. PUBLIKACJA NR 1.

Applying Proteomics and Integrative „Omics” Strategies to Decipher the Chronic Kidney Disease-Related Atherosclerosis

3. PUBLIKACJA NR 2.

Proteomic Profiling of Leukocytes Reveals Dysregulation of Adhesion and Integrin Proteins In Chronic Kidney Disease-Related Atherosclerosis

4. PUBLIKACJA NR 3.

Mass-Spectrometry-Based Lipidomics Reveals Differential Changes in the Accumulated Lipid Classes in Chronic Kidney Disease

Poznań, 13.09.2021r.

Mgr inż. Joanna Tracz
Zakład Proteomiki Biomedycznej
Instytut Chemii Bioorganicznej PAN
ul. Noskowskiego 12/14
61-704 Poznań

**OŚWIADCZENIE KANDYDATA O WŁASNYM WKŁADZIE W PUBLIKACJE
NAUKOWE WCHODZĄCE W SKŁAD ROZPRAWY DOKTORSKIEJ**

Tytuł artykułu naukowego: „*Applying Proteomics and Integrative „Omics” Strategies to Decipher the Chronic Kidney Disease-Related Atherosclerosis*”

Autorzy: J. Tracz, M. Luczak*

Czasopismo: International Journal of Molecular Sciences

Data opublikowania: 13-07-2021

Ja, Joanna Tracz, oświadczam, że mój wkład autorski w artykuł naukowy o tytule „Applying Proteomics and Integrative „Omics” Strategies to Decipher the Chronic Kidney Disease-Related Atherosclerosis” polegał na:

- Zgromadzeniu i przeanalizowaniu dostępnej literatury naukowej niezbędnej do stworzenia pracy oraz przygotowaniu pierwszej wersji manuskryptu;
- Utworzeniu zawartych w artykule rycin oraz tabeli.


.....
Podpis kandydata

Tytuł artykułu naukowego: „*Proteomic Profiling of Leukocytes Reveals Dysregulation of Adhesion and Integrin Proteins in Chronic Kidney Disease-Related Atherosclerosis*”

Autorzy: J. Tracz, L. Handschuh, M. Lalowski, Ł. Marczak, K. Kostka-Jeziorny, B. Perek, M. Wanic-Kossowska, A. Podkowińska, A. Tykarski, D. Formanowicz, M. Luczak*

Czasopismo: Journal of Proteome Research

Data opublikowania: 3-05-2021

Ja, Joanna Tracz, oświadczam, że mój wkład autorski w artykuł naukowy o tytule „Proteomic Profiling of Leukocytes Reveals Dysregulation of Adhesion and Integrin Proteins in Chronic Kidney Disease-Related Atherosclerosis” polegał na:

- Zebraniu i przygotowaniu materiału badawczego do wszystkich eksperymentów opisanych w pracy;
- Zoptymalizowaniu i przeprowadzeniu wszystkich eksperymentów proteomicznych opartych o techniki spektrometrii mas;
- Zoptymalizowaniu i przeprowadzeniu wszystkich eksperymentów walidacyjnych z wykorzystaniem technik immunoenzymatycznych – western blot i ELISA oraz analiz z użyciem metody MRM;
- Zoptymalizowaniu i przeprowadzeniu izolacji RNA, reakcji odwrotnej transkrypcji, badania poziomu transkryptów z wykorzystaniem techniki ddPCR oraz analiz statystycznych i korelacyjnych uzyskanych wyników;
- Wizualizacji uzyskanych wyników w postaci ryciny 1, 2, 3 oraz 5;
- Przygotowaniu i napisaniu wstępu literaturowego oraz rozdziału opisującego metodykę, a także zebraniu literatury do dyskusji zawartych w pracy wyników.


.....
Podpis kandydata

Tytuł artykułu naukowego: „*Mass Spectrometry-Based Lipidomics Reveals Differential Changes in the Accumulated Lipid Classes in Chronic Kidney Disease*”

Autorzy: Ł. Marczak*, J. Idkowiak, **J. Tracz**, M. Stobiecki, B. Perek, K. Kostka-Jeziorny, A. Tykarski, M. Wanic-Kossowska, M. Borowski, M. Osuch, D. Formanowicz, M. Luczak*

Czasopismo: Metabolites

Data opublikowania: 27-04-2021

Ja, Joanna Tracz, oświadczam, że mój wkład autorski w artykuł naukowy o tytule „*Mass Spectrometry-Based Lipidomics Reveals Differential Changes in the Accumulated Lipid Classes in Chronic Kidney Disease*” polegał na:

- Zebraniu i przygotowaniu materiału badawczego do wszystkich eksperymentów opisanych w pracy;
- Przeprowadzeniu profilowania metabolomicznego osocza z wykorzystaniem techniki GC-MS;
- Analizie chromatogramów i widm masowych niskocząsteczkowych metabolitów oraz opracowaniu uzyskanych wyników metabolomicznych;
- Przeprowadzeniu analizy statystycznej oraz korelacyjnej uzyskanych wyników;
- Udziale w tworzeniu rycin 7 i 8;
- Przeglądzie dostępnej literatury oraz przygotowaniu pierwotnej wersji wstępu literaturowego oraz dyskusji uzyskanych wyników.

.....
Joanna Tracz
Podpis kandydata

Poznań, 13.09.2021r.

Dr hab. Magdalena Łuczak, prof. IChB PAN
Zakład Proteomiki Biomedycznej
Instytut Chemii Bioorganicznej PAN
ul. Noskowskiego 12/14
61-704 Poznań

**OŚWIADCZENIE AUTORA KORESPONDENCYJNEGO O WKŁADZIE
KANDYDATA W ARTYKUŁY ZAWARTE W ROZPRAWIE DOKTORSKIEJ**

Tytuł artykułu naukowego: „*Applying Proteomics and Integrative „Omics” Strategies to Decipher the Chronic Kidney Disease-Related Atherosclerosis*”

Autorzy: J. Tracz, M. Łuczak*

Czasopismo: International Journal of Molecular Sciences

Data opublikowania: 13-07-2021

Ja, Magdalena Łuczak, oświadczam, że wkład autorski mgr inż. Joanny Tracz w artykuł naukowy o tytule „Applying Proteomics and Integrative „Omics” Strategies to Decipher the Chronic Kidney Disease-Related Atherosclerosis” polegał na:

- Zgromadzeniu i przeanalizowaniu dostępnej literatury naukowej niezbędnej do stworzenia pracy oraz przygotowaniu pierwszej wersji manuskryptu;
- Utworzeniu wszystkich zawartych w artykule rycin oraz tabeli.

Natomiast mój wkład, jako autora korespondencyjnego, polegał na:

- Przygotowaniu koncepcji pracy;
- Edycji stworzonego przez doktorantkę manuskryptu;
- Nadzorowaniu prac i pomocy merytorycznej;
- Uzyskaniu finansowania niezbędnego do opublikowania pracy w czasopiśmie „open access”.


.....
Podpis autora korespondencyjnego

Tytuł artykułu naukowego: „*Proteomic Profiling of Leukocytes Reveals Dysregulation of Adhesion and Integrin Proteins in Chronic Kidney Disease-Related Atherosclerosis*”

Autorzy: J. Tracz, L. Handschuh, M. Lalowski, Ł. Marczak, K. Kostka-Jeziorny, B. Perek, M. Wanic-Kossowska, A. Podkowińska, A. Tykarski, D. Formanowicz, M. Luczak*

Czasopismo: Journal of Proteome Research

Data opublikowania: 3-05-2021

Ja, Magdalena Łuczak, oświadczam, że wkład autorski mgr inż. Joanny Tracz w artykuł naukowy o tytule „*Proteomic Profiling of Leukocytes Reveals Dysregulation of Adhesion and Integrin Proteins in Chronic Kidney Disease-Related Atherosclerosis*” polegał na:

- Zebraniu i przygotowaniu materiału badawczego do wszystkich eksperymentów opisanych w pracy;
- Zoptymalizowaniu i przeprowadzeniu wszystkich eksperymentów proteomicznych opartych o techniki spektrometrii mas;
- Zoptymalizowaniu i przeprowadzeniu wszystkich eksperymentów walidacyjnych z wykorzystaniem technik immunoenzymatycznych – western blot i ELISA oraz analiz z użyciem metody MRM;
- Zoptymalizowaniu i przeprowadzeniu izolacji RNA, reakcji odwrotnej transkrypcji, badania poziomu transkryptów z wykorzystaniem techniki ddPCR oraz analiz statystycznych i korelacyjnych uzyskanych wyników;
- Wizualizacji uzyskanych wyników w postaci ryciny 1, 2, 3 oraz 5;
- Przygotowaniu i napisaniu wstępu literaturowego oraz rozdziału opisującego metodykę, a także zebraniu literatury do dyskusji zawartych w pracy wyników.

Natomiast mój wkład, jako autora korespondencyjnego, polegał na:

- Zaplanowaniu koncepcji badań oraz uzyskaniu funduszy na realizację wszystkich eksperymentów;
- Nadzorowaniu i pomocy merytorycznej podczas badań oraz pisania pracy;
- Interpretacji uzyskanych przez doktorantkę wyników;
- Wizualizacji wyników w postaci ryciny 4 i 6;
- Edycji przygotowanego przez doktorantkę manuskryptu oraz jego finalne przygotowanie do publikacji.

.....*Magdalena Łuczak*.....
Podpis autora korespondencyjnego

Tytuł artykułu naukowego: „*Mass Spectrometry-Based Lipidomics Reveals Differential Changes in the Accumulated Lipid Classes in Chronic Kidney Disease*”

Autorzy: Ł. Marczak*, J. Idkowiak, **J. Tracz**, M. Stobiecki, B. Perek, K. Kostka-Jeziorny, A. Tykarski, M. Wanic-Kossowska, M. Borowski, M. Osuch, D. Formanowicz, M. Luczak*

Czasopismo: Metabolites

Data opublikowania: 27-04-2021

Ja, Magdalena Łuczak, oświadczam, że wkład autorski mgr inż. Joanny Tracz w artykuł naukowy o tytule „*Mass Spectrometry-Based Lipidomics Reveals Differential Changes in the Accumulated Lipid Classes in Chronic Kidney Disease*” polegał na:

- Zebraniu i przygotowaniu materiału badawczego do wszystkich eksperymentów opisanych w pracy;
- Przeprowadzeniu profilowania metabolomicznego osocza z wykorzystaniem techniki GC-MS;
- Analizie chromatogramów i widm masowych niskocząsteczkowych metabolitów oraz opracowaniu uzyskanych wyników metabolomicznych;
- Przeprowadzeniu analizy statystycznej oraz korelacyjnej uzyskanych wyników;
- Udziale w tworzeniu rycin 7 i 8;
- Przeglądzie dostępnej literatury oraz przygotowaniu pierwotnej wersji wstępu literaturowego i dyskusji uzyskanych wyników.

Natomiast mój wkład, jako autora korespondencyjnego, polegał na:

- Zaplanowaniu koncepcji badań oraz uzyskaniu funduszy na realizację wszystkich eksperymentów;
- Nadzorowaniu i pomocy merytorycznej podczas badań oraz pisania pracy;
- Interpretacji uzyskanych przez doktorantkę wyników;
- Wizualizacji uzyskanych wyników w postaci rycin 1-4;
- Edycji przygotowanego manuskryptu oraz jego finalne przygotowanie do publikacji.


.....
Podpis autora korespondencyjnego

Poznań, 13.09.2021r.

Dr Łukasz Marczak
Pracownia Spektrometrii Mas
Instytut Chemii Bioorganicznej PAN
ul. Noskowskiego 12/14
61-704 Poznań

OŚWIADCZENIE AUTORA KORESPONDENCYJNEGO O WKŁADZIE KANDYDATA W ARTYKUŁY ZAWARTE W ROZPRAWIE DOKTORSKIEJ

Tytuł artykułu naukowego: „*Mass Spectrometry-Based Lipidomics Reveals Differential Changes in the Accumulated Lipid Classes in Chronic Kidney Disease*”.

Autorzy: Ł. Marczak*, J. Idkowiak, **J. Tracz**, M. Stobiecki, B. Perek, K. Kostka-Jeziorny, A. Tykarski, M. Wanic-Kossowska, M. Borowski, M. Osuch, D. Formanowicz, M. Luczak*

Czasopismo: Metabolites

Data opublikowania: 27-04-2021

Ja, Łukasz Marczak, oświadczam, że wkład autorski mgr inż. Joanny Tracz w artykuł naukowy o tytule „*Mass Spectrometry-Based Lipidomics Reveals Differential Changes in the Accumulated Lipid Classes in Chronic Kidney Disease*” polegał na:

- Zebraniu i przygotowaniu materiału badawczego do wszystkich eksperymentów opisanych w pracy;
- Przeprowadzeniu profilowania metabolomicznego osocza z wykorzystaniem techniki GC-MS;
- Analizie chromatogramów i widm masowych niskocząsteczkowych metabolitów oraz opracowaniu uzyskanych wyników metabolomicznych;
- Przeprowadzeniu analizy statystycznej oraz korelacyjnej uzyskanych wyników;
- Udziale w tworzeniu rycin 7 i 8;
- Przeglądzie dostępnej literatury oraz przygotowaniu pierwotnej wersji wstępu literaturowego oraz dyskusji uzyskanych wyników.

Natomiast mój wkład, jako autora korespondencyjnego, polegał na:

- Zaplanowaniu eksperymentów lipidomicznych;
- Nadzorowaniu i wsparciu merytorycznym podczas prowadzenia badań oraz analizy uzyskanych wyników;
- Opracowaniu uzyskanych wyników lipidomicznych oraz ich analizie bioinformatycznej;



- Wizualizacji uzyskanych wyników w postaci rycin 5 i 6;
- Przygotowaniu manuskryptu artykułu.

Julian Kowalski

.....
Podpis autora korespondencyjnego



Review

Applying Proteomics and Integrative “Omics” Strategies to Decipher the Chronic Kidney Disease-Related Atherosclerosis

Joanna Tracz and Magdalena Luczak *

European Centre for Bioinformatics and Genomics, Institute of Bioorganic Chemistry,
Polish Academy of Sciences, 61-704 Poznan, Poland; joanna.a.tracz@gmail.com

* Correspondence: magdalu@ibch.poznan.pl

Abstract: Patients with chronic kidney disease (CKD) are at increased risk of atherosclerosis and premature mortality, mainly due to cardiovascular events. However, well-known risk factors, which promote “classical” atherosclerosis are alone insufficient to explain the high prevalence of atherosclerosis-related to CKD (CKD-A). The complexity of the molecular mechanisms underlying the acceleration of CKD-A is still to be defined. To obtain a holistic picture of these changes, comprehensive proteomic approaches have been developed including global protein profiling followed by functional bioinformatics analyses of dysregulated pathways. Furthermore, proteomics surveys in combination with other “omics” techniques, i.e., transcriptomics and metabolomics as well as physiological assays provide a solid ground for interpretation of observed phenomena in the context of disease pathology. This review discusses the comprehensive application of various “omics” approaches, with emphasis on proteomics, to tackle the molecular mechanisms underlying CKD-A progression. We summarize here the recent findings derived from global proteomic approaches and underline the potential of utilizing integrative systems biology, to gain a deeper insight into the pathogenesis of CKD-A and other disorders.



Citation: Tracz, J.; Luczak, M. Applying Proteomics and Integrative “Omics” Strategies to Decipher the Chronic Kidney Disease-Related Atherosclerosis. *Int. J. Mol. Sci.* **2021**, *22*, 7492. <https://doi.org/10.3390/ijms22147492>

Academic Editor: Abdelnaby Khalyfa

Received: 10 June 2021

Accepted: 8 July 2021

Published: 13 July 2021

Publisher’s Note: MDPI stays neutral with regard to jurisdictional claims in published maps and institutional affiliations.



Copyright: © 2021 by the authors. Licensee MDPI, Basel, Switzerland. This article is an open access article distributed under the terms and conditions of the Creative Commons Attribution (CC BY) license (<https://creativecommons.org/licenses/by/4.0/>).

Keywords: chronic kidney disease; cardiovascular disease; atherosclerosis; multiomics; proteomics

1. Introduction

Chronic kidney disease (CKD) is defined as a loss of renal function manifested as a progressive reduction of the glomerular filtration rate (GFR) present for at least 3 months and/or albuminuria, and abnormal kidney morphology [1,2]. CKD is divided into five stages with increasing severity and the transition to stage 3b is the point at which the diseases become irreversible. Patients with stage 5 (CKD5) develop end-stage renal disease (ESRD), display kidney failure with eGFR values below 15 mL/min/1.73 m², and ultimately require a dialysis or kidney transplantation [2,3]. The number of people undergoing renal replacement therapy exceeds 2.5 million and is estimated to be doubled by 2030 [4]. Annual mortality due to CKD increased by 33.7% over the 2007–2017 period [5], and reached similar numbers as colon cancer [6], thereby posing CKD as a one of the main causes of mortality and morbidity worldwide [4,7]. The mortality in CKD, especially in ESRD, is however, not driven by a kidney failure but by the cardiovascular complications caused by accelerated atherosclerosis [8]. CKD patients are exposed to an increased risk of cardiovascular disease (CVD), and its prevalence along with cardiovascular mortality increases alongside declining kidney function [9,10]. Multiple epidemiological studies demonstrated that CKD patients are more prone to develop CVD, triggering over 60% of deaths due to cardiovascular events: stroke or myocardial infarction, while in individuals with normal kidney function this value accounted for less than 30% [11,12]. For ESRD patients, the risk of CVD is 20–1000-fold higher as compared to general population, and raises in proportion to the decrease of eGFR [13]. Nevertheless, even the early stage CKD patients indicate the initial symptoms of CVD, including hypertension or ischemic heart

disease and reveal 1.5-fold higher risk of CVD-induced death as compared to general population [9,14]. Cardiovascular complications in CKD are mainly caused by atherosclerosis, and its high prevalence indicates the close functional association of CVD with kidney disease. This phenomenon can be explained by the clustering of several traditional risk factors, including dyslipidemia, hypertension and diabetes, which are characteristic for “classical” atherosclerosis, and the other ones, uremia-related, which are more specific to CKD. In “classical” atherosclerosis, a direct correlation with progress of dyslipidemia is observed. This disturbance is recognized as a fundamental step for the development of complex interplay of hemodynamics, lipid metabolism, and thrombotic processes that initiate chronic inflammation in the arterial wall, and progress towards development of atherosclerotic plaques [15]. In chronic kidney disease-related atherosclerosis (CKD-A), non-traditional risk factors, including accumulation of uremic toxins, inflammation, oxidative stress, malnutrition, disturbances of the calcium-phosphate metabolism, are also considered [16,17]. The effect of uremic and traditional risk factors can accelerate atherosclerosis in CKD [16,18,19]. However, many individuals with CKD reveal a phenomenon called “reverse epidemiology”, and display decreased serum cholesterol, body mass, and blood pressure that are more strongly related to the higher risk of atherosclerosis [20]. All this points towards the non-obvious relationship between CKD and risk of atherosclerosis. In this respect, CKD-A appears as a complex multifactorial disease with many dysregulated processes and pathways. Moreover, CKD patients are often excluded from the large trials of cardiovascular outcomes, well-established diagnostic modalities, and treatment strategies for atherosclerosis and cardiovascular disease [21]. Therefore, studies presenting direct analyses of both conditions, CKD and “classical” CVD, are extremely rare in the literature. The vast majority of them compared CKD to healthy controls, which is the main limitation in unraveling the differences in mechanisms accelerating atherosclerosis in CKD and “classical” CVD. Several excellent reviews have outlined the general features of CKD [22,23]. A report presenting the current state-of-the-art of risk factors and increased cardiovascular morbidity/mortality in CKD has been recently published [24].

In this review, we focus on the utilization of comprehensive “omics” applications, with emphasis on proteomics, to the analysis of molecular mechanisms of CKD-related atherosclerosis. We aimed to underline the possibilities and large potential value of integrative “omics” studies to decipher the disease-related molecular mechanisms. Furthermore, the research on CKD and “classical” CVD and their functional interrelations will aid in better understanding of these mechanisms.

2. Key Concepts of Proteomics in Disease Analysis

Proteins are effectors of biological functions and dysregulation of their abundance results in pathological imbalance of an organism. Proteomics aids in the characterization of proteome dynamics, including abundance, function, interactions and modifications of proteins in various types of biological fluids, cells and tissues over time and disease conditions. During the last decade, a broad spectrum of “omics” studies on CKD and CVD, including proteomic ones, has been conducted to determine the specific indicators of disease development.

One of the most common proteomic approaches in analysis of pathological condition relates to the identification of biomarkers. Reviews discussing various “omics” attempts for discovery of clinically relevant biomarkers have recently been published [25–27]. Therefore, only a few issues will be mentioned in this review. Protein biomarkers are molecular indicators of perturbed biological processes, physiological pathways, or pharmacological responses to treatment. The knowledge about their level provides useful information for early detection of subtle pathological disturbances and disease progression, and is considered as an introductory phase to focused personalized medicine studies [28]. However, the putative biomarkers have to pass through rigorous validation phase to be implemented in clinical setting. More specifically, the early phase studies have to determine their accuracy, reliability, interpretability, and feasibility in the diagnostic laboratory, with a relatively

minimal cost per sample. To determine if a biomarker is “promising”, it is recommended to report its significant association with the clinical outcome and the assessment of sensitivity and specificity [29]. Moreover, the candidate biomarker has to be appropriately validated in vivo, in animal models first and then in cohorts of patients, in independent clinical studies. Normal and prognostic concentration values should embrace the differences matched by gender and age, thereby assisting in clinical decision making [30].

Various proteomic studies have been performed in CKD and CVD, and many putative biomarkers were proposed to aid the diagnosis of CKD or CVD [31–34]. For instance, neutrophil gelatinase-associated lipocalin (NGAL) and urinary kidney injury molecule (KIM-1) were suggested for an early CKD detection [35,36]. A review that outlined recent advances in the discovery and validation of biomarkers for CKD prediction has been published by Zhang et al. [37]. Most of the studies, however, are not able to meet the above-mentioned criteria mainly due to insufficient accuracy and the sensitivity, low predictive power, the heterogeneous results as well as the lack of validation. An interesting solution that increases the predictive power of biomarkers is a multi-marker strategy, involving combinatorial panel of proteins representing multiple pathways perturbed in a given disease. For instance, the CKD273 classifier, developed by Good et al. [38], is a panel based on capillary electrophoresis/mass spectrometry method (CE-MS), frequently used in the CKD diagnostics, especially on urine samples (reviewed by [39]). On the other hand, lncRNAs may be useful as potential biomarkers for the early diagnosis and prognosis of many diseases, including patients with CKD. The review summarizing the role of lncRNAs in kidney diseases, and their function as prognostic biomarkers has recently been published [40].

Studies targeting single entities might be useful for preventive and therapeutic approaches, and guidelines for biomarker identification and qualification in clinical proteomics have been presented some time ago [41]. Nevertheless, the value of such biomarkers and translatability of preclinical discoveries to human applications is still under debate, and many challenges and bottlenecks are associated with the transformation of biomarkers into potential clinical assays [42,43]. Moreover, many suggested protein biomarkers require detailed mass spectrometry analysis, which might be preclusive for broad utilization in clinical settings on a large scale. To this day, only a few urinary biomarkers, including KIM-1, clusterin (apolipoprotein J), albumin, β 2-microglobulin and cystatin C are considered as valid by Food and Drug Administration (FDA) and European Medicines Agency (EMA). The most suited biomarkers, associated with CKD progression have not been yet discovered and implemented into medical practice. Therefore, proteomic approaches focused on biomarkers searching are relevant, but have limited practicability.

However, high-throughput proteomics might be also utilized to recognize complex disease processes and the molecular mechanisms of a pathological condition as well as verification of results obtained with other techniques (Figure 1).

An advancement in proteomic approaches, mainly mass spectrometry techniques and affinity assays, has played a meaningful role in this respect. Comparative proteomic analysis on a large-scale might be useful to create hypotheses, and to determine targets and dynamic interactions between proteins or associations between processes and pathways underlying disease. Such a proteomic approach can utilize many different targeted and non-targeted techniques. Recently, affinity-based proteomics i.e., proximity extension and aptamer-based assays, have been presented as targeted methods to the quantitative, high-specific evaluation of multiple proteins [44,45]. These techniques seem to be very promising especially in analysis of low-abundance proteins, in samples with wide dynamic range of protein concentrations, i.e., plasma or serum.

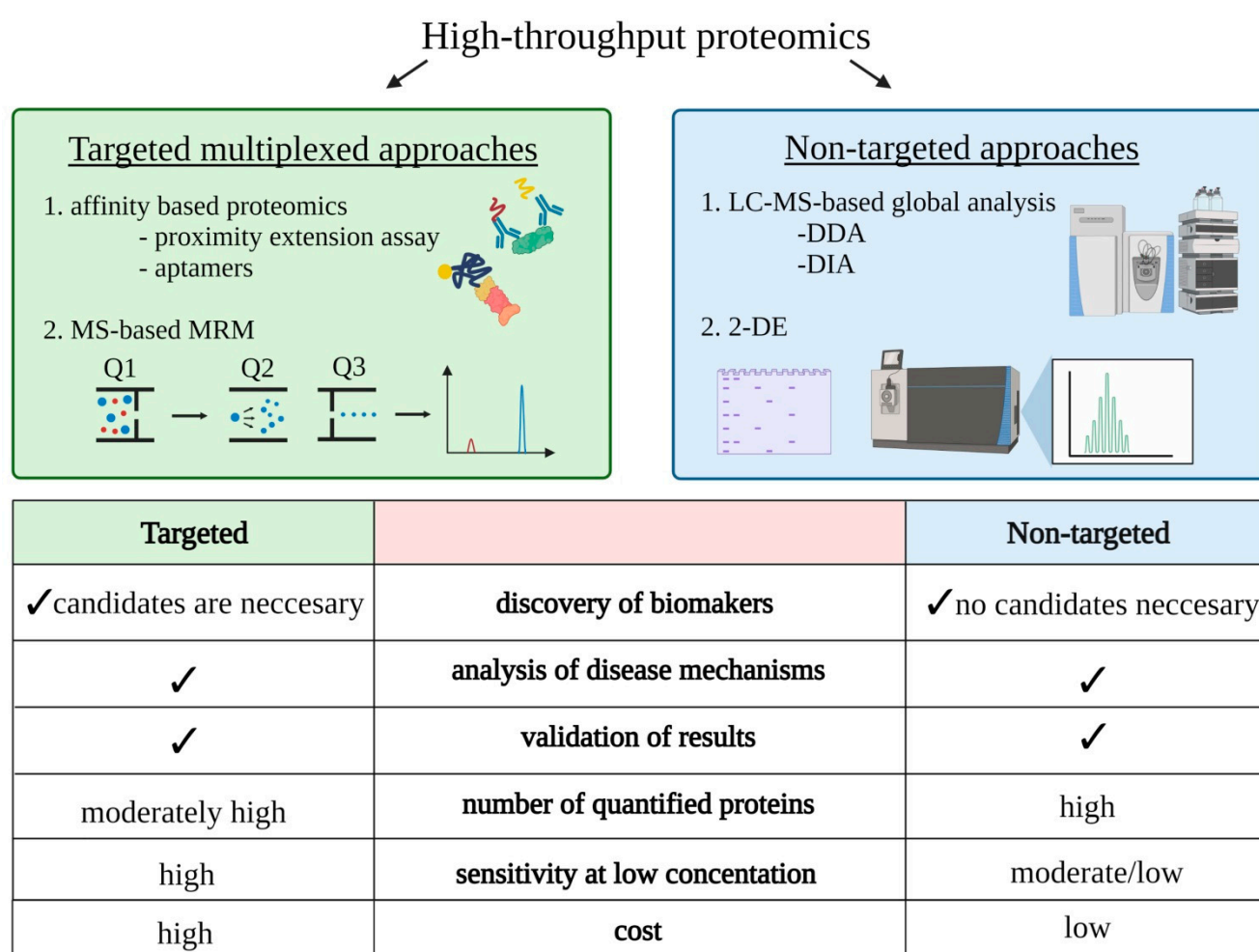


Figure 1. Characteristics of the targeted and non-targeted proteomic approaches. MRM—multiple-reaction monitoring; DDA—data-dependent acquisition; DIA—data-independent acquisition; 2DE—two-dimensional electrophoresis.

In proximity extension assay (PEA), a pair of oligonucleotide-labeled antibodies binds to epitopes on the surface of a protein [46]. After the antibodies recognize target molecule, the oligonucleotide sequences hybridize, and the added DNA polymerase leads to an extension of the oligonucleotide sequence. The reaction product is detected and quantified by real-time PCR and the result converted into the amount of examined protein [44]. The immunoassay is multiplexable and can detect up to 92 protein biomarkers in 96-plex format simultaneously without a loss of specificity [47]. Aptamer-based proteomic technology is based on single-stranded oligonucleotides linked with a fluorophore and a photocleavable linker to capture target proteins from a biological sample with a high specificity without utilizing antibodies. The new generation of aptamers, called “SOMAmer” (Slow Off-rate Modified Aptamer), is capable to bind proteins with subnanomolar affinities and without any nonspecific interactions. SOMAmers can be combined in multiplexed detection assay (called SOMAscan), and in this form efficiently quantify more than a thousand proteins at a very low limit of detection, high reproducibility and utilizing a minimal amount of biological samples [45].

Mass spectrometry-based proteomics represents one of the most sensitive methods utilizing to untangle the molecular mechanisms of a disease. This technique can be applied in targeted and non-targeted mode. Application of targeted multiple-reaction monitoring (MRM) mass spectrometry allows specific, highly reproducible and sensitive quantitative analyses of hundreds of proteins in a single experiment [48,49]. It offers not only relative but also absolute quantitation of proteins when isotopically labeled internal standards are utilized. Importantly, the identification of low-abundance proteins in samples with wide

dynamic range of protein concentrations is possible. However, being a targeted method, only a limited number of known proteins can be evaluated, which can be an obstacle when a rare biological condition is explored. In consequence, MRM approach is mainly utilized for biomarker validation studies of newly identified protein targets.

Non-targeted MS-based methods does not reveal this obstacle and enable the identification and quantitation of thousands of proteins making it an ideal approach in elucidation of the underlying molecular events associated with disease development and progression. However, identification of low-abundance proteins in complex samples is sometimes challenging. The obtained datasets of differentially expressed proteins (DEPs) among multiple biological conditions serve as an input for subsequent functional bioinformatics analyses linking changes in protein abundance with information about disturbed processes and interaction between them in studied pathological condition. Identified DEPs are analyzed in the context of Gene Ontology (GO), and proteins are assigned to particular biological process, molecular function or cellular component categories. KEGG (www.genome.jp/kegg/pathway.html; accessed on 16 March 2021), Reactome (<https://reactome.org/>; accessed on 16 March 2021), BioCarta (<https://maayanlab.cloud/Harmonizome/dataset/Biocarta+Pathways>; accessed on 16 March 2021) are most commonly used. In the next step, the enrichment analysis is performed to examine whether any identified functional GO-term in the data set is statistically enriched in relation to its frequency in the genome [50]. Moreover, biological process and molecular function analysis might be fortified with physiological pathway analysis, which is more meaningful since it provides more detailed information about the changes. Identification of the disturbed pathways between two biological conditions supports clarifying the pathophysiology of disease progression. Among the tools for the GO-terms identification and enrichment, open-source software: DAVID (<https://david.ncifcrf.gov/>), PANTHER (<http://pantherdb.org/>; accessed on 16 March 2021), and ConsensusPathDB (<http://cpdb.molgen.mpg.de/>; accessed on 16 March 2021) can be highlighted [51–53]. Some commercial software, i.e., the Ingenuity Pathway Analysis (IPA; Ingenuity systems, Redwood City, CA, USA; www.ingenuity.com; accessed on 16 March 2021) and Advaita (www.advaitabio.com/ipathwayguide; accessed on 16 March 2021), have additional built-in scientific literature-based databases allowing indicating the directionality of the observed changes and thus predicting an inhibition or activation of identified pathways/functions. Moreover, these programs allow the functional interpretation of the results derived from other “omics” studies, gathering the information at the gene, transcript and metabolite levels, providing a more comprehensive molecular view of examined biological processes (Figure 2).

Genomics reveals specific mutations related to disease prognosis. Transcriptomic analyses indicate whether the disturbed abundance identified at the protein level is directly related to changes in mRNA expression or arises from post-translational machinery. It is difficult to obtain a good correlation between the level of mRNA expression and the observed abundance of the associated proteins [54]. However, the recent study presented the possibility of predicting protein copy numbers from the transcriptome analysis by considering RNA-to-protein (RTP) conversion factor across several human tissues and cell lines [55]. Metabolomics and lipidomics reflect the metabolic status of cells or tissues but are sensitive to various stimuli, which results in a large degree of variability of observed changes. Nonetheless, combination of all aforementioned approaches in biomedical research delivers one of the most powerful methodologies to understand the complex molecular mechanisms of disease progression (Figure 2). The integration of such approaches constitutes a starting point for functional validation and physiological experiments targeting the unraveled mechanisms, in vitro in cell lines or in vivo, using animal models of studied pathological condition.

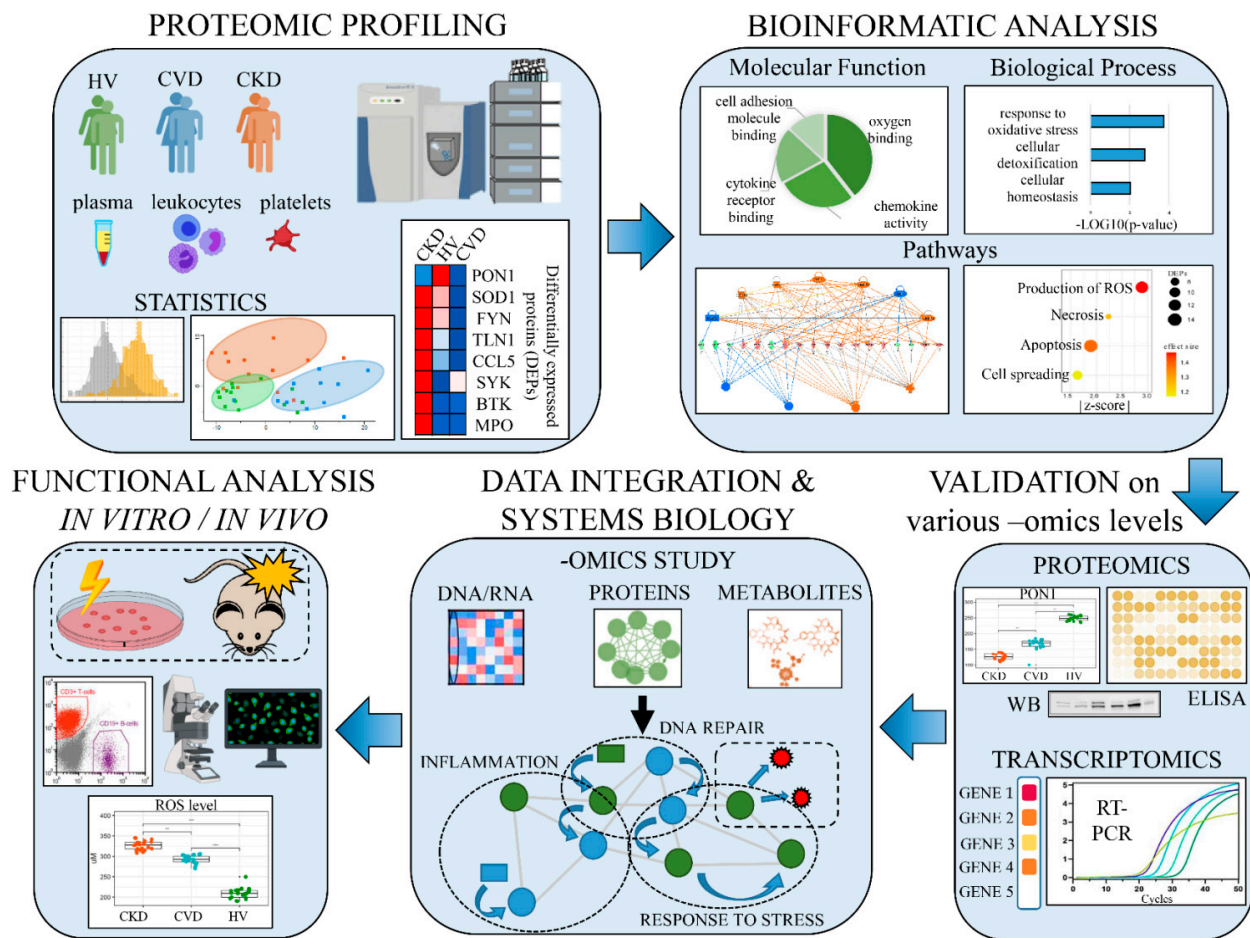


Figure 2. The analysis pipeline targeting the molecular mechanisms of CKD-A utilizing an integrated multiomics strategy.

In recent years, the number of systematic studies utilizing multi-approach has increased considerably. An excellent example of such a comprehensive pipeline to understand the molecular mechanism of selected aspect of atherosclerotic plaque development is presented in the study by Venturini and co-workers [56]. In this study, the authors have integrated high-throughput proteomics and metabolomics with bioinformatic analysis supplemented with physiological experiments to demonstrate the differences occurring in endothelium under atheroprone and atheroprotective shear stress, a hemodynamic force playing a role in atherosclerosis development. Alterations in lipid and lipoprotein abundance and metabolism at proteome and metabolome levels were presented and the key molecules involved in response to atheroprone flow were identified. The low-density lipoprotein receptor (LDLR) demonstrated a significant downregulation in its abundance and disturbances in the glycosylation pattern, and the changes were validated by immunohistochemistry and Western blot analysis. Moreover, by utilizing an integrative “omics” approach, a modulation of LDLR with statin was shown to be partially recovering the normal, atheroprotective profile of endothelial cells, thereby pinpointing to a new treatment strategy and demonstrating pleiotropic effect of statin activity [56].

3. Application of Proteomics to Understanding Molecular Mechanism of CKD-A

Such comprehensive analyses mentioned above, are not very frequent in CKD-related atherosclerosis as researchers focus rather on biomarker searches than on high-throughput and multilevel elucidation of molecular changes. Thus far, only a few studies utilizing the global proteomics and functional bioinformatics, to the study of biological processes and pathways disturbed during CKD and CKD-A progression have been published (Table 1).

Table 1. Summary of presented in the literature studies applying “omics” approaches to the analysis of mechanisms in CKD-A.

Studied Mechanism/Process in CKD-A	Applied “Omics” Strategy	References
Unique dyslipidemia	Lipidomics	[57]
Alterations in lipid transport- and metabolism-related molecules	MS-based proteomics Transcriptomics Metabolomics	[58–65]
Disturbances in chemical composition, structure and functionality of HDL	MS-based proteomics Lipidomics	[58–64,66]
Association of vascular calcification with accelerated inflammation and the progression of CKD	MS-based proteomics	[67–72]
Relationships between uremic toxins and development of vascular calcification	MS-based proteomics Aptamer-based proteomics Metabolomics	[69,73,74]
The mechanism of inflammation and atherogenesis development in renal and non-renal conditions	MS-based proteomics Transcriptomics Aptamer-based proteomics	[75–79]
The mechanism of VSMC calcification	MS-based proteomics	[80]
Enhanced inflammatory state or inflammation imbalance	MS-based proteomics	[67,68,76,79,81–84]
Disturbances in ECM turnover, endothelial adhesion and transmigration	MS-based proteomics Metabolomics Transcriptomics	[79,84–87]
Dysregulation of hemostasis and coagulation process	MS-based proteomics	[67,68,75,79,81,82,86,87]
The mechanism of hypoxia and oxidative stress	MS-based proteomics Transcriptomics	[84]

3.1. Proteomic and Lipidomic Analyses on Lipid Metabolism in CKD-A

Among the major factors contributing to the risk of atherosclerosis are disturbances in lipid metabolism and transport. In the general population, the high concentration of total cholesterol and its atherogenic fraction, LDL, is associated with the pathogenesis of atherosclerosis and the prevalence of cardiovascular events [88]. Additionally, the low concentration of anti-atherogenic high-density lipoprotein, HDL, is regarded as contributing to the CVD progression [89]. Hypercholesterolemia can be controlled by statins, but this treatment is only partially effective in patients with mild to moderate CKD and does not reduce cardiovascular morbidity and mortality at the advanced stage of CKD [90–92]. Therefore, nature and molecular mechanism(s) behind dyslipidemia seem to be different in CKD, and this phenomenon is called “reverse epidemiology” [20,93]. In fact, the CKD patients are often characterized by hypertriglyceridemia, which is consistent with symptoms observed in “classical” CVD, however, low total cholesterol, HDL and normal or even low LDL concentration are often observed [94]. Unique dyslipidemia distinguishing patients with atherosclerosis-related and nonrelated to CKD has recently been presented utilizing a shotgun lipidomics approach [57]. The putative functional link between the low cholesterol level correlated with kidney dysfunction supports the postulated “reverse epidemiology”. On the other hand, the upregulation of triacylglycerols in CKD and downregulation of cholesterol/cholesteryl esters, sphingomyelins, phosphatidylcholines, phosphatidylethanolamines and ceramides as compared to CVD group underlines the differences between CKD-A and “classical” CVD.

In addition, proteomic approaches have proven to be very useful in elucidation and providing insights into these alterations in CKD. In CVD non-related to kidney dysfunction, HDL particles have strong anti-inflammatory, antioxidant and antithrombotic properties [89,95]. On the other hand, many proteomic studies suggested that HDL may become dysfunctional or even pro-inflammatory in CKD due to chemical modification or remodeling of its protein composition [58–62]. Among others, the changes in the HDL proteome in ESRD patients in comparison to control subjects were identified and linked with the dysregulation of lipoprotein metabolism, immune response, or platelet activation [61,62]. Moreover, altered protein components of HDL were positively correlated with vascular calcification in CKD and this phenomenon was also related to atherosclerosis progression and CKD severity [63,68]. More importantly, similar alterations in HDL protein composition were identified when plasma proteome of CKD patients was compared to non-renal CVD patients, suggesting dysfunctionality of HDL [64]. Combination of global proteomic profiling with bioinformatics and functional studies of monocytes, together with physiological experiments and validation of obtained results, confirmed defective anti-inflammatory activity of HDL in ESRD patients [60]. Therefore, a link between dysfunctional character of HDL, enhanced inflammation and cardiovascular mortality in CKD was indicated. Complementary proteomic approach based on screening and targeted mass spectrometry demonstrated that the protein cargo of HDL was significantly altered in ESRD subjects [61]. The changes in HDL proteome were furthermore accompanied by derangements in HDL lipid composition, mainly by decreased phospholipid and increased triglyceride content as related with functional impairment of HDL in CKD patients [59]. By utilizing the targeted proteomic approach for analysis of HDL fraction in CKD, it was shown that HDL might also lose its atheroprotective functionality evoked by chemical modifications, such as acylation or palmitoylation that negatively affect reverse cholesterol transport, and can be associated with the high cholesterol efflux [66,96,97]. Recent studies have demonstrated that oxidative stress can modify the HDL protein components leading to dysfunctionality of HDL, and thus to non-effective cholesterol efflux and atherosclerosis acceleration [98,99]. Aforementioned changes in HDL composition were not identified in “classical” CVD, but the opposite situation was observed, i.e., the low level of apo A-IV is one of the important factors affecting atherosclerosis development, whereas in CKD the inverse correlation was demonstrated [61,68,100].

Summarizing, comprehensive “omics” approaches supplemented with Gene Ontology analysis and biochemical, and physiological studies revealed that HDL-related dyslipidemia in CKD patients seems not to be related to the HDL level but rather to its chemical nature and thus functional impairment reflected in deficiency of anti-atherogenic and anti-inflammatory properties. As a result, a decline in the cardioprotective features of HDL is observed in CKD, in contrast to “classical” CVD.

Disturbances related to lipids and lipoproteins in kidney disease revealed by comprehensive “omics” approaches were demonstrated not only for HDL plasma particles. The application of multiomics study of murine kidney, combining transcriptomics, high-throughput label-free proteomics, and metabolomics coupled with bioinformatic analysis, confirmed a significant alterations in gene expression levels and protein abundance, primarily of those involved in lipid metabolism [65]. In addition, downregulation of total phosphatidylcholines, phosphatidylethanolamines, and sphingomyelins in age-related CKD mice was revealed, and the vitamin A pathway was implicated in this process.

3.2. “Omics” Strategies to Decipher the Vascular Calcification Mechanism in CKD-A

The vascular calcification, as a pathological deposition of calcium and phosphorus derivatives and other mineral substances in the arterial wall, constitutes the other common metabolic derangement that contributes to the development of CKD-related atherosclerosis [101]. Although, calcification is also observed in “classical” CVD [102], this process seems to be more frequent and extensive in CKD patients due to often occurring mineral and bone disorders and also has prognostic implications [103,104]. Nevertheless, its mech-

anism remains elusive. Proteomic approaches to tackle the relationship between vascular calcification and atherosclerosis progression in CKD have been undertaken [69–72]. These studies revealed that vascular calcification is strongly connected with accelerated inflammation [70], and associated with the progression of CKD [67,68,70,105]. Both the vascular calcification and inflammation are strongly exacerbated by uremia and circulating in the blood uremic toxins, i.e., indoxyl sulfate (IS) and p-cresyl sulfate (pCS) [106–108]. Exposure of cells to serum uremic toxins in CKD results in morphological alterations and vascular calcification linked with CKD-related atherosclerosis [72,109].

The accumulation of uremia-related factors has been demonstrated to evoke vascular dysfunction in animals and humans with CKD, and was associated with the higher mortality and CVD progression in CKD patients [75,110–113]. The application of the isobaric tag for relative and absolute quantitation (iTRAQ) label-based proteomics to understand the global alterations during IS- and pCS-treatment revealed that coagulation pathways, hyperglycemia and insulin resistance accompany the development of arterial calcification in CKD model [73]. The deeper insight into the mechanism of IS influence on a pro-inflammatory phenotype and thus atherogenesis in CKD has been proposed by Nakano and co-workers [74]. In this elegant example of integrated “omics” approach, the authors combined global proteomics and transcriptomic analysis to confirm that IS induces inflammation in macrophages of CKD patients. The bioinformatic analyses were used to identify the signaling mechanisms responsible for observed activation of macrophages, and as a result the Notch signaling and the ubiquitin-proteasome pathways were identified. Comprehensive validation on the transcriptome and proteome levels, using Western blotting, flow cytometry and microscope analyses was performed to independently confirm the observed findings. To address the mechanism of disturbed signaling and proteasome pathways, the authors utilized in-depth mechanistic analysis *in vitro* and *in vivo*, comprising CKD cell lines and mouse model to follow the molecular events underlying the studied processes. Finally, utilizing siRNA-based silencing technique they identified the particular molecules responsible for transport of IS and its induced effect of the inflammatory processes in macrophages. The presented study constitutes the perfect systems biology approach, combining the number of genomic, transcriptomic and proteomic techniques together with bioinformatics for elucidation of molecular mechanism behind IS-induced inflammation, leading to the progression of atherosclerosis in CKD.

Phosphate can be considered as another uremic toxin involved in vascular calcification, and thus arteriosclerosis and an increased risk of cardiovascular mortality [114]. In CKD, this phenomenon is uniquely functionally related to fibroblast growth factor-23 (FGF23) that strongly increases phosphate level and thus evokes toxic effects on the endothelium and cardiovascular system. The positive correlation between elevated serum FGF23 levels and CVD events, and mortality in ESRD patients has been demonstrated [115]. By utilizing comprehensive analyses based on aptamer-based proteomic platform, combined with the high-throughput metabolomics, glycerol-3-phosphate has been revealed as a potential kidney-derived modulator responsible for the FGF23-mediated disturbances in phosphate homeostasis in humans [69]. Moreover, application of genome editing technology, and *in vitro* and *in vivo* mechanistic analysis conducted on cell lines and mouse model resulted in elucidation of a sequence of physiological events underlying this mechanism. This finding provided evidence necessary to understand the molecular mechanism of hyperphosphatemia during the kidney injury and its effect on the vascular system. Moreover, it has also suggested a new therapeutic strategy in atherosclerosis related to kidney disease [69]. Therefore, an evidence supporting the effects of uremic toxins on vascular dysfunction and the progression of atherosclerosis is available, although, the mechanism leading to CVD is not yet fully elucidated.

It has been also suggested that in patients with ESRD, vascular calcification is mediated by decreased ability of vascular smooth muscle cells (VSMCs) to inhibit mineralization process due to vesicle-mediated mechanism [116]. Global proteomic approach in combination with bioinformatics and advanced mechanistic analysis *in vitro* were utilized to

investigate the regulation of matrix vesicles biogenesis in VSMC calcification [80]. The authors demonstrated and validated that VSMC-derived exosomes were involved in this process, and indicated disturbances in calcium ions homeostasis, cell adhesion and motion, and regulation of cell death as the key processes responsible for the observed phenotype. They confirmed the *in vitro* results utilizing the aortic samples from ESRD patients to present exosomes deposited in pre-calcified vessels and suggested a potential mechanism of the VSMC calcification in CKD, due to increased exosomes release at sites of vascular injury. This study elegantly demonstrated a mechanism that links calcification with the development of CKD-related atherosclerosis.

In another interesting study, the authors utilized “omics” approaches, including proteomics, transcriptomics, metabolomics combined with Gene Ontology analyses to evaluate how the monocyte genome responds to the up- and down-regulation of a miR-223 which is a pleiotropic inflammatory regulator of metabolic-related diseases, including CKD [117]. These results indicate that miR-223 alters osteoclastogenesis and macrophage differentiation via the targeting, among others, the NF- κ B pathway and implicates in the progression of calcification process.

3.3. Proteomics and Metabolomics in Analysis of Inflammation and Endothelial Dysfunction in CKD-A

The dysfunctional impact of uremic toxins on vascular endothelium plays an important role in CKD-A progression. Due to endothelial dysfunction caused in CKD by inflammation or oxidative stress, the disturbances in cell activation, adhesion and migration occur, and in consequence structural integrity of extracellular matrix (ECM) is altered [118–120]. As a result, atherosclerosis and CVD accelerate. Translational proteomic studies have been used to demonstrate the changes occurring in endothelial cells under uremic serum exposure [85,86]. The mechanisms evoked by uremic factors on the endothelial dysfunction and thus atherosclerosis were closely linked to enhanced oxidative stress and induction of pro-thrombotic, pro-inflammatory, and pro-proliferative state. Moreover, histone deacetylase (HDAC), as a key modulator of the uremic-induced endothelial phenotype has been identified [86]. In addition, the authors proposed defibrotide as an endothelial protective compound demonstrating the inhibitory effect on HDAC up-regulation related to uremic medium and suggested the possible mechanism of this inhibition [86].

Combination of metabolomic and proteomic approaches fortified with advanced statistics has also added a piece of a puzzle to this story. Nkuipou-Kenfack et al. [87] pinpointed the alterations in the ECM turnover and fibrosis that occur in the advanced stage of CKD and further enriched the landscape of CKD-A molecular mechanisms. Enhanced endothelial adhesion and transmigration in the uremic conditions have also been demonstrated in study of Trojanowicz and co-workers [121]. The authors exposed a link between ECM, adhesion, transmigration and inflammatory communication signaling pathways and the atherosclerosis progression in CKD. Another insight into these mechanisms derived from a proteomics has been given by Glorieux et al. [81]. In this study, 2054 proteins were identified, and 333 of them displayed an altered abundance in ESRD plasma. The selected results were further verified in an independent cohort of patients using ELISA. Functional analyses performed with IPA and Cytoscape software revealed disturbed pathways related to systemic inflammation, acute phase response, complement and coagulation systems, platelet degranulation, calcium ion-dependent exocytosis, production of nitric oxide and reactive oxygen species. All of these pathways were closely associated with atherosclerosis signaling, moreover, severity of these disturbances correlated with CKD progression [81]. Similar results were presented in our previous studies [67,68,82]. We demonstrated that proteins involved in inflammation, blood coagulation, oxidative stress, vascular damage, and calcification process, exhibited greater alterations in patients with advanced CKD, and that these alterations were connected with progression of atherosclerosis.

Relationship of IS and pCS with 181 cardiovascular-related proteins involved in endothelial function, cell adhesion, complement system, phosphate homeostasis and inflammation, has also been recently analyzed by PEA [75]. Both pCS and IS were positively

associated with the increased risk of acute coronary syndrome and with FGF23, involved in CVD morbidity and mortality in renal patients.

The colon microbiome plays a pivotal role in uremic toxins formation in CKD, including IS and pCS [122]. A deeper understanding of this relationship has been recently demonstrated by comprehensive “omics” analysis in CKD rats [83]. The authors showed an altered composition and reduced diversity of the bacterial population, especially depletion of the anti-inflammatory bacteria, as a major cause of inflammation imbalance. These findings were related to changes in blood pressure and kidney parameters, and accompanied by marked alteration of plasma metabolites linked to the inflammation, oxidative stress and metabolism of lipids, amino acids and polyamines. Importantly, possible therapeutic strategy was proposed as treatment with poricoic acid A and fungus *Poria cocos* (*Wolfiporia extensa*) that manipulated microbial dysbiosis and attenuated hypertension, oxidative stress, inflammation, and decline of the renal function in CKD rat model. Finally, some of these results were successfully validated with Western blotting and immunohistochemistry. A relationship between uremic toxins, inflammation, CKD and CVD has been suggested by another, comprehensive “omics” study [76]. In this multi-proteomics approach the global changes in mouse kidney proteome and phosphoproteome upon septic infection were analyzed. Among others, the authors demonstrated that pathways associated with oxidative stress and pyroptosis regulate observed kidney dysfunction. A detailed characterization of the role of inflammation and mechanistic insights into sepsis-associated kidney disease were revealed.

Another interesting study has recently been presented by Yang et al. [77] utilizing modified aptamer based-technology. The authors with IPA software recognized cardiovascular and renal disease-related pathways for the 217 proteins correlated with eGFR, including angiogenesis, control of blood pressure and cardiac fibrosis. Thus, an introduction to the biological basis of cardiovascular relationships with renal and non-renal conditions has been demonstrated. However, taking into account that 1130 individual proteins were measured in this excellent study, in 938 plasma samples, many of these data were unexploited. A few protein predictors of cardiovascular mortality in ESRD patients has been demonstrated recently in the study based on PEA [78]. Nevertheless, majority of data that could have been explored by in-depth bioinformatics were completely omitted.

Specific attention should also be given to diabetes, as a factor strongly associated with the inflammation and development of both CKD and CVD [123]. Although the kidney function decline is one of the most frequent complications in diabetes, nephropathy itself leads also to cardiovascular disease. The relationship between diabetes and CKD has been extensively reviewed, e.g., [124,125]. The pathological link between diabetes and atherosclerosis is also well-documented by others [126]. While the large number of proteomic or even multiomics investigations of diabetic kidney disease (DKD) have been presented, our knowledge about these mechanisms is limited [127–129]. This is mainly because diabetes is linked also with a variety of other comorbidities. Thus, studies on atherosclerosis in DKD pose a challenge since it is difficult to separate the effects and reasons behind CKD and CVD, and other atherogenic factors in diabetic patients shall be taken into account. Therefore, the analysis non-diabetic CKD patients seems to be more appropriate, to understand the mechanisms accompanying the progression of atherosclerosis.

3.4. The Potential and Future Perspectives of “Omics” Approaches in Understanding Molecular Mechanism of CKD-A

Proteomic analyses of CKD-A offer considerable opportunity in terms of type of samples. A lot of CKD and CKD-A proteomic studies focus on plasma [81,130], and serum [131], although urine comprises the most commonly used type of sample [132,133]. Proteomics of kidney tissue is doable in animal models [134], but in humans such analysis requires taking a tissue biopsy that is difficult to obtain due to clinical or ethical reasons. However, analysis of vessel/aorta samples deriving from surgical interventions in CKD and CVD patients might be useful source of information, especially in the context of

calcification process [80]. Unfortunately, these studies are mainly limited to CVD not related to kidney dysfunction so far [135,136].

Additionally, the very low number of proteomic studies was conducted utilizing blood cells, especially leukocytes. As mentioned above, CKD and CVD are closely related to alterations in inflammatory processes, and several researchers demonstrated that plasma/serum proteins involved in inflammation exhibited significant alterations in both diseases [137,138]. However, our previous studies indicated an upregulation of systemic inflammation during CKD development and confirmed that this phenomenon is more pronounced in CKD as compared to the “classical” CVD [68]. Therefore, leukocytes shall be considered as a next source of greater importance in proteomic studies on CKD-A. Scholze and co-workers have analyzed monocytes in non-dialyzed and dialyzed CKD patients, but large-scale “omics” studies have not been performed [139]. Recently, we have demonstrated a complementary proteomic approach to assess CKD and “classical” CVD with distinct atherosclerosis progression. A label-free approach based on LC-MS/MS and functional bioinformatic analyses were used to profile CKD and CVD leukocyte proteins. The dysregulation of proteins involved in different phases of leukocytes’ transmigration process and upregulation of apoptosis-related proteins in CKD as compared to CVD, was presented [79]. We suggested that the disturbances in leukocyte extravasation proteins may alter cell integrity and trigger cell death at the advanced stage of CKD. Importantly, the obtained results were validated by MRM, ELISA, Western blotting, and at the mRNA level by ddPCR and flow cytometry and microscopy analyses.

Similarly, platelets might represent a valuable resource for global/targeted “omics” studies. Dysregulation of coagulation cascade and related proteins has been presented multiple times utilizing patients’ plasma material [68,73,81,82], but according to our knowledge only one study has utilized proteomics on CKD platelets [140]. In this work, the authors demonstrated the alterations in cytoskeletal proteins, presence of the oxidative stress and cell interactions in uremic platelets, the processes also linked with atherosclerosis. Therefore, there is a large hidden potential in the “omics” studies of vessel samples, leukocytes and platelets in CKD-A. Thus, an ideal comprehensive “omics” approach to elucidate the mechanisms behind CKD-A should utilize several types of samples in one study. All mentioned types of samples may easily be analyzed with different proteomic approaches, including LC-MS, CE-MS or, already used less frequently: 2-DE and subsequent MS-based analyses.

Comprehensive proteomic approach, based on different sample specimens and analyzing CKD progression, has very recently been presented by Kim et al. [84]. The authors combined searches of potential urine CKD biomarkers with an analysis of mechanisms underlying the progression from CKD to ESRD. They utilized label-free and label-based quantitative proteomic approaches to investigate the urine proteome changes in the material derived from patients with different stage of CKD progression and rat kidney tissues with moderate-to-severe renal failure. Furthermore, human primary glomerular and proximal tubular epithelial cells were analyzed under hypoxia and normoxia. As a result, proteins related to CKD progression were identified and confirmed by Western blotting, qRT-PCR, and immunohistochemistry. More than 2900 DEPs were identified and utilized for the analysis of cellular pathways and protein-protein interactions associated with CKD severity. Unsurprisingly, immune response and inflammatory processes were upregulated, whereas cell adhesion and migration revealed down-regulation in urine of advanced CKD. Interestingly, activation of cell movement, cell survival, inflammatory response and organization of cytoskeleton, and significant inhibition of fatty acid and nucleic acid metabolism, and regulation of mRNA processing were revealed in injured kidney tissue in rat model. These results were fortified with comprehensive elaboration of proteomic changes associated with fibrosis in hypoxia-treated epithelial cells. This multi-sample proteomics study provides an ideal combination of multiomics approach, and in vitro or in vivo analyses targeting the mechanisms and processes involved in disease progression.

The ongoing rapid development of high-throughput proteomic technologies raises our capacity of large-scale studies leading to the identification/quantification of an increasing number of involved proteins. Since the origination of the proteomics concept, a huge volume of proteomics data has been collected, resulting in rapid development of a plethora of various proteomic bioinformatic platforms and computational tools, including machine-learning approaches. Bioinformatic analysis of biological functions and signaling pathways in the context of their mutual relationships is the foundation for elucidating the molecular mechanisms underlying the disease development and progression. Many high-throughput proteomic studies generating a large datasets involving hundreds to thousands of proteins in a single experiment have been demonstrated also in CKD [45,77,78,141,142]. Unfortunately, despite an unlimited potential and possibilities of these studies, the authors mainly focused on individual proteins/biomarkers. In our view, scrutinizing of a measured protein dataset in comprehensive bioinformatics surveys shall rather serve towards the holistic realization of systems biology approaches, combined with more targeted, functional analysis. This strategy might be useful for providing the complete depiction of molecular mechanisms in CKD-A.

There is also a need to improve the transparency in “omics” research, by including the availability of the raw data and protocols that should be accessible for further use by other scientists. However, due to the complexity of hosting and integration of complete “omics” datasets there is currently no public repository for multiomics data and this limitation has recently been reviewed [143]. Such a multi-platform would add a new possibility and boost a potential of multi-dimensional analysis of diseases. Moreover, to learn how genes, proteins and metabolites interact and influence on CKD-A molecular mechanism(s), new software for integration and analysis of multiomics data should be developed and optimized.

4. Conclusions

Despite the failure of proteomics attempts to recognize useful clinical biomarkers in CKD, a number of lessons were learned during these studies, including elaboration of standard protocols for sample proper collection, processing and storage [144]. Moreover, there are enormous, unexploited and already existing datasets derived from multiple CKD-related studies that can be adopted in a meta-analysis utilizing functional bioinformatics in the context of processes and pathways altered during CKD-A acceleration. Combining and a post hoc analysis of these data can provide a systematic picture of CKD-A and elucidation of mechanisms involved in the development of atherosclerosis.

Another unexplored area in CKD-A “omics” analysis relates to leukocyte and platelet as fractions of blood cells strongly associated with inflammatory or coagulation processes and oxidative stress, with suggested involvement in CKD-A development.

Ultimately, although, the close connection between kidney dysfunction and atherosclerosis is widely recognized, and differences between “classical” CVD and CKD-A are underlined, almost all demonstrated studies rely on analysis of either CKD or CVD patients. Taking into account that, especially early stage CKD patients, reveal the same symptoms and take similar medications as non-renal CVD patients, in-depth analysis of both entities conducted in one study may provide more meaningful information about unique character of CKD-A. Interpretation of these results will help in better understanding of the complex pathophysiology and provide novel insights into CKD-A complexity.

Author Contributions: Conceptualization, M.L.; writing—original draft preparation, J.T.; writing—review and editing, M.L.; visualization, J.T.; supervision, M.L.; funding acquisition, M.L. Both authors have read and agreed to the published version of the manuscript.

Funding: This research was funded by the National Science Centre, Poland under Grant No. 2015/19/B/ NZ2/02450), to M.L.

Acknowledgments: The authors wish to acknowledge Maciej Lalowski for critical reading of the manuscript. The figures were generated using the web-based tool BioRender (BioRender.com; accessed on 16 March 2021).

Conflicts of Interest: The authors declare no conflict of interest.

References

1. Levin, A.; Stevens, P.E.; Bilous, R.W.; Coresh, J.; De Francisco, A.L.M.; De Jong, P.E.; Griffith, K.E.; Hemmelgarn, B.R.; Iseki, K.; Lamb, E.J.; et al. Kidney disease: Improving global outcomes (KDIGO) CKD work group. KDIGO 2012 clinical practice guideline for the evaluation and management of chronic kidney disease. *Kidney Int. Suppl.* **2013**, *3*, 1–150. [[CrossRef](#)]
2. UK, National Clinical Guideline Centre. *Chronic Kidney Disease (Partial Update): Early Identification and Management of Chronic Kidney Disease in Adults in Primary and Secondary Care*; National Institute for Health and Care Excellence: London, UK, 2014.
3. Webster, A.C.; Nagler, E.V.; Morton, R.L.; Masson, P. Chronic Kidney Disease. *Lancet* **2017**, *389*, 1238–1252. [[CrossRef](#)]
4. Bikbov, B.; Purcell, C.A.; Levey, A.S.; Smith, M.; Abdoli, A.; Abebe, M.; Adebayo, O.M.; Afarideh, M.; Agarwal, S.K.; Agudelo-Botero, M.; et al. Global, regional, and national burden of chronic kidney disease, 1990–2017: A systematic analysis for the Global Burden of Disease Study 2017. *Lancet* **2020**, *395*, 709–733. [[CrossRef](#)]
5. Roth, G.A.; Abate, D.; Abate, K.H.; Abay, S.M.; Abbafati, C.; Abbasi, N.; Abastabar, H.; Abd-Allah, F.; Abdela, J.; Abdelalim, A.; et al. Global, regional, and national age-sex-specific mortality for 282 causes of death in 195 countries and territories, 1980–2017: A systematic analysis for the Global Burden of Disease Study 2017. *Lancet* **2018**, *392*, 1736–1788. [[CrossRef](#)]
6. Naylor, K.L.; Kim, S.J.; McArthur, E.; Garg, A.X.; McCallum, M.K.; Knoll, G.A. Mortality in Incident Maintenance Dialysis Patients Versus Incident Solid Organ Cancer Patients: A Population-Based Cohort. *Am. J. Kidney Dis.* **2019**, *73*, 765–776. [[CrossRef](#)] [[PubMed](#)]
7. Cockwell, P.; Fisher, L.-A. The global burden of chronic kidney disease. *Lancet* **2020**, *395*, 662–664. [[CrossRef](#)]
8. Vallianou, N.G.; Mitesh, S.; Gkogkou, A.; Geladari, E. Chronic Kidney Disease and Cardiovascular Disease: Is there Any Relationship? *Curr. Cardiol. Rev.* **2019**, *15*, 55–63. [[CrossRef](#)]
9. Gansevoort, R.T.; Correa-Rotter, R.; Hemmelgarn, B.R.; Jafar, T.H.; Heerspink, H.J.L.; Mann, J.F.; Matsushita, K.; Wen, C.P. Chronic kidney disease and cardiovascular risk: Epidemiology, mechanisms, and prevention. *Lancet* **2013**, *382*, 339–352. [[CrossRef](#)]
10. Wanner, C.; Amann, K.; Shoji, T. The heart and vascular system in dialysis. *Lancet* **2016**, *388*, 276–284. [[CrossRef](#)]
11. Wen, C.P.; Cheng, T.Y.D.; Tsai, M.K.; Chang, Y.C.; Chan, H.T.; Tsai, S.P.; Chiang, P.H.; Hsu, C.C.; Sung, P.K.; Hsu, Y.H.; et al. All-cause mortality attributable to chronic kidney disease: A prospective cohort study based on 462 293 adults in Taiwan. *Lancet* **2008**, *371*, 2173–2182. [[CrossRef](#)]
12. Hemmelgarn, B.R.; Manns, B.J.; Lloyd, A.; James, M.T.; Klarenbach, S.; Quinn, R.R.; Wiebe, N.; Tonelli, M. Alberta Kidney Disease Network Relation between kidney function, proteinuria, and adverse outcomes. *JAMA* **2010**, *303*, 423–429. [[CrossRef](#)] [[PubMed](#)]
13. Schiffrin, E.L.; Lipman, M.L.; Mann, J.F.E. Chronic kidney disease: Effects on the cardiovascular system. *Circulation* **2007**, *116*, 85–97. [[CrossRef](#)] [[PubMed](#)]
14. Liu, M.; Li, X.C.; Lu, L.; Cao, Y.; Sun, R.R.; Chen, S.; Zhang, P.Y. Cardiovascular disease and its relationship with chronic kidney disease. *Eur. Rev. Med. Pharmacol. Sci.* **2014**, *18*, 2918–2926.
15. Libby, P.; Ridker, P.M.; Hansson, G.K. Progress and challenges in translating the biology of atherosclerosis. *Nature* **2011**, *473*, 317–325. [[CrossRef](#)] [[PubMed](#)]
16. Chen, J.; Mohler, E.R.; Xie, D.; Shlipak, M.; Townsend, R.R.; Appel, L.J.; Ojo, A.; Schreiber, M.; Nessel, L.; Zhang, X.; et al. Traditional and non-traditional risk factors for incident peripheral arterial disease among patients with chronic kidney disease. *Nephrol. Dial. Transplant.* **2016**, *31*, 1145–1151. [[CrossRef](#)]
17. Weiner, D.E.; Tighiouart, H.; Elsayed, E.F.; Griffith, J.L.; Salem, D.N.; Levey, A.S.; Sarnak, M.J. The relationship between nontraditional risk factors and outcomes in individuals with stage 3 to 4 CKD. *Am. J. Kidney Dis.* **2008**, *51*, 212–223. [[CrossRef](#)] [[PubMed](#)]
18. Major, R.W.; Cheng, M.R.I.; Grant, R.A.; Shantikumar, S.; Xu, G.; Oozeerally, I.; Brunskill, N.J.; Gray, L.J. Cardiovascular disease risk factors in chronic kidney disease: A systematic review and meta-analysis. *PLoS ONE* **2018**, *13*, e0192895. [[CrossRef](#)]
19. Kendrick, J.; Chonchol, M.B. Nontraditional risk factors for cardiovascular disease in patients with chronic kidney disease. *Nat. Clin. Pract. Nephrol.* **2008**, *4*, 672–681. [[CrossRef](#)]
20. Kalantar-Zadeh, K.; Block, G.; Humphreys, M.H.; Kopple, J.D. Reverse epidemiology of cardiovascular risk factors in maintenance dialysis patients. *Kidney Int.* **2003**, *63*, 793–808. [[CrossRef](#)]
21. Maini, R.; Wong, D.B.; Addison, D.; Chiang, E.; Weisbord, S.D.; Jneid, H. Persistent underrepresentation of kidney disease in randomized, controlled trials of cardiovascular disease in the contemporary era. *J. Am. Soc. Nephrol.* **2018**, *29*, 2782–2786. [[CrossRef](#)]
22. Romagnani, P.; Remuzzi, G.; Glassock, R.; Levin, A.; Jager, K.J.; Tonelli, M.; Massy, Z.; Wanner, C.; Anders, H.-J. Chronic kidney disease. *Nat. Rev. Dis. Prim.* **2017**, *3*, 17088. [[CrossRef](#)] [[PubMed](#)]
23. Daenen, K.; Andries, A.; Mekahli, D.; Schepdael, A.V.; Jouret, F.; Bammens, B. Oxidative stress in chronic kidney disease. *Iran. J. Kidney Dis.* **2015**, *9*, 165. [[CrossRef](#)]
24. Valdivielso, J.M.; Rodríguez-Puyol, D.; Pascual, J.; Barrios, C.; Bermúdez-López, M.; Sánchez-Niño, M.D.; Pérez-Fernández, M.; Ortiz, A. Atherosclerosis in Chronic Kidney Disease. *Arterioscler. Thromb. Vasc. Biol.* **2019**, *39*, 1938–1966. [[CrossRef](#)]
25. Tummalapalli, L.; Nadkarni, G.N.; Coca, S.G. Biomarkers for predicting outcomes in chronic kidney disease. *Curr. Opin. Nephrol. Hypertens.* **2016**, *25*, 480–486. [[CrossRef](#)]

26. Saucedo, A.L.; Perales-Quintana, M.M.; Paniagua-Vega, D.; Sanchez-Martinez, C.; Cordero-Perez, P.; Minsky, N.W. Chronic Kidney Disease and the Search for New Biomarkers for Early Diagnosis. *Curr. Med. Chem.* **2018**, *25*, 3719–3747. [[CrossRef](#)]
27. Taherkhani, A.; Farrokhi Yekta, R.; Mohseni, M.; Saidijam, M.; Arefi Oskouie, A. Chronic kidney disease: A review of proteomic and metabolomic approaches to membranous glomerulonephritis, focal segmental glomerulosclerosis, and IgA nephropathy biomarkers. *Proteome Sci.* **2019**, *17*, 7. [[CrossRef](#)]
28. Mayeux, R. Biomarkers: Potential Uses and Limitations. *NeuroRx* **2004**, *1*, 182–188. [[CrossRef](#)] [[PubMed](#)]
29. Parikh, C.R.; Thiessen-Philbrook, H. Key concepts and limitations of statistical methods for evaluating biomarkers of kidney disease. *J. Am. Soc. Nephrol.* **2014**, *25*, 1621–1629. [[CrossRef](#)]
30. Drucker, E.; Krapfenbauer, K. Pitfalls and limitations in translation from biomarker discovery to clinical utility in predictive and personalised medicine. *EPMA J.* **2013**, *4*, 1–10. [[CrossRef](#)] [[PubMed](#)]
31. Zhang, Z.-Y.; Ravassa, S.; Pejchinovski, M.; Yang, W.-Y.; Züribig, P.; López, B.; Wei, F.-F.; Thijs, L.; Jacobs, L.; González, A.; et al. A Urinary Fragment of Mucin-1 Subunit α is a Novel Biomarker Associated with Renal Dysfunction in the General Population. *Kidney Int. Rep.* **2017**, *2*, 811–820. [[CrossRef](#)]
32. Siwy, J.; Züribig, P.; Argiles, A.; Beige, J.; Haubitz, M.; Jankowski, J.; Julian, B.A.; Linde, P.G.; Marx, D.; Mischak, H.; et al. Noninvasive diagnosis of chronic kidney diseases using urinary proteome analysis. *Nephrol. Dial. Transplant.* **2017**, *32*, 2079–2089. [[CrossRef](#)] [[PubMed](#)]
33. Knoflach, M.; Kiechl, S.; Mantovani, A.; Cuccovillo, I.; Bottazzi, B.; Xu, Q.; Xiao, Q.; Gasperi, A.; Mayr, A.; Kehrer, M.; et al. Pentraxin-3 as a marker of advanced atherosclerosis results from the Bruneck, ARMY and ARFY Studies. *PLoS ONE* **2012**, *7*, e31474. [[CrossRef](#)]
34. Martínez, P.J.; Baldán-Martín, M.; López, J.A.; Martín-Lorenzo, M.; Santiago-Hernández, A.; Agudiez, M.; Cabrera, M.; Calvo, E.; Vázquez, J.; Ruiz-Hurtado, G.; et al. Identification of six cardiovascular risk biomarkers in the young population: A promising tool for early prevention. *Atherosclerosis* **2019**, *282*, 67–74. [[CrossRef](#)]
35. Han, W.K.; Bailly, V.; Abichandani, R.; Thadhani, R.; Bonventre, J.V. Kidney Injury Molecule-1 (KIM-1): A novel biomarker for human renal proximal tubule injury. *Kidney Int.* **2002**, *62*, 237–244. [[CrossRef](#)]
36. Mishra, J.; Qing, M.A.; Prada, A.; Mitsnefes, M.; Zahedi, K.; Yang, J.; Barasch, J.; Devarajan, P. Identification of neutrophil gelatinase-associated lipocalin as a novel early urinary biomarker for ischemic renal injury. *J. Am. Soc. Nephrol.* **2003**, *14*, 2534–2543. [[CrossRef](#)] [[PubMed](#)]
37. Zhang, W.R.; Parikh, C.R. Biomarkers of Acute and Chronic Kidney Disease. *Annu. Rev. Physiol.* **2019**, *81*, 309–333. [[CrossRef](#)]
38. Good, D.M.; Züribig, P.; Argilés, À.; Bauer, H.W.; Behrens, G.; Coon, J.J.; Dakna, M.; Decramer, S.; Delles, C.; Dominiczak, A.F.; et al. Naturally occurring human urinary peptides for use in diagnosis of chronic kidney disease. *Mol. Cell. Proteom.* **2010**, *9*, 2424–2437. [[CrossRef](#)] [[PubMed](#)]
39. Persson, F.; Rossing, P. Urinary Proteomics and Precision Medicine for Chronic Kidney Disease: Current Status and Future Perspectives. *Proteom. Clin. Appl.* **2019**, *13*, 1800176. [[CrossRef](#)] [[PubMed](#)]
40. Moreno, J.A.; Hamza, E.; Guerrero-Hue, M.; Rayego-Mateos, S.; García-Caballero, C.; Vallejo-Mudarra, M.; Metzinger, L.; Metzinger-Le Meuth, V. Non-Coding RNAs in Kidney Diseases: The Long and Short of Them. *Int. J. Mol. Sci.* **2021**, *22*, 6077. [[CrossRef](#)]
41. Mischak, H.; Allmaier, G.; Apweiler, R.; Attwood, T.; Baumann, M.; Benigni, A.; Bennett, S.E.; Bischoff, R.; Bongcam-Rudloff, E.; Capasso, G.; et al. Recommendations for biomarker identification and qualification in clinical proteomics. *Sci. Transl. Med.* **2010**, *2*. [[CrossRef](#)]
42. Gromova, M.; Vaggelas, A.; Dallmann, G.; Seimetz, D. Biomarkers: Opportunities and Challenges for Drug Development in the Current Regulatory Landscape. *Biomark. Insights* **2020**, *15*, 117727192097465. [[CrossRef](#)]
43. Gupta, S.; Venkatesh, A.; Ray, S.; Srivastava, S. Challenges and prospects for biomarker research: A current perspective from the developing world. *Biochim. Biophys. Acta Proteins Proteom.* **2014**, *1844*, 899–908. [[CrossRef](#)]
44. Lundberg, M.; Eriksson, A.; Tran, B.; Assarsson, E.; Fredriksson, S. Homogeneous antibody-based proximity extension assays provide sensitive and specific detection of low-abundant proteins in human blood. *Nucleic Acids Res.* **2011**, *39*, e102. [[CrossRef](#)]
45. Gold, L.; Ayers, D.; Bertino, J.; Bock, C.; Bock, A.; Brody, E.; Carter, J.; Cunningham, V.; Dalby, A.; Eaton, B.; et al. Aptamer-based multiplexed proteomic technology for biomarker discovery. *Nat. Preced.* **2010**. [[CrossRef](#)]
46. Fredriksson, S.; Gullberg, M.; Jarvius, J.; Olsson, C.; Pietras, K.; Gústafsdóttir, S.M.; Ostman, A.; Landegren, U. Protein detection using proximity-dependent DNA ligation assays. *Nat. Biotechnol.* **2002**, *20*, 473–477. [[CrossRef](#)]
47. Assarsson, E.; Lundberg, M.; Holmquist, G.; Björkstén, J.; Thorsen, S.B.; Ekman, D.; Eriksson, A.; Rennel Dickens, E.; Ohlsson, S.; Edfeldt, G.; et al. Homogenous 96-plex PEA immunoassay exhibiting high sensitivity, specificity, and excellent scalability. *PLoS ONE* **2014**, *9*, e95192. [[CrossRef](#)] [[PubMed](#)]
48. Percy, A.J.; Chambers, A.G.; Smith, D.S.; Borchers, C.H. Standardized Protocols for Quality Control of MRM-based Plasma Proteomic Workflows. *J. Proteome Res.* **2013**, *12*, 222–233. [[CrossRef](#)]
49. Rezeli, M.; Sjödin, K.; Lindberg, H.; Gidlöf, O.; Lindahl, B.; Jernberg, T.; Spaak, J.; Erlinge, D.; Marko-Varga, G. Quantitation of 87 Proteins by nLC-MRM/MS in Human Plasma: Workflow for Large-Scale Analysis of Biobank Samples. *J. Proteome Res.* **2017**, *16*, 3242–3254. [[CrossRef](#)] [[PubMed](#)]
50. Schmidt, A.; Forne, I.; Imhof, A. Bioinformatic analysis of proteomics data. *BMC Syst. Biol.* **2014**, *8*, S3. [[CrossRef](#)] [[PubMed](#)]

51. Mi, H.; Muruganujan, A.; Casagrande, J.T.; Thomas, P.D. Large-scale gene function analysis with the panther classification system. *Nat. Protoc.* **2013**, *8*, 1551–1566. [[CrossRef](#)] [[PubMed](#)]
52. Huang, D.W.; Sherman, B.T.; Lempicki, R.A. Systematic and integrative analysis of large gene lists using DAVID bioinformatics resources. *Nat. Protoc.* **2009**, *4*, 44–57. [[CrossRef](#)] [[PubMed](#)]
53. Kamburov, A.; Wierling, C.; Lehrach, H.; Herwig, R. ConsensusPathDB—A database for integrating human functional interaction networks. *Nucleic Acids Res.* **2009**, *37*, D623–D628. [[CrossRef](#)] [[PubMed](#)]
54. Schwanhüsser, B.; Busse, D.; Li, N.; Dittmar, G.; Schuchhardt, J.; Wolf, J.; Chen, W.; Selbach, M. Global quantification of mammalian gene expression control. *Nature* **2011**, *473*, 337–342. [[CrossRef](#)] [[PubMed](#)]
55. Edfors, F.; Danielsson, F.; Hallström, B.M.; Käll, L.; Lundberg, E.; Pontén, F.; Forsström, B.; Uhlén, M. Gene-specific correlation of RNA and protein levels in human cells and tissues. *Mol. Syst. Biol.* **2016**, *12*, 883. [[CrossRef](#)]
56. Venturini, G.; Malagrino, P.A.; Padilha, K.; Tanaka, L.Y.; Laurindo, F.R.; Dariolli, R.; Carvalho, V.M.; Cardozo, K.H.M.; Krieger, J.E.; Pereira, A.d.C. Integrated proteomics and metabolomics analysis reveals differential lipid metabolism in human umbilical vein endothelial cells under high and low shear stress. *Am. J. Physiol. Cell Physiol.* **2019**, *317*, C326–C338. [[CrossRef](#)]
57. Marczak, L.; Idkowiak, J.; Tracz, J.; Stobiecki, M.; Perek, B.; Kostka-Jeziorny, K.; Tykarski, A.; Wanic-Kossowska, M.; Borowski, M.; Osuch, M.; et al. Mass spectrometry-based lipidomics reveals differential changes in the accumulated lipid classes in chronic kidney disease. *Metabolites* **2021**, *11*, 275. [[CrossRef](#)] [[PubMed](#)]
58. Rubinow, K.B.; Henderson, C.M.; Robinson-Cohen, C.; Himmelfarb, J.; de Boer, I.H.; Vaisar, T.; Kestenbaum, B.; Hoofnagle, A.N. Kidney function is associated with an altered protein composition of high-density lipoprotein. *Kidney Int.* **2017**, *92*, 1526–1535. [[CrossRef](#)]
59. Holzer, M.; Birner-Gruenberger, R.; Stojakovic, T.; El-Gamal, D.; Binder, V.; Wadsack, C.; Heinemann, A.; Marsche, G. Uremia alters HDL composition and function. *J. Am. Soc. Nephrol.* **2011**, *22*, 1631–1641. [[CrossRef](#)]
60. Weichhart, T.; Kopecky, C.; Kubicek, M.; Haidinger, M.; Döllner, D.; Katholnig, K.; Suarna, C.; Eller, P.; Tölle, M.; Gerner, C.; et al. Serum amyloid A in uremic HDL promotes inflammation. *J. Am. Soc. Nephrol.* **2012**, *23*, 934–947. [[CrossRef](#)]
61. Shao, B.; De Boer, I.; Tang, C.; Mayer, P.S.; Zelnick, L.; Afkarian, M.; Heinecke, J.W.; Himmelfarb, J. A Cluster of Proteins Implicated in Kidney Disease Is Increased in High-Density Lipoprotein Isolated from Hemodialysis Subjects. *J. Proteome Res.* **2015**, *14*, 2792–2806. [[CrossRef](#)]
62. Mangé, A.; Goux, A.; Badiou, S.; Patrier, L.; Canaud, B.; Maudelonde, T.; Cristol, J.-P.; Solassol, J. HDL proteome in hemodialysis patients: A quantitative nanoflow liquid chromatography-tandem mass spectrometry approach. *PLoS ONE* **2012**, *7*, e34107. [[CrossRef](#)] [[PubMed](#)]
63. Gordon, S.M.; Chung, J.H.; Playford, M.P.; Dey, A.K.; Sviridov, D.; Seifuddin, F.; Chen, Y.C.; Pirooznia, M.; Chen, M.Y.; Mehta, N.N.; et al. High density lipoprotein proteome is associated with cardiovascular risk factors and atherosclerosis burden as evaluated by coronary CT angiography. *Atherosclerosis* **2018**, *278*, 278–285. [[CrossRef](#)]
64. Luczak, M.; Formanowicz, D.; Marczak, L.; Suszyńska-Zajczyk, J.; Pawliczak, E.; Wanic-Kossowska, M.; Stobiecki, M. ITRAQ-based proteomic analysis of plasma reveals abnormalities in lipid metabolism proteins in chronic kidney disease-related atherosclerosis. *Sci. Rep.* **2016**, *6*, 32511. [[CrossRef](#)] [[PubMed](#)]
65. Braun, F.; Rinschen, M.M.; Bartels, V.; Frommolt, P.; Habermann, B.; Hoeijmakers, J.H.J.; Schumacher, B.; Dollé, M.E.T.; Müller, R.-U.; Benzing, T.; et al. Altered lipid metabolism in the aging kidney identified by three layered omic analysis. *Ageing* **2016**, *8*, 441–457. [[CrossRef](#)] [[PubMed](#)]
66. Seckler, H.D.S.; Fornelli, L.; Mutharasan, R.K.; Thaxton, C.S.; Fellers, R.; Daviglius, M.; Sniderman, A.; Rader, D.; Kelleher, N.L.; Lloyd-Jones, D.M.; et al. A Targeted, Differential Top-Down Proteomic Methodology for Comparison of ApoA-I Proteoforms in Individuals with High and Low HDL Efflux Capacity. *J. Proteome Res.* **2018**, *17*, 2156–2164. [[CrossRef](#)] [[PubMed](#)]
67. Luczak, M.; Formanowicz, D.; Marczak, L.; Pawliczak, E.; Wanic-Kossowska, M.; Figlerowicz, M.; Stobiecki, M. Deeper insight into chronic kidney disease-related atherosclerosis: Comparative proteomic studies of blood plasma using 2DE and mass spectrometry. *J. Transl. Med.* **2015**, *13*, 20. [[CrossRef](#)]
68. Luczak, M.; Suszynska-Zajczyk, J.; Marczak, L.; Formanowicz, D.; Pawliczak, E.; Wanic-Kossowska, M.; Stobiecki, M. Label-free quantitative proteomics reveals differences in molecular mechanism of atherosclerosis related and non-related to chronic kidney disease. *Int. J. Mol. Sci.* **2016**, *17*, 631. [[CrossRef](#)]
69. Simic, P.; Kim, W.; Zhou, W.; Pierce, K.A.; Chang, W.; Sykes, D.B.; Aziz, N.B.; Elmariah, S.; Ngo, D.; Pajevic, P.D.; et al. Glycerol-3-phosphate is an FGF23 regulator derived from the injured kidney. *J. Clin. Investig.* **2020**, *130*, 1513–1526. [[CrossRef](#)]
70. Mihai, S.; Codrici, E.; Popescu, I.D.; Enciu, A.-M.; Rusu, E.; Zilisteanu, D.; Albulescu, R.; Anton, G.; Tanase, C. Proteomic Biomarkers Panel: New Insights in Chronic Kidney Disease. *Dis. Markers* **2016**, *2016*, 3185232. [[CrossRef](#)]
71. Oliveira, E.; Araújo, J.E.; Gómez-Meire, S.; Lodeiro, C.; Perez-Melon, C.; Iglesias-Lamas, E.; Otero-Glez, A.; Capelo, J.L.; Santos, H.M. Proteomics analysis of the peritoneal dialysate effluent reveals the presence of calciumregulation proteins and acute inflammatory response. *Clin. Proteom.* **2014**, *11*. [[CrossRef](#)]
72. Wang, C.; Tang, Y.; Wang, Y.; Li, G.; Wang, L.; Li, Y. Label-free quantitative proteomics identifies Smarca4 is involved in vascular calcification. *Ren. Fail.* **2019**, *41*, 220–228. [[CrossRef](#)] [[PubMed](#)]
73. Opdebeeck, B.; Maudsley, S.; Azmi, A.; De Maré, A.; De Leger, W.; Meijers, B.; Verhulst, A.; Evenepoel, P.; D’Haese, P.C.; Neven, E. Indoxyl Sulfate and p-Cresyl Sulfate Promote Vascular Calcification and Associate with Glucose Intolerance. *J. Am. Soc. Nephrol.* **2019**, *30*, 751–766. [[CrossRef](#)]

74. Nakano, T.; Katsuki, S.; Chen, M.; Decano, J.L.; Halu, A.; Lee, L.H.; Pestana, D.V.S.; Kum, A.S.T.; Kuromoto, R.K.; Golden, W.S.; et al. Uremic Toxin Indoxyl Sulfate Promotes Proinflammatory Macrophage Activation Via the Interplay of OATP2B1 and Dll4-Notch Signaling: Potential Mechanism for Accelerated Atherogenesis in Chronic Kidney Disease. *Circulation* **2019**, *139*, 78–96. [[CrossRef](#)] [[PubMed](#)]
75. Wu, P.-H.; Lin, Y.-T.; Chiu, Y.-W.; Baldanzi, G.; Huang, J.-C.; Liang, S.-S.; Lee, S.-C.; Chen, S.-C.; Hsu, Y.-L.; Kuo, M.-C.; et al. The relationship of indoxyl sulfate and p-cresyl sulfate with target cardiovascular proteins in hemodialysis patients. *Sci. Rep.* **2021**, *11*, 3786. [[CrossRef](#)]
76. Lin, Y.H.; Platt, M.P.; Fu, H.; Gui, Y.; Wang, Y.; Gonzalez-Juarbe, N.; Zhou, D.; Yu, Y. Global Proteome and Phosphoproteome Characterization of Sepsis-induced Kidney Injury. *Mol. Cell. Proteom.* **2020**, *19*, 2030–2046. [[CrossRef](#)]
77. Yang, J.; Brody, E.N.; Murthy, A.C.; Mehler, R.E.; Weiss, S.J.; DeLisle, R.K.; Ostroff, R.; Williams, S.A.; Ganz, P. Impact of Kidney Function on the Blood Proteome and on Protein Cardiovascular Risk Biomarkers in Patients With Stable Coronary Heart Disease. *J. Am. Heart Assoc.* **2020**, *9*, e016463. [[CrossRef](#)]
78. Feldreich, T.; Nowak, C.; Fall, T.; Carlsson, A.C.; Carrero, J.J.; Ripsweden, J.; Qureshi, A.R.; Heimbürger, O.; Barany, P.; Stenvinkel, P.; et al. Circulating proteins as predictors of cardiovascular mortality in end-stage renal disease. *J. Nephrol.* **2019**, *32*, 111–119. [[CrossRef](#)]
79. Tracz, J.; Handschuh, L.; Lalowski, M.; Marczak, Ł.; Kostka-Jeziorny, K.; Perek, B.; Wanic-Kossowska, M.; Podkowińska, A.; Tykarski, A.; Formanowicz, D.; et al. Proteomic Profiling of Leukocytes Reveals Dysregulation of Adhesion and Integrin Proteins in Chronic Kidney Disease-Related Atherosclerosis. *J. Proteome Res.* **2021**, *20*, 3067. [[CrossRef](#)]
80. Kapustin, A.N.; Chatrou, M.L.L.; Drozdov, I.; Zheng, Y.; Davidson, S.M.; Soong, D.; Furmanik, M.; Sanchis, P.; De Rosales, R.T.M.; Alvarez-Hernandez, D.; et al. Vascular Smooth Muscle Cell Calcification Is Mediated by Regulated Exosome Secretion. *Circ. Res.* **2015**, *116*, 1312–1323. [[CrossRef](#)] [[PubMed](#)]
81. Glorieux, G.; Mullen, W.; Durantou, F.; Filip, S.; Gayraud, N.; Husi, H.; Schepers, E.; Neiryneck, N.; Schanstra, J.P.; Jankowski, J.; et al. New insights in molecular mechanisms involved in chronic kidney disease using high-resolution plasma proteome analysis. *Nephrol. Dial. Transplant.* **2015**, *30*, 1842–1852. [[CrossRef](#)]
82. Luczak, M.; Formanowicz, D.; Pawliczak, E.; Wanic-Kossowska, M.; Wykretowicz, A.; Figlerowicz, M. Chronic kidney disease-related atherosclerosis—Proteomic studies of blood plasma. *Proteome Sci.* **2011**, *9*, 25. [[CrossRef](#)]
83. Feng, Y.L.; Cao, G.; Chen, D.Q.; Vaziri, N.D.; Chen, L.; Zhang, J.; Wang, M.; Guo, Y.; Zhao, Y.Y. Microbiome–metabolomics reveals gut microbiota associated with glycine-conjugated metabolites and polyamine metabolism in chronic kidney disease. *Cell. Mol. Life Sci.* **2019**, *76*, 4961–4978. [[CrossRef](#)]
84. Kim, J.E.; Han, D.; Jeong, J.S.; Moon, J.J.; Moon, H.K.; Lee, S.; Kim, Y.C.; Yoo, K.D.; Lee, J.W.; Kim, D.K.; et al. Multisample Mass Spectrometry-Based Approach for Discovering Injury Markers in Chronic Kidney Disease. *Mol. Cell. Proteom.* **2021**, *20*, 100037. [[CrossRef](#)]
85. Carbó, C.; Arderiu, G.; Escolar, G.; Fusté, B.; Cases, A.; Carrascal, M.; Abián, J.; Díaz-Ricart, M. Differential Expression of Proteins From Cultured Endothelial Cells Exposed to Uremic Versus Normal Serum. *Am. J. Kidney Dis.* **2008**, *51*, 603–612. [[CrossRef](#)]
86. Palomo, M.; Vera, M.; Martin, S.; Torramadé-Moix, S.; Martínez-Sánchez, J.; Belen Moreno, A.; Carreras, E.; Escolar, G.; Cases, A.; Díaz-Ricart, M. Up-regulation of HDACs, a harbinger of uraemic endothelial dysfunction, is prevented by defibrotide. *J. Cell. Mol. Med.* **2020**, *24*, 1713–1723. [[CrossRef](#)]
87. Nkuipou-Kenfack, E.; Durantou, F.; Gayraud, N.; Argilés, À.; Lundin, U.; Weinberger, K.M.; Dakna, M.; Delles, C.; Mullen, W.; Husi, H.; et al. Assessment of metabolomic and proteomic biomarkers in detection and prognosis of progression of renal function in chronic kidney disease. *PLoS ONE* **2014**, *9*, e96955. [[CrossRef](#)]
88. Hao, W.; Friedman, A. The LDL-HDL Profile Determines the Risk of Atherosclerosis: A Mathematical Model. *PLoS ONE* **2014**, *9*, e90497. [[CrossRef](#)] [[PubMed](#)]
89. Bandea, S.; Farmer, J. High-Density Lipoprotein and Atherosclerosis: The Role of Antioxidant Activity. *Curr. Atheroscler. Rep.* **2012**, *14*, 101–107. [[CrossRef](#)] [[PubMed](#)]
90. Fellström, B.C.; Jardine, A.G.; Schmieder, R.E.; Holdaas, H.; Bannister, K.; Beutler, J.; Chae, D.-W.; Chevaile, A.; Cobbe, S.M.; Grönhagen-Riska, C.; et al. Rosuvastatin and Cardiovascular Events in Patients Undergoing Hemodialysis. *N. Engl. J. Med.* **2009**, *360*, 1395–1407. [[CrossRef](#)] [[PubMed](#)]
91. Mathew, R.O.; Bangalore, S.; Lavelle, M.P.; Pellikka, P.A.; Sidhu, M.S.; Boden, W.E.; Asif, A. Diagnosis and management of atherosclerotic cardiovascular disease in chronic kidney disease: A review. *Kidney Int.* **2017**, *91*, 797–807. [[CrossRef](#)] [[PubMed](#)]
92. Ortiz, A.; Covic, A.; Fliser, D.; Fouque, D.; Goldsmith, D.; Kanbay, M.; Mallamaci, F.; Massy, Z.A.; Rossignol, P.; Vanholder, R.; et al. Epidemiology, contributors to, and clinical trials of mortality risk in chronic kidney failure. *Lancet* **2014**, *383*, 1831–1843. [[CrossRef](#)]
93. Fleischmann, E.H.; Bower, J.D.; Salahudeen, A.K. Risk factor paradox in hemodialysis: Better nutrition as a partial explanation. *ASAIO J.* **2001**, *47*. [[CrossRef](#)] [[PubMed](#)]
94. Kaysen, G.A. New insights into lipid metabolism in chronic kidney disease. *J. Ren. Nutr.* **2011**, *21*, 120–123. [[CrossRef](#)] [[PubMed](#)]
95. van der Stoep, M.; Korporaal, S.J.A.; Van Eck, M. High-density lipoprotein as a modulator of platelet and coagulation responses. *Cardiovasc. Res.* **2014**, *103*, 362–371. [[CrossRef](#)]
96. Navab, M.; Ananthramiah, G.M.; Reddy, S.T.; Van Lenten, B.J.; Ansell, B.J.; Fonarow, G.C.; Vahabzadeh, K.; Hama, S.; Hough, G.; Kamranpour, N.; et al. The oxidation hypothesis of atherogenesis: The role of oxidized phospholipids and HDL. *J. Lipid. Res.* **2004**, *45*, 993–1007. [[CrossRef](#)] [[PubMed](#)]

97. Marsche, G.; Furtmüller, P.G.; Obinger, C.; Sattler, W.; Malle, E. Hypochlorite-modified high-density lipoprotein acts as a sink for myeloperoxidase in vitro. *Cardiovasc. Res.* **2008**, *79*, 187–194. [[CrossRef](#)] [[PubMed](#)]
98. Huang, Y.; Wu, Z.; Riwanoto, M.; Gao, S.; Levison, B.S.; Gu, X.; Fu, X.; Wagner, M.A.; Besler, C.; Gerstenecker, G.; et al. Myeloperoxidase, paraoxonase-1, and HDL form a functional ternary complex. *J. Clin. Investig.* **2013**, *123*, 3815–3828. [[CrossRef](#)]
99. Kratzer, A.; Giral, H.; Landmesser, U. High-density lipoproteins as modulators of endothelial cell functions: Alterations in patients with coronary artery disease. *Cardiovasc. Res.* **2014**, *103*, 350–361. [[CrossRef](#)]
100. Kronenberg, F.; Kuen, E.; Ritz, E.; König, P.; Kraatz, G.; Lhotta, K.; Mann, J.F.; Müller, G.A.; Neyer, U.; Riegel, W.; et al. Apolipoprotein A-IV serum concentrations are elevated in patients with mild and moderate renal failure. *J. Am. Soc. Nephrol.* **2002**, *13*, 461–469. [[CrossRef](#)]
101. Karohl, C.; D'Marco Gascón, L.; Raggi, P. Noninvasive imaging for assessment of calcification in chronic kidney disease. *Nat. Rev. Nephrol.* **2011**, *7*, 567–577. [[CrossRef](#)]
102. Otsuka, F.; Sakakura, K.; Yahagi, K.; Joner, M.; Virmani, R. Has our understanding of calcification in human coronary atherosclerosis progressed? *Arterioscler. Thromb. Vasc. Biol.* **2014**, *34*, 724–736. [[CrossRef](#)] [[PubMed](#)]
103. Garland, J.S.; Holden, R.M.; Groome, P.A.; Lam, M.; Nolan, R.L.; Morton, A.R.; Pickett, W. Prevalence and Associations of Coronary Artery Calcification in Patients With Stages 3 to 5 CKD Without Cardiovascular Disease. *Am. J. Kidney Dis.* **2008**, *52*, 849–858. [[CrossRef](#)] [[PubMed](#)]
104. Nakamura, S.; Ishibashi-Ueda, H.; Niizuma, S.; Yoshihara, F.; Horio, T.; Kawano, Y. Coronary calcification in patients with chronic kidney disease and coronary artery disease. *Clin. J. Am. Soc. Nephrol.* **2009**, *4*, 1892–1900. [[CrossRef](#)]
105. Matsubara, K.; Stenvinkel, P.; Qureshi, A.R.; Carrero, J.J.; Axelsson, J.; Heimbürger, O.; Bárány, P.; Alvestrand, A.; Lindholm, B.; Suliman, M.E. Inflammation modifies the association of osteoprotegerin with mortality in chronic kidney disease. *J. Nephrol.* **2009**, *22*, 774–782. [[PubMed](#)]
106. Stockler-Pinto, M.B.; Saldanha, J.F.; Yi, D.; Mafra, D.; Fouque, D.; Soulage, C.O. The uremic toxin indoxyl sulfate exacerbates reactive oxygen species production and inflammation in 3T3-L1 adipose cells. *Free Radic. Res.* **2016**, *50*, 337–344. [[CrossRef](#)] [[PubMed](#)]
107. Lin, C.-J.; Wu, V.; Wu, P.-C.; Wu, C.-J. Meta-Analysis of the Associations of p-Cresyl Sulfate (PCS) and Indoxyl Sulfate (IS) with Cardiovascular Events and All-Cause Mortality in Patients with Chronic Renal Failure. *PLoS ONE* **2015**, *10*, e0132589. [[CrossRef](#)] [[PubMed](#)]
108. Ito, S.; Osaka, M.; Edamatsu, T.; Itoh, Y.; Yoshida, M. Crucial Role of the Aryl Hydrocarbon Receptor (AhR) in Indoxyl Sulfate-Induced Vascular Inflammation. *J. Atheroscler. Thromb.* **2016**, *23*, 960–975. [[CrossRef](#)] [[PubMed](#)]
109. Serradell, M.; Diaz-Ricart, M.; Cases, A.; Zurbano, M.; López-Pedret, J.; Arranz, O.; Ordinas, A.; Escolar, G. Uremic medium causes expression, redistribution and shedding of adhesion molecules in cultured endothelial cells. *Haematologica* **2002**, *87*, 1053–1061.
110. Barreto, F.C.; Barreto, D.V.; Liabeuf, S.; Meert, N.; Glorieux, G.; Temmar, M.; Choukroun, G.; Vanholder, R.; Massy, Z.A.; European Uremic Toxin Work Group (EUTox), on behalf of the E.U.T.W.G. Serum indoxyl sulfate is associated with vascular disease and mortality in chronic kidney disease patients. *Clin. J. Am. Soc. Nephrol.* **2009**, *4*, 1551–1558. [[CrossRef](#)]
111. Liabeuf, S.; Barreto, D.V.; Barreto, F.C.; Meert, N.; Glorieux, G.; Schepers, E.; Temmar, M.; Choukroun, G.; Vanholder, R.; Massy, Z.A.; et al. Free p-cresylsulphate is a predictor of mortality in patients at different stages of chronic kidney disease. *Nephrol. Dial. Transplant.* **2010**, *25*, 1183–1191. [[CrossRef](#)]
112. Meijers, B.K.I.; Van kerckhoven, S.; Verbeke, K.; Dehaen, W.; Vanrenterghem, Y.; Hoylaerts, M.F.; Evenepoel, P. The Uremic Retention Solute p-Cresyl Sulfate and Markers of Endothelial Damage. *Am. J. Kidney Dis.* **2009**, *54*, 891–901. [[CrossRef](#)]
113. Watanabe, H.; Miyamoto, Y.; Honda, D.; Tanaka, H.; Wu, Q.; Endo, M.; Noguchi, T.; Kadowaki, D.; Ishima, Y.; Kotani, S.; et al. P-Cresyl sulfate causes renal tubular cell damage by inducing oxidative stress by activation of NADPH oxidase. *Kidney Int.* **2013**, *83*, 582–592. [[CrossRef](#)]
114. Cozzolino, M.; Ciceri, P.; Galassi, A.; Mangano, M.; Carugo, S.; Capelli, I.; Cianciolo, G. The Key Role of Phosphate on Vascular Calcification. *Toxins* **2019**, *11*, 213. [[CrossRef](#)] [[PubMed](#)]
115. Gao, S.; Xu, J.; Zhang, S.; Jin, J. Meta-Analysis of the Association between Fibroblast Growth Factor 23 and Mortality and Cardiovascular Events in Hemodialysis Patients. *Blood Purif.* **2019**, *47*, 24–30. [[CrossRef](#)]
116. Reynolds, J.L.; Joannides, A.J.; Skepper, J.N.; McNair, R.; Schurgers, L.J.; Proudfoot, D.; Jahnke-Dechent, W.; Weissberg, P.L.; Shanahan, C.M. Human vascular smooth muscle cells undergo vesicle-mediated calcification in response to changes in extracellular calcium and phosphate concentrations: A potential mechanism for accelerated vascular calcification in ESRD. *J. Am. Soc. Nephrol.* **2004**, *15*, 2857–2867. [[CrossRef](#)]
117. M'baya-Moutoula, E.; Louvet, L.; Molinié, R.; Guerrero, I.C.; Cerutti, C.; Fourdinier, O.; Nourry, V.; Gutierrez, L.; Morlière, P.; Mesnard, F.; et al. A multi-omics analysis of the regulatory changes induced by miR-223 in a monocyte/macrophage cell line. *Biochim. Biophys. Acta Mol. Basis Dis.* **2018**, *1864*, 2664–2678. [[CrossRef](#)] [[PubMed](#)]
118. Gimbrone, M.A.; García-Cardena, G. Endothelial Cell Dysfunction and the Pathobiology of Atherosclerosis. *Circ. Res.* **2016**, *118*, 620–636. [[CrossRef](#)] [[PubMed](#)]
119. Ley, K.; Laudanna, C.; Cybulsky, M.I.; Nourshargh, S. Getting to the site of inflammation: The leukocyte adhesion cascade updated. *Nat. Rev. Immunol.* **2007**, *7*, 678–689. [[CrossRef](#)]
120. Mohindra, R.; Agrawal, D.K.; Thankam, F.G. Altered Vascular Extracellular Matrix in the Pathogenesis of Atherosclerosis. *J. Cardiovasc. Transl. Res.* **2021**, 1–14. [[CrossRef](#)]

121. Trojanowicz, B.; Ulrich, C.; Kohler, F.; Bode, V.; Seibert, E.; Fiedler, R.; Girndt, M. Monocytic angiotensin-converting enzyme 2 relates to atherosclerosis in patients with chronic kidney disease. *Nephrol. Dial. Transplant.* **2016**, *32*, gfw206. [[CrossRef](#)] [[PubMed](#)]
122. Yang, C.-Y.; Tarng, D.-C. Diet, gut microbiome and indoxyl sulphate in chronic kidney disease patients. *Nephrology* **2018**, *23*, 16–20. [[CrossRef](#)] [[PubMed](#)]
123. Fowler, M.J. Microvascular and Macrovascular Complications of Diabetes. *Clin. Diabetes* **2008**, *26*, 77–82. [[CrossRef](#)]
124. Abe, M.; Kalantar-Zadeh, K. Haemodialysis-induced hypoglycaemia and glycaemic disarrays. *Nat. Rev. Nephrol.* **2015**, *11*, 302–313. [[CrossRef](#)]
125. Pecoits-Filho, R.; Abensur, H.; Betônico, C.C.R.; Machado, A.D.; Parente, E.B.; Queiroz, M.; Salles, J.E.N.; Titan, S.; Vencio, S. Interactions between kidney disease and diabetes: Dangerous liaisons. *Diabetol. Metab. Syndr.* **2016**, *8*, 50. [[CrossRef](#)] [[PubMed](#)]
126. La Sala, L.; Prattichizzo, F.; Ceriello, A. The link between diabetes and atherosclerosis. *Eur. J. Prev. Cardiol.* **2019**, *26*, 15–24. [[CrossRef](#)] [[PubMed](#)]
127. Klein, J.; Caubet, C.; Camus, M.; Makridakis, M.; Denis, C.; Gilet, M.; Feuillet, G.; Rascalou, S.; Neau, E.; Garrigues, L.; et al. Connectivity mapping of glomerular proteins identifies dimethylaminoparthenolide as a new inhibitor of diabetic kidney disease. *Sci. Rep.* **2020**, *10*, 14898. [[CrossRef](#)]
128. Santana, M.F.M.; Lira, A.L.A.; Pinto, R.S.; Minanni, C.A.; Silva, A.R.M.; Sawada, M.I.B.A.C.; Nakandakare, E.R.; Correa-Giannella, M.L.C.; Queiroz, M.S.; Ronsein, G.E.; et al. Enrichment of apolipoprotein A-IV and apolipoprotein D in the HDL proteome is associated with HDL functions in diabetic kidney disease without dialysis. *Lipids Health Dis.* **2020**, *19*, 205. [[CrossRef](#)] [[PubMed](#)]
129. Wen, J.; Ma, Z.; Livingston, M.J.; Zhang, W.; Yuan, Y.; Guo, C.; Liu, Y.; Fu, P.; Dong, Z. Decreased secretion and profibrotic activity of tubular exosomes in diabetic kidney disease. *Am. J. Physiol. Ren. Physiol.* **2020**, *319*, F664–F673. [[CrossRef](#)]
130. Gajjala, P.R.; Bruck, H.; Noels, H.; Heinze, G.; Ceccarelli, F.; Kribben, A.; Saez-Rodriguez, J.; Marx, N.; Zidek, W.; Jankowski, J.; et al. Novel plasma peptide markers involved in the pathology of CKD identified using mass spectrometric approach. *J. Mol. Med.* **2019**, *97*, 1451–1463. [[CrossRef](#)]
131. Romanova, Y.; Laikov, A.; Markelova, M.; Khadiullina, R.; Makseev, A.; Hasanova, M.; Rizvanov, A.; Khaiboullina, S.; Salafutdinov, I. Proteomic analysis of human serum from patients with chronic kidney disease. *Biomolecules* **2020**, *10*, 257. [[CrossRef](#)]
132. Konvalinka, A.; Batruch, I.; Tokar, T.; Dimitromanolakis, A.; Reid, S.; Song, X.; Pei, Y.; Drabovich, A.P.; Diamandis, E.P.; Jurisica, I.; et al. Quantification of angiotensin II-regulated proteins in urine of patients with polycystic and other chronic kidney diseases by selected reaction monitoring. *Clin. Proteom.* **2016**, *13*, 16. [[CrossRef](#)]
133. Øvrehus, M.A.; Zúrbig, P.; Vikse, B.E.; Hallan, S.I. Urinary proteomics in chronic kidney disease: Diagnosis and risk of progression beyond albuminuria. *Clin. Proteom.* **2015**, *12*. [[CrossRef](#)]
134. Jiang, S.; He, H.; Tan, L.; Wang, L.; Su, Z.; Liu, Y.; Zhu, H.; Zhang, M.; Hou, F.F.; Li, A. Proteomic and phosphoproteomic analysis of renal cortex in a salt-load rat model of advanced kidney damage. *Sci. Rep.* **2016**, *6*, 35906. [[CrossRef](#)] [[PubMed](#)]
135. Herrington, D.M.; Mao, C.; Parker, S.J.; Fu, Z.; Yu, G.; Chen, L.; Venkatraman, V.; Fu, Y.; Wang, Y.; Howard, T.D.; et al. Proteomic Architecture of Human Coronary and Aortic Atherosclerosis. *Circulation* **2018**, *137*, 2741–2756. [[CrossRef](#)] [[PubMed](#)]
136. Olson, F.J.; Sihlbom, C.; Davidsson, P.; Hulthe, J.; Fagerberg, B.; Bergström, G. Consistent differences in protein distribution along the longitudinal axis in symptomatic carotid atherosclerotic plaques. *Biochem. Biophys. Res. Commun.* **2010**, *401*, 574–580. [[CrossRef](#)] [[PubMed](#)]
137. Wallentin, L.; Eriksson, N.; Olszowka, M.; Grammer, T.B.; Hagström, E.; Held, C.; Kleber, M.E.; Koenig, W.; März, W.; Stewart, R.A.H.; et al. Plasma proteins associated with cardiovascular death in patients with chronic coronary heart disease: A retrospective study. *PLoS Med.* **2021**, *18*, e1003513. [[CrossRef](#)]
138. Yong, K.; Ooi, E.M.; Dogra, G.; Mannion, M.; Boudville, N.; Chan, D.; Lim, E.M.; Lim, W.H. Cytokine Elevated interleukin-12 and interleukin-18 in chronic kidney disease are not associated with arterial stiffness. *Cytokine* **2013**, *64*, 39–42. [[CrossRef](#)]
139. Scholze, A.; Krueger, K.; Diedrich, M.; Räh, C.; Torges, A.; Jankowski, V.; Maier, A.; Thilo, F.; Zidek, W.; Tepel, M. Superoxide dismutase type 1 in monocytes of chronic kidney disease patients. *Amino Acids* **2011**, *41*, 427–438. [[CrossRef](#)]
140. Marques, M.; Sacristán, D.; Mateos-Cáceres, P.J.; Herrero, J.; Arribas, M.J.; González-Armengol, J.J.; Villegas, A.; Macaya, C.; Barrientos, A.; López-Farré, A.J. Different protein expression in normal and dysfunctional platelets from uremic patients. *J. Nephrol.* **2010**, *23*, 90–101. [[PubMed](#)]
141. Carlsson, A.C.; Ingelsson, E.; Sundström, J.; Carrero, J.J.; Gustafsson, S.; Feldreich, T.; Stenemo, M.; Larsson, A.; Lind, L.; Ärnlöv, J. Use of proteomics to investigate kidney function decline over 5 years. *Clin. J. Am. Soc. Nephrol.* **2017**, *12*, 1226–1235. [[CrossRef](#)]
142. Feldreich, T.; Nowak, C.; Carlsson, A.C.; Östgren, C.J.; Nyström, F.H.; Sundström, J.; Carrero-Roig, J.J.; Leppert, J.; Hedberg, P.; Giedraitis, V.; et al. The association between plasma proteomics and incident cardiovascular disease identifies MMP-12 as a promising cardiovascular risk marker in patients with chronic kidney disease. *Atherosclerosis* **2020**, *307*, 11–15. [[CrossRef](#)] [[PubMed](#)]
143. Conesa, A.; Beck, S. Making multi-omics data accessible to researchers. *Sci. Data* **2019**, *6*, 1–4. [[CrossRef](#)] [[PubMed](#)]
144. Hsu, C.Y.; Ballard, S.; Battle, D.; Bonventre, J.V.; Böttinger, E.P.; Feldman, H.I.; Klein, J.B.; Coresh, J.; Eckfeldt, J.H.; Inker, L.A.; et al. Cross-disciplinary biomarkers research: Lessons learned by the CKD biomarkers consortium. *Clin. J. Am. Soc. Nephrol.* **2015**, *10*, 894–902. [[CrossRef](#)] [[PubMed](#)]

Proteomic Profiling of Leukocytes Reveals Dysregulation of Adhesion and Integrin Proteins in Chronic Kidney Disease-Related Atherosclerosis

Joanna Tracz, Luiza Handschuh, Maciej Lalowski, Łukasz Marczak, Katarzyna Kostka-Jeziorny, Bartłomiej Perek, Maria Wanic-Kossowska, Alina Podkowińska, Andrzej Tykarski, Dorota Formanowicz, and Magdalena Luczak*



Cite This: *J. Proteome Res.* 2021, 20, 3053–3067



Read Online

ACCESS |



Metrics & More



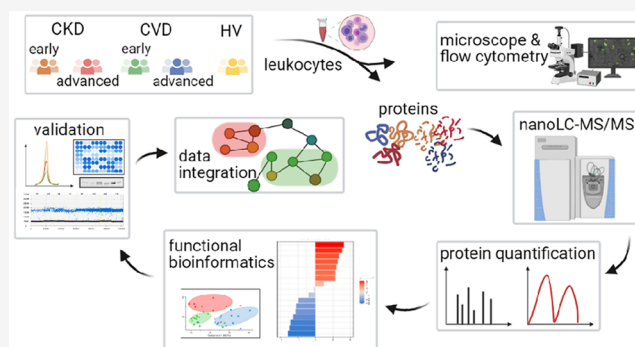
Article Recommendations



Supporting Information

ABSTRACT: A progressive loss of functional nephrons defines chronic kidney disease (CKD). Complications related to cardiovascular disease (CVD) are the principal causes of mortality in CKD; however, the acceleration of CVD in CKD remains unresolved. Our study used a complementary proteomic approach to assess mild and advanced CKD patients with different atherosclerosis stages and two groups of patients with different classical CVD progression but without renal dysfunction. We utilized a label-free approach based on LC-MS/MS and functional bioinformatic analyses to profile CKD and CVD leukocyte proteins. We revealed dysregulation of proteins involved in different phases of leukocytes' diapedesis process that is very pronounced in CKD's advanced stage. We also showed an upregulation of apoptosis-related proteins in CKD as compared to CVD. The differential abundance of selected proteins was validated by multiple reaction monitoring, ELISA, Western blotting, and at the mRNA level by ddPCR. An increased rate of apoptosis was then functionally confirmed on the cellular level. Hence, we suggest that the disturbances in leukocyte extravasation proteins may alter cell integrity and trigger cell death, as demonstrated by flow cytometry and microscopy analyses. Our proteomics data set has been deposited to the ProteomeXchange Consortium via the PRIDE repository with the data set identifier PXD018596.

KEYWORDS: chronic kidney disease, cardiovascular disease, adhesion, integrin, proteomics, mass spectrometry



1. INTRODUCTION

Chronic kidney disease (CKD) is a global health problem with a constantly enhancing rate, defined and categorized by a progressive loss of functional nephrons resulting in a gradual reduction of glomerular filtration rate (GFR) and proteinuria.¹ However, not an impaired kidney function *per se*, but accelerated atherosclerosis followed by cardiovascular disease (CVD) complications represent the principal causes of mortality in CKD.² The severity of CVD in CKD increases along with renal damage progression;³ hence, patients with kidney failure often demonstrate even a 20-fold increase in cardiovascular mortality risk than in the general population.⁴ The vast majority of CKD patients succumb to cardiovascular death prior to developing kidney failure.⁵

Interestingly, in marked contrast to the general population, well-established risk factors, like hypertension, high serum cholesterol level, or obesity, appear to be associated with markedly higher survival rates in CKD. These paradoxical observations have been termed as “reverse epidemiology” and disclose that traditionally recognized risk factors might

inadequately explain the high incidence of CVD in CKD patients.⁶ It has also been demonstrated that other risk factors, including endothelial dysfunction, vascular calcification, volume overload, oxidative stress, and inflammation, may play a key role in the high incidence of CVD risk in CKD. This issue seems to be of vital importance; however, due to many confounding factors, patients with CKD are often excluded from CVD-oriented studies, which limits the understanding of their high-risk, CKD-related atherosclerosis.⁷

It should be emphasized that CKD is currently treated as an oxidative stress- and inflammatory-mediated CVD, underlined by accelerated atherosclerosis (for a review, see ref 8). This phenomenon is very complex; thus deeper insights into the

Received: November 4, 2020

Published: May 3, 2021



Table 1. Characteristics of the Study Population^a

	HV	group				p-value	p-value without HVs
		CKD1-2	CKD5	CVD1	CVD2		
age [years]	43 ± 6	66 ± 8	65 ± 17	62 ± 15	63 ± 9	<0.0001	0.25
male/female	16/8	18/8	18/9	17/10	16/6	0.92	0.86
BMI [kg/m ²]	24 ± 2	29 ± 4	25 ± 3	29 ± 5	26 ± 4	0.13	0.33
obesity (BMI > 30 kg/m ²)	0	3	0	4	1	<0.0001	<0.0001
arterial hypertension	0	26	27	27	22	<0.0001	1.00
hyperlipidemia	0	26	2	27	22	<0.0001	<0.0001
CAD/previous myocardial infarction	0/0	0/0	27/15	0/0	22/17	<0.0001	<0.0001
previous PCI	0	0	18	0	22	<0.0001	<0.0001
PVD	0	0	2	0	4	<0.0001	<0.0001
neurological events	0	0	1	0	4	<0.0001	<0.0001
eGFR [mL/min/1.73 m ²]	95.3 ± 13.9	68.0 ± 5.1	8.5 ± 3.9	106.4 ± 13.4	90.7 ± 10.7	<0.0001	<0.0001
glucose [mM]	4.0 ± 0.6	5.4 ± 0.4	5.6 ± 0.4	5.5 ± 0.5	5.1 ± 0.3	0.02	0.07
total cholesterol [mg/dL]	190.5 ± 23.9	170.8 ± 50.1	157.2 ± 29.3	189 ± 92	175 ± 37	0.01	0.10
HDL cholesterol [mg/dL]	50.3 ± 13.1	63.8 ± 20.1	45.7 ± 11.7	65.1 ± 17.8	56.3 ± 12.8	<0.0001	<0.0001
LDL cholesterol [mg/dL]	123.0 ± 2	87.5 ± 44.2	84.4 ± 28.9	102.2 ± 47	95.8 ± 29.8	<0.0001	0.38
triglycerides [mg/dL]	91.3 ± 41.0	103.6 ± 41.1	135.7 ± 77.4	131.3 ± 93.1	113.0 ± 41.3	0.23	0.73
hsCRP [mg/L]	1.7 ± 1.9	2.4 ± 2.3	22.2 ± 29.8	2.3 ± 1.9	2.2 ± 3.0	<0.0001	<0.0001
WBC [10 ⁹ /L]	6.1 ± 1.5	7.2 ± 2.4	7.1 ± 2.4	6.9 ± 2.4	8.8 ± 6.7	0.44	0.91
NEUT [10 ⁹ /L]	3.2 ± 1.0	4.5 ± 1.7	4.6 ± 2	4.3 ± 2.2	4.3 ± 1.1	0.04	0.88
EOS [10 ⁹ /L]	0.18 ± 0.1	0.18 ± 0.13	0.22 ± 0.14	0.1 ± 0.1	0.13 ± 0.04	0.11	0.16
BASO [10 ⁹ /L]	0.03 ± 0.01	0.03 ± 0.02	0.03 ± 0.23	0.03 ± 0.01	0.03 ± 0.02	0.97	0.81
LYMPH [10 ⁹ /L]	2.1 ± 0.6	1.9 ± 0.5	1.4 ± 0.8	1.7 ± 0.6	1.9 ± 0.6	<0.0001	0.12
MONO [10 ⁹ /L]	0.4 ± 0.1	0.4 ± 0.2	0.7 ± 0.2	0.4 ± 0.1	0.4 ± 0.1	<0.0001	<0.0001
RBC [10 ¹² /L]	4.5 ± 0.4	4.7 ± 0.4	3.2 ± 0.5	4.5 ± 0.4	4.8 ± 1.2	<0.0001	<0.0001
PLT [10 ⁹ /L]	262.1 ± 78.5	243.9 ± 87.9	205.0 ± 65.8	249.8 ± 54.2	236 ± 78.5	0.01	0.02
<i>antiplatelet treatment</i>	0	21	19	18	18	<0.0001	0.51
acetylsalicylic acid	0	18	12	15	16	<0.0001	0.11
acetylsalicylic acid + ticagrelor	0	2	3	2	1	<0.0001	0.86
acetylsalicylic acid + clopidogrel	0	1	3	1	1	<0.0001	0.61
<i>hypertension treatment</i>	0	26	27	27	22	<0.0001	1.00
β-blocker	0	18	16	19	18	<0.0001	0.40
diuretics	0	13	13	12	13	<0.0001	0.91
ACEI	0	18	2	14	2	<0.0001	<0.0001
CCB	0	6	11	7	6	<0.0001	0.50
ARB	0	4	2	5	2	<0.0001	0.59
statin (atorvastatin or rosuvastatin)	0	23	17	19	22	<0.0001	0.02

^aMean value ± SD. Abbreviations: HV, healthy volunteer; BMI, body mass index; CAD, coronary artery disease; PCI, percutaneous coronary interventions; PVD, peripheral vascular disease; eGFR, estimated glomerular filtration rate; hsCRP, high-sensitivity C-reactive protein; WBC, white blood cells; EOS, eosinophils; BASO, basophils; LYMPH, lymphocytes; MONO, monocytes; RBC, red blood cells; PLT, platelets; ACE, angiotensin-converting enzyme inhibitors; CCB, calcium channel blocker; ARB, angiotensin receptor blocker. The chi-square test was used for categorical variables (gender, drug treatment, the prevalence of hypertension, obesity, hyperlipidemia, CAD, PCI, PVD, and events). For other variables, the Mann–Whitney U-test was used.

relationships between the many disrupted metabolic pathways involved in CKD pathology are strongly recommended.

Although the close connection between kidney dysfunction and atherosclerosis is widely recognized, almost all existing studies rely on comparing CKD or CVD patients separately to healthy controls. Therefore, only direct analysis of both conditions may provide information about the differences underlying atherosclerotic CVD related and non-related to CKD.

Since atherosclerosis is regulated by a complex interplay of circulating plasma proteins and inflammatory cells, and soluble forms of these molecules could be detected in plasma, the analysis of a repertoire of constitutive proteins in leukocytes during CKD-related atherosclerosis progression could be

critical. Many proteomic studies presenting alterations in plasma protein profiles from patients with either CKD or CVD have previously been published.^{9,10} We earlier presented a comparative proteomic analysis of plasma from CKD and CVD patients and demonstrated that proteins involved in inflammation exhibited more significant alterations in individuals with CKD-related atherosclerosis.¹¹

In this study, we utilized a label-free proteomics approach to increase our knowledge about the alteration of leukocyte proteins in CKD and CVD. We aimed to assess mild and advanced CKD patients with different CKD-related atherosclerosis progression and two groups of CVD patients with non-CKD-related atherosclerosis. The obtained results were confirmed by ELISA, digital droplet PCR (ddPCR), and

multiple reaction monitoring (MRM). Cells were subsequently evaluated by microscopy and flow cytometry, and then functionally analyzed by a network approach. Measurements of adhesion molecules with a known role in atherosclerosis development and circulating in plasma were also performed to validate selected findings.

2. MATERIAL AND METHODS

2.1. Experimental Groups and Sample Preparation

The study protocol conformed to the Ethical Guidelines of the World Medical Association Declaration of Helsinki. Before the project commenced, appropriate approval was obtained from the Bioethical Commission of the Poznan University of Medical Sciences, Poland (no. 926/16). All patients qualified for this study underwent a clinical examination and provided signed informed consent before participation. The study involved 220 patients divided into four experimental groups (named CKD1-2, CKD5, CVD1, and CVD2, respectively) and 48 healthy volunteers. During 2016–2017, samples were collected from dialysis stations and Poznan University of Medical Sciences' four clinical departments.

The CKD patients were divided into two groups based on NICE Clinical Guidelines¹² and according to their levels of eGFR.¹³ The first group, named CKD1-2, encompassed patients at the initial stage of CKD with a mean eGFR of 68 mL/min/1.73 m². The second CKD group, called CKD5, included ESRD patients treated with hemodialysis, mean eGFR of 8.5 mL/min/1.73 m². The study was also carried out on two groups of CVD patients varying in the degree of CVD clinical manifestation (CVD1 and CVD2) but without kidney dysfunction and thus eGFR > 90 mL/min/1.73 m².

The CKD1-2 and CVD1 groups included patients with no previous cardiovascular events and vascular interventions; they were burdened with commonly accepted risk factors of atherosclerosis development, i.e., hypertension and hyperlipidemia, with non-obstructive coronary artery disease (non-hemodynamically significant stenosis less than 30%) confirmed by coronarography. Both groups differed only in kidney function.

Patients comprising the CVD2 and CKD5 groups had advanced atherosclerosis, confirmed by coronarography clinically manifested as coronary artery disease (CAD) with a history of at least one acute coronary syndrome and/or after the vascular intervention. Again, only kidney function differentiated these groups. Thus, the following groups were involved in this study:

- (I) Group CVD1 - normal kidney function; hypertension, hyperlipidemia, and non-obstructive coronary artery disease
- (II) Group CVD2 - normal kidney function; symptomatic CVD
- (III) Group CKD1-2 - an early stage of kidney disease; hypertension, hyperlipidemia, and non-obstructive coronary artery disease
- (IV) Group CKD5 - severe kidney disease; symptomatic CVD

All patient groups were examined by coronarography, echocardiography, electrocardiography, and Doppler ultrasonography. The characteristics of all experimental groups are presented in Table 1.

The set exclusion criteria for patients included diabetes, active acute infection, and malignant tumors. In order to avoid

problems associated with different treatments, patient groups were also matched concerning types of statins used and hypertension and antiplatelet drugs. Patients treated with anticoagulants were also excluded from the analysis. Ultimately, 126 samples were selected for LC-MS analyses performed in triplicate.

Blood samples were collected, and at the same time, standard biochemical examinations were performed. In the case of hemodialyzed patients, blood samples were drawn prior to the second hemodialysis session of the week, as recommended. White blood cells were isolated using the RBC lysis solution procedure as described.¹⁴ Plasma samples were also frozen at -80 °C until analysis. The cell pellet containing leukocytes was analyzed by fluorescence microscopy and flow cytometry to assess the morphology, preparation quality, and apoptosis/necrosis rate. Cells were stained with Hoechst 33342 (Thermo Fisher Scientific, Waltham, MA, USA). The rates of apoptotic and necrotic cells were evaluated with dual staining with CellEvent Casp3/7-FITC (Thermo Fisher Scientific, Waltham, MA, USA) according to the manufacturer's protocol and propidium iodide (1.25 µg/mL; Sigma-Aldrich, Milwaukee, WI, USA) fluorescent dyes. The intensity of green fluorescence was analyzed with 488 nm excitation by an Accuri C6 flow cytometer (Becton Dickinson (BD), Franklin Lakes, NJ, USA). Leukocytes were gated by size and granularity to assess particular subpopulations of cells. For confocal microscopy, cells were placed on a glass slide, coverslipped, and analyzed with a Leica TCS SP5 microscope (Leica Microsystems, Wetzlar, Germany) with a Plan Apo 63 × 1.4 NA oil-immersion objective. Sequentially scanned images were collected at Ex/Em = 502/510–550 nm for living cells, 535/610–650 nm for apoptotic cells, and 405/450–500 nm for nuclei staining. Leica LAS AF and Leica LAS X software with a deconvolution module were used for image processing and fluorescence analysis, respectively.

The rest of the leukocytes was aliquoted, frozen, and stored in a vapor phase of liquid N₂ until analysis. For ddPCR analysis, cell pellets were suspended in a mirVana Ambion miRNA Isolation Kit lysis buffer (Thermo Fisher Scientific, Waltham MA, USA) and immediately frozen at -80 °C.

2.2. Protein Preparation and Nano LC-MS/MS Analysis

The cell pellets of leukocytes were suspended in 8 M urea/0.2% SDS and homogenized using Precellys24 homogenizer (Bertin Technologies, Villeurbanne, France) in three, 30-s cycles at 5500 rpm. Next, the samples were sonicated on ice for 10 min. Proteins were precipitated with six volumes of cold acetone and then washed with 80% acetone to remove SDS. The protein pellet was resuspended in 25 µL of 50 mM ammonium bicarbonate, vortexed for 1 h at RT, and sonicated for 10 min using an ultrasonic bath. After that, the samples were centrifuged at 23000g for 10 min at 4 °C, and the supernatants were used for protein concentration assay (2D-Quant Kit, GE Healthcare, Uppsala, Sweden). A 30 µg portion of the protein mixture was reduced with 5.6 mM DTT for 5 min at 95 °C and then alkylated with 5 mM iodoacetamide for 20 min at RT. The samples were digested with 0.2 µg of trypsin (Promega, Mannheim, Germany) overnight at 37 °C. The peptide mixtures were analyzed by nano-LC-MS/MS using a Dionex UltiMate 3000 RSLCnano System coupled with Q-Exactive Orbitrap mass spectrometer (Thermo Fisher Scientific, Waltham, MA, USA) in one batch as described.¹¹ Following LC-MS/MS analysis, the raw files were analyzed to

evaluate the quality of the performed runs by Proteome Discoverer (PD), version 1.4.14 (Thermo Fisher Scientific, Waltham, MA, USA), as described.¹¹ The reproducibility of the biological and technical replicates was assessed by scatter plotting, and the correlation coefficient was determined based on the label-free quantification (LFQ) intensities. Only samples with Pearson correlation coefficients above 0.8 (125 out of 126) were included in quantitative surveys (Table S1).

2.3. Quantitative Analysis of Proteomic Data

The raw files were quantitatively analyzed by MaxQuant (MQ),¹⁵ version 1.5.1.2. The identification of proteins at $\leq 1\%$ FDR was performed against the UniProt complete human proteome set (release 10-03-2019) using tolerance levels of 10 ppm for MS and 0.08 Da for MS/MS, and two missed cleavages were allowed. The carbamidomethylation of cysteines was set as a fixed modification, and the oxidation of methionine was allowed as a variable modification. The analysis of the samples was based on the LFQ intensities. The normalized MQ data were analyzed with Perseus software, version 1.6.1.3 (<https://maxquant.net/perseus/>). The MQ data were filtered to exclude false-positive identifications (contaminants, reverse identifications, and proteins “only identified by site”). Only proteins detected in all samples were taken into account in the quantitative analyses (no missing values). The fold changes in the level of the proteins were assessed by comparing the mean intensities among all experimental groups.

2.4. Validation of Results with Quantitative ddPCR

Ten patients' samples from each experimental group were chosen for ddPCR analysis. Total RNA was extracted from the leukocytes with a mirVana miRNA Isolation Kit and DNase-digested with a TURBO DNA-free Kit according to the manufacturers' protocols. RNA quantity was determined using a NanoDrop 2000 spectrophotometer. The quality of RNA was assessed with a Bioanalyzer 2100 with a Total RNA Pico Assay (Agilent Technologies, Santa Clara, USA). RNA (0.5 μg per sample) was used for reverse transcription by SuperScript III RT and oligo(dT) (Thermo Fisher Scientific, Waltham, MA, USA). The reaction mixtures were incubated for 1.5 h at 50 °C. Six pairs of primers, unique for each gene, i.e., *TLN1*, *NAMPT*, *MMP8*, *TAGLN2*, *PXN*, and *ITGAM*, are presented in Table S2. The ddPCR assays and data analysis were performed as described previously.¹⁶ The level of each gene was calculated as the ratio of the absolute transcript level of genes to the geometric mean of the absolute transcript level of reference genes, *PGK1* and *GAPDH*.

2.5. Immunoassay Analysis

Ten patients' samples from each experimental group were chosen for immunoanalysis. The protein concentration was measured using a commercially available ELISA kit (Elabscience, China). ELISA validation was prepared for integrin beta-2 (*ITGB2*), integrin alpha-M (*ITGAM*), talin-1 (*TLN1*), and vinculin (*VCL*), identified in LC-MS/MS analysis. The concentrations of three known plasma integrin ligands, vascular cell adhesion protein 1 (*VCAM1*), intercellular adhesion molecule 1 (*ICAM1*), and E-selectin, were also measured. All assays were prepared according to the manufacturers' instructions, including appropriate positive and negative controls.

For Western blot (WB) validation, equal amounts of proteins (30 μg) were separated by SDS-PAGE (4–15%;

Biorad, Hercules, USA). Due to the high molecular weight of *TLN1* (270 kDa; ~ 2540 amino acids), the electrophoretic runs were extended beyond the point that dye reached the bottom of the gel, allowing for better separation of proteins in this molecular range. The proteins were transferred overnight to a PVDF membrane. Blots were blocked with TBST containing 4% BSA and incubated overnight with the anti-*TLN1* primary antibodies. Chemiluminescent detection was performed using the ChemiDoc XRS imaging system.

2.6. Validation of Results with Quantitative Multiple Reaction Monitoring

Twenty-five patients' samples from each experimental group were chosen for MRM validation. A list of peptides and transitions for *VCAM1*, *ICAM1*, *ANXA2*, and *EGLN* was created by the open software Skyline 20.1.0.31.¹⁷ Two unique peptides and two transitions with rank 1 or 2 for each peptide were chosen. Two isotope-labeled peptides were spiked into samples and used as an internal standard. An overview of MRM analysis is presented in Table S3. Proteins were in-solution digested with trypsin, as described previously.¹¹ LC-MS/MS analysis was conducted using the UFLC system coupled to an ESI triple-quadrupole mass spectrometer (LC-MS-8060, Shimadzu, Kyoto, Japan). The separation of samples was achieved on an Acquity UPLC Peptide CSH C18 column, 1.7 μm i.d., particle size of 2 μm and pore size of 130 Å (150 \times 1.0 mm; Waters, Milford, USA). The LC conditions were optimized as follows: solvent A was 0.1% formic acid in the water, and solvent B was 0.1% formic acid in acetonitrile. The gradient program for pump B was set as follows: 0.01–20 min, 10–65%; 20–25 min, 95%; and 25–30 min, 10%. The flow rate was set to 0.1 mL min^{-1} , and the column temperature was set at 40 °C. LabSolutions software (Shimadzu, Kyoto, Japan) was used to control the instruments as well as to acquire and process the data. Skyline software was used for MRM peak integration, normalization, and relative abundance calculations.

2.7. Statistical Analysis

Statistical analyses were performed using Perseus 1.6.1.3, Statistica 12.0 software (StatSoft, Inc., Kraków, Poland), or R ver. 3.6.0 and R Studio ver. 1.2.1335. All plots were made in R Studio, and the following packages were used: *dplyr*, *ggplot2*, *reshape2*, *ggsignif*, and *ggpubr*. Chi-square test was used for categorical variables. Data distribution was assessed using a Shapiro–Wilk test and Leven's test to evaluate the equality of variances. The data were statistically analyzed using a Mann–Whitney U-test or Student's unpaired *t*-test when appropriate. More than two groups were compared using one-way ANOVA or Kruskal–Wallis for non-parametric data, followed by post hoc multiple comparison testing. Statistical significance was accepted as $p < 0.05$. The Benjamini–Hochberg FDR was set to 5%.

Statistical power was calculated based on the number of biological replicates, FDR adjusted p-value and coefficients of variation calculated for all proteins. Because overall variation was below 30% for each experimental group, fold change 1.4 was chosen according to ref 18. Additionally, the effect size (Hedges's *g*) was calculated according to Cohen's *d*¹⁹ formula corrected by Hedges's.²⁰ All differential proteins with Hedges's *g* below 0.5 were excluded from the final list of differential proteins. Therefore, a protein was considered to be differentially expressed if the difference between at least two groups was statistically significant ($p < 0.05$), the effect size was above 0.5, and the fold change was above 1.4. Only DEPs identified

with a minimum of two unique peptides, at >99% confidence level were accepted.

The correlations between variables were defined by the Pearson coefficients, and *p*-values less than 0.05 were considered significant. Multivariate analyses were carried out by unsupervised principal component analysis (PCA) and hierarchical clustering. For hierarchical clustering and heat map visualization, data were normalized to *z*-score.

2.8. Bioinformatic Analysis

Bioinformatic analysis was conducted using Perseus and Ingenuity Pathway Analysis software (Ingenuity Systems, Redwood City, USA). All identified proteins were annotated according to their Gene Ontology in the cellular compartment, canonical pathway, and biological function category using UniProtKB list. Differentially expressed proteins (DEPs; (*p*-value <0.05; fold change ≥ 1.4 ; effect size >0.5; ≥ 2 unique peptides) were subjected to the enrichment analysis to determine the top cellular compartment, canonical pathways, biological functions, and upstream regulators associated with the observed differences in protein profiles. Also, downstream effect analyses were performed from which the most affected categories were extracted. Enrichment analysis was performed using the right-tailed Fisher's exact test with Benjamini–Hochberg (B-H) multiple corrections. Based on obtained *p*-value, this test estimates the probability that the association between a set of molecules and a function or pathway is not random. Moreover, the IPA regulation *z*-score algorithm was also used to predict the direction of change for a given function or pathway. A negative *z*-score indicates inhibition, and positive predicts activation. In order to enhance the stringency of our analysis, functions with *z*-scores ≥ 2 (for activation) and ≤ -2 (for inhibition) were considered as those in which the directionality was assigned.²¹ The *z*-score was not calculated if there were no available data in the Ingenuity Knowledge Base concerning the functional involvement of the given DEPs. In case the directionalities of changes in the data set and those predicted by the Ingenuity Knowledge Base were not corresponding, a “biased” *z*-score was defined.

2.9. Data Availability

The mass spectrometry proteomics data have been deposited to the PRIDE Archive (<http://www.ebi.ac.uk/pride/archive/>) via the PRIDE partner repository with the data set identifier PXD018596 (<https://www.ebi.ac.uk/pride/archive/projects/PXD018596>).

3. RESULTS

The whole leukocyte fraction of peripheral blood was collected from two experimental groups with CKD (CKD1-2 and CKD5), two groups with CVD (CVD1 and CVD2), and healthy volunteers (HVs). Based on similar symptoms and results of medical examinations, the equal status of atherosclerosis progression was concluded for CKD1-2/CVD1 groups as well as for CKD5/CVD2 groups. A characteristic of each analyzed group is presented in Table 1. Samples did not differ in their white blood cells number. Also, the number of granulocytes and lymphocytes, which constitute approximately 90% of all leukocyte population, did not reveal statistical differences (according to Mann–Whitney U-test) between CVD or CKD patients groups. Only the number of monocytes was elevated in CKD5 compared to other groups (Table 1). Fluorescence microscopy and flow cytometry were utilized to evaluate the quality of collected samples and the

percentage of leukocyte subpopulations (Figure S1). The obtained results confirmed the data derived from medical examinations and revealed an increased number of monocytes in CKD5 samples (average $9.6\% \pm 1.06$) as compared to other patient groups (average $6.5\% \pm 0.39$) ($p < 0.01$). Therefore, correlation analyses between the identified proteins and the number of particular blood cells and leukocyte subpopulations were performed, in order to exclude the probable influence of this observation on obtained proteomic results (see results for DEPs below and in Table S4).

Isolated cells were lysed, and proteins were analyzed by nano-LC-MS/MS, which resulted in the identification and quantitation of 2845 proteins in total. Enrichment analysis using Fisher's exact test determined the presence of 2320 proteins with intracellular localization (B-H-corrected *p*-value 6.68×10^{-268}), and 525 extracellular proteins. Since the analyzed experimental groups slightly differed in the context of statin and anticoagulant treatment (Table 1), we also statistically evaluated if proteins with differential abundances were related to the applied therapy. Then the data were filtered, and only proteins detected in all samples (1687) were taken into account in the quantitative analyses. A total of 149 differentially expressed proteins (DEPs), whose abundance was significantly altered amid analyzed groups (Table S5), were included in the subsequent bioinformatic surveys. Enrichment analysis in the context of compartmental localization was performed for DEPs, and the results were compared with those obtained for all proteins identified in the study. According to the value of enrichment factor and B-H-corrected FDR *p*-value, the distribution of all categories was similar in both sets of proteins (Figure S2).

PCA revealed that CKD5 and CVD2 differed most significantly between each other and separated from the other groups (Figure S3). The obtained quantitative data confirmed this result—118 proteins out of 149 revealed significant differences only when the CKD5 and CVD2 groups were compared. Among 118 proteins differentiating CKD5 and CVD2 groups, 107 of them showed a “large” effect size with a value above 0.8. Moreover, the average effect size for this set of DEPs was 1.24, suggesting their significant influence on differentiating both groups. These DEPs were further queried by hierarchical clustering. In the CVD2 group, an abundance of 53 proteins was decreased as compared to CKD5, while 65 proteins were downregulated in CKD5 in comparison to CVD2 (Figure S4). Several of these proteins differentiated also CKD5 from other experimental groups (Table S5).

To reveal possible relationships, in the next step, 118 DEPs were correlated using the Pearson correlation, and the resulting matrix was visualized as a heat map (Figure S5). More details about these correlations are presented in other parts of the study (Table S6).

Correlation analyses were also performed between DEPs and the number of particular cells subpopulations and results from medical examinations. No correlated DEPs were identified. Even the number of monocytes revealed Pearson coefficients below 0.3 and above -0.3 . Thus, there were no DEPs correlating with the number of monocytes. However, monocytes negatively correlated with eGFR ($r = -0.63$), suggesting a putative relationship with CKD progression (Table S4).

The abundance of eight proteins (ITGAM, ITGB2, PXN, TLN1, VCL, MMP8, NAMPT, and ANXA2) was validated using an ELISA, WB, MRM, or ddPCR approach. The

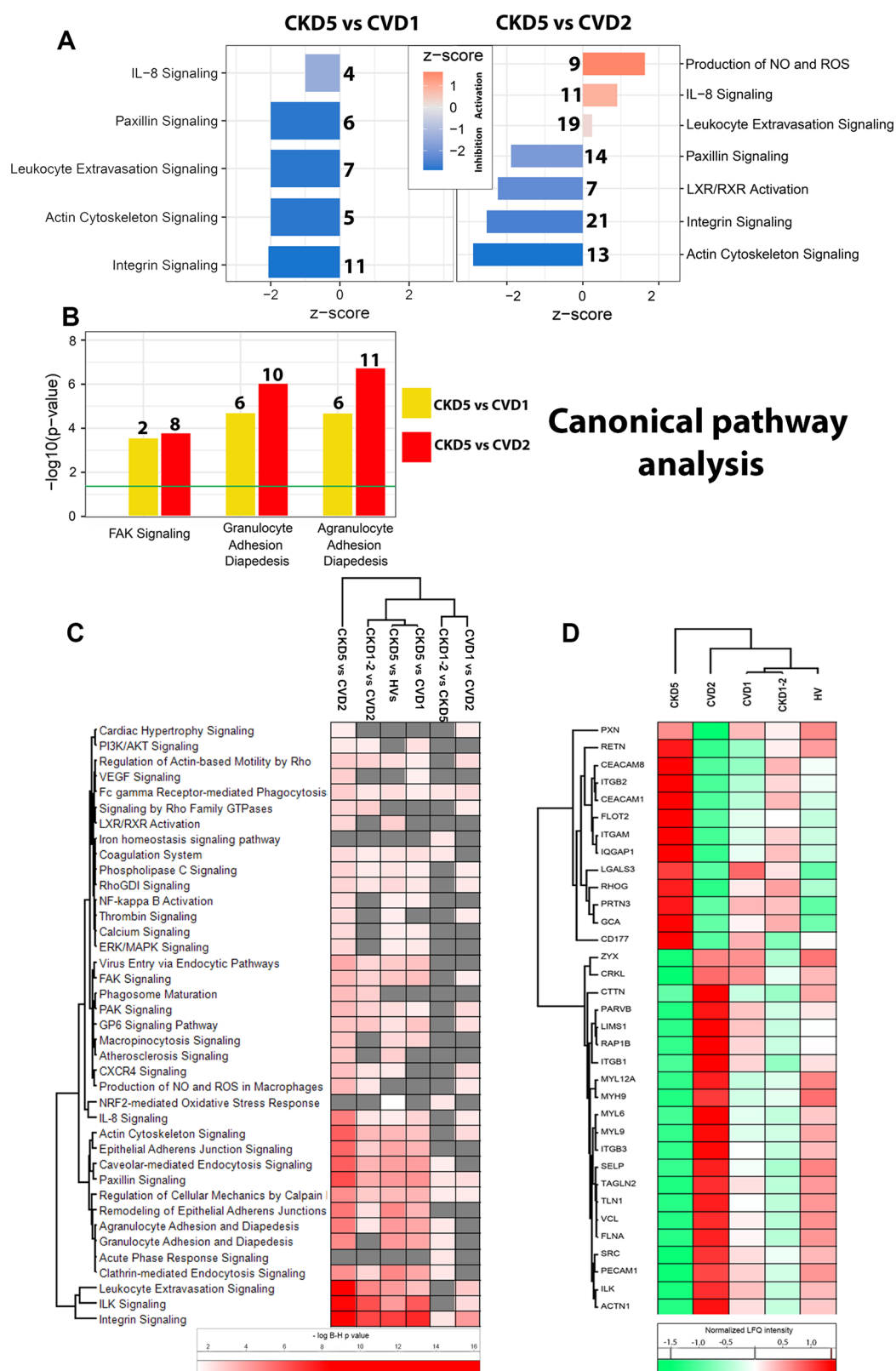


Figure 1. Canonical pathway analysis. (A) The chart of the top statistically enriched pathways according to Ingenuity Pathway Analysis (IPA) calculations presents z-scores and the number of DEPs (bold) associated with each pathway. Comparisons CKD5 vs CVD1 and CVD2 are presented. Inhibited in CKD5 pathways are marked in blue. Pathways activated in CKD5 are depicted in red. (B) Top canonical pathways without predicted z-scores but significantly enriched according to IPA derived Fisher's test. A threshold of $-\log_{10}$ B-H-corrected p -value 1.3 (green line) represents a p -value 0.05. Numbers indicate the number of DEPs associated with each pathway. (C) The heat map presents the top statistically enriched pathways in all comparisons. Functions that were not enriched in a particular comparison are presented in gray. (D) The heat map presents abundances of DEPs involved in actin cytoskeleton, integrin signaling, and leukocyte extravasation—the most statistically enriched pathways in the study. A detailed list of annotations is presented in Table S7.

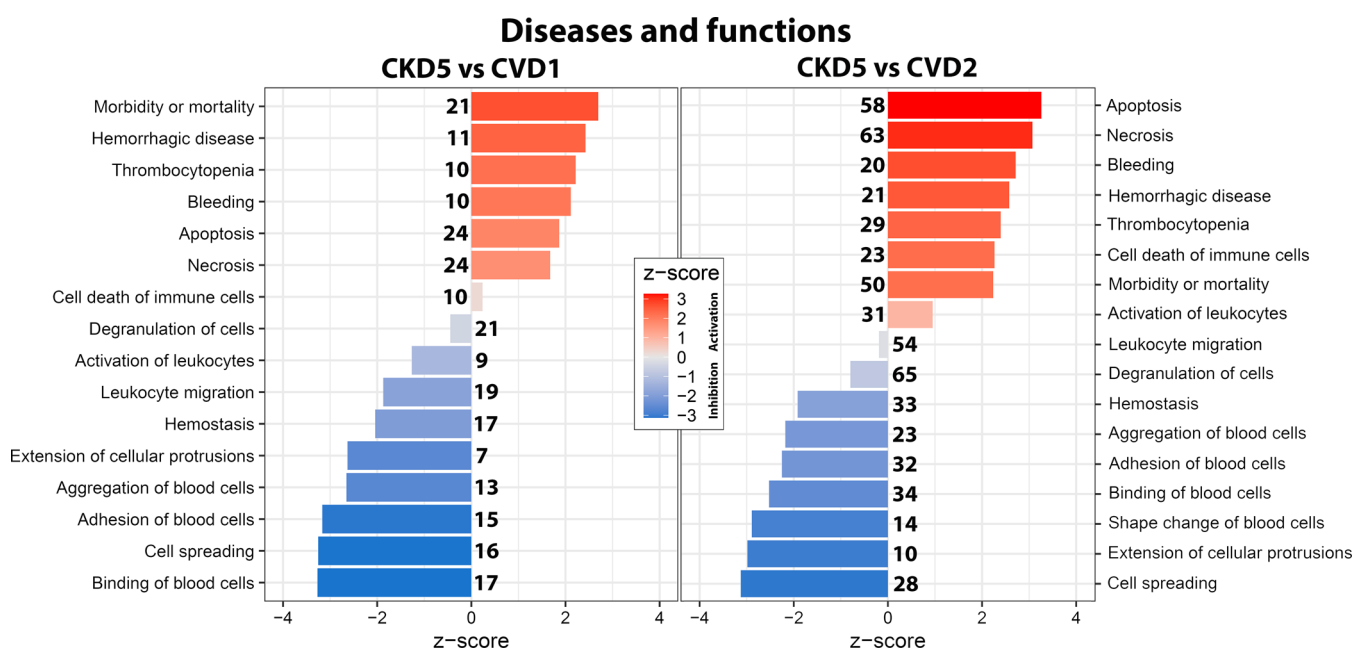


Figure 2. Functional analyses of DEPs identified in CKD5 vs CVD1/CVD2 comparisons. The chart of the top statistically enriched functional categories according to IPA calculations presents z-scores and the number of identified DEPs (numbers in bold) associated with each category. Inhibited categories in CKD5 are marked in blue. Functions activated in CKD5 are marked in red. A detailed list of annotations is presented in Table S7.

abundance of TLN1 was confirmed utilizing two different methods, MRM and WB.

3.1. Integrin and Actin Cytoskeleton Signaling Pathways Are Highlighted in CKD vs CVD Comparison

To assign the functional relationships, the DEPs were queried utilizing Ingenuity canonical pathways classification (Figure 1A,B). Six comparisons between experimental groups with the highest number of identified DEPs were chosen for IPA analysis (Figure 1C). Overall, 37 different canonical pathways were overrepresented according to B-H *p*-value (Table S7) and statistically enriched in CKD5 versus CVD2 comparison. The top-ranked canonical pathways included integrin signaling and leukocyte extravasation signaling as well as ILK, paxillin, and actin cytoskeleton signaling (Figure 1A–C).

We also analyzed the directionality of the overrepresented canonical pathways. For this purpose, we used the IPA z-score algorithm to identify pathway categories that are expected to be activated (positive z-score) or inhibited (negative z-score) between analyzed experimental groups. We revealed that actin cytoskeleton, integrin, and paxillin signaling pathways were the most inhibited in CKD5 compared to CVD2 and CVD1 (Figure 1A). On the other hand, the leukocyte extravasation signaling pathway, sharing many proteins with integrin and actin signaling pathways and being the second most overrepresented pathway, did not reveal any significant directionality (z-score \sim 0) (Figure 1A). We thus decided to more closely examine the abundance of 34 DEPs assigned by IPA analyses to the actin cytoskeleton, integrin signaling, and leukocyte extravasation categories. By comparing the abundance of these proteins, we found that 13 of the 34 DEPs were upregulated in CKD5 (Figure 1D). Some of these proteins were also increased in the CKD1-2 group (9 out of 34).

3.2. Leukocyte Migration and Diapedesis-Related Proteins Are Dysregulated in CKD vs CVD

To gain more functional insight, we further analyzed DEPs in the context of associated functions and diseases (Figure 2). This analysis confirmed the results obtained in the canonical pathway study and revealed overrepresented categories associated with leukocyte activation and migration. Some of them (cell spreading, shape change of blood cells, binding, adhesion, and aggregation of blood cells) were predicted to be inhibited in CKD5 when compared to CVD2 and CVD1. However, overrepresented functions related to cell movement and degranulation did not disclose any significant directionality as suggested by their z-scores.

To confirm the validity of our findings, the differential abundance of selected proteins involved in integrin and actin cytoskeletons signaling during the leukocyte diapedesis process (ITGAM, ITGB2, PXN, TLN1, and VCL) was further assessed. It was evaluated by ELISA (ITGB2, ITGAM, and VCL), MRM (ANXA2), and WB (TLN1), and at the mRNA level by ddPCR (ITGAM, PXN, and TLN1). Validation at the protein level partially confirmed proteomic findings and bioinformatic predictions. The expression of PXN and ITGAM was not altered at the mRNA level, suggesting that differential changes may be related to posttranslational events (Figure 3A). Since integrins can bind to a number of adhesion molecules produced by endothelial cells and released to plasma, we subsequently scrutinized an abundance of well-characterized plasma integrin ligands: VCAM1, ICAM1, and E-selectin (Figure 3B). Level of expression of these plasma adhesion molecules was significantly elevated in CKD5 as compared to CVD2 and HVs, which was confirmed by two independent methods, MRM and ELISA. Previously, it has been demonstrated that endoglin (EGLN) inhibits the synthesis of several members of the integrin family and regulates integrin-mediated cell adhesion (reviewed in ref 22), and we thus decided to check the level of this protein in

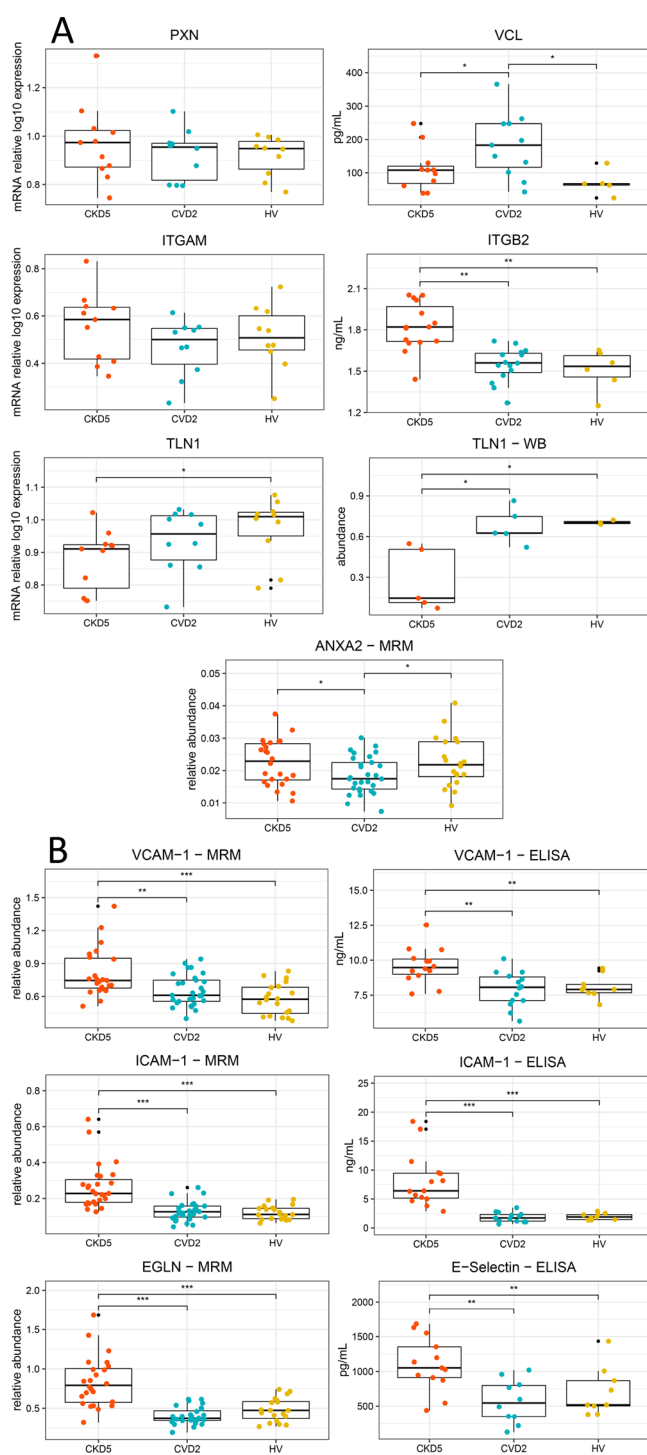


Figure 3. (A) Validation using ddPCR (PXN, ITGAM, TLN1), ELISA (ITGB2, VCL), MRM (ANXA2), and WB (TLN1) methods. Boxes on plots represent interquartile ranges and median. (B) Quantitative ELISA and MRM measurements of selected proteins involved in the integrin signaling pathway, synthesized by endothelium and secreted to plasma. Mann–Whitney U-test. * $p < 0.05$, ** $p < 0.01$, *** $p < 0.001$; $n = 10$ (ELISA), $n = 25$ (MRM), $n = 5$ (WB) in each group.

plasma. The abundance of the soluble form of endoglin was twice higher in CKD5 in comparison to CVD2 and HVs (Figure 3B).

Taken together, utilizing different targeted and non-targeted proteomic approaches, we detected 17 upregulated and 21

downregulated proteins in CKD5 that were functionally related to the actin cytoskeleton, integrin cascade, and leukocyte migration signaling. These experimental results are graphically illustrated in Figure 4. The majority of proteins involved in the initial steps of leukocyte capture from the bloodstream and rolling on the luminal surface of endothelial cells were differentially upregulated (depicted in red color). Increased expression was also detected for ligands and their receptors expressed on endothelium and leukocytes, i.e., E-selectin (SELE), ICAM1, VCAM1, and ICAM3, as well as for some associated proteins, involved in leukocyte adhesion. Both components of integrin MAC1/ $\alpha M\beta 2$ (ITGB2 and ITGAM), specifically expressed by neutrophils and monocytes, were upregulated in CKD5. Among this group of proteins, only P-selectin (SELP) was downregulated. The binding of leukocytes' integrins to their extracellular ligands triggers signaling cascades designated as “outside-in signaling”, which leads to the strengthening of leukocyte adhesion and their movement. We found that most DEPs participating in the later phase of transmigration, apart from paxillin, were downregulated (marked in green in Figure 4). The expression of actin-binding proteins, i.e., VCL, TLN1, ZYX, and proteins regulating the reorganization and polarization of actin cytoskeleton during movement and diapedesis, was decreased. Therefore, the observed changes may partially explain the lack of specified directionality (suggested by biased-z-score) for integrin and actin cytoskeleton signaling and diapedesis-related categories. Correlation analysis revealed that many proteins belonging to both groups of proteins (depicted in Figure 4, in red and green) were associated with each other, i.e., ITGAM negatively correlated with TLN1 ($r = -0.74$), TAGLN2 ($r = -0.73$), FLNA ($r = -0.72$), or VCL ($r = -0.69$). On the other hand, proteins found to be in the same functional group displayed very strong and positive relationships; i.e., ITGB2 correlated with ITGAM ($r = 0.86$), and TLN1 as revealed by Pearson correlation coefficients above 0.9 for VCL, FLNA, or TAGLN1 (0.95, 0.97, and 0.93, respectively; Table S6).

3.3. Advanced CKD Group Discloses a Higher Rate of Apoptosis

Moreover, the obtained results revealed dysregulation of processes related to cell death and survival. The necrosis and apoptosis pathways were activated in the CKD5 as compared to CVD2 (z-scores of 3.07 and 3.26, respectively, Figure 2) and CKD1-2 (z-scores of 1.96 and 2.88, Table S7). Activation of these processes was also predicted in CKD5 group versus CVD1 comparison, albeit with a less pronounced effect (z-scores of 1.67 and 1.86, respectively). Similarly, morbidity/mortality and cell death of immune cells were identified as activated in CKD5 compared to CVD2 (z-scores of 2.69 and 2.64, respectively) and CVD1 (z-scores of 2.23 and 0.23, respectively).

Flow cytometric analysis of necrosis and apoptosis rate in examined cells, performed by staining with CellEvent Casp3/7 in conjunction with propidium iodide, confirmed these predictions (Figure 5A). The percentage of live cells in CVD2 samples was calculated at $95.74\% \pm 2.95$, whereas CKD5 samples demonstrated on average $76\% \pm 6.38$ of live cells, and these differences were statistically significant ($p < 0.001$), (Figure 5B). Specifically, the number of late apoptotic cells was highly increased in CKD5 compared to CVD2 ($14\% \pm 2$ as compared to $3.7\% \pm 0.7$; $p < 0.001$). More than 20 DEPs related to cell death and survival were identified, all of

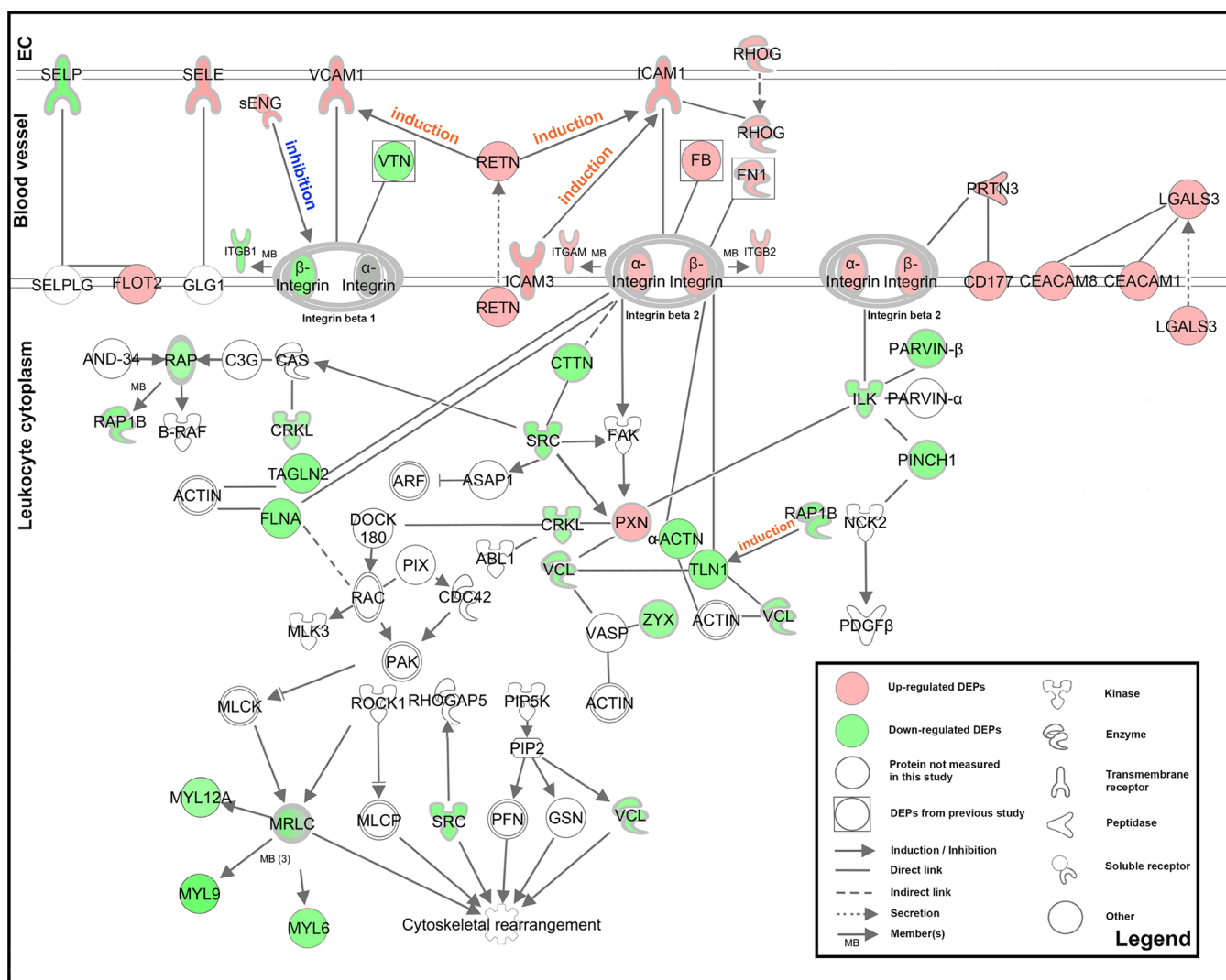


Figure 4. Pathway illustrating the involvement of DEPs identified in CKD5 vs CVD2 comparison in integrin/actin signaling processes during leukocyte extravasation. An increase in CKD5 expression (depicted in red) was detected for ligands and their receptors expressed on both endothelium and leukocyte surface, as well as for proteins regulating activation and adhesion. Downregulation observed in CKD5 (depicted in green) was characteristic for actin-binding proteins and proteins regulating the reorganization and polarization of actin cytoskeleton during diapedesis. Three DEPs identified in the previous study, namely vitronectin (VTN), fibrinogen (FB), and fibronectin 1 (FN1) (depicted by squares),¹¹ and corroborated by the current findings, were added as components of the pathways.

them found to be upregulated in CKD5. Majority of these proteins positively correlated with each other (Table S6). Moreover, a Pearson's correlation test revealed that many of these proteins were negatively correlated with eGFR, i.e., NCF1, NCF2, NAMPT, MMP8, MMP9, ANXA1, ANXA3, and ANXA11 (all with $r < -0.5$). It suggests that upregulation of necrosis and apoptosis processes is closely associated with the progression of renal dysfunction. To validate this finding, two proteins categorized by IPA software as participated in apoptosis, NAMPT and MMP8, were validated by ddPCR method at the mRNA level (Figure 5C). Correlation analysis between particular DEPs revealed that many identified proteins involved in apoptotic processes displayed a positive relationship with a group of upregulated proteins engaged in cell adhesion and migration. For instance, ITGAM and ITGB2 correlated with MMP9, NCF1, NCF2, ANXA1, and ANXA3 with average correlation coefficients of 0.77 and 0.61, respectively. Similarly, the same apoptotic proteins were found to be negatively correlated with many downregulated

in CKD5 diapedesis proteins (see details in Table S6). This observation suggests that alterations in the abundance of proteins related to integrin and actin cytoskeleton pathways, and cell adhesion and movement, can be closely associated with an elevated rate of apoptosis and mortality in CKD5 cells observed in proteomics and microscopy/flow cytometry analyses.

Apart from cell death and survival, the functions linked to hemostasis, i.e., thrombocytopenia and hemorrhagic disease (19 and 21 DEPs, respectively), were activated in CKD5 as compared to CVD2 (z -scores 2.39 and 2.57), and to a lesser extent versus CVD1 (z -scores 2.21 and 2.42, Figure 2) and CKD1-2 (z -scores 2 for both, Table S7).

Irrespective of cardiovascular background, we also tried to reveal how the progression of CKD influences the composition of leukocytes' proteome. For this purpose, we compared both groups of CKD and HVs. Functional analysis revealed categories enriched specifically in CKD1-2 as compared to CKD5. For instance, the flux of ions (z -score 2.17), ion

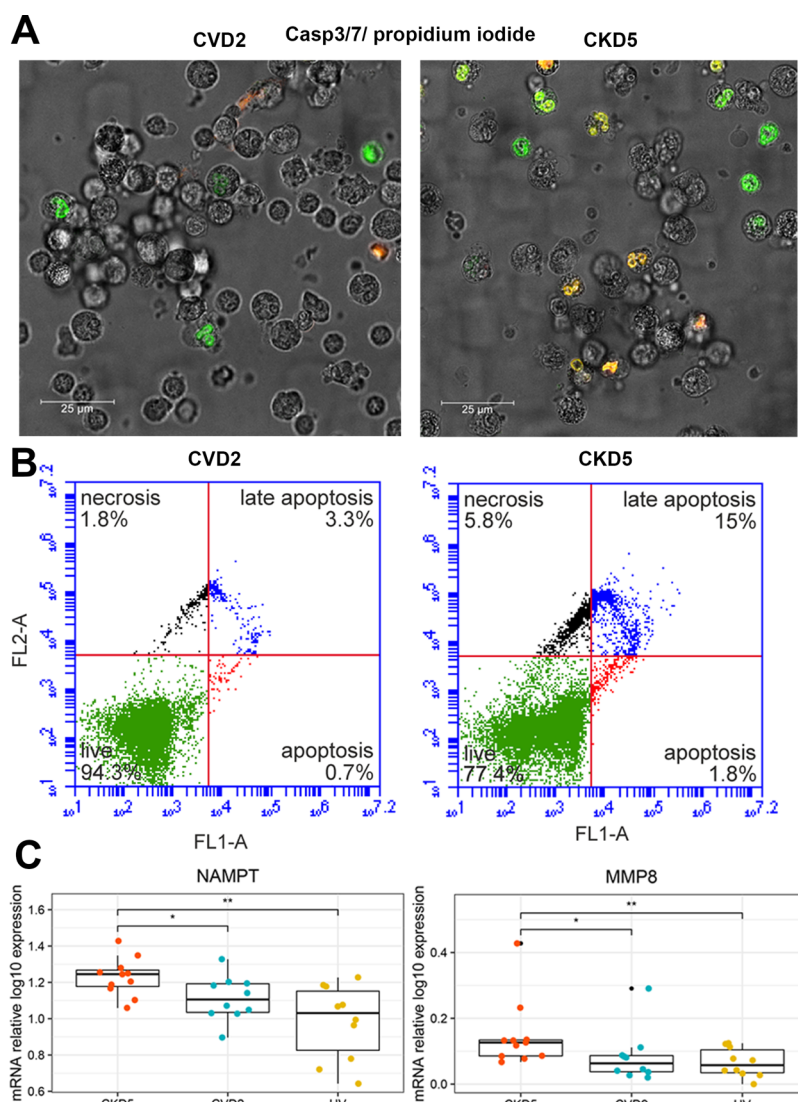


Figure 5. Upregulation of apoptosis in CKD5. Dysregulation of processes related to cell death revealed by bioinformatic analysis confirmed by (A) confocal microscopy (green, apoptotic cells; orange, dead cells) and (B) flow cytometric analysis assessing apoptosis/necrosis in representative CVD2 and CKD5 samples. (C) Validation of *NAMPT* and *MMP8* at the transcriptome level using ddPCR, corroborated the results of proteome profiling using nano-LC-MS/MS. Mann–Whitney U: * $p < 0.05$, ** $p < 0.01$; $n = 10$ in each group.

homeostasis of cells (z-score 2.23), cell viability (z-score 2.71), cellular infiltration by leukocytes (z-score 2.21), and homing of cells (z-score 2.39) were more pronounced at the initial stage of CKD (Table S7 and Figure S6). Comparing both CKD groups also revealed categories related to the blood coagulation cascade and hemostasis, and suggested that these processes are more perturbed at the advanced stage of CKD. Also, functions related to apoptosis and necrosis were clearly upregulated in CKD5 compared to CKD1-2. However, these differences were not as pronounced when comparing CKD5 to CVD2 (Table S7).

Many functional categories were statistically enriched also in CVD1 as compared to CVD2. Stimulation of cells, the immune response of leukocytes, migration of leukocytes, atherosclerosis, and occlusion of arteries were predicted to be activated in CVD1 in comparison to CVD2, with z-scores close to 2 (1.95–1.98). On the other hand, several “general inflammation” categories, like organ inflammation (z-score 1.87), were upregulated in CVD2 group as compared to CVD1.

Finally, we analyzed a proteomic profile of healthy volunteers in comparison to particular patients’ groups. Not surprisingly, the highest differences were revealed in HVs vs CKD5 comparison. Although enriched canonical pathway and function categories were similar to those indicated in the comparison between CKD5 and other groups of patients, the intensity of observed differences was very often higher based on z-score values. For example, z-score for hemostasis function was revealed as 2.0 for CKD1-2 vs CKD5 comparison, whereas for HVs vs CKD5 this value was more significant and amounted to 2.7 (Table S7).

3.4. TGFB1, SRF, and GATA1 Are the Primary Upstream Regulators at the Protein Level

To identify the regulators predicted to be activated or suppressed in the cascade, the DEPs were functionally linked to upstream network drivers. Transforming Growth Factor Beta 1 (TGFB1) was identified as a top upstream regulator in all comparisons, according to B-H-corrected p -value. However, according to a z-score (−1.70 and −1.73 for CKD5 vs CVD2 and CKD5 vs CVD1 comparisons, respectively) directionality

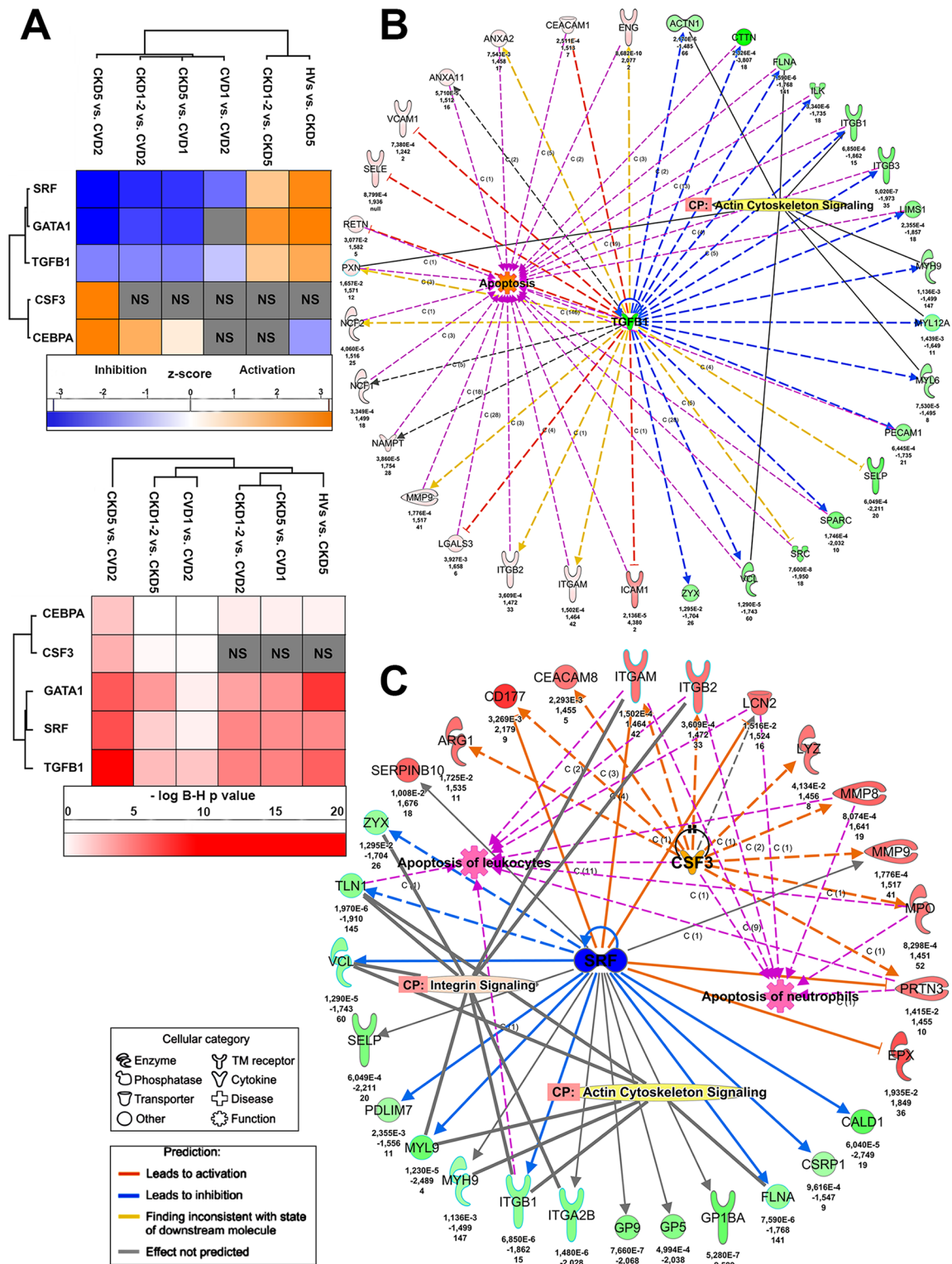


Figure 6. Upstream regulators analysis using Ingenuity Pathway Analysis software. (A) The top upstream regulators with predicted activation/inhibition state according to calculated z-score (the upper heat map) and B-H-corrected p-value (the lower heat map). Functions overrepresented according to B-H-corrected p-value but without calculated z-scores are present in gray. Functions not enriched according to B-H-corrected p-value are present in gray with NS. A detailed list of annotations is presented in the Table S7. (B) The network displays predicted interactions between DEPs identified in CKD5 vs CVD2 comparison and the top upstream regulator according to B-H-corrected p-value: TGFB1. Links with apoptosis and actin cytoskeleton categories are presented. (C) The network displays predicted interactions between DEPs identified in CKD5 vs CVD2 comparison and the top upstream regulators, according to z-score: SRF and CSF3. Links with apoptosis and integrin signaling categories are presented. The downregulated in CKD5 compared to CVD2 proteins are shown in green and upregulated ones in red. The arrows indicate the directionality of changes. Solid and dashed lines indicate experimentally confirmed and predicted interactions, respectively. Numbers by the nodes in panels B and C refer to B-H-corrected p-values, fold changes, and the number of unique peptides, respectively.

was not predicted, suggesting crosstalk with other cellular processes which may influence the score (Figure 6A and Table S7). To functionally bridge these findings, we further connected 33 DEPs predicted to be regulated by TGFB1 (Figure 6B). The network analysis revealed that TGFB1 is an upstream regulator of a cell migration process, including actin cytoskeleton organization and signaling (dysregulated in CKD5), and regulates apoptotic/necrotic processes (upregulated in CKD5). This result is consistent with the dysregulation of canonical pathways and biological functions observed in CVD and CKD. The top upstream regulators with predicted inhibition included transcription factors: serum response factor (SRF) and GATA-binding factor 1 (GATA1) (Figure 6A, Table S7). Twenty-two DEPs were predicted to be regulated by SRF, and 15 of them were downregulated in CKD5 in comparison to CVD2 (Figure 6C). Colony stimulating factor 3 (CSF3) and CCAAT enhancer binding protein alpha (CEBPA) were predicted to be the top positive regulators of the networks, uniquely in CKD5 versus CVD2 comparison. Eleven DEPs involved in cell death/survival categories and processes related to inflammation were predicted to be downstream targets for CSF3 and upregulated in their expression in CKD5 versus CVD2 comparison (Figure 6C). Moreover, other proteins predicted to be upregulated due to reduced expression level of SRF, constituted a part of these functional categories. The proteins negatively regulated by SRF belong to cell–cell aggregation, adhesion, and transmigration processes and integrin, paxillin, and actin cytoskeleton signaling pathways. Although, the relationship between SRF and atherosclerosis in classical CVD patients is not novel, the underlying alterations observed in CKD and the differences between CKD and CVD have not yet been presented.

4. DISCUSSION

Although CKD is a disorder associated with a loss of renal function, these patients are exposed to a high risk of atherosclerosis. The predominant causes of their deaths are cardiovascular events.^{23,24} Atherosclerosis is an inflammatory disease, and during its progression, various types of immune cells play essential roles in the initiation and progression of atherosclerotic plaques. During the progression of atherosclerosis unrelated to kidney dysfunction, monocytes are recruited to the intima and, due to dyslipidemia, differentiate into foam cells, which triggers atherosclerotic plaque formation.²⁵ The accumulation of inflammatory cells and lipids in the arteries leads to the formation of mature plaques and the thickening of their walls. In contrast, due to “reverse epidemiology”, CKD patients do not reveal typical dyslipidemia, and their plaques show more inorganic character.²⁶ Nonetheless, systemic inflammation is undoubtedly elevated in CKD (reviewed in ref 27).

Our previous studies utilizing patients' plasma samples indicated an upregulation of systemic inflammation during CKD development and confirmed that this phenomenon is more pronounced in CKD compared to the “classical” CVD.¹¹ At present, in order to provide deeper insights into the inflammation-based mechanisms underlying atherosclerosis-related and non-related to CKD, we utilized the proteomic approach to investigate the global protein profiles of the immune system cells, focusing on leukocytes isolated from the patients at the initial and advanced stages of CKD and CVD. We also subsequently scrutinized the abundance of molecules produced by endothelial cells and released to plasma to link

the literature findings with proteomic results. Correlation analysis revealed that there is no association between identified DEPs and the particular leukocyte subpopulations. The number of monocytes, which differentiated CKD5 from the other groups, did not show any correlation with DEPs. However, considering that monocytes compose below 10% of all leukocytes, this result is not surprising. Nevertheless, we demonstrated that monocytes negatively correlated with CKD progression what was presented before,²⁸ but never revealed in the currently presented experimental setup.

Our results show that CKD5 and CVD2 groups, representing patients with similar advanced symptoms of CVD but differing in renal function, reveal the most differences in proteomic profiles. The CKD1-2 and CVD1 groups, which signify patients with initial atherosclerosis symptoms, showed a high level of similarity in their protein profiles. These results are consistent with those presented in our previous study utilizing plasma samples.^{11,29} In the present study, we demonstrated for the first time that CKD leukocytes phenotypically differ from those derived from CVD patients, in the dynamics of their biological pathways and processes related to cell–cell adhesion and transmigration machinery (as judged by the differential expression of several pathway components). Several canonical pathways and processes related to leukocyte rolling and adhesion and the subsequent migration to the sites of inflammation were found dysregulated in comparison amid CKD5 and CVD2. In other comparisons, i.e., CKD5 vs CVD1 and CKD1-2 vs CVD2, these pathways were also found to be statistically differentially enriched, but with lesser significance. Notably, only early steps, but not initial, of leukocyte adhesion and rolling on the surface of endothelial cells were differentially upregulated in CKD compared to CVD (Figure 4). P-selectin is responsible for the initial stage of leukocyte arrest on endothelium, but its level of expression was decreased in CKD5. Importantly, maximal expression of this protein has been observed after 10 min of leukocyte activation, after which E-selectin and other proteins identified as upregulated in our study take over its role.³⁰

Selectins interact with receptors present on the surface of leukocytes with marginal affinity, which results in a reduction of leukocytes velocity. The tight binding and arrest of leukocytes on endothelium are mediated by the interaction of integrins with their ligands, which leads to the strengthening of adhesion.³¹ Several reports have demonstrated the increased level of ligands, i.e., VCAM1 and ICAM1 in CVD patients as the factor promoting atherosclerosis development,^{32–34} to our knowledge, this is the first study directly comparing CKD and CVD patients in this context. The upregulation of integrins in CKD in comparison to CVD has not been demonstrated earlier. Crawling of the leukocytes to endothelial junctions is almost exclusively dependent on interactions between leukocyte-specific $\beta 2$ integrins MAC1 and LFA-1 and their ligands, ICAM1 and ICAM3.^{35,36} The increased expression level of ICAM1, ICAM3, and other molecules interacting with them and $\beta 2$ integrins MAC1 and LFA-1 suggest the upregulation of MAC1/LFA4-ICAM-dependent crawling mechanism determining the subsequent stage of the leukocyte adhesion cascade. These integrins play vital roles in leukocyte targeting to the atherosclerotic plaques.³¹ Their upregulation can affect the ability of leukocytes to adhere to the endothelium and promote the local accumulation of the leukocytes on endothelium, which supports pro-inflammatory conditions and atherosclerotic plaques' development.

Endoglin is another transmembrane molecule that interacts with β 1-type integrin and promotes leukocytes' migration to the inflammatory site.³⁷ However, it has been presented that the soluble form of endoglin inhibits leukocyte extravasation.³⁸ We demonstrated an increased abundance of this specific form of endoglin. It may explain the decreased level of ITGB1, a component of β 1 integrin VLA-4. Furthermore, the reduced expression level of vitronectin, one of the ligands for β 1 integrin in CKD5 was previously demonstrated by us.¹¹

In a physiological state, adhesion of leukocytes to endothelial cells leads to cell motility, by controlling cytoskeletal rearrangements causing transendothelial migration. Actin cytoskeleton assembly and its dynamics are pivotal for cell migration and immune response involving leukocytes. In our study, almost all DEPs participating in the later transmigration phase were downregulated in the CKD5 group (Figure 4). Among those were actin-binding proteins as well as proteins regulating the reorganization of the actin cytoskeleton. Paxillin acts as an adaptor stabilizing the linkage of VLA-4 to actin cytoskeleton during leukocyte adhesion upon exposure to fluid flow and transmission of mechanical force,³⁹ which partially can explain its increased expression level.

Leukocytes can sense and resist high external forces from flowing blood through RAP1 and PI3K regulation of actin polymerization.⁴⁰ In our analysis, downregulation of RAP1 and disturbances in expression of other proteins regulating the cytoskeleton among the CKD5 and CVD2 groups were identified. Rullo and co-workers⁴⁰ suggested that reinforcement of tension-bearing structures by actin is critical for adaptation of cells to the external force. Therefore, decreased ability of CKD5 cells to actin cytoskeleton reorganization during the transmigration process might be compensated by the mechanism of stabilization of leukocytes on the surface of endothelium by integrin-related mechanism(s). Both phenomena might influence endothelial dysfunction and acceleration of atherosclerosis progression.

Under these circumstances, the observed upregulation of processes related to apoptosis in CKD5 further confirmed by flow cytometry and confocal microscopy analysis is not surprising (Figure 5). The misbalance between different phases of leukocyte extravasation may lead to the alteration of cellular integrity and trigger cell death. We have not detected differences in the number of leukocytes. It has been shown, however, that even though neutrophils undergo apoptosis, they are still able to prolong their longevity and survive for many hours before disintegration.⁴¹ Moreover, a direct relationship between apoptosis and loss of cytoskeletal functions has been demonstrated.⁴² On the other hand, the increased apoptosis resulting from oxidative stress in CKD is known (reviewed by⁴³). Uremia and circulating uremic toxins evoke an imbalance between antioxidant protection and reactive oxygen species production, resulting in endothelial dysfunction leading to advanced CKD. Our previous study described that oxidative stress is more pronounced in CKD-related atherosclerosis than in classical CVD.¹¹ We also suggested that due to the progression of kidney dysfunction, CVD acceleration can be different at the initial and advanced stages of CKD, which might partially explain the differences between CKD5 and CVD2 profiles. In this study, we added another piece of the puzzle to the story: dysregulation in leukocytes' adhesion and extravasation processes.

However, apart from associations between CKD and CVD, we also confirmed that the progression of CKD and CVD itself

influences on the composition of leukocytes' proteome. We have shown an upregulation of proteins related to inflammatory processes in advanced CVD. We have also indicated an ionic homeostasis and blood coagulation cascade, specifically associated with CKD progression.

Limitations inherent in this study should also be taken into account. Although this study sheds some light on the mechanism of chronic kidney disease-related atherosclerosis, the clinical significance and statistical power would undoubtedly benefit from more numerous cohorts. Nevertheless, our results underline the importance and necessity of studying and comparing patients with CKD and CVD in one study, and constitute a promising prelude for future work.

5. CONCLUSIONS

In the present study, we utilized proteomic profiling of leukocytes and demonstrated for the first time a dysregulation of proteins involved in different phases of leukocytes' transmigration which are very pronounced at the advanced stage of CKD. Moreover, the upregulation of proteins related to apoptotic cell death was also observed, which was functionally confirmed on the cellular level. The observed misbalance can lead to inflammation and, as a consequence, endothelial dysfunction and atherosclerotic plaque development.

■ ASSOCIATED CONTENT

SI Supporting Information

The Supporting Information is available free of charge at <https://pubs.acs.org/doi/10.1021/acs.jproteome.0c00883>.

Figure S1, microscopy and flow cytometry analysis of isolated cells; Figure S2, enrichment analysis in the context of compartmental localization; Figure S3, unsupervised principal component analysis; Figure S4, heat maps presenting abundance of identified DEPs; Figure S5, correlation coefficient matrix for DEPs in CKD5 vs CVD2 comparison; Figure S6, IPA functional analysis; Figure S7, TLN1 immunoblots for entire membranes (PDF)

Table S1, Pearson's correlation coefficients between the label-free quantification intensities from replicates in all experimental groups (XLSX)

Table S2, list of primers used in ddPCR analysis (XLSX)

Table S3, list of peptide transitions with precursor and product masses, charges, retention times, and collision energies used for MRM analysis (XLSX)

Table S4, results of correlation analyses between the identified DEPs and eGFR, including the number of particular blood cells and leukocyte subpopulations (XLSX)

Table S5, complete list of DEPs identified in the study: names of proteins, number of identified peptides, p-values, fold changes, effect size for all group comparisons, and UniProt accession numbers (XLSX)

Table S6, results of Pearson's correlation analyses between the DEPs identified in CKD5 vs CVD2 comparison (XLSX)

Table S7: A detailed list of IPA annotation results for canonical pathway, diseases/functions and upstream regulator categories with $-\log_{10}$ B-H corrected p-values and z-scores (XLSX)

AUTHOR INFORMATION**Corresponding Author**

Magdalena Luczak – Institute of Bioorganic Chemistry, Polish Academy of Sciences, 61-704 Poznan, Poland; orcid.org/0000-0002-2182-5699; Email: magdalul@ibch.poznan.pl

Authors

Joanna Tracz – Institute of Bioorganic Chemistry, Polish Academy of Sciences, 61-704 Poznan, Poland; orcid.org/0000-0003-0962-5114

Luiza Handschuh – Institute of Bioorganic Chemistry, Polish Academy of Sciences, 61-704 Poznan, Poland

Maciej Lalowski – Institute of Bioorganic Chemistry, Polish Academy of Sciences, 61-704 Poznan, Poland; Helsinki Institute for Life Science (HiLIFE) and Faculty of Medicine, Biochemistry/Developmental Biology, Meilahti Clinical Proteomics Core Facility, University of Helsinki, 00100 Helsinki, Finland

Łukasz Marczak – Institute of Bioorganic Chemistry, Polish Academy of Sciences, 61-704 Poznan, Poland; orcid.org/0000-0001-8602-0077

Katarzyna Kostka-Jeziorny – Department of Hypertension, Angiology and Internal Disease, Poznan University of Medical Sciences, 61-848 Poznan, Poland

Bartłomiej Perek – Department of Cardiac Surgery and Transplantology, Poznan University of Medical Sciences, 61-848 Poznan, Poland

Maria Wanic-Kossowska – Department of Nephrology, Transplantology and Internal Medicine, Poznan University of Medical Sciences, 60-355 Poznan, Poland

Alina Podkowińska – Dialysis Station Dravis sp. z o.o., 60-631 Poznan, Poland

Andrzej Tykarski – Department of Hypertension, Angiology and Internal Disease, Poznan University of Medical Sciences, 61-848 Poznan, Poland

Dorota Formanowicz – Department of Medical Chemistry and Laboratory Medicine, Poznan University of Medical Sciences, 60-806 Poznan, Poland

Complete contact information is available at:

<https://pubs.acs.org/10.1021/acs.jproteome.0c00883>

Author Contributions

J. Tracz: investigation, validation, writing - original draft; L. Handschuh, L. Marczak: investigation; M. Lalowski: formal analysis, writing - review and editing; K. Kostka-Jeziorny, B. Perek, A. Podkowińska, A. Tykarski and M. Wanic-Kossowska: resources; D. Formanowicz: conceptualization, resources, writing - review and editing; M. Luczak: conceptualization, formal analysis, visualization, writing - review and editing, supervision, funding acquisition. All authors read and approved the final version of a manuscript.

Notes

The authors declare no competing financial interest.

ACKNOWLEDGMENTS

This work was supported by the National Science Centre, Poland, under grant no. 2015/19/B/NZ2/02450, to M. Luczak. The authors wish to thank Dr. Agnieszka Fedoruk-Wyszomirska and Dr. Dorota Gurda (Institute of Bioorganic Chemistry PAS) for support in confocal microscopy and flow

cytometry. The graphical abstract was generated using the web-based tool BioRender (Biorender.com).

REFERENCES

- (1) Levin, A.; Stevens, P. E.; Bilous, R. W.; Coresh, J.; De Francisco, A. L. M.; De Jong, P. E.; Griffith, K. E.; Hemmelgarn, B. R.; Iseki, K.; Lamb, E. J.; Levey, A. S.; Riella, M. C.; Shlipak, M. G.; Wang, H.; White, C. T.; Winearls, C. G. Kidney Disease: Improving Global Outcomes (KDIGO) CKD Work Group. KDIGO 2012 Clinical Practice Guideline for the Evaluation and Management of Chronic Kidney Disease. *Kidney Int. Suppl.* **2013**, *3*, 1–150.
- (2) Gansevoort, R. T.; Correa-Rotter, R.; Hemmelgarn, B. R.; Jafar, T. H.; Heerspink, H. J. L.; Mann, J. F.; Matsushita, K.; Wen, C. P. Chronic Kidney Disease and Cardiovascular Risk: Epidemiology, Mechanisms, and Prevention. *Lancet* **2013**, *382*, 339–352.
- (3) Go, A. S.; Chertow, G. M.; Fan, D.; McCulloch, C. E.; Hsu, C. Y. Chronic Kidney Disease and the Risks of Death, Cardiovascular Events, and Hospitalization. *N. Engl. J. Med.* **2004**, *351* (13), 1296–1305.
- (4) De Jager, D. J.; Grootendorst, D. C.; Jager, K. J.; Van Dijk, P. C.; Tomas, L. M. J.; Ansell, D.; Collart, F.; Finne, P.; Heaf, J. G.; De Meester, J.; Wetzels, J. F. M.; Rosendaal, F. R.; Dekker, F. W. Cardiovascular and Noncardiovascular Mortality among Patients Starting Dialysis. *JAMA - J. Am. Med. Assoc.* **2009**, *302* (16), 1782–1789.
- (5) Van Der Velde, M.; Matsushita, K.; Coresh, J.; Astor, B. C.; Woodward, M.; Levey, A.; De Jong, P.; Gansevoort, R. T.; El-Nahas, M.; Eckardt, K. U.; Kasiske, B. L.; Ninomiya, T.; Chalmers, J.; MacMahon, S.; Tonelli, M.; Hemmelgarn, B.; Sacks, F.; Curhan, G.; Collins, A. J.; Li, S.; Chen, S. C.; Hawaii Cohort, K. P.; Lee, B. J.; Ishani, A.; Neaton, J.; Svendsen, K.; Mann, J. F. E.; Yusuf, S.; Teo, K. K.; Gao, P.; Nelson, R. G.; Knowler, W. C.; Bilo, H. J.; Joosten, H.; Kleefstra, N.; Groenier, K. H.; Auguste, P.; Veldhuis, K.; Wang, Y.; Camarata, L.; Thomas, B.; Manley, T. Lower Estimated Glomerular Filtration Rate and Higher Albuminuria Are Associated with All-Cause and Cardiovascular Mortality. A Collaborative Meta-Analysis of High-Risk Population Cohorts. *Kidney Int.* **2011**, *79* (12), 1341–1352.
- (6) Kalantar-Zadeh, K.; Block, G.; Humphreys, M. H.; Kopple, J. D. Reverse Epidemiology of Cardiovascular Risk Factors in Maintenance Dialysis Patients. *Kidney Int.* **2003**, *63*, 793–808.
- (7) Maini, R.; Wong, D. B.; Addison, D.; Chiang, E.; Weisbord, S. D.; Jneid, H. Persistent Underrepresentation of Kidney Disease in Randomized, Controlled Trials of Cardiovascular Disease in the Contemporary Era. *J. Am. Soc. Nephrol.* **2018**, *29* (12), 2782–2786.
- (8) Podkowińska, A.; Formanowicz, D. Chronic Kidney Disease as Oxidative Stress- and Inflammatory-Mediated Cardiovascular Disease. *Antioxidants* **2020**, *9* (8), 752.
- (9) Romanova, Y.; Laikov, A.; Markelova, M.; Khadiullina, R.; Makseev, A.; Hasanova, M.; Rizvanov, A.; Khaiboullina, S.; Salafutdinov, I. Proteomic Analysis of Human Serum from Patients with Chronic Kidney Disease. *Biomolecules* **2020**, *10* (2), 257.
- (10) Lygirou, V.; Latosinska, A.; Makridakis, M.; Mullen, W.; Delles, C.; Schanstra, J. P.; Zoidakis, J.; Pieske, B.; Mischak, H.; Vlahou, A. Plasma Proteomic Analysis Reveals Altered Protein Abundances in Cardiovascular Disease. *J. Transl. Med.* **2018**, *16* (1), 104.
- (11) Luczak, M.; Suszynska-Zajczyk, J.; Marczak, L.; Formanowicz, D.; Pawliczak, E.; Wanic-Kossowska, M.; Stobiecki, M. Label-Free Quantitative Proteomics Reveals Differences in Molecular Mechanism of Atherosclerosis Related and Non-Related to Chronic Kidney Disease. *Int. J. Mol. Sci.* **2016**, *17*, 631.
- (12) *Chronic Kidney Disease (Partial Update): Early Identification and Management of Chronic Kidney Disease in Adults in Primary and Secondary Care*, NICE Clinical Guidelines, No. 182; National Institute for Health and Care Excellence: London, UK, 2014.
- (13) Levey, A. S.; Bosch, J. P.; Lewis, J. B.; Greene, T.; Rogers, N.; Roth, D. A More Accurate Method to Estimate Glomerular Filtration Rate from Serum Creatinine: A New Prediction Equation.

Modification of Diet in Renal Disease Study Group. *Ann. Intern. Med.* **1999**, *130* (6), 461–470.

(14) Dagur, P. K.; McCoy, J. P. Collection, Storage, and Preparation of Human Blood Cells. *Curr. Protoc. Cytom.* **2015**, *73*, 5.1.1–5.1.16.

(15) Cox, J.; Mann, M. MaxQuant Enables High Peptide Identification Rates, Individualized p.p.b.-Range Mass Accuracies and Proteome-Wide Protein Quantification. *Nat. Biotechnol.* **2008**, *26* (12), 1367–1372.

(16) Handschuh, L.; Wojciechowski, P.; Kazmierczak, M.; Marcinkowska-Swojak, M.; Luczak, M.; Lewandowski, K.; Komarnicki, M.; Blazewicz, J.; Figlerowicz, M.; Kozlowski, P. NPM1 Alternative Transcripts Are Upregulated in Acute Myeloid and Lymphoblastic Leukemia and Their Expression Level Affects Patient Outcome. *J. Transl. Med.* **2018**, *16*, 232.

(17) MacLean, B.; Tomazela, D. M.; Shulman, N.; Chambers, M.; Finney, G. L.; Frewen, B.; Kern, R.; Tabb, D. L.; Liebler, D. C.; MacCoss, M. J. Skyline: An Open Source Document Editor for Creating and Analyzing Targeted Proteomics Experiments. *Bioinformatics* **2010**, *26* (7), 966–968.

(18) Levin, Y. The Role of Statistical Power Analysis in Quantitative Proteomics. *Proteomics* **2011**, *11* (12), 2565–2567.

(19) Cohen, J. A Power Primer. *Psychol. Bull.* **1992**, *112* (1), 155–159.

(20) Hedges, L. V.; Olkin, I. *Statistical Methods for Meta-Analysis*; Academic Press, 1985.

(21) Pezzini, F.; Bianchi, M.; Benfatto, S.; Griggio, F.; Doccini, S.; Carozzo, R.; Dapkunas, A.; Delledonne, M.; Santorelli, F. M.; Lalowski, M. M.; Simonati, A. The Networks of Genes Encoding Palmitoylated Proteins in Axonal and Synaptic Compartments Are Affected in PPT1 Overexpressing Neuronal-like Cells. *Front. Mol. Neurosci.* **2017**, *10*, 266.

(22) Rossi, E.; Lopez-Novoa, J. M.; Bernabeu, C. Endoglin Involvement 1 in Integrin-Mediated Cell Adhesion as a Putative Pathogenic Mechanism in Hereditary Hemorrhagic Telangiectasia Type 1 (HHT1). *Front. Genet.* **2015**, *5*, 457.

(23) Muntner, P.; He, J.; Astor, B. C.; Folsom, A. R.; Coresh, J. Traditional and Nontraditional Risk Factors Predict Coronary Heart Disease in Chronic Kidney Disease: Results from the Atherosclerosis Risk in Communities Study. *J. Am. Soc. Nephrol.* **2005**, *16* (2), 529–538.

(24) Recio-Mayoral, A.; Banerjee, D.; Streather, C.; Kaski, J. C. Endothelial Dysfunction, Inflammation and Atherosclerosis in Chronic Kidney Disease – a Cross-Sectional Study of Predialysis, Dialysis and Kidney-Transplantation Patients. *Atherosclerosis* **2011**, *216* (2), 446–451.

(25) Woollard, K. J.; Geissmann, F. Monocytes in Atherosclerosis: Subsets and Functions. *Nat. Rev. Cardiol.* **2010**, *7* (2), 77–86.

(26) Schwarz, U.; Buzello, M.; Ritz, E.; Stein, G.; Raabe, G.; Wiest, G.; Mall, G.; Amann, K. Morphology of Coronary Atherosclerotic Lesions in Patients with End-Stage Renal Failure Patients and Age and Sex Matched Non-Uraemic. *Nephrol., Dial., Transplant.* **2000**, *15*, 218–223.

(27) Campean, V.; Neureiter, D.; Varga, I.; Runk, F.; Reiman, A.; Garlachs, C.; Achenbach, S.; Nonnast-Daniel, B.; Amann, K. Atherosclerosis and Vascular Calcification in Chronic Renal Failure. *Kidney Blood Pressure Res.* **2006**, *28* (5–6), 280–289.

(28) Bowe, B.; Xie, Y.; Xian, H.; Li, T.; Al-Aly, Z. Association between Monocyte Count and Risk of Incident CKD and Progression to ESRD. *Clin. J. Am. Soc. Nephrol.* **2017**, *12* (4), 603–613.

(29) Luczak, M.; Formanowicz, D.; Marczak, E.; Suszyńska-Zajczyk, J.; Pawliczak, E.; Wanic-Kossowska, M.; Stobiecki, M. ITRAQ-Based Proteomic Analysis of Plasma Reveals Abnormalities in Lipid Metabolism Proteins in Chronic Kidney Disease-Related Atherosclerosis. *Sci. Rep.* **2016**, *6*, 32511.

(30) Heemskerck, N.; Van Rijssel, J.; Van Buul, J. D. Rho-GTPase Signaling in Leukocyte Extravasation: An Endothelial Point of View. *Cell Adhesion and Migration.* **2014**, *8* (2), 67–75.

(31) Finney, A. C.; Stokes, K. Y.; Pattillo, C. B.; Orr, A. W. Integrin Signaling in Atherosclerosis. *Cell. Mol. Life Sci.* **2017**, *74* (12), 2263–2282.

(32) Davies, M. J.; Gordon, J. L.; Gearing, A. J. H.; Pigott, R.; Woolf, N.; Katz, D.; Kyriakopoulos, A. The Expression of the Adhesion Molecules ICAM-1, VCAM-1, PECAM, and E-Selectin in Human Atherosclerosis. *J. Pathol.* **1993**, *171* (3), 223–229.

(33) Gross, M. D.; Bielski, S. J.; Suarez-Lopez, J. R.; Reiner, A. P.; Bailey, K.; Thyagarajan, B.; Carr, J. J.; Duprez, D. A.; Jacobs, D. R., Jr. Circulating Soluble Intercellular Adhesion Molecule 1 and Subclinical Atherosclerosis: The Coronary Artery Risk Development in Young Adults Study. *Clin. Chem.* **2012**, *58* (2), 411–420.

(34) Luc, G.; Arveiler, D.; Evans, A.; Amouyel, P.; Ferrieres, J.; Bard, J.-M.; Elkhail, L.; Fruchart, J.-C.; Ducimetiere, P. Circulating Soluble Adhesion Molecules ICAM-1 and VCAM-1 and Incident Coronary Heart Disease: The PRIME Study. *Atherosclerosis* **2003**, *170* (1), 169–176.

(35) Hepper, I.; Schymeinsky, J.; Weckbach, L. T.; Jakob, S. M.; Frommhold, D.; Sixt, M.; Laschinger, M.; Sperandio, M.; Walzog, B. The Mammalian Actin-Binding Protein 1 Is Critical for Spreading and Intraluminal Crawling of Neutrophils under Flow Conditions. *J. Immunol.* **2012**, *188* (9), 4590–4601.

(36) Phillipson, M.; Heit, B.; Colarusso, P.; Liu, L.; Ballantyne, C. M.; Kubers, P. Intraluminal Crawling of Neutrophils to Emigration Sites: A Molecularly Distinct Process from Adhesion in the Recruitment Cascade. *J. Exp. Med.* **2006**, *203* (12), 2569–2575.

(37) Rossi, E.; Bernabeu, C.; Smadja, D. M. Endoglin as an Adhesion Molecule in Mature and Progenitor Endothelial Cells: A Function beyond TGF- β . *Front. Med.* **2019**, *6*, 10.

(38) Rossi, E.; Sanz-Rodriguez, F.; Eleno, N.; Düwell, A.; Blanco, F. J.; Langa, C.; Botella, L. M.; Cabañas, C.; Lopez-Novoa, J. M.; Bernabeu, C. Endothelial Endoglin Is Involved in Inflammation: Role in Leukocyte Adhesion and Transmigration. *Blood* **2013**, *121* (2), 403–415.

(39) Alon, R.; Feigelson, S. W.; Manevich, E.; Rose, D. M.; Schmitz, J.; Overby, D. R.; Winter, E.; Grabovsky, V.; Shinder, V.; Matthews, B. D.; Sokolovsky-Eisenberg, M.; Ingber, D. E.; Benoit, M.; Ginsberg, M. H. A4 β 1-Dependent Adhesion Strengthening under Mechanical Strain Is Regulated by Paxillin Association with the A4-Cytoplasmic Domain. *J. Cell Biol.* **2005**, *171* (6), 1073–1084.

(40) Rullo, J.; Becker, H.; Hyduk, S. J.; Wong, J. C.; Digby, G.; Arora, P. D.; Cano, A. P.; Hartwig, J.; McCulloch, C. A.; Cybulsky, M. I. Actin Polymerization Stabilizes A4 β 1 Integrin Anchors That Mediate Monocyte Adhesion. *J. Cell Biol.* **2012**, *197* (1), 115–129.

(41) Lee, A.; Whyte, M. K. B.; Haslett, C. Inhibition of Apoptosis and Prolongation of Neutrophil Functional Longevity by Inflammatory Mediators. *J. Leukocyte Biol.* **1993**, *54*, 283–288.

(42) Whyte, M. K.; Meagher, L. C.; MacDermot, J.; Haslett, C. Impairment of Function in Aging Neutrophils Is Associated with Apoptosis. *J. Immunol.* **1993**, *150* (11), 5124–5134.

(43) Modaresi, A.; Nafar, M.; Sahraei, Z. Oxidative Stress in Chronic Kidney Disease. *Iran. J. Kidney Dis.* **2015**, *9* (3), 165–179.

SUPPORTING INFORMATION

Proteomic profiling of leukocytes reveals dysregulation of adhesion and integrin proteins in chronic kidney disease-related atherosclerosis

Joanna Tracz¹, Luiza Handschuh¹, Maciej Lalowski^{1,2}, Łukasz Marczak¹, Katarzyna Kostka-Jeziorny³, Bartłomiej Perek⁴, Maria Wanic-Kossowska⁵, Alina Podkowińska⁶, Andrzej Tykarski³, Dorota Formanowicz⁷, Magdalena Luczak^{1*}

¹ Institute of Bioorganic Chemistry, Polish Academy of Sciences, Noskowskiego 12/14, 61-704 Poznan, Poland;

² Helsinki Institute for Life Science (HiLIFE) and Faculty of Medicine, Biochemistry/Developmental Biology, Meilahti Clinical Proteomics Core Facility, University of Helsinki

³ Department of Hypertension, Angiology and Internal Disease, Poznan University of Medical Sciences, Długa 1/2, 61-848, Poznan, Poland;

⁴ Department of Cardiac Surgery and Transplantology, Poznan University of Medical Sciences, Długa 1/2, 61-848, Poznan, Poland;

⁵ Department of Nephrology, Transplantology and Internal Medicine, Poznan University of Medical Sciences, Przybyszewskiego 49, 60-355 Poznan, Poland;

⁶ Dialysis station Dravis sp. z o.o., Dojazd 34, 60-631 Poznan, Poland

⁷ Chair and Department of Medical Chemistry and Laboratory Medicine, Poznan University of Medical Sciences, Rokietnicka 8, 60-806, Poznan, Poland.

TABLE OF CONTENTS

The following supporting information is available free of charge at ACS website

<http://pubs.acs.org>

List of Figures

Figure S1

Microscopy and flow cytometry analysis of isolated cells

Figure S2

Enrichment analysis in the context of compartmental localization

Figure S3

Unsupervised principal component analysis (PCA)

Figure S4

Heat maps presenting abundance of identified DEPs

Figure S5

Correlation coefficient matrix for DEPs in CKD5 vs CVD2 comparison

Figure S6

IPA functional analysis

Figure S7

TLN1 immunoblot – entire membrane

List of Tables

Table S1

Pearson's correlation coefficients between the LFQ (label-free quantification) intensities from replicates in all experimental groups

Table S2

List of primers used in ddPCR analysis

Table S3

List of peptide transitions with precursor and product masses, charges, retention times and collision energies used for MRM analysis

Table S4

The results of correlation analyses between the identified DEPs and eGFR, the number of particular blood cells and leukocyte subpopulations

Table S5

Complete list of differentially expressed proteins (DEPs) identified in the study. The names of proteins, the number of identified peptides, p-values, fold changes, effect size for all group comparisons and UniProt accessions

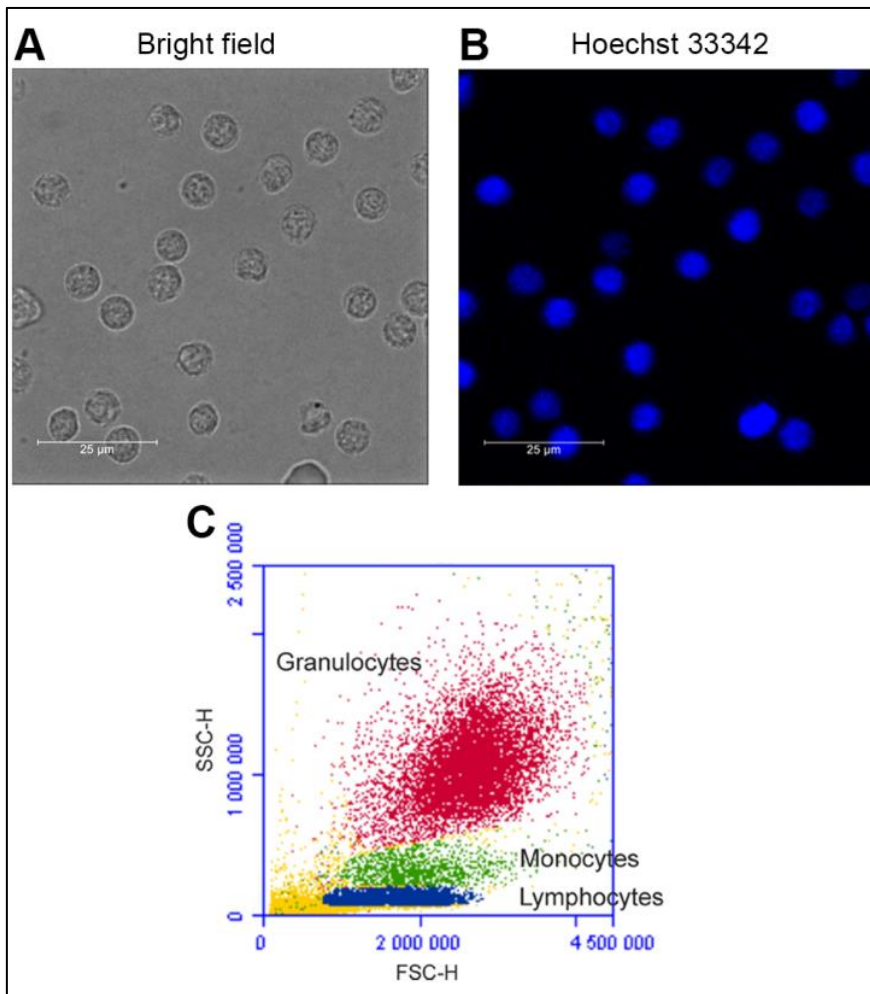
Table S6

The results of Pearson's correlation analyses between the DEPs identified in CKD5 vs CVD2 comparison

Table S7

A detailed list of IPA annotation results for canonical pathway, diseases/functions and upstream regulator categories with $-\log_{10}$ B-H corrected p-values and z-scores

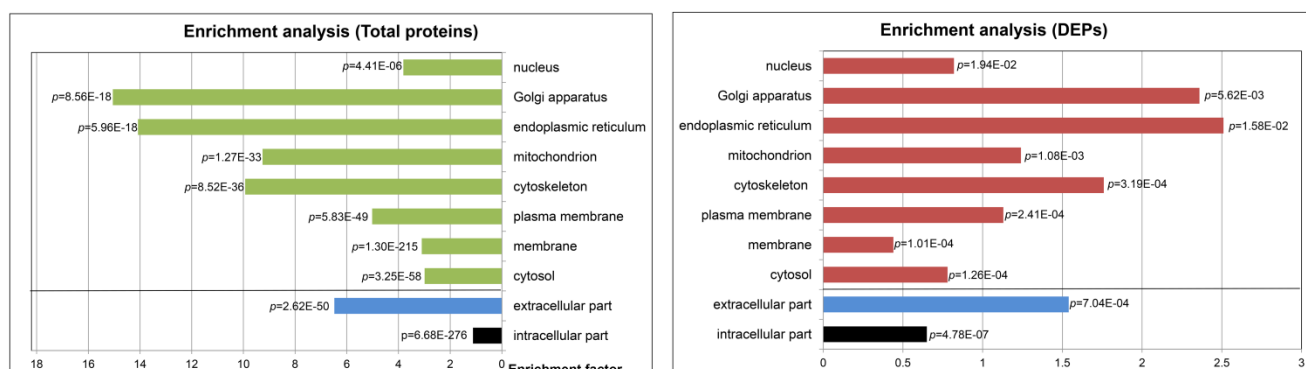
Figure S1: Microscopy and flow cytometry analysis of isolated cells



Isolated cells were evaluated using fluorescence microscopy and flow cytometry. Bright field (A) and fluorescence images of leukocytes after staining with Hoechst 33342 (B); (C) Gating of isolated leukocyte subpopulations by flow cytometry.

Figure S2

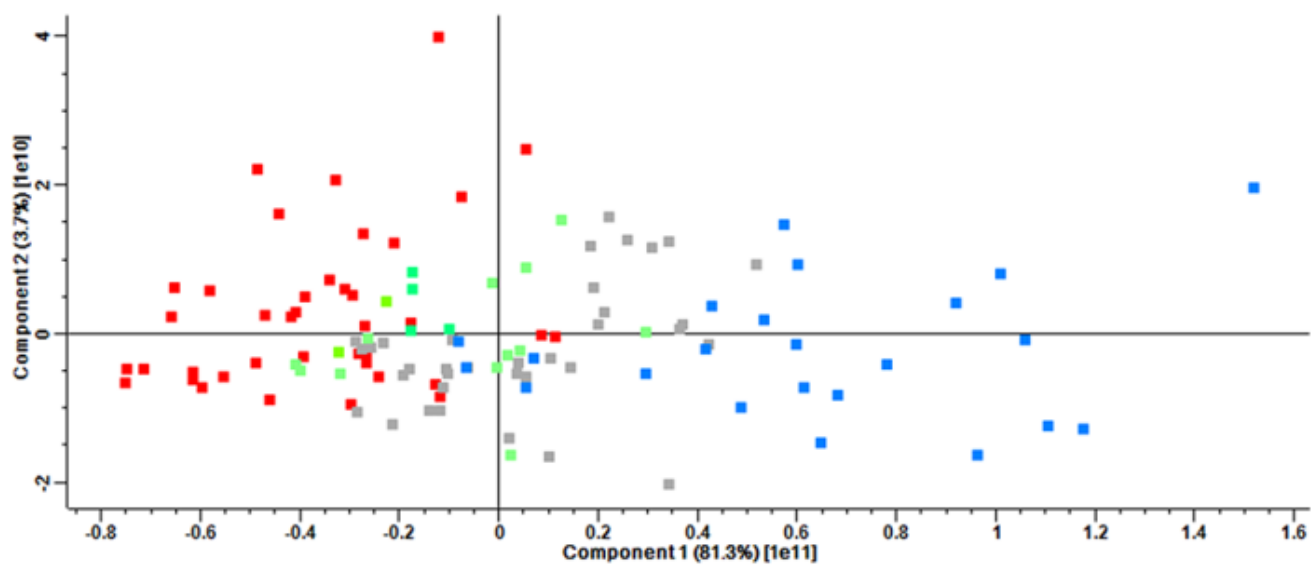
Enrichment analysis in the context of compartmental localization



Enrichment analysis in the context of compartmental localization was performed for all identified proteins and DEPs. Fisher's exact with B-H correction at FDR of 2% was used.

Figure S3

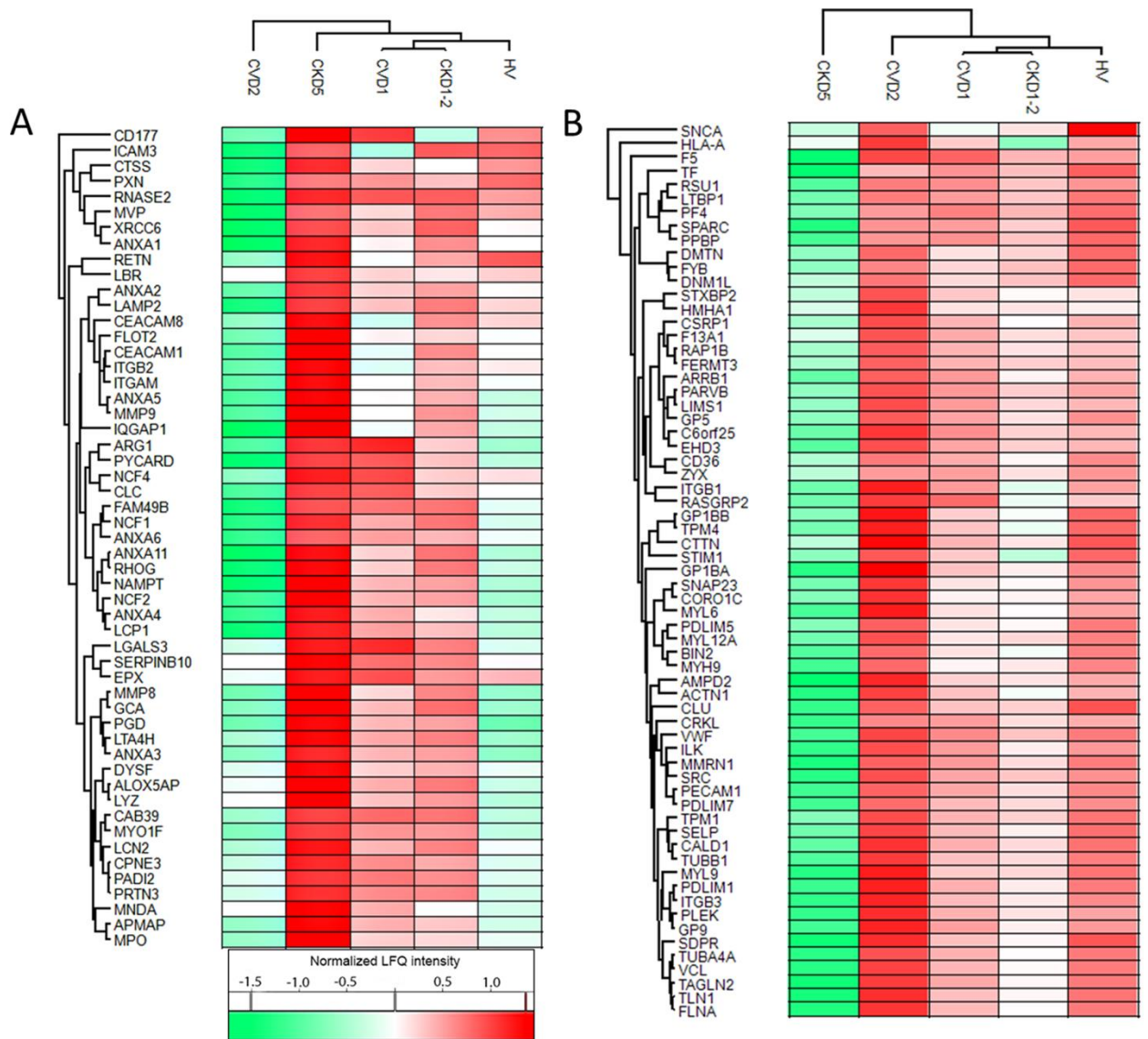
Unsupervised principal component analysis (PCA)



PCA performed on the total number of proteins identified in CKD5 (red), CVD2 (blue), CKD1-2 (green) and CVD1 (grey) experimental groups.

Figure S4

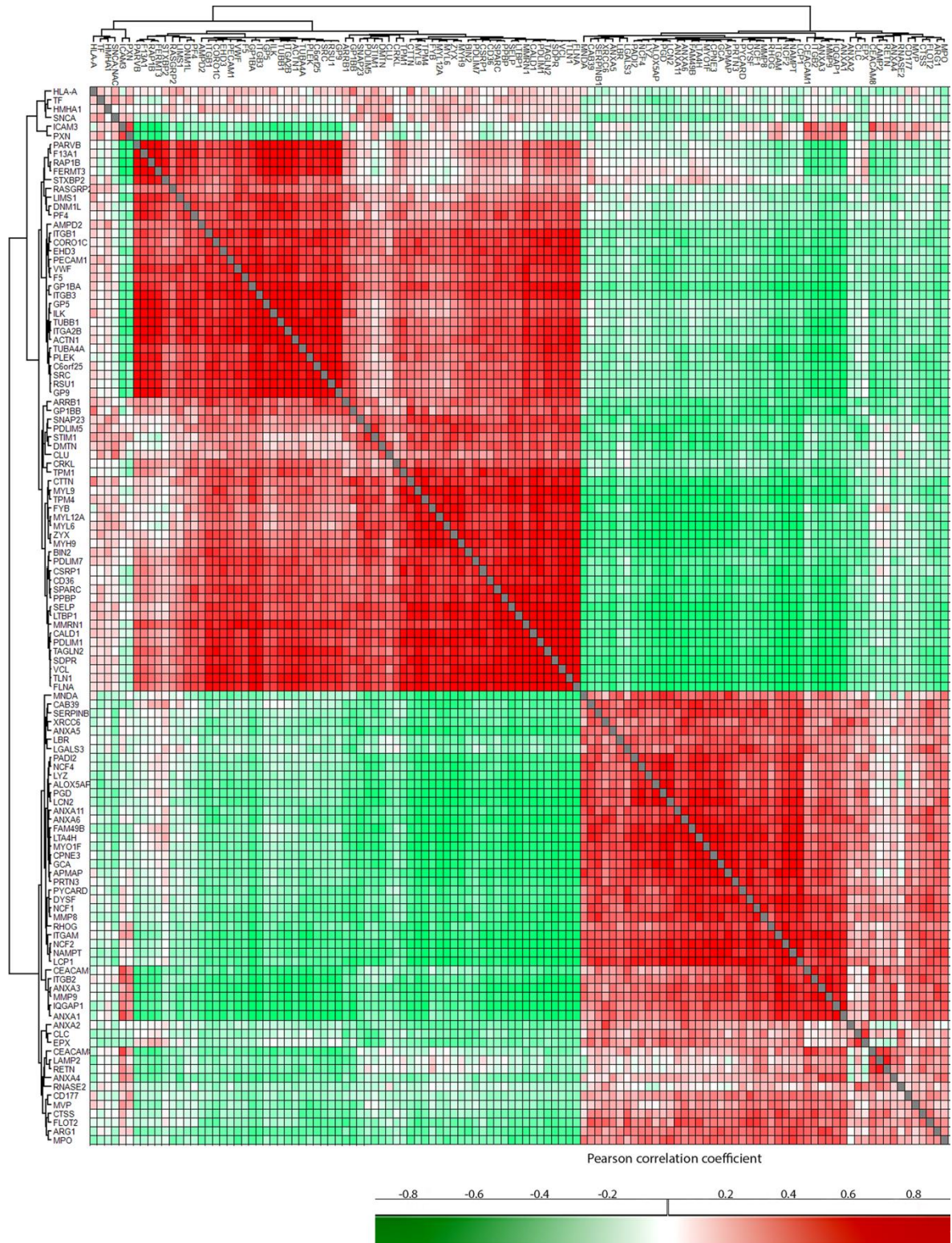
Heat maps presenting abundance of identified DEPs



Heat maps presenting abundance of downregulated in CVD2 (**A**) or in CKD5 (**B**) proteins in the background of other experimental groups.

Figure S5

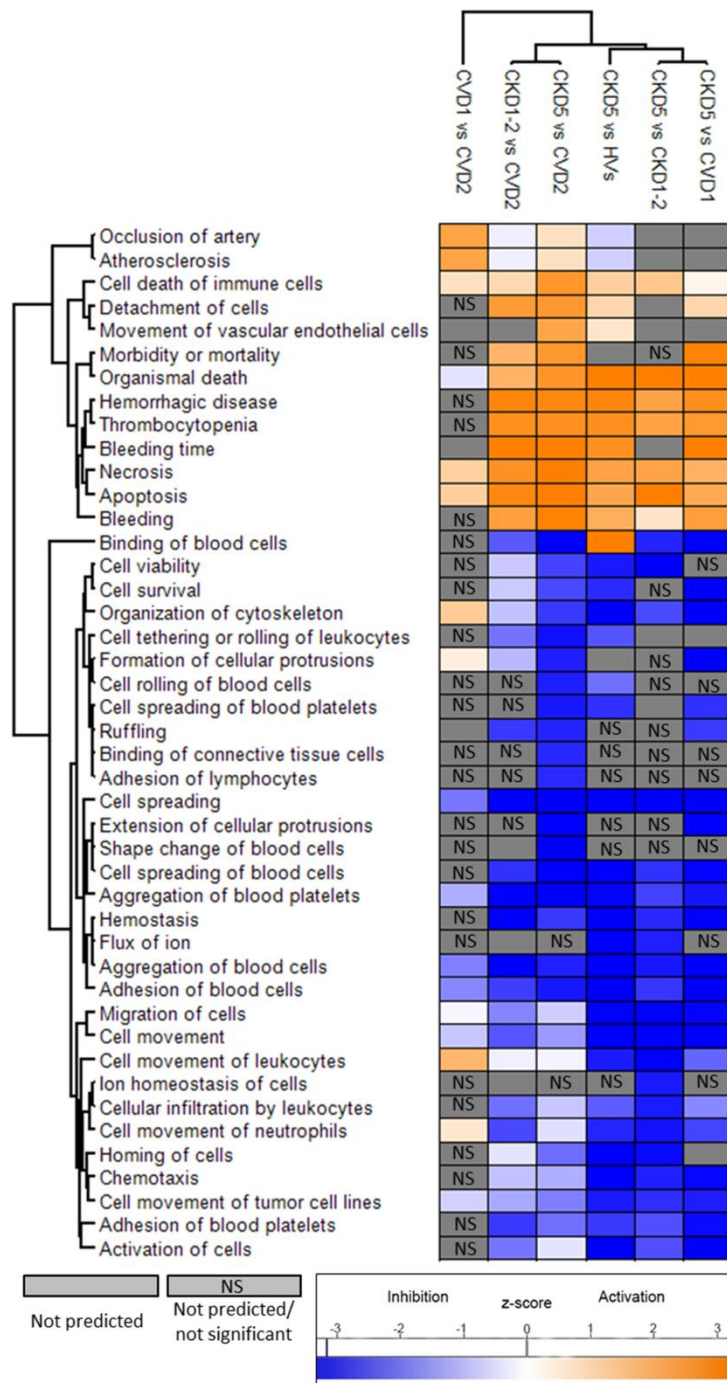
Correlation coefficient matrix for DEPs in CKD5 vs CVD2 comparison



Heat map representation of Pearson's correlations for the abundances of DEPs identified in CKD5 vs CVD2 comparison.

Figure S6

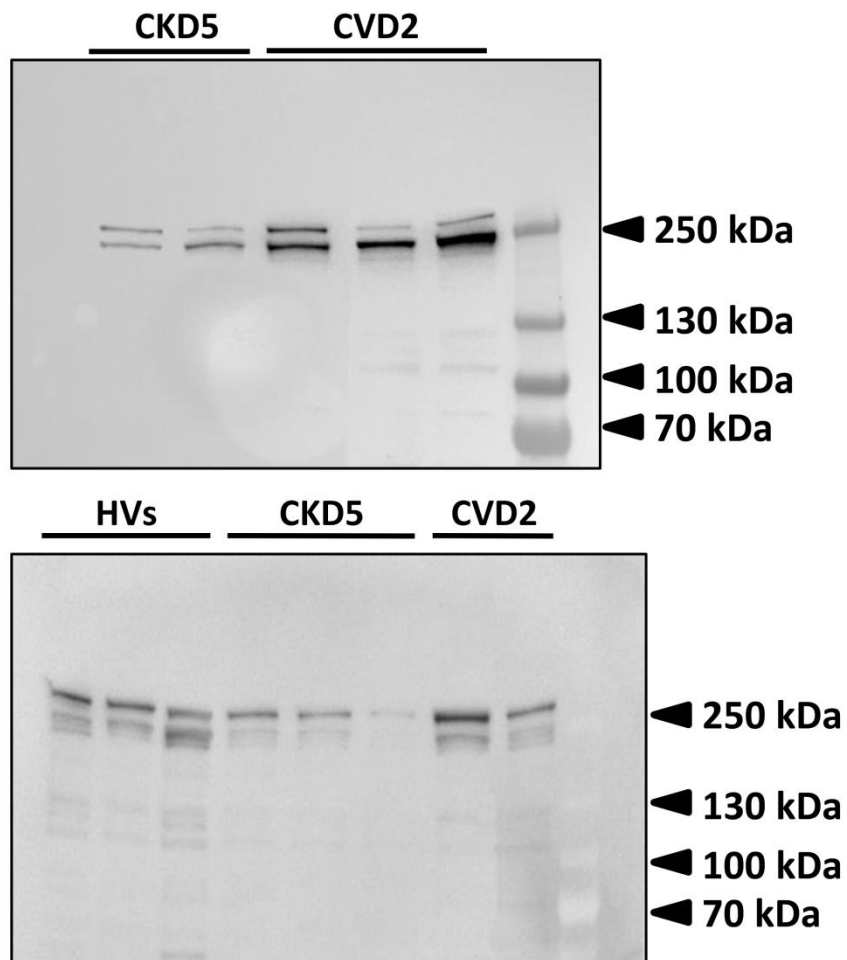
IPA functional analysis



IPA functional analysis performed for 6 different comparisons. Categories with significant z-scores are presented in blue inhibition; z-score ≤ -2) or orange (activation; z-score ≥ 2). Functions overrepresented according to B-H corrected p-values but without calculated z-scores are presented in grey. Functions not enriched according to B-H corrected p-values are shown in grey and marked as NS. A detailed list of annotations with B-H p-values and z-scores is presented in Table S7.

Figure S7

TLN1 immunoblot – entire membranes



Entire membranes for the Western blot in Figure 3. 30 μ g of proteins were separated by 4-15% SDS-PAGE. Blots were incubated with the anti- TLN1 primary antibodies. Chemiluminescent detection was performed using the ChemiDoc XRS imaging system







Tabele, zawarte jako suplement artykułu nr 2 nie zostały załączone do niniejszej rozprawy ze względu na swoją złożoność, natomiast są dostępne do pobrania w poniższym linku:

<https://pubs.acs.org/doi/abs/10.1021/acs.jproteome.0c00883>

- Table S1: Pearson's correlation coefficients between the label-free quantification intensities from replicates in all experimental groups.
- Table S2: list of primers used in ddPCR analysis.
- Table S3: list of peptide transitions with precursor and product masses, charges, retention times, and collision energies used for MRM analysis.
- Table S4: results of correlation analyses between the identified DEPs and eGFR, including the number of particular blood cells and leukocyte subpopulations.
- Table S5: complete list of DEPs identified in the study: names of proteins, number of identified peptides, *p*-values, fold changes, effect size for all group comparisons, and UniProt accession numbers.
- Table S6: results of Pearson's correlation analyses between the DEPs identified in CKD5 vs CVD2 comparison.
- Table S7: A detailed list of IPA annotation results for canonical pathway, diseases/functions and upstream regulator categories with $-\log_{10}$ B-H corrected *p*-values and α -scores.

Article

Mass Spectrometry-Based Lipidomics Reveals Differential Changes in the Accumulated Lipid Classes in Chronic Kidney Disease

Lukasz Marczak ^{1,*}, Jakub Idkowiak ^{1,2}, Joanna Tracz ³, Maciej Stobiecki ¹ , Bartłomiej Perek ⁴ , Katarzyna Kostka-Jeziorny ⁵ , Andrzej Tykarski ⁵, Maria Wanic-Kossowska ⁶, Marcin Borowski ⁷ , Marcin Osuch ⁸, Dorota Formanowicz ⁹  and Magdalena Luczak ^{3,*} 

- ¹ Department of Natural Products Biochemistry, Institute of Bioorganic Chemistry Polish Academy of Sciences, 61-704 Poznan, Poland; jakubidkowiak1@gmail.com (J.I.); mackis@ibch.poznan.pl (M.S.)
- ² Department of Analytical Chemistry, Faculty of Chemical Technology, University of Pardubice, 532 10 Pardubice, Czech Republic
- ³ Department of Biomedical Proteomics, Institute of Bioorganic Chemistry Polish Academy of Sciences, 61-704 Poznan, Poland; joanna.a.tracz@gmail.com
- ⁴ Department of Cardiac Surgery and Transplantology, Poznan University of Medical Sciences, 61-001 Poznan, Poland; bperek@ump.edu.pl
- ⁵ Department of Hypertension, Angiology and Internal Disease, Poznan University of Medical Sciences, 61-001 Poznan, Poland; kostkajeziorny@gmail.com (K.K.-J.); tykarski@o2.pl (A.T.)
- ⁶ Department of Nephrology, Transplantology and Internal Medicine, Poznan University of Medical Sciences, 60-355 Poznan, Poland; wanic.kossowska.maria@gmail.com
- ⁷ Institute of Computing Science, Poznan University of Technology, 60-965 Poznan, Poland; Marcin.Borowski@cs.put.poznan.pl
- ⁸ Department of Molecular and Systems Biology, Institute of Bioorganic Chemistry Polish Academy of Sciences, 61-704 Poznan, Poland; mosuch@ibch.poznan.pl
- ⁹ Chair and Department of Medical Chemistry and Laboratory Medicine, Poznan University of Medical Sciences, 60-806 Poznan, Poland; doforman@ump.edu.pl
- * Correspondence: lukasmar@ibch.poznan.pl (L.M.); magdalu@ibch.poznan.pl (M.L.)



check for updates

Citation: Marczak, L.; Idkowiak, J.; Tracz, J.; Stobiecki, M.; Perek, B.; Kostka-Jeziorny, K.; Tykarski, A.; Wanic-Kossowska, M.; Borowski, M.; Osuch, M.; et al. Mass Spectrometry-Based Lipidomics Reveals Differential Changes in the Accumulated Lipid Classes in Chronic Kidney Disease. *Metabolites* **2021**, *11*, 275. <https://doi.org/10.3390/metabo11050275>

Academic Editor: Robert J. Brown

Received: 16 April 2021

Accepted: 23 April 2021

Published: 27 April 2021

Publisher's Note: MDPI stays neutral with regard to jurisdictional claims in published maps and institutional affiliations.



Copyright: © 2021 by the authors. Licensee MDPI, Basel, Switzerland. This article is an open access article distributed under the terms and conditions of the Creative Commons Attribution (CC BY) license (<https://creativecommons.org/licenses/by/4.0/>).

Abstract: Chronic kidney disease (CKD) is characterized by the progressive loss of functional nephrons. Although cardiovascular disease (CVD) complications and atherosclerosis are the leading causes of morbidity and mortality in CKD, the mechanism by which the progression of CVD accelerates remains unclear. To reveal the molecular mechanisms associated with atherosclerosis linked to CKD, we applied a shotgun lipidomics approach fortified with standard laboratory analytical methods and gas chromatography-mass spectrometry technique on selected lipid components and precursors to analyze the plasma lipidome in CKD and classical CVD patients. The MS-based lipidome profiling revealed the upregulation of triacylglycerols in CKD and downregulation of cholesterol/cholesteryl esters, sphingomyelins, phosphatidylcholines, phosphatidylethanolamines and ceramides as compared to CVD group and controls. We have further observed a decreased abundance of seven fatty acids in CKD with strong inter-correlation. In contrast, the level of glycerol was elevated in CKD in comparison to all analyzed groups. Our results revealed the putative existence of a functional causative link—the low cholesterol level correlated with lower estimated glomerular filtration rate and kidney dysfunction that supports the postulated “reverse epidemiology” theory and suggest that the lipidomic background of atherosclerosis-related to CKD is unique and might be associated with other cellular factors, i.e., inflammation.

Keywords: chronic kidney disease; cardiovascular disease; lipid profiling; lipidomics; mass spectrometry

1. Introduction

Chronic kidney disease (CKD) represents a kidney function disorder, which lasts at least three months and results from progressive damage of nephrons [1,2]. Despite

the recognition of CKD as a major health problem worldwide, the awareness among patients and healthcare providers remains low [3]. CKD diagnosis is mainly based on decreased value of estimated glomerular filtration rate factor (eGFR), abnormal urinary albumin-to-creatinine ratio or occurrence of proteinuria [2,3].

Patients with CKD are at increased risk of cardiovascular diseases (CVD) [4]. The first stages of CKD (CKD1-2) reveal a mild reduction in kidney function and initial symptoms of CVD. Patients with stage 5 (CKD5) develop an end-stage renal disease (ESRD) and advanced CVD. Hypertension is found in about 70% of CKD and 80–90% of end-stage renal disease (ESRD) patients [5,6]. At early CKD stages, the likelihood of developing CVD increases two to three-fold due to deterioration of kidney function [6,7]. Furthermore, ESRD patients are at 20 to 1000-times higher risk of CVD as compared to the general population [8]. Moreover, the mortality rate related to cardiovascular events in CKD is almost three times higher than that for individuals without kidney dysfunction [4,9]. In classical CVD, dyslipidemia is recognized as one of the initial steps of atherosclerosis development resulting in subsequent cardiovascular complications. Elevated concentration of total cholesterol, followed by an increase in the atherogenic fraction of low-density lipoprotein (LDL) components, along with a low concentration of anti-atherogenic high-density lipoproteins (HDL) are crucial during atherosclerosis development [10]. However, in dialyzed CKD patients, an inverse association between cholesterol level and mortality, known as “reverse epidemiology”, has been reported [11–13]. The unique character of premature atherosclerosis in CKD has been unceasingly suggested [14–17]. Moreover, it has been postulated that the inverse relationship between cholesterol level and mortality in dialyzed CKD patients may be caused by several cholesterol-lowering factors, including malnutrition and systemic inflammation [18].

In our previous studies, we have shown that in CKD-related atherosclerosis (CKD-A) patients’ abnormalities in the accumulation of proteins involved in lipid transport and metabolism in plasma can be observed as compared to healthy people and persons with classical CVD without kidney dysfunction [19]. Consequently, a detailed study of lipidome alterations in CKD-A patients seemed worth pursuing. In CKD, the use of lipidomic profiling has been largely limited to the analysis of selected lipids, like cholesterol, its esters, triacylglycerols, and biochemical assemblies, e.g., HDL and LDL fractions [20]. However, in recent years, different accumulation of phospholipids and serum sulfatides in CKD patients, as well as first lipid biomarkers accompanying progression to ESRD, have been reported [20,21]. In these studies, experimental groups consisting mainly of patients with kidney dysfunction compared to age-matched controls have been considered. In turn, changes in lipid accumulation in patients with classical CVD, nonrelated to kidney dysfunction, have been investigated using different analytical approaches [22–24]. While lipid composition changes were observed in many inflammatory diseases, the alterations in CKD-A patients have been less assessed. To the best of our knowledge, lipid profiling in CKD-A and the association between CKD-A and dyslipidemia development remain undefined. Thus, detailed studies on lipidome in patients with CKD-A are of clinical importance.

The lipidomic approach relying on mass spectrometry has been frequently used in CVD investigations [22–26]. At present, direct infusion mass spectrometry, called “shotgun lipidomics”, and liquid chromatography-mass spectrometry (LC-MS) analysis constitute the most robust analytical approaches [27,28]. The interest concerning the high-throughput, precisely-reproducible and comprehensive shotgun approach in blood plasma lipidome screening is growing [27]. Moreover, new and improved protocols for shotgun lipidomics have been recently introduced, yielding unique lipid identification and data handling tools. These procedures cover method for plasma lipid extraction, analysis of obtained fractions with high-resolution mass spectrometers or triple quadrupoles equipped with a specific type of nano-electrospray ion source (nanoESI), but also bioinformatics and statistical typing of lipidomic signature [27,29,30].

This study focuses on plasma lipid profile alterations resulting from CVD development-related and nonrelated to CKD. We applied a shotgun lipidomics analytical approach to analyze plasma lipidome composition in two groups of CKD patients with different severity of the disease and underlying atherosclerosis, and a group of patients with the advanced stage of CVD but without any kidney dysfunction. Healthy volunteers without CKD and CVD were included in the study as a reference group. Furthermore, we utilized the analysis of lipid precursors and components using GC-MS. Such studies, based on complementary mass spectrometry approaches fortified with standard medical tests may shed light on the molecular mechanisms associated with atherosclerosis, related or nonrelated to CKD.

2. Results

This study investigated the disease-related differences in the lipidome of patients with atherosclerosis either related or nonrelated to CKD, and healthy volunteers. To achieve it, total lipid extracts from plasma were analyzed by the screening lipidomics approach. Further lipid blood measurement was conducted using standard medical examinations (Table 1). Finally, analysis of the selected precursors and components of lipids was performed. Since the composition of analyzed experimental groups slightly differed, we statistically evaluated if the identified lipids were related to statin, blood pressure, anticoagulant treatment, or gender. Such compounds were not identified in our study.

Table 1. Demographic data and clinical characteristics of the study. Mean value \pm SD. $p < 0.05$ was considered to be statistically significant. eGFR—estimated glomerular filtration rate, BMI—body mass index, hsCRP—high-sensitivity C-reactive protein. Chi-square test was used for categorical variables, while for other variables, Mann–Whitney U-test was utilized.

	HV	CKD1-2	CKD5	CVD	<i>p</i> -Value
Age [years]	51 \pm 16	63 \pm 5	61 \pm 14	58 \pm 10	0.04
Males	75%	75%	75%	75%	0.64
eGFR [ml/min/1.73 m ²]	102 \pm 11	70 \pm 6	6 \pm 4	96 \pm 11	<0.01
BMI [kg/m ²]	24 \pm 2	29 \pm 4	25 \pm 3	28 \pm 4	0.08
Arterial hypertension	0%	100%	100%	100%	<0.01
Glucose [mM]	4 \pm 0.5	5.6 \pm 0.5	5.8 \pm 0.4	5.41 \pm 0.6	<0.01
Anticoagulant treatment	0%	79%	54%	87.5%	<0.01
Statin treatment	0%	87.5%	67%	75%	<0.01
Blood pressure treatment	0%	100%	100%	100%	<0.01
Total cholesterol [mg/dL]	190 \pm 24	199 \pm 46	170 \pm 29	187 \pm 49	<0.01
HDL cholesterol [mg/dL]	65 \pm 16	62 \pm 19	44 \pm 10	53 \pm 13	<0.01
LDL cholesterol [mg/dL]	90 \pm 28	131 \pm 39	84 \pm 27	101 \pm 41	<0.01
Triacylglycerols [mg/dL]	101 \pm 56	129 \pm 66	127 \pm 60	101 \pm 42	<0.01
hsCRP [mg/L]	1.53 \pm 0.4	2.32 \pm 2.1	16.67 \pm 11	2.17 \pm 4.6	<0.01

Laboratory tests have revealed that the concentration of total cholesterol, LDL and HDL fraction was significantly decreased in the CKD5 group, and exhibited the lowest levels as compared to other patients' groups and healthy volunteers (HVs). The highest concentration of total cholesterol and LDL fraction has been measured in the CKD1-2 group. The levels of TAGs (triacylglycerols) were similar in both, CKD5 and CKD1-2, and revealed evident differences as compared to HVs and CVD group. CKD5 group displayed the lowest concentration of HDL in comparison to others. For this group, the highest concentration of C-reactive protein (CRP) was characteristic. Patients from CKD5 and CVD groups revealed a similar level of progression of atherosclerosis and CVD, however, all the above lipids measurements differed among these groups. The parameters presented in Table 1 served as variables for correlation analyses. The negative correlation between eGFR and CRP ($r = -0.82$) and glucose was demonstrated ($r = -0.59$). As expected, total cholesterol also revealed a positive correlation with LDL fraction ($r = 0.58$). However, HDL positively correlated with eGFR ($r = 0.68$) and negatively with glucose level ($r = -0.53$) and CRP ($r = -0.51$). The details of correlation analyses are presented in Table S1.

2.1. Lipid Classes Analysis Using Shotgun Approach

Utilizing plasma lipid profiling with a mass spectrometry approach, the presence of 14 lipid subclasses was revealed, including phosphatidylcholines (PC and PC-O), phosphatidylethanolamines (PE and PE-O), phosphatidylinositols (PI), lysophosphatidylcholines (LPC), lysophosphatidylethanolamines (LPE), phosphatidylserines (PS), sphingomyelins (SM), ceramides (Cer), hexosylceramides (HexCer), triacylglycerols (TAGs), diacylglycerols (DAG), and cholesterol/cholesteryl esters (CE). At first, the overall composition of lipid classes was compared. For this purpose, the average accumulation of each class of lipids was calculated and the data were scrutinized by one-way ANOVA/Kruskal–Wallis and t-test/U-Mann–Whitney tests. Nine out of 14 classes of lipids (CE, LPC, PE-O, Cer, PC, TAG, PS, LPE, and SM) were significantly altered amid the studied groups and revealed the false discovery rate (FDR) adjusted p -values below 0.05. HVs and CKD5 represented the most differentiating groups and exhibited the altered accumulation of all lipid classes. Details of the analysis are presented in Table S2. Principal component analysis encompassing all lipid species confirmed this observation and revealed that CKD5 and HVs varied most significantly from each other and the other groups (Figure 1A). Additionally, CKD5 and CVD groups demonstrated statistically significant differences in the accumulation of six classes of lipids (Figure 1AB). PCA did not separate HV and CKD1-2 groups (Figure 1A, marked in black (CKD1-2) and green (HVs)). Observed differences were further confirmed by hierarchical cluster analysis (HCA, Figure 1C), in which the abundances of particular lipid classes in the studied groups can be observed. HCA merged two studied groups of CKD (CKD5 and CKD1-2) into one cluster, while the second cluster was represented by HV and CVD groups. HCA also revealed the upregulation of TAGs, DAGs, and PEs in both CKD groups and downregulation of CE, SM, PC, PE-O, and Cer as compared to CVD and HV cluster.

The partial least squares discriminant analysis (PLS-DA) also confirmed differences observed between HVs, CVD, CKD1-2, and CKD5, as these groups separate from each other in the presented score plot (Figure S1).

Details of this analysis are presented in Figure 2. Both CKD1-2 and CKD5 disclosed the highest level of TAGs as compared to HVs and CVD group (Figure 2A), which corroborated the results of standard medical examinations. In contrast, the lowest level of CEs was identified in the CKD5 group (Figure 2B), which confirmed the results of standard lipid profiling and suggested the correctness of performed MS/MS measurements. CKD1-2 and CKD5 groups differed in LPE accumulation only (Figure 2C). However, we also demonstrated a decrease in accumulation of PC, Cer, PE-O, and SM, in CKD5 patients in comparison to CVD (Figure 2D–G). Furthermore, CKD1-2 and CVD groups showed statistically significant differences in TAG, Cer and PE-O accumulation (Figure 2A,E,F). Downregulation of PSs and LPC was further shown in all patients' groups compared to HVs (Figure 2H,I).

To reveal the possible relationship between analyzed classes of lipids, in the next step, fourteen classes of lipids were correlated using Pearson's correlation, and the resulting matrix was visualized as a heat map (Figure 3). Correlation analysis revealed that lipids belonging to similar classes were associated with each other, i.e., PC positively correlated with PC-O ($r = 0.49$) and PE-O ($r = 0.59$), and LPE with LPC ($r = 0.69$). Moreover, a Pearson's correlation test revealed that SMs were correlated with PE-O ($r = 0.66$), PC-O ($r = 0.68$), CE ($r = 0.61$), and Cer ($r = 0.49$). Additionally, CE group correlated with PC ($r = 0.65$). The only inverse correlation was found between TAG and PS ($r = -0.51$). The details of correlation analyses are presented in Table S3.

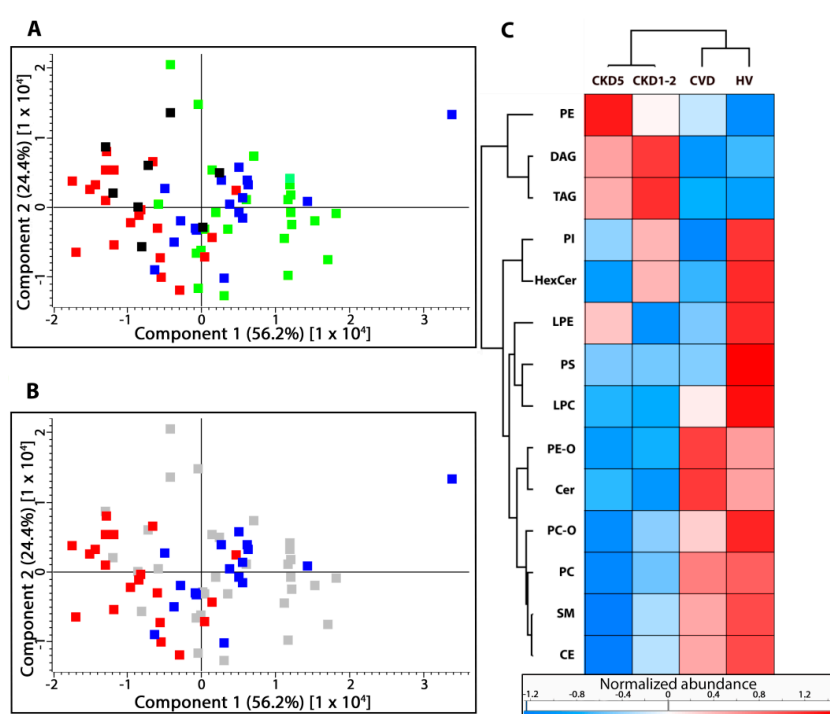


Figure 1. Unsupervised principal component analysis (PCA) performed on the total number of lipids identified in (A) stage 5 chronic kidney disease (CKD5) (red), cardiovascular disease (CVD) (blue), stage 1 and 2 chronic kidney disease (CKD1-2) (black), and healthy volunteers (HVs) (green) experimental groups. (B) To highlight the observed differences, only CKD5 (red) and CVD (blue) are marked. Other groups are presented in grey. (C) Hierarchical clustering analysis of identified lipid classes. PC, PC-O- phosphatidylcholines; PE, PE-O—phosphatidylethanolamines; PI—phosphatidylinositols; LPC—lysophosphatidylcholines; LPE—lysophosphatidylethanolamines; PS—phosphatidylserines; SM—sphingomyelins; Cer—ceramides; HexCer—hexosylceramides; TAG—triacylglycerols; DAG—diacylglycerols; CE—cholesterol and cholesteryl esters.

The correlation analyses were also performed utilizing the analyzed classes of lipids and medical parameters presented in Table 1. Correlation between CE group and total cholesterol level measured in medical examinations corroborated the obtained results ($r = 0.495$). Pearson's correlation test revealed that CE also correlated with CRP ($r = 0.46$), and eGFR ($r = 0.47$). Additionally, LPC group negatively correlated with glucose levels ($r = -0.403$). Other parameters demonstrated only medium or weak correlation ($r = 0.23$ – 0.40 ; Table S3).

2.2. Lipid Species Analysis Utilizing Shotgun Approach

In the next step, the changes in the particular lipid species abundance were found. High-throughput shotgun analysis of blood plasma allowed for the identification and quantification of 253 lipid species in total, including 24 Cers, 10 CEs, 12 DAGs, 45 TAGs, 14 LPCs, 6 LPEs, 24 PC-Os, 12 PIs, 14 PE-Os, 21 PEs, 4 PSs, and 28 SMs, 9 HexCers and 30 PCs. All of them were included in the subsequent statistical surveys and a particular lipid was considered to be differentially accumulated between at least two groups if the difference was statistically significant ($p < 0.05$), at the fold change of ± 1.5 . The list of differentially accumulated lipids sorted according to appropriate statistical tests is presented in Table S4. The statistical comparison of quantitative lipidomic data revealed 61 lipid species differentiating all experimental groups (ANOVA/Kruskal–Wallis, FDR-adjusted p -value < 0.05). Ninety-one differentially accumulated lipid species were identified when separate comparisons were performed for all groups using t -test or U-Mann–Whitney test. These analyses demonstrated an altered accumulation of 28 and 50 lipid species when HVs were compared to CKD1-2 and CKD5 groups, respectively. Twenty-three lipid species differentiated HVs

and CVD group. Differential accumulation of 24 and 17 lipid species, was revealed when CKD1-2 was compared to CVD and CKD5 group. Twenty-three differentially accumulated lipids were identified in CKD5 vs. CVD comparison.

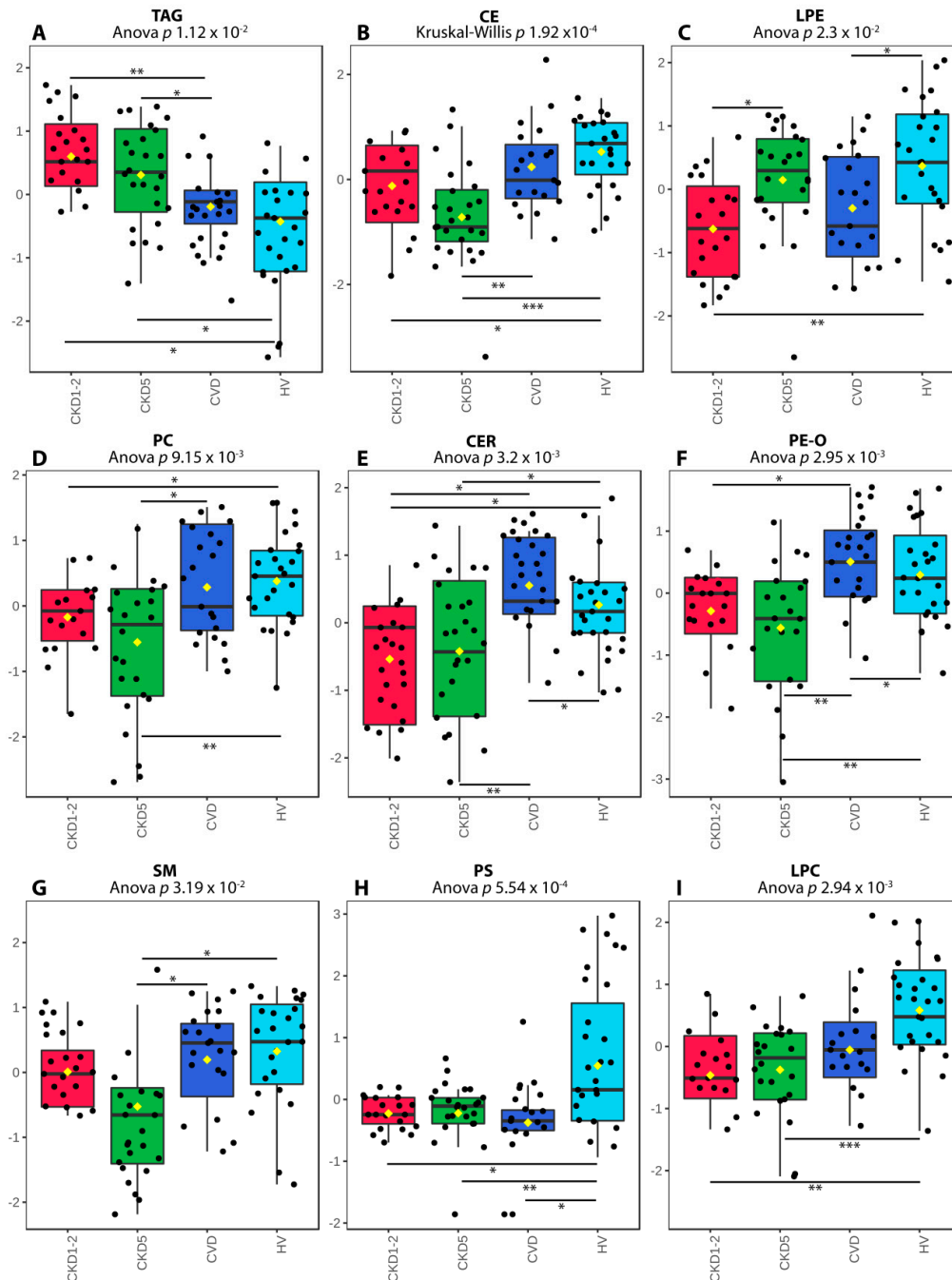


Figure 2. Differentially accumulated lipid classes sorted according to Anova/Kruskal–Wallis p -values: (A) triacylglycerols (TAG). (B) cholesterol and cholesterol esters (CE). (C) lysophosphatidylcholines (LPE). (D) phosphatidylcholines (PC). (E) ceramides (CER). (F) phosphatidylethanolamines (PE-O). (G) sphingomyelins (SM). (H) phosphatidylserines (PS). (I) lysophosphatidylcholines (LPC). A box on a plot presents interquartile ranges and medians. The black dots correspond to the normalized accumulation of lipid classes in all samples. The notch indicates the 95% confidence interval around the median of each group. The mean level is indicated with a yellow diamond. Bars and asterisks show the results of U-Mann–Whitney/ t -test: * $p < 0.05$, ** $p < 0.01$, *** $p < 0.001$; $n = 25$ in each group.

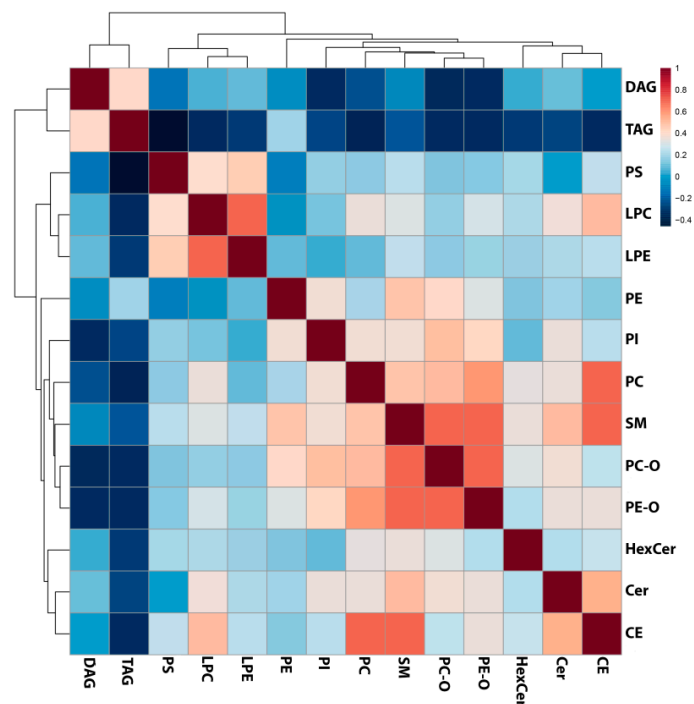


Figure 3. Results of the Pearson's correlation analysis performed for all identified lipid classes and presented as a heat map with the corresponding hierarchical tree. Color saturation corresponds to the value of Pearson's correlation coefficient.

The high accumulation of TAGs characterized both CKD1-2 and CKD5 and considerably differentiated these groups from the other ones (Figure 4). Accumulation of 14 TAGs (all differential ones) was on average 2.03 and 2.13 times higher in CKD1-2 or CKD5 than in CVD group. Furthermore, all identified TAGs were also upregulated when CKD1-2 or CKD5 groups were compared to HV, with average fold changes of 1.78 and 1.67, respectively. The exemplary TAG [52:2] profile is presented in Figure 4A. We also identified two DAGs: [34:3] and [32:0], with similar abundance profiles as TAGs. The results obtained for specific CEs were consistent with the data gained for all classes of lipids (Figure 4B). Five differentially accumulated CE species were identified and found to be downregulated in the CKD5 group. The respective fold changes ranged between 0.3 and 0.62 in CKD5 vs. HV comparison and 0.52–0.62 in CKD5 vs. CVD comparison. The representative CE [20:3] profile is presented in Figure 4B. The robust difference in the accumulation of particular lipid species was identified when HVs and CKD5 groups were compared. The levels of 49 different molecules were found to be altered, including five downregulated CEs in CKD5 as compared to HV. In addition, seven differentially regulated SM (Figure 4G), seven LPC (Figure 4I), five PC (Figure 4D), three PC-O, three PE-O (Figure 4F), two PS (Figure 4H), two Cer, one PI and one LPE were decreased in their abundance in CKD5, in comparison to HVs. On the other hand, seven upregulated TAGs (Figure 4A), two DAGs and five PE were identified in CKD5. A similar difference, but to a lower extent, was identified when HV was compared with CKD1-2. In particular, nine TAGs (Figure 4A) and one DAG were found to be upregulated in CKD1-2, while one SM (Figure 4G), six LPCs (Figure 4I), two PS (Figure 4H), two PCs (Figure 4D), one PE-O, two Cer, two LPE (Figure 4C), one CE and one PI were downregulated in CKD1-2 in comparison to HV group.

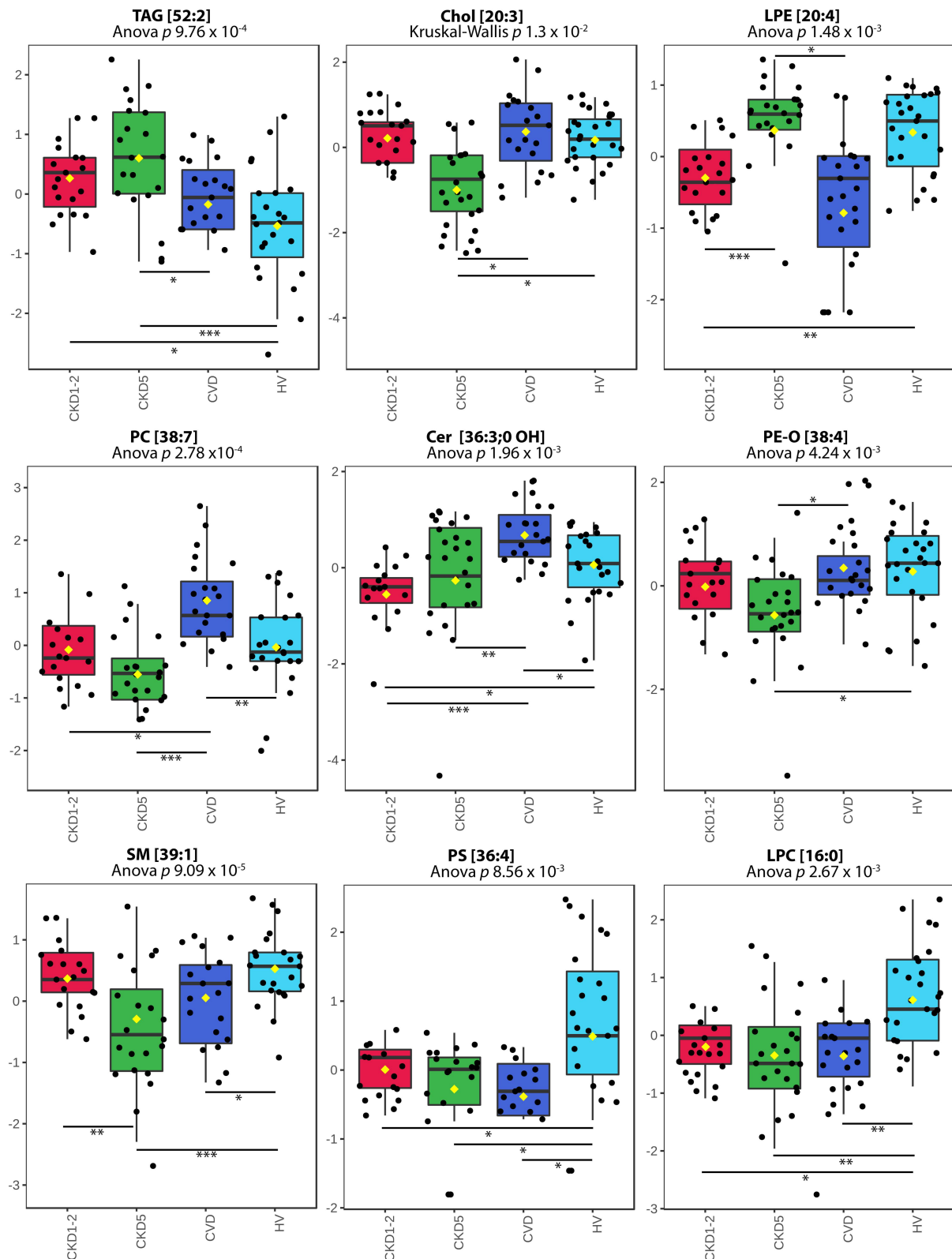


Figure 4. Abundances of representative species for all classes of lipids. (A) TAG [52:2]. (B) Chol [20:3]. (C) LPE [20:4]. (D) PC [38:7]. (E) CER [36:3;0, OH]. (F) PE-O [38:4]. (G) SM [39:1]. (H) PS [36:4]. (I) LPC [16:0]. A box on plot presents the interquartile ranges and medians. The black dots correspond to the normalized accumulation of selected lipid species in all samples. The notch indicates the 95% confidence interval around the median for each group. The mean level is indicated with a yellow diamond. Bars and asterisks show the results of U-Mann-Whitney/*t*-test: * $p < 0.05$, ** $p < 0.01$, *** $p < 0.001$; $n = 25$ in each group.

Subsequently, we compared two groups of CKD patients. We have observed that CKD1-2 and CKD5 patients displayed a similar lipid profile but differed in the accumulation of PC/PC-O, which were upregulated, and PEs that were found to be downregulated in CKD1-2 vs. CKD5 comparison.

Furthermore, the differences between CKD and CVD patients were disclosed. Apart from the upregulation of TAGs and downregulation of CEs in CKD compared to CVD, also two DAGs revealed the same directionality of change. All identified differential phospholipid species, i.e., nine PCs, three PE-Os, one PC-O, two PEs were downregulated in both CKD groups (as compared to CVD). Additionally, three SM and three Cer accumulated at significantly lower levels in both CKD groups.

In the next step, the enrichment analysis was performed in LION software to show a possible overrepresentation of functional terms related to lipid functions, cellular components, or lipid classification (Figure 5). Lipid identifiers were ranked by logarithmic transformation and fold-change values.

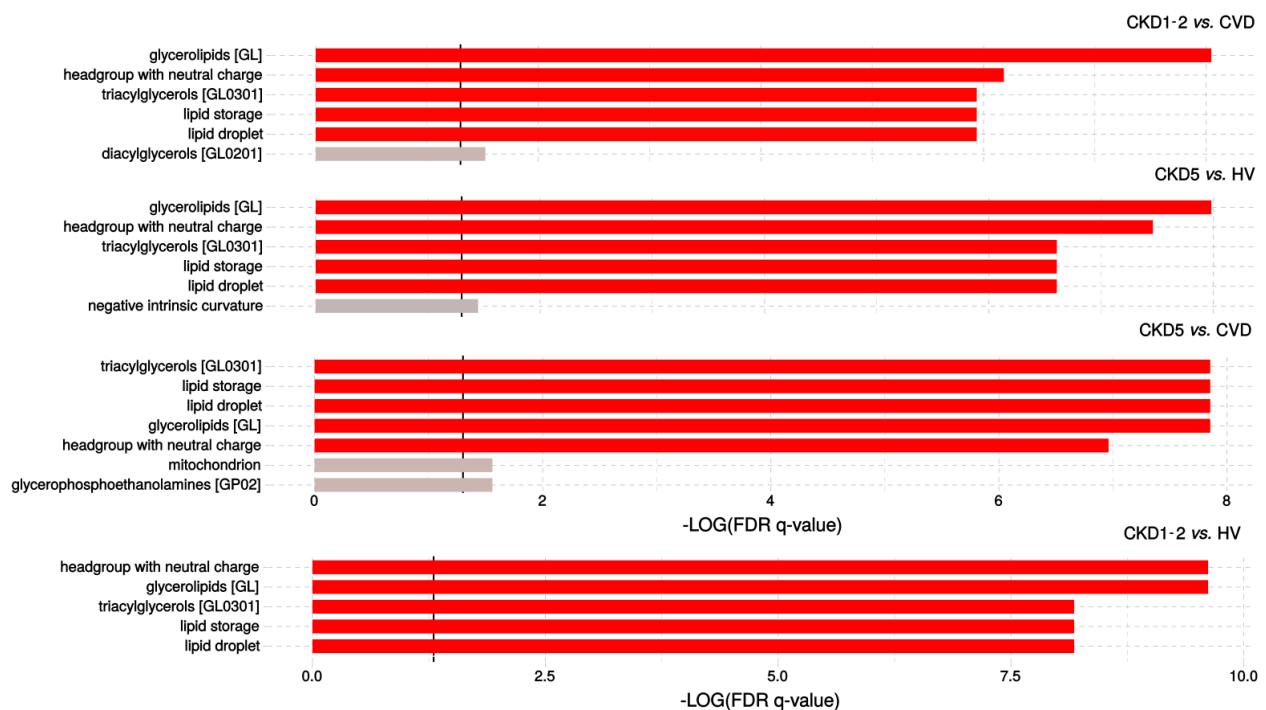


Figure 5. LION-term enrichment analysis of CKD1-2 vs. CVD, CKD5 vs. HV, CKD5 vs. CVD and CKD1-2 vs. HVs presented in the “ranking mode”. The gray vertical lines indicate the threshold of $-\log_{10}$ False discovery rate (FDR)-corrected p -value 0.05 (q -value 1.3). Red bars present terms with FDR-corrected p -value < 0.01 ($q > 2$).

Seven different features including lipid storage and formation of lipid droplets, were overrepresented according to FDR-corrected Kolmogorov–Smirnov p -value and statistically enriched in the CKD5 vs. CVD2 comparison. The results also suggested that triacylglycerols and glycerophosphoethanolamines are important in the differentiation of CKD5 and CVD patients. In the case of CKD1-2 vs. CVD comparison, similar results concerning functions in lipid storage have been found, but glycerolipids and lipids with neutral head groups were the main enriched group. Almost the same results were observed in comparison of CKD5 to HVs, and CKD1-2 vs. HV. Interestingly, no important enrichment was observed in the comparison of CVD to HV. The detailed information of this analysis is presented in Table S5.

To gain more functional insight, we further analyzed associations between identified classes of lipids (Figure 6). The plots illustrate overall changes observed in the lipidome of two the most significant group comparisons and revealed downregulation of PCs in CKD5 in comparison to CVD group and upregulation of PEs in CKD5 in comparison to HVs.

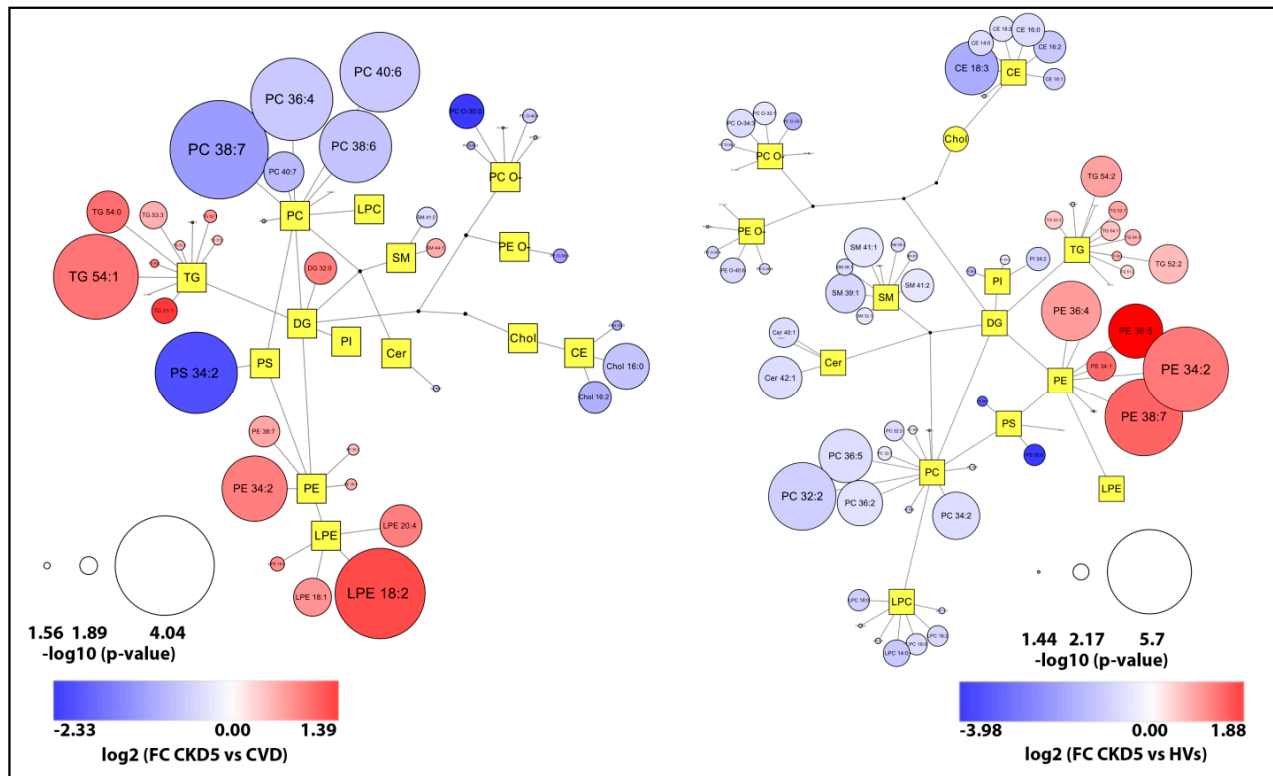


Figure 6. Network visualization of the most dysregulated lipid species found in CKD5 vs. CVD (left panel) and CKD5 vs. HV comparisons. Graphs express lipidomic pathways connections with clustering into individual lipid classes prepared using the Cytoscape software. Circles correspond to detected lipid species, the circle size articulates the significance according to Mann Whitney U test p -value, while the color gradient explains the degree of variations (red/blue) according to the calculated fold change.

2.3. Analysis of Selected Lipid Precursor and Components Using GC-MS Profiling

To gain more information about the observed changes, we subsequently chose the 14 most common precursors or components of lipids, including saturated, unsaturated fatty acids, glycerol, glyceric acid, and cholesterol, and performed the GC-MS metabolomic analysis utilizing separate cohorts. The low-molecular-weight compounds were quantified based on their peaks integrated from extracted-ion chromatograms (EIC). The results of this analysis are presented in Table S6. We have identified seven fatty acids, glycerol and cholesterol as differentiating lipid species among the analyzed experimental groups (Figure 7).

Data obtained for cholesterol corroborated the results of lipid profiling and standard medical tests, and revealed its lowest level in the CKD5 group (Figure 7H). However, a statistically significant change was only observed in CKD5 vs. HV comparison. All analyzed fatty acids revealed the lowest abundance in CKD5 plasma. However, substantial differences between particular groups of patients have also been detected (Figure 7A–G). For instance, CKD1-2 and CKD5 patients differed only in the level of palmitic acid (Figure 7B), although all fatty acids were significantly altered when CKD5 patients were compared to CVD ones (Figure 7A–G).

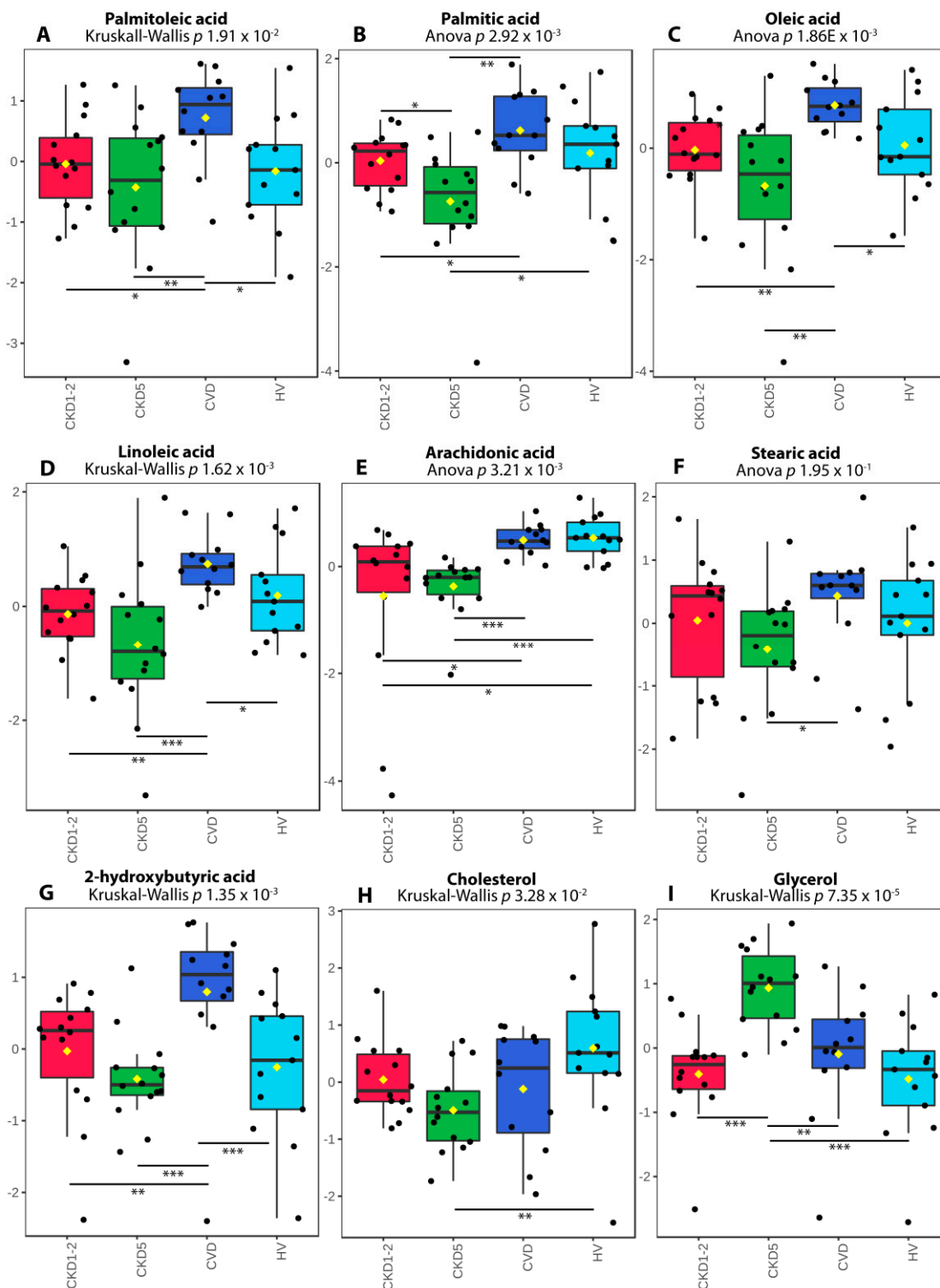


Figure 7. The abundance of differentially accumulated fatty acids, cholesterol and glycerol revealed in GC-MS analysis. (A) Palmitoleic acid. (B) Palmitic acid. (C) Oleic acid. (D) Linoleic acid. (E) Arachidonic acid. (F) Stearic acid. (G) 2-hydroxybutyric acid. (H) Cholesterol. (I) Glycerol. A box on plot presents interquartile ranges and medians. The black dots represent the normalized accumulation of molecules in all samples. The notch indicates the 95% confidence interval around the median of each group. The mean level is indicated with a yellow diamond. Bars and asterisks show results of U-Mann-Whitney/*t*-test: * $p < 0.05$, ** $p < 0.01$, *** $p < 0.001$; $n = 14$ in each group.

The opposite result was also disclosed—the CKD5 group revealed the highest abundance of this molecule, which differed significantly as compared to CVD, CKD1-2 and

HVs (Figure 7I). Moreover, four identified fatty acids: linoleic, palmitic, palmitoleic and oleic acids strongly, positively correlated with each other, with $\rho > 0.75$ (Figure 8; Table S7). Palmitic acid strongly correlated with stearic acid, with $\rho = 0.73$. We also correlated the abundance of identified compounds with eGFR. The analysis revealed that lower eGFR corresponded to a lower abundance of arachidonic acid ($\rho = 0.7$), palmitic acid ($\rho = 0.42$), oleic acid ($\rho = 0.43$), linoleic acid ($\rho = 0.47$), and cholesterol ($\rho = 0.49$). On the other hand, glycerol showed an inverse relationship with eGFR ($\rho = -0.46$). Additionally, CRP revealed a correlation with arachidonic ($\rho = -0.45$) and palmitic acid ($\rho = -0.40$).

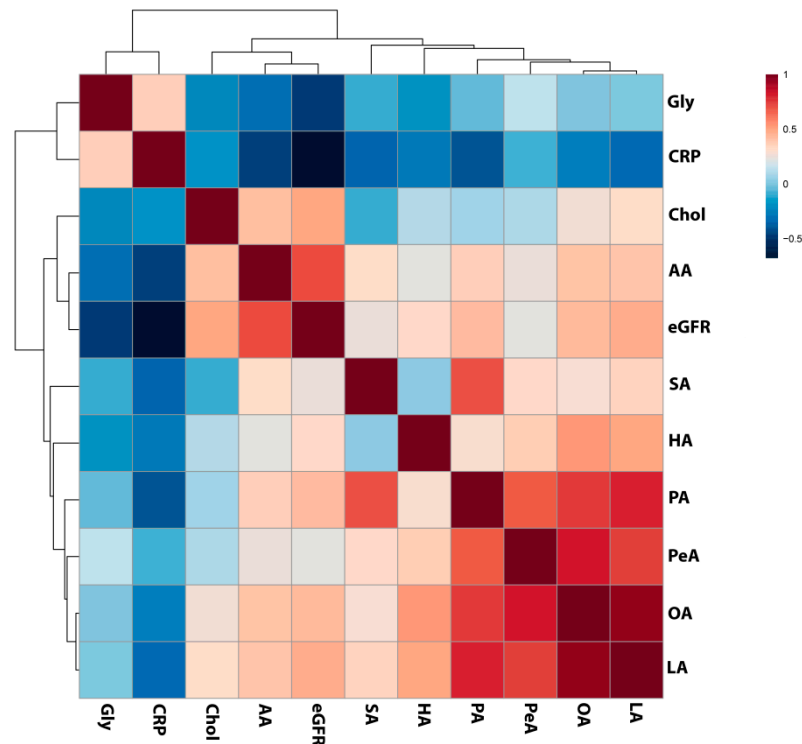


Figure 8. Results of the Spearman's rank correlation test performed for compounds identified in GC/MS analyses as differentially accumulated between analyzed experimental groups and estimated glomerular filtration rate (eGFR) and C-reactive protein (CRP) level presented as a heat map with the corresponding hierarchical tree. Color saturation corresponds to the value of Spearman's correlation coefficient. Gly—glycerol, Chol—cholesterol, AA—arachidonic acid, SA—stearic acid, HA—hydroxybutyric acid, PA—palmitic acid, PeA—palmitoleic acid, OA—oleic acid, LA—linoleic acid.

3. Discussion

The results of our previous proteome analyses showed that the accumulation of proteins involved in lipid metabolism and transport differed considerably in patients with CKD-A and atherosclerosis nonrelated to CKD, i.e., found in CVD patients [19]. In this study, we aimed to investigate changes in the blood plasma lipidome, in CKD and CVD patients. In routine clinical practice, lipid measurement based on the estimation of lipid concentration does not allow for the complex characterization of alterations in the plasma lipid profile. Human blood plasma lipidome can be characterized as highly diverse and thereby, more precise and accurate analysis needs to be performed to reveal the subtle abnormalities. The results of lipidome screening in CKD by mass spectrometry or hyphenated techniques have been published recently. For instance, Reis et al. analyzed LDL fractions in CKD patients and controls, and identified 352 lipid species. They demonstrated that the disease progression was associated with evident changes in lipid profile, while the results of clinical, biochemical tests might appear normal [20]. Using LC-MS several phosphatidylethanolamines and monoacylglycerols related to CKD progression were

identified [21]. However, to the best of our knowledge, our study demonstrated for the first time the comparison between patients with atherosclerosis-related and unrelated to CKD.

Among CKD patients, unique dyslipidemia which affects CVD progression is frequently observed and characterized as resistant to standard interventions [31]. Elevated levels of triacylglycerols (TAGs) and normal or reduced HDL and LDL are often seen [2,12,31]. Mikolasevic et al. indicated that hypertriglyceridemia occurs in 40–60% of CKD1-4 individuals and 45% of hemodialyzed patients [32]. Previous studies demonstrated a link between decreased catabolism of TAGs-rich lipoproteins (i.e., VLDL, LDL, and chylomicrons), caused by downregulation of certain genes involved in lipid metabolism and transport, and higher accumulation of TAGs in the blood of patients with CKD [33]. Authors suggested that the presence of uremic toxins inhibits lipid processing enzymes and alters lipoprotein particles' composition, which was considered to represent the main mechanisms of hypertriglyceridemia in patients with kidney dysfunction. Interestingly, the relation between impaired catabolism of TAG-carrying particles, the elevated abundance of TAGs, proteins participating in mentioned processes, and inflammation progression was suggested.

Therefore, the higher abundance of TAGs observed in CKD is not surprising. TAGs are esters derived directly from glycerol and fatty acid molecules. Interestingly, we observed a decreased abundance of seven fatty acids (commonly present in TAG structure) in CKD, especially in CKD5 patients, and four of them; palmitic, palmitoleic, oleic and linoleic, were strongly correlated with each other. In contrast, the level of glycerol was elevated in CKD5 in comparison to all analyzed experimental groups. Treatment with glycerol causes severe renal dysfunction, which includes renal structural abnormalities, renal oxidative stress, inflammation and apoptosis, and this molecule is frequently used to induce kidney injury in animal models [34–36]. However, a high level of endogenous glycerol in humans has not been observed so far. It is also noteworthy that arachidonic, palmitic, oleic and linoleic acid positively associated with renal function, whereas glycerol was inversely associated with eGFR and CRP. Fatty acids in kidney disease are sporadically described in the literature. Nevertheless, the correlation between the level of plasma fatty acids in CKD and disease progression and mortality has been previously demonstrated [37]. Stearic acid abundance was decreased in CKD patients, which is in line with our findings [38]. In this study, also oleic and linoleic acid were correlated with kidney dysfunction parameters, and the authors suggested an association with CKD. Furthermore, downregulation of oleic, linoleic and arachidonic acids was observed in hemodialyzed patients as compared to the control group [39]. Moreover, the relative abundance of saturated fatty acids and mono-unsaturated fatty acids was associated with lipid disorders and cardiomyopathy in CKD [39]. The positive relationship between saturated fatty acids accumulation and vascular calcification, the most common complications related to atherosclerosis progression in CKD, has also been reported [40]. Furthermore, the reduced level of 2-hydroxybutyric acid was observed in advanced renal patients [41]. The authors suggested that the presence of decreased level of 2-hydroxybutyric acid is related to the declining of H₂S generation process, which was confirmed by the reduced expression of enzymes involved in these reactions. The downregulation of H₂S-synthesis and related enzymes was also presented in an animal model of CKD [42] and in the circulating leukocytes of ESRD patients [43,44]. As an anti-inflammatory, anti-oxidant and anti-apoptotic compound, H₂S has been associated with cardiovascular and kidney disease. Therefore, the differences in the CKD and CVD level of 2-hydroxybutyric acid, a metabolite related to H₂S production, but also other identified fatty acids once again underlines the differences between molecular mechanisms underlying disease progression in CKD and CVD.

We have earlier suggested that dysregulated metabolism of pro-atherogenic and anti-atherogenic protein fractions of lipoproteins transporting primarily TAGs is far more advanced in CKD than patients with the classical cardiovascular disorder without kidney dysfunction [45]. Apolipoprotein B and apolipoprotein A1 are critical for lipoprotein formation, stability and clearance, while apolipoprotein A4 is involved in reverse cholesterol

transport and plays an anti-atherogenic and antioxidative role. Our previous studies revealed the altered levels of these proteins in CKD as compared to HVs and CVD patients. Therefore, the impaired accumulation of TAGs can be a consequence of processes associated with lipoprotein particles' changed composition.

Furthermore, low HDL levels were found in 35–50% of cases of CKD1-5 [32]. Our results concerning the clinical indices showed significantly decreased total cholesterol levels, LDL and HDL in CKD5 compared to others, despite advanced atherosclerosis and high incidence of cardiovascular events observed in this group. The lowest concentration of total cholesterol was observed for the CKD5 group, as revealed by three independent, complementary approaches: shotgun lipid profiling, standard medical tests and GC-MS quantification. Moreover, we also showed a correlation between the cholesterol level, and eGFR and thus demonstrated that the lower cholesterol level might be related to kidney dysfunction progression. The negative association between cholesterol levels and mortalities in dialyzed patients known as “reverse epidemiology” was postulated in a few studies [12,31,46,47]. Some studies suggested that LDL lowering therapy can relatively reduce the risk of mortality among renal failure patients [2]. In contrast, Kilpatrick et al. demonstrated that adjustments for inflammation and malnutrition led to equivocal results, and did not confirm the thesis of the increased mortality in the group of CKD5 patients with low LDL [47]. In our study, the inflammation process was significantly elevated in CKD5 patients as depicted by the level of C-reactive protein. Moreover, we have earlier demonstrated that proteins involved in inflammation exhibited more significant alterations in individuals with CKD-related atherosclerosis [48]. Therefore, severe malnutrition and inflammation development should be considered as the most critical factors responsible for CVD progression in CKD.

Previously, we have also demonstrated an absence of a correlation between the protein components of LDL and LDL level, and indicated that LDL might be more atherogenic in CKD-A vs. classical CVD patients [19]. Large differences in accumulation of many lipid species between CVD and CKD5 groups, with similar atherosclerosis progress, observed in the current study, strengthen our hypothesis that different molecular mechanisms are involved in atherosclerosis-related and nonrelated to CKD. Apart from TAGs, the highest differences in CKD5 vs. CVD comparison were observed for CEs, PCs, PE-Os, SMs and Cers. However, in contrast to TAGs, all of these classes revealed decreased abundance in CKD5 compared to CVD. Moreover, changes in abundances of many of these classes were strongly correlated with each other. It should be stated that the dialysis procedure itself shall not cause the loss of hydrophobic molecules, but the loss of some proteins like albumin, which may bind lipid particles, is possible [49]. Moreover, samples were collected before the hemodialysis session which excludes the influence of treatment.

It is worth mentioning that CKD5 and CVD groups of patients with similar symptoms and progress of atherosclerosis (based on medical records) differed in the accumulation of 23 from a total of 91 differentiating lipid species. On the other hand, the comparison between CVD and CKD1-2 groups, which are considerably different in the severity of atherosclerosis, also revealed 24 differentially accumulated compounds. However, distinct lipid species were identified as differentially accumulated in both comparisons. These observations support our hypothesis that the CVD acceleration mechanism may differ at initial and advanced CKD stages, in which the inflammation processes are more pronounced. Accumulation of 17 different lipid species differentiated CKD1-2 and CKD5 groups, and these compounds could serve as disease progression indicators in CKD.

A few studies have shown that sphingomyelin is associated with cardiovascular disease progression [50]. Moreover, CKD sphingomyelin was found to be significantly and directly associated with GFR decline [51]. Our results seem to be contrasting with them, however, studies comparing both groups, CKD and CVD at the same have not been conducted in this aspect.

The molecular complexity of the CKD-A should also be taken into account. Although precise relation(s) between differentially accumulated lipid species and genes or enzymes

involved in lipid homeostasis was not investigated, we can refer to the other results. Some researchers suggested that significantly increased cellular accumulation of CEs and DAGs can be linked with the activation of the mitogen-activated protein kinase and protein kinase C pathways involved in the process of inflammatory milieu development [21]. Moreover, the intensified biosynthesis of particular PEs could confirm the protein kinase C activation, leading directly to the degradation of membrane components and influencing the downstream membrane-protein physiological processes [21]. Further research shall be conducted on the role of inflammation caused by progressive kidney damage and its influence on the process of cardiovascular disorder development.

Considering a functional analysis of results we should emphasize that lipidomics is still a novel strategy in system biology sciences and all the available tools are still in their early development. LION is as far as we know the only tool allowing for reasonably effective enrichment analysis of lipid species. Our results strongly suggest that the main function of lipids involved in the progression of CKD is lipid storage and formation of lipid droplets, it also shows that these lipids are mainly TAGs and DAGs, but also phospholipids of a different kind. As lipid droplets are reservoirs of cholesterols in mammalian cells, the dysregulation of their formation may be of important function especially in the development of atherosclerosis and it may explain why we observe these changes both in CKD and CVD patients.

The limitations of the current study are related to the identification of only a portion of the plasma lipidome. Another limitation is the lack of common and verified methods for validation of lipid analytes that we can utilize in, for instance, proteomic studies. Therefore, we supplemented the lipid profiling with standard medical assessments of lipoprotein fractions and GC/MS analysis of selected lipid components and precursors. Utilizing such complementary methods, we successfully validated the cholesterol levels in all analyzed experimental groups. The dietary habits of studied participants were not analyzed in this study. Nonetheless, the assumption about the dietary variation equal in all groups of individuals can be considered. Finally, an additional research in larger CKD and CVD cohorts is required to validate the findings presented in this small-scale study.

To the best of our knowledge, the study comparing lipid profiles of patients with atherosclerosis-related and nonrelated to CKD has not been presented before. These findings, combined with lipid precursors and components analysis and clinical indices, confirmed our previous hypothesis that atherosclerosis underlying CVD in CKD may be uniquely assessed, differentiating it from patients with classical CVD without kidney disease. The mechanism of atherosclerosis progression in CKD is not yet fully elucidated, and is likely of multifactorial origin. Based on our results, it seems plausible that atherosclerosis in patients with CKD is more considerable than in CVD, and is associated with inflammation. Malnutrition and increasing concentration of uremic toxins that influence lipid metabolism and transport and inhibit the enzymes involved in lipid homeostasis can act as acceleratory factors. Hence, the targeted screening of lipid classes engaged in the inflammation process and analysis of oxidized forms of metabolites is worth pursuing in future studies, to reveal the mechanisms beyond the progression of CVD in CKD. In summary, our findings support the importance of exploring the lipid profiles to elucidate the underlying molecular mechanisms and pinpoint the new lipid-lowering strategies in CKD-A.

4. Materials and Methods

4.1. Subject and Samples

The study has been approved by the Bioethics Committee at the Poznan University of Medical Sciences (resolution no. 926/16). Our study protocol conformed to the Ethical Guidelines of the World Medical Association Declaration of Helsinki. All participating individuals provided signed informed consent for inclusion. One hundred individuals divided into four groups of equal size were involved in the survey (Table 1). Individuals with diabetes mellitus, acute inflammatory processes, and malignant tumors were excluded

from the study. To further characterize the studied groups, eGFR (calculated by the formula developed by Levey et al. [52]), body mass index (BMI), high sensitivity C-reactive protein (hsCRP), and the full lipid profile were determined.

The systolic and diastolic blood pressure was measured, and medical history was established in all studied groups. Healthy volunteers and patients were qualified to appropriate experimental groups based on obtained clinical measurements and medical history. According to the National Institute for Health and Care Excellence guidelines, CKD patients were divided into two groups, i.e., CKD1-2 and CKD5 [53]. The CKD1-2 group was restricted to 25 patients at the initial CKD stages (mean eGFR 70 mL/min/1.73 m²) with hypertension, hyperlipidemia, diagnosed with nonobstructive coronary artery disease (CAD)—confirmed by coronarography, but without cardiovascular events in their medical history. The CKD5 and CVD groups included 25 patients each, displaying advanced atherosclerosis confirmed by coronarography and clinically manifested as severe CAD, with a history of at least one acute cardiac incident and/or status after the vascular intervention. The factor differentiating these two groups was the status of kidney function, the CKD5 patients with mean eGFR 6 mL/min/1.73 m² represented ESRD patients treated with hemodialysis for at least two years, three times per week. Subjects from the CVD group exhibited normal kidney function with mean eGFR 96 mL/min/1.73 m². The last group, which served as a control group, consisted of 25 age-matched healthy volunteers (HVs) with a mean eGFR of 102 mL/min/1.73 m².

A closed monovette system containing EDTA was applied for peripheral blood collection. Plasma samples were stored at −80 °C until analysis.

4.2. Lipid Extraction Method

Lipid separation was carried out according to the MTBE extraction protocol proposed by Matyash and co-workers [29]. Briefly, 20 µL of each plasma sample was diluted with 80 µL of water in glass tubes with teflon-coated caps. Subsequently, 10 µL of methanolic solution of labeled standard (16:0-d31-18:1 PC, 1 µg, from Avanti lipids), 750 µL of methanol and 2.5 mL of MTBE were added, and the mixtures were vortexed for 1 h at RT. Phase separation was induced by the addition of 625 µL of water. Upon 10 min incubation at RT, the mixtures were centrifuged at 1000× g for 10 min, 2 mL of upper organic phases were then collected and dried under a nitrogen stream at 37 °C. Lipids were resuspended prior to analysis in 500 µL of MS-mix buffer containing 7.5 mM ammonium acetate, in chloroform, 2-propanol and methanol (1:2:4 v/v/v).

4.3. Mass Spectrometry Analysis of Lipid Fractions (Shotgun-Based Lipidomics)

Lipid profiling of blood plasma samples was performed using Q-Exactive Orbitrap mass spectrometer (Thermo Fisher Scientific, Bremen, Germany) equipped with TriVersa NanoMate robotic nanoflow ESI ion source (Advion BioSciences Ltd., Ithaca, NY, USA). The nanoelectrospray chips with nozzles' diameter of 5.5 µm were used to obtain stable ion spray, and Chipsoft software (ver. 8.3.1.1018, Advion BioSciences Ltd., Ithaca, NY, USA) was applied to control ESI ion source. The system was calibrated using Pierce™ LTQ Velos ESI Positive Ion Calibration Solution (Thermo Fisher Scientific, Rockford, IL, USA). 10 µL of the sample was infused directly into the mass spectrometer, and after ion current stabilization, data were acquired for 10 min. The source was operated at a gas pressure of 1.25 psi, and the optimum ionization voltage was set to 1.05 kV. Briefly, MS data were acquired in positive ion mode within the range of *m/z* 300–1500 at the resolution of 140,000 (at *m/z* 200, FWHM). Automatic gain control was set to a target value of 3.0×10^6 , and ion injection time (IT) at 100 ms. Targeted MS/MS experiments were carried out using higher-energy collisional dissociation mode (HCD) to assist in the identification of lipid species.

In order to control the quality of measurements, we have used pooled plasma samples derived from all samples as well as pools prepared for each group of patients separately. These samples were injected following every 8 samples in sequence. The reproducibility of the biological and technical replicates was assessed by the scatter plotting and the

correlation coefficient determined based on the signal intensities. Samples with Pearson's correlation coefficients above 0.9 were considered as those with good quality suitable for further analysis.

4.4. Data Processing and Identification of Lipid Species

Raw MS data were converted into mzXML format and further processed with LipidXplorer software (ver. 1.2.7, Max Planck Institute of Cell Biology and Genetics, Dresden, Germany) [54]. Profiles were obtained by averaging 8 min of recorded mass spectra, from the second minute to the ninth minute within ten minutes of sample delivery time. The first 60 s of sample injection was allowed for electrospray and analyte flow stabilization, based on total ion current (TIC) variation. Subsequently, an alignment procedure was performed to match the related peaks within the whole dataset. Defined signals in mass spectra for further processing and consideration were selected by setting the threshold value to 1500 (S/N ~3). The identification of lipid species was performed following Graessler et al. [25]. The LipidXplorer software was used, and MFQL files for the identification of lipids in human blood plasma were supplied from the MFQL library (available at: https://wiki.mpi-cbg.de/lipidx/MFQL_library, access on 12 March 2020). Particular lipid species were identified based on accurately determined masses, i.e., mass accuracy higher than 5 ppm in MS⁺ (the top-down lipidomics approach). The fragmentation patterns of selected lipids were additionally analyzed for the presence of specific signals derived from headgroups or bases, in order to confirm the subclass annotations: for LPC, PC and SM at m/z 184.07—phosphocholine headgroup, for CE at m/z 369.35—cholesterol base, and for ceramides at m/z 264.26—for the sphingosine d18:1 backbone; for PE and PS the neutral losses were observed of 141.02 Da (phosphoethanolamine), and of 185.01 Da for phosphoserine, respectively (<https://lipidomics-standards-initiative.org/resources/lipid-class-specific-fragments>, access on 9 April 2021). The annotations were additionally compared with the data from the LipidMaps and the Human Metabolome Database library. Following the recommendations by MSI (Metabolite Standard Initiative), the compound names were assigned within each class according to the second and third level of identification. The second level indicates the putatively annotated compounds based on physicochemical properties and/or spectral similarity with public/commercial spectral libraries. The third level designates the putatively characterized compound classes based on characteristic physicochemical properties of a chemical class of compounds, or by spectral similarity to known compounds of a chemical class. Both levels of identification designate them as putatively annotated compounds, according to Sumner and co-workers [55].

All identified lipids were analyzed separately, and average abundance for each lipid class was also calculated. The average accumulation was based on the normalized accumulation of all identified lipids that belonged to the same class.

4.5. Functional Analysis

LION (Lipid Ontology—<http://www.lipidontology.com/>, access on 9 April 2021) tool was used for enrichment analysis and lipids' association with pathways [56]. For this purpose, tables with quantitative information were prepared according to instruction present on the website and “Ranking Mode” for data pretreatment was used. Lipid identifiers were ranked by logarithmic transformation and fold-change values. The 1-tailed Kolmogorov–Smirnov tests were used as “global” statistics to assess enrichment of LION-terms over a ranked (by “local” statistics) list of lipids.

In addition to the results from LION, plots in which the core structure reflects basic (simplified) lipid metabolism were prepared. The up- and downregulated lipids in a target group were presented as circles, where the size is related to the statistical significance (Mann Whitney U test p -value), and the color to the fold change, respectively. The plots capture overall changes observed in the lipidome of one group, compared to control (or another

group). Graphs were prepared using the Cytoscape software (<http://www.cytoscape.org>, access on 9 April 2021).

4.6. GC-MS Analysis of Plasma Samples for Identification of Selected Lipid-Related Compounds

Twenty-five microliter aliquots of plasma samples were deproteinized with 4 volumes of cold methanol and stored in a freezer for 20 min at $-20\text{ }^{\circ}\text{C}$. Samples were centrifuged at $11,000\times g$ for 5 min, and supernatants were transferred to Eppendorf tubes. Samples were then dried in a vacuum centrifuge, resuspended in 20 μL of methoxyamine hydrochloride (20 mg/mL in dry pyridine), and vortexed in a thermomixer for 1.5 h at $37\text{ }^{\circ}\text{C}$. Fifty μL of MSTFA (*N*-Methyl-*N*-(trimethylsilyl)-trifluoroacetamide) was then added to each sample, vortexed for 30 min at $37\text{ }^{\circ}\text{C}$ and centrifuged at $11,000\times g$ for 10 min. From each sample, 50 μL of the mixture was subsequently transferred to a conical glass vial prior to GC separation. One- μL aliquots of the derivatized samples were injected using PTV-injection in the splitless mode. Metabolites were analyzed using GC-MS system (TRACE 1310 GC oven with TSQ8000 triple quad MS; Thermo Fisher Scientific, Rockford, IL, USA), equipped with DB-5MS column (30 m \times 0.25 mm \times 0.25 μm ; J&W Scientific, Agilent Technologies, Santa Clara, CA, USA). Chromatographic separation conditions in gradient mode were kept as follows: $70\text{ }^{\circ}\text{C}$ for 2 min, followed by $10\text{ }^{\circ}\text{C}/\text{min}$ up to $300\text{ }^{\circ}\text{C}$, at $300\text{ }^{\circ}\text{C}$ ($10'$). PTV injector was used for sample injection with a temperature gradient from 40 to $250\text{ }^{\circ}\text{C}$, column interface was kept at $250\text{ }^{\circ}\text{C}$, and source temperature at $250\text{ }^{\circ}\text{C}$. The ion source operated in 50–850 m/z range, in EI positive mode, and electron energy was set to 70 eV. As TMS (trimethylsilyl) derivatives, the compounds were identified after comparisons of registered mass spectra with those present in the NIST library. Identified compounds were quantified, and extracted ion chromatograms (EIC) of selected m/z values, corresponding to specific compounds, together with specific retention times for given compounds, were used. First, the unique masses were chosen based on library spectra, and EIC peaks were integrated to measure their areas, and respective values were exported into tables. Furthermore, the total ion current was measured by integration of all TIC peaks, and used for compounds normalization.

4.7. Statistical Analysis

The raw MS data were normalized to total ion current (TIC) and statistically analyzed using Perseus ver. 1.5.8.5 [57], and MetaboAnalyst [58]. Data were logarithmized, and sample quality was assessed by calculating the presence of lipids in the samples (cut off was set to 80%). For subsequent analysis, only lipids present across 80% of all samples in each group were retained. In the GC-MS analysis of selected lipid-related compounds, only compounds present in all samples were analyzed (no missing values). Chi-square test was used for categorical variables. Data distribution was assessed using Shapiro–Wilk and Leven’s tests to evaluate the equality of variances. The data were statistically analyzed using a U-Mann–Whitney test or a Student’s unpaired t-test when appropriate. More than two groups were compared using one-way ANOVA or Kruskal–Wallis for nonparametric data with FDR correction, followed by post-hoc multiple comparison testing. Statistical significance was accepted at $p < 0.05$. Particular lipids were considered to be differentially accumulated if apart from the p -value < 0.05 , the difference between at least 2 groups was at the fold change of ± 1.5 .

To analyze the average abundance of each lipid class, only p -values were taken into account. The correlations between variables were defined by Pearson’s coefficients (for parametric data) or using the Spearman’s rank correlation test (for nonparametric data). A p -value of < 0.05 was considered statistically significant. Multivariate analyses were carried out by untargeted principal component analysis (PCA) and hierarchical clustering. For hierarchical clustering and heat map visualization, the data were normalized to a Z-score. Partial least squares discriminant analysis (PLS-DA) was additionally performed using the SIMCA software ver. 13.0.0.0 (Umetrics AB, Umeå, Sweden) to check for the potential

differences between groups. The data were not split additionally into the training and testing set. Data were log-transformed and Pareto-scaled before the analysis.

Supplementary Materials: The following are available online at <https://www.mdpi.com/article/10.3390/metabo11050275/s1>, Table S1: Pearson's correlation coefficients calculated for clinical data, Table S2: A list of identified lipid classes in plasma of HVs, CKD1-2, CKD5 and CVD patients. Table provides information about the name of lipid class, average abundances and SD for all analyzed experimental groups, ANOVA/K-W *p*-value and *q*-value and fold changes for all group comparisons, Table S3: Pearson's correlation coefficients calculated for identified lipid classes presented as a heat map in Figure 1 and clinical data. The calculations were derived from MetaboAnalyst software. Significant correlation (*p*-value < 0.05) is marked in bold, Table S4: Complete list of differentially accumulated lipid species in plasma of HVs, CKD1-2, CKD5 and CVD patients. Table provides information about the name of lipid class, average abundances and SD for all analyzed experimental groups, ANOVA/K-W *p*-value and *q*-value and fold changes for all group comparisons, Table S5: A detailed list of the enrichment analysis performed in LION. Table provides information about lipid functions, cellular components or lipid classification with term ID, number of annotated lipids, *p*-value and FDR-corrected Kolmogorov–Smirnov *p*-value (*q*-value), Table S6: A list of low-molecular-weight compounds quantified using extracted-ion chromatogram (EIC) and GC-MS analysis. Table provides information about the name of compound, retention time (RT), and *m/z* value characteristic for the given compound derived from NIST database (Quant Mass), average abundances and SD for all analyzed experimental groups, ANOVA/K-W *p*-value and *q*-value and fold changes for all group comparisons, Table S7: Spearman's correlation coefficients calculated for low-molecular-weight compounds quantified using extracted-ion chromatogram (EIC) and GC-MS analysis and clinical data presented in Figure 8, Figure S1: Partial least squares discriminant analysis (PLS-DA) performed on the total number of lipids identified in CKD5 (green), CVD (dark blue), CKD1-2 (red), and HVs (blue) experimental groups.

Author Contributions: Conceptualization, L.M. and M.L.; funding acquisition, M.L.; investigation, J.I., J.T., M.B. and M.O.; methodology, L.M., J.I. and J.T.; resources, B.P., K.K.-J., A.T., M.W.-K. and D.F.; supervision, L.M. and M.L.; validation, J.T.; visualization, M.L.; writing—original draft, L.M. and M.S.; writing—review and editing, D.F. and M.L. All authors have read and agreed to the published version of the manuscript.

Funding: This research was funded by the National Science Centre, Poland under Grant no. 2015/19/B/NZ2/02450, to M.L.

Institutional Review Board Statement: The study was conducted according to the guidelines of the Declaration of Helsinki, and approved by the Bioethics Committee of Poznan University of Medical Sciences (resolution no. 926/16; 15 September 2016).

Informed Consent Statement: Informed consent was obtained from all subjects involved in the study.

Data Availability Statement: The data presented in this study are available on request from the corresponding author. The data are not publicly available due to the specificity and complexity of data sets obtained with shotgun approach.

Acknowledgments: The graphical abstract was generated using the web-based tool BioRender (Biorender.com, accessed on 26 April 2021).

Conflicts of Interest: The authors declare no conflict of interests. The funders had no role in the design of the study; in the collection, analyses, or interpretation of data; in the writing of the manuscript, or in the decision to publish the results.

References

1. Levin, A.; Stevens, P.; Bilous, R. Kidney Disease: Improving Global Outcomes (KDIGO) CKD Work Group. KDIGO 2012 clinical practice guideline for the evaluation and management of chronic kidney disease. *Kidney Int. Suppl.* **2013**, *3*, 1e150.
2. Yamamoto, S.; Kon, V. Mechanisms for increased cardiovascular disease in chronic kidney dysfunction. *Curr. Opin. Nephrol. Hypertens.* **2009**, *18*, 181–188. [[CrossRef](#)] [[PubMed](#)]
3. Ecder, T. Early diagnosis saves lives: Focus on patients with chronic kidney disease. *Kidney Int. Suppl.* **2013**, *3*, 335–336. [[CrossRef](#)] [[PubMed](#)]

4. Briasoulis, A.; Bakris, G.L. Chronic Kidney Disease as a Coronary Artery Disease Risk Equivalent. *Curr. Cardiol. Rep.* **2013**, *15*, 340. [[CrossRef](#)] [[PubMed](#)]
5. De Santo, N.G.; Cirillo, M.; Perna, A.; De Santo, L.S.; Anastasio, P.; Pollastro, M.R.; De Santo, R.M.; Iorio, L.; Cotrufo, M.; Rossi, F. The heart in uremia: Role of hypertension, hypotension, and sleep apnea. *Am. J. Kidney Dis.* **2001**, *38*, S38–S46. [[CrossRef](#)]
6. Olechnowicz-Tietz, S.; Gluba, A.; Paradowska, A.; Banach, M.; Rysz, J. The risk of atherosclerosis in patients with chronic kidney disease. *Int. Urol. Nephrol.* **2013**, *45*, 1605–1612. [[CrossRef](#)] [[PubMed](#)]
7. Levey, A.S.; Beto, J.A.; Coronado, B.E.; Eknoyan, G.; Foley, R.N.; Kasiske, B.L.; Klag, M.J.; Mailloux, L.U.; Manske, C.L.; Meyer, K.B.; et al. Controlling the epidemic of cardiovascular disease in chronic renal disease: What do we know? What do we need to learn? Where do we go from here? National Kidney Foundation Task Force on Cardiovascular Disease. *Am. J. Kidney Dis.* **1998**, *32*, 853–906. [[CrossRef](#)]
8. Schiffrin, E.L.; Lipman, M.L.; Mann, J.F.E. Chronic kidney disease: Effects on the cardiovascular system. *Circulation* **2007**, *116*, 85–97. [[CrossRef](#)]
9. De Jager, D.J.; Grootendorst, D.C.; Jager, K.J.; Van Dijk, P.C.; Tomas, L.M.J.; Ansell, D.; Collart, F.; Finne, P.; Heaf, J.G.; De Meester, J.; et al. Cardiovascular and noncardiovascular mortality among patients starting dialysis. *JAMA J. Am. Med. Assoc.* **2009**, *302*, 1782–1789. [[CrossRef](#)]
10. Manjunath, C.N.; Rawal, J.R.; Irani, P.M.; Madhu, K. Atherogenic dyslipidemia. *Indian J. Endocrinol. Metab.* **2013**, *17*, 969–976. [[CrossRef](#)]
11. Kalantar-Zadeh, K.; Block, G.; Humphreys, M.H.; Kopple, J.D. Reverse epidemiology of cardiovascular risk factors in maintenance dialysis patients. *Kidney Int.* **2003**, *63*, 793–808. [[CrossRef](#)]
12. Liu, Y.; Coresh, J.; Eustace, J.A.; Longenecker, J.C.; Jaar, B.; Fink, N.E.; Tracy, R.P.; Powe, N.R.; Klag, M.J. Association Between Cholesterol Level and Mortality in Dialysis Patients. *JAMA* **2004**, *291*, 451. [[CrossRef](#)] [[PubMed](#)]
13. Baigent, C.; Landray, M.J.; Wheeler, D.C. Misleading associations between cholesterol and vascular outcomes in dialysis patients: The need for randomized trials. *Semin. Dial.* **2007**, *20*, 498–503. [[CrossRef](#)] [[PubMed](#)]
14. Nogueira, J.; Weir, M. The unique character of cardiovascular disease in chronic kidney disease and its implications for treatment with lipid-lowering drugs. *Clin. J. Am. Soc. Nephrol.* **2007**, *2*, 766–785. [[CrossRef](#)] [[PubMed](#)]
15. Valdivielso, J.M.; Rodríguez-Puyol, D.; Pascual, J.; Barrios, C.; Bermúdez-López, M.; Sánchez-Niño, M.D.; Pérez-Fernández, M.; Ortiz, A. Atherosclerosis in Chronic Kidney Disease. *Arterioscler. Thromb. Vasc. Biol.* **2019**, *39*, 1938–1966. [[CrossRef](#)]
16. Cai, Q.; Mukku, V.K.; Ahmad, M. Coronary artery disease in patients with chronic kidney disease: A clinical update. *Curr. Cardiol. Rev.* **2013**, *9*, 331–339. [[CrossRef](#)]
17. Tannock, L. *Dyslipidemia in Chronic Kidney Disease*; MDText.com, Inc.: Portland, OR, USA, 2000.
18. Obialo, C.I.; Ofili, E.O.; Norris, K.C. Statins and Cardiovascular Disease Outcomes in Chronic Kidney Disease: Reaffirmation vs. Repudiation. *Int. J. Environ. Res. Public Health* **2018**, *15*, 2733. [[CrossRef](#)]
19. Luczak, M.; Formanowicz, D.; Marczak, Ł.; Suszyńska-Zajczyk, J.; Pawliczak, E.; Wanic-Kossowska, M.; Stobiecki, M. ITRAQ-based proteomic analysis of plasma reveals abnormalities in lipid metabolism proteins in chronic kidney disease-related atherosclerosis. *Sci. Rep.* **2016**, *6*, 32511. [[CrossRef](#)]
20. Reis, A.; Rudnitskaya, A.; Chariyavilaskul, P.; Dhaun, N.; Melville, V.; Goddard, J.; Webb, D.J.; Pitt, A.R.; Spickett, C.M. Top-down lipidomics of low density lipoprotein reveal altered lipid profiles in advanced chronic kidney disease. *J. Lipid Res.* **2015**, *56*, 413–422. [[CrossRef](#)]
21. Afshinnia, F.; Rajendiran, T.M.; Karnovsky, A.; Soni, T.; Wang, X.; Xie, D.; Yang, W.; Shafi, T.; Weir, M.R.; He, J.; et al. Lipidomic Signature of Progression of Chronic Kidney Disease in the Chronic Renal Insufficiency Cohort. *Kidney Int. Rep.* **2016**, *1*, 256–268. [[CrossRef](#)]
22. Ekroos, K.; Jänis, M.; Tarasov, K.; Hurme, R.; Laaksonen, R. Lipidomics: A Tool for Studies of Atherosclerosis. *Curr. Atheroscler. Rep.* **2010**, *12*, 273–281. [[CrossRef](#)] [[PubMed](#)]
23. Zhao, Y.-Y.; Cheng, X.; Lin, R.-C. Lipidomics Applications for Discovering Biomarkers of Diseases in Clinical Chemistry. *Int. Rev. Cell Mol. Biol.* **2014**, *313*, 1–26. [[CrossRef](#)]
24. Holčápek, M.; Červená, B.; Cifková, E.; Lísa, M.; Chagovets, V.; Vostálová, J.; Bancířová, M.; Galuszka, J.; Hill, M. Lipidomic analysis of plasma, erythrocytes and lipoprotein fractions of cardiovascular disease patients using UHPLC/MS, MALDI-MS and multivariate data analysis. *J. Chromatogr. B* **2015**, *990*, 52–63. [[CrossRef](#)] [[PubMed](#)]
25. Graessler, J.; Schwudke, D.; Schwarz, P.E.H.; Herzog, R.; Shevchenko, A.; Bornstein, S.R. Top-down lipidomics reveals ether lipid deficiency in blood plasma of hypertensive patients. *PLoS ONE* **2009**, *4*, e6261. [[CrossRef](#)]
26. Holčápek, M.; Liebisch, G.; Ekroos, K. Lipidomic Analysis. *Anal. Chem.* **2018**, *90*, 4249–4257. [[CrossRef](#)]
27. Surma, M.A.; Herzog, R.; Vasilj, A.; Klose, C.; Christinat, N.; Morin-Rivron, D.; Simons, K.; Masoodi, M.; Sampaio, J.L. An automated shotgun lipidomics platform for high throughput, comprehensive, and quantitative analysis of blood plasma intact lipids. *Eur. J. Lipid Sci. Technol.* **2015**, *117*, 1540–1549. [[CrossRef](#)] [[PubMed](#)]
28. Cajka, T.; Fiehn, O. Comprehensive analysis of lipids in biological systems by liquid chromatography-mass spectrometry. *Trends Analyt. Chem.* **2014**, *61*, 192. [[CrossRef](#)] [[PubMed](#)]
29. Matyash, V.; Liebisch, G.; Kurzchalia, T.V.; Shevchenko, A.; Schwudke, D. Lipid extraction by methyl-tert-butyl ether for high-throughput lipidomics. *J. Lipid Res.* **2008**, *49*, 1137–1146. [[CrossRef](#)]

30. Schwudke, D.; Schuhmann, K.; Herzog, R.; Bornstein, S.R.; Shevchenko, A. Shotgun Lipidomics on High Resolution Mass Spectrometers. *Cold Spring Harb. Perspect. Biol.* **2011**, *3*, a004614. [[CrossRef](#)] [[PubMed](#)]
31. Pandya, V.; Rao, A.; Chaudhary, K. Lipid abnormalities in kidney disease and management strategies. *World J. Nephrol.* **2015**, *4*, 83–91. [[CrossRef](#)]
32. Mikolasevic, I.; Žutelija, M.; Mavrinac, V.; Orlic, L. Dyslipidemia in patients with chronic kidney disease: Etiology and management. *Int. J. Nephrol. Renovasc. Dis.* **2017**, *10*, 35–45. [[CrossRef](#)]
33. Tsimihodimos, V.; Dounousi, E.; Siamopoulos, K.C. Dyslipidemia in Chronic Kidney Disease: An Approach to Pathogenesis and Treatment. *Am. J. Nephrol.* **2008**, *28*, 958–973. [[CrossRef](#)] [[PubMed](#)]
34. Kim, J.H.; Lee, S.S.; Jung, M.H.; Yeo, H.D.; Kim, H.J.; Yang, J.I.; Roh, G.S.; Chang, S.H.; Park, D.J. N-acetylcysteine attenuates glycerol-induced acute kidney injury by regulating MAPKs and Bcl-2 family proteins. *Nephrol. Dial. Transplant.* **2010**, *25*, 1435–1443. [[CrossRef](#)]
35. Homsí, E.; Janino, P.; De Faria, J.B.L. Role of caspases on cell death, inflammation, and cell cycle in glycerol-induced acute renal failure. *Kidney Int.* **2006**, *69*, 1385–1392. [[CrossRef](#)] [[PubMed](#)]
36. Soares, S.; Souza, L.C.R.; Cronin, M.T.; Waaga-Gasser, A.M.; Grossi, M.F.; Franco, G.R.; Tagliati, C.A. Biomarkers and in vitro strategies for nephrotoxicity and renal disease assessment. *Nephrol. Ren. Dis.* **2020**, *5*. [[CrossRef](#)]
37. Shearer, G.C.; Carrero, J.J.; Heimbürger, O.; Barany, P.; Stenvinkel, P. Plasma Fatty Acids in Chronic Kidney Disease: Nervonic Acid Predicts Mortality. *J. Ren. Nutr.* **2012**, *22*, 277–283. [[CrossRef](#)] [[PubMed](#)]
38. Szczuko, M.; Kaczkan, M.; Drozd, A.; Maciejewska, D.; Palma, J.; Owczarzak, A.; Marczuk, N.; Rutkowski, P.; Małgorzewicz, S. Comparison of Fatty Acid Profiles in a Group of Female Patients with Chronic Kidney Diseases (CKD) and Metabolic Syndrome (MetS)—Similar Trends of Changes, Different Pathophysiology. *Int. J. Mol. Sci.* **2019**, *20*, 1719. [[CrossRef](#)]
39. Varga, Z.; Kárpáti, I.; Paragh, G.; Buris, L.; Kakuk, G. Relative abundance of some free fatty acids in plasma of uremic patients: Relationship between fatty acids, lipid parameters, and diseases. *Nephron* **1997**, *77*, 417–421. [[CrossRef](#)]
40. Ting, T.C.; Miyazaki-Anzai, S.; Masuda, M.; Levi, M.; Demer, L.L.; Tintut, Y.; Miyazaki, M. Increased lipogenesis and stearate accelerate vascular calcification in calcifying vascular cells. *J. Biol. Chem.* **2011**, *286*, 23938–23949. [[CrossRef](#)] [[PubMed](#)]
41. Martín-Lorenzo, M.; Gonzalez-Calero, L.; Ramos-Barron, A.; Sanchez-Niño, M.D.; Gomez-Alamillo, C.; García-Segura, J.M.; Ortiz, A.; Arias, M.; Vivanco, F.; Alvarez-Llamas, G. Urine metabolomics insight into acute kidney injury point to oxidative stress disruptions in energy generation and H₂S availability. *J. Mol. Med.* **2017**, *95*, 1399–1409. [[CrossRef](#)] [[PubMed](#)]
42. Aminzadeh, M.A.; Vaziri, N.D. Downregulation of the renal and hepatic hydrogen sulfide (H₂S)-producing enzymes and capacity in chronic kidney disease. *Nephrol. Dial. Transplant.* **2012**, *27*, 498–504. [[CrossRef](#)] [[PubMed](#)]
43. Perna, A.F.; Luciano, M.G.; Ingrosso, D.; Pulzella, P.; Sepe, I.; Lanza, D.; Violetti, E.; Capasso, R.; Lombardi, C.; De Santo, N.G. Hydrogen sulphide-generating pathways in haemodialysis patients: A study on relevant metabolites and transcriptional regulation of genes encoding for key enzymes. *Nephrol. Dial. Transplant.* **2009**, *24*, 3756–3763. [[CrossRef](#)] [[PubMed](#)]
44. Perna, A.F.; Luciano, M.G.; Ingrosso, D.; Raiola, I.; Pulzella, P.; Sepe, I.; Lanza, D.; Violetti, E.; Capasso, R.; Lombardi, C.; et al. Hydrogen sulfide, the third gaseous signaling molecule with cardiovascular properties, is decreased in hemodialysis patients. *J. Ren. Nutr.* **2010**, *20*, S11–S14. [[CrossRef](#)]
45. Luczak, M.; Formanowicz, D.; Marczak, Ł.; Pawliczak, E.; Wanic-Kossowska, M.; Figlerowicz, M.; Stobiecki, M. Deeper insight into chronic kidney disease-related atherosclerosis: Comparative proteomic studies of blood plasma using 2DE and mass spectrometry. *J. Transl. Med.* **2015**, *13*, 20. [[CrossRef](#)]
46. Iseki, K.; Ikemiya, Y.; Iseki, C.; Takishita, S. Proteinuria and the risk of developing end-stage renal disease. *Kidney Int.* **2003**, *63*, 1468–1474. [[CrossRef](#)]
47. Kilpatrick, R.D.; McAllister, C.J.; Kovesdy, C.P.; Derose, S.F.; Kopple, J.D.; Kalantar-Zadeh, K. Association between Serum Lipids and Survival in Hemodialysis Patients and Impact of Race. *J. Am. Soc. Nephrol.* **2007**, *18*, 293–303. [[CrossRef](#)]
48. Luczak, M.; Suszynska-Zajczyk, J.; Marczak, Ł.; Formanowicz, D.; Pawliczak, E.; Wanic-Kossowska, M.; Stobiecki, M. Label-free quantitative proteomics reveals differences in molecular mechanism of atherosclerosis related and non-related to chronic kidney disease. *Int. J. Mol. Sci.* **2016**, *17*, 631. [[CrossRef](#)] [[PubMed](#)]
49. Gayraud, N.; Ficheux, A.; Durantón, F.; Guzman, C.; Szwarc, I.; Vetromile, F.; Cazeveille, C.; Brunet, P.; Servel, M.-F.; Argilés, À.; et al. Consequences of increasing convection onto patient care and protein removal in hemodialysis. *PLoS ONE* **2017**, *12*, e0171179. [[CrossRef](#)] [[PubMed](#)]
50. Yeboah, J.; McNamara, C.; Jiang, X.C.; Tabas, I.; Herrington, D.M.; Burke, G.L.; Shea, S. Association of plasma sphingomyelin levels and incident coronary heart disease events in an adult population: Multi-ethnic study of atherosclerosis. *Arterioscler. Thromb. Vasc. Biol.* **2010**, *30*, 628–633. [[CrossRef](#)] [[PubMed](#)]
51. Pongrac Barlovic, D.; Harjutsalo, V.; Sandholm, N.; Forsblom, C.; Groop, P.H. Sphingomyelin and progression of renal and coronary heart disease in individuals with type 1 diabetes. *Diabetologia* **2020**, *63*, 1847–1856. [[CrossRef](#)] [[PubMed](#)]
52. Levey, A.S.; Bosch, J.P.; Lewis, J.B.; Greene, T.; Rogers, N.; Roth, D. A More Accurate Method To Estimate Glomerular Filtration Rate from Serum Creatinine: A New Prediction Equation. *Ann. Intern. Med.* **1999**, *130*, 461. [[CrossRef](#)] [[PubMed](#)]
53. National Clinical Guideline Centre (UK). *Chronic Kidney Disease (Partial Update): Early Identification and Management of Chronic Kidney Disease in Adults in Primary and Secondary Care*; NICE Clinical Guidelines, No. 182; National Clinical Guideline Centre: London, UK, 2014; pp. 113–120.

54. Herzog, R.; Schuhmann, K.; Schwudke, D.; Sampaio, J.L.; Bornstein, S.R.; Schroeder, M.; Shevchenko, A. LipidXplorer: A software for consensual cross-platform lipidomics. *PLoS ONE* **2012**, *7*, e29851. [[CrossRef](#)] [[PubMed](#)]
55. Sumner, L.W.; Amberg, A.; Barrett, D.; Beale, M.H.; Beger, R.; Daykin, C.A.; Fan, T.W.-M.; Fiehn, O.; Goodacre, R.; Griffin, J.L.; et al. Proposed minimum reporting standards for chemical analysis Chemical Analysis Working Group (CAWG) Metabolomics Standards Initiative (MSI). *Metabolomics* **2007**, *3*, 211–221. [[CrossRef](#)] [[PubMed](#)]
56. Molenaar, M.R.; Jeucken, A.; Wassenaar, T.A.; van de Lest, C.H.A.; Brouwers, J.F.; Helms, J.B. LION/web: A web-based ontology enrichment tool for lipidomic data analysis. *Gigascience* **2019**, *8*, giz061. [[CrossRef](#)]
57. Cox, J.; Mann, M. MaxQuant enables high peptide identification rates, individualized p.p.b.-range mass accuracies and proteome-wide protein quantification. *Nat. Biotechnol.* **2008**, *26*, 1367–1372. [[CrossRef](#)]
58. Xia, J.; Psychogios, N.; Young, N.; Wishart, D.S. MetaboAnalyst: A web server for metabolomic data analysis and interpretation. *Nucleic Acids Res.* **2009**, *37*, W652–W660. [[CrossRef](#)] [[PubMed](#)]

Supplementary Materials

Mass Spectrometry-Based Lipidomics Reveals Differential Changes in the Accumulated Lipid Classes in Chronic Kidney Disease

Lukasz Marczak^{1,*}, Jakub Idkowiak^{1,2}, Joanna Tracz³, Maciej Stobiecki¹, Bartłomiej Perek⁴, Katarzyna Kostka-Jeziorny⁵, Andrzej Tykarski⁵, Maria Wanic-Kossowska⁶, Marcin Borowski⁷, Marcin Osuch⁸, Dorota Formanowicz⁹ and Magdalena Luczak^{3,*}

¹ Department of Natural Products Biochemistry, Institute of Bioorganic Chemistry Polish Academy of Sciences, 61-704 Poznan, Poland; jakubidkowiak1@gmail.com (J.I.); mackis@ibch.poznan.pl (M.S.)

² Department of Analytical Chemistry, Faculty of Chemical Technology, University of Pardubice, 532 10 Pardubice, Czech Republic

³ Department of Biomedical Proteomics, Institute of Bioorganic Chemistry Polish Academy of Sciences, 61-704 Poznan, Poland; joanna.a.tracz@gmail.com

⁴ Department of Cardiac Surgery and Transplantology, Poznan University of Medical Sciences, 61-001 Poznan, Poland; bperek@ump.edu.pl

⁵ Department of Hypertension, Angiology and Internal Disease, Poznan University of Medical Sciences, 61-001 Poznan, Poland; kostkajeziorny@gmail.com (K.K.-J.); tykarski@o2.pl (A.T.)

⁶ Department of Nephrology, Transplantology and Internal Medicine, Poznan University of Medical Sciences, 60-355 Poznan, Poland; wanic.kossowska.maria@gmail.com

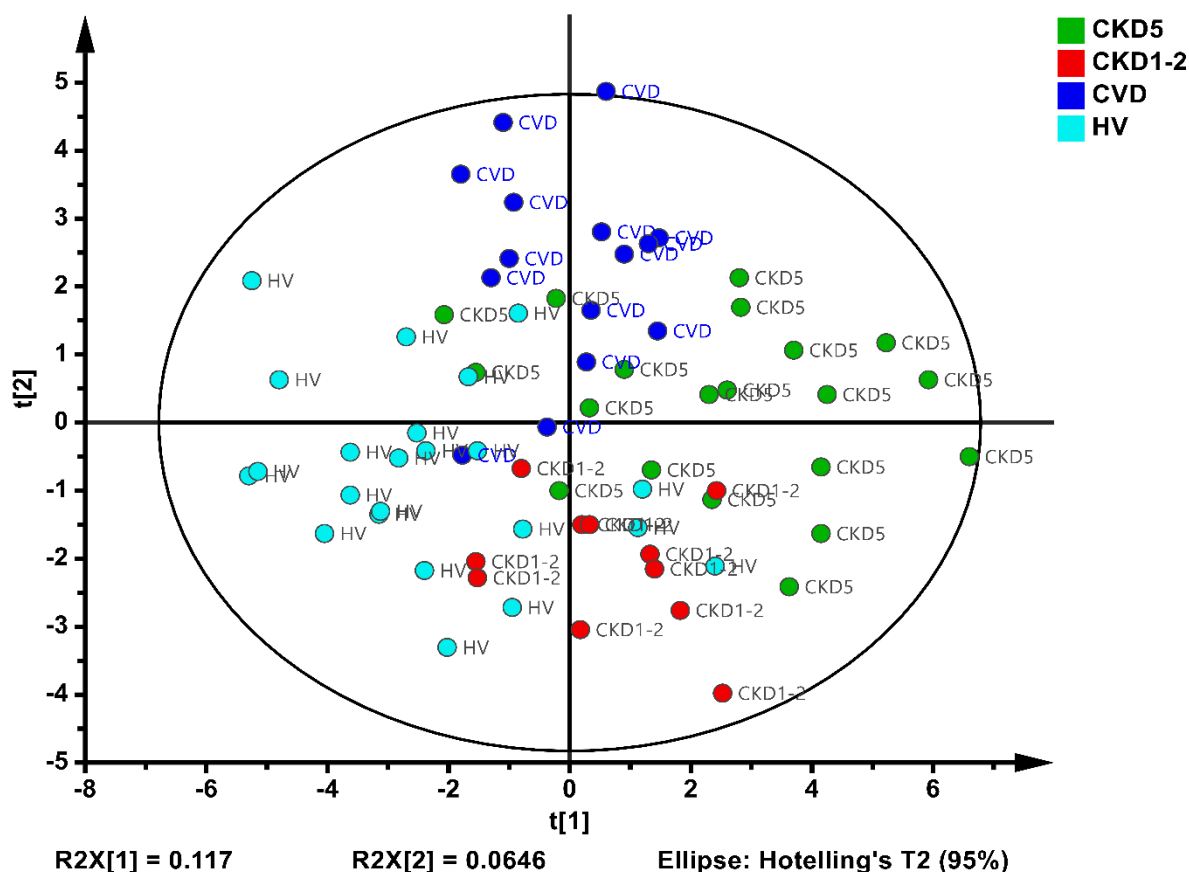
⁷ Institute of Computing Science, Poznan University of Technology, 60-965 Poznan, Poland; Marcin.Borowski@cs.put.poznan.pl

⁸ Department of Molecular and Systems Biology, Institute of Bioorganic Chemistry Polish Academy of Sciences, 61-704 Poznan, Poland; mosuch@ibch.poznan.pl

⁹ Chair and Department of Medical Chemistry and Laboratory Medicine, Poznan University of Medical Sciences, 60-806 Poznan, Poland; doforman@ump.edu.pl

* Correspondence: lukasmar@ibch.poznan.pl (L.M.); magdalu@ibch.poznan.pl (M.L.)

Figure S1: Partial least squares discriminant analysis (PLS-DA) performed on the total number of lipids identified in CKD5 (green), CVD (dark blue), CKD1-2 (red), and HVs (blue) experimental groups.



Tabele, zawarte jako suplement artykułu nr 3 nie zostały załączone do niniejszej rozprawy ze względu na swoją złożoność, natomiast są dostępne do pobrania w poniższym linku:

<https://www.mdpi.com/2218-1989/11/5/275#supplementary>

- Table S1: Pearson's correlation coefficients calculated for clinical data.
- Table S2: A list of identified lipid classes in plasma of HVs, CKD1-2, CKD5 and CVD patients. Table provides information about the name of lipid class, average abundances and SD for all analyzed experimental groups, ANOVA/K-W p -value and q -value and fold changes for all group comparisons.
- Table S3: Pearson's correlation coefficients calculated for identified lipid classes presented as a heat map in Figure 1 and clinical data. The calculations were derived from MetaboAnalyst software. Significant correlation (p -value < 0.05) is marked in bold.
- Table S4: Complete list of differentially accumulated lipid species in plasma of HVs, CKD1-2, CKD5 and CVD patients. Table provides information about the name of lipid class, average abundances and SD for all analyzed experimental groups, ANOVA/K-W p -value and q -value and fold changes for all group comparisons.
- Table S5: A detailed list of the enrichment analysis performed in LION. Table provides information about lipid functions, cellular components or lipid classification with term ID, number of annotated lipids, p -value and FDR-corrected Kolmogorov–Smirnov p -value (q -value).
- Table S6: A list of low-molecular-weight compounds quantified using extracted-ion chromatogram (EIC) and GC-MS analysis. Table provides information about the name of compound, retention time (RT), and m/z value characteristic for the given compound derived from NIST database (Quant Mass), average abundances and SD for all analyzed experimental groups, ANOVA/K-W p -value and q -value and fold changes for all group comparisons.
- Table S7: Spearman's correlation coefficients calculated for low-molecular-weight compounds quantified using extracted-ion chromatogram (EIC) and GC-MS analysis and clinical data presented in Figure 8.